Multipoint Conformal Blocks in Conformal Field Theories

Dissertation
zur Erlangung des Doktorgrades
an der Fakultät für Mathematik, Informatik und Naturwissenschaften
Fachbereich Physik
der Universität Hamburg

vorgelegt von

Lorenzo Quintavalle

Hamburg

2022

Gutachter/innen der Dissertation:	Prof. Dr. Volker Schomerus Prof. Dr. Gleb Arutyunov
Zusammensetzung der Prüfungskommission:	Prof. Dr. Bernd Kniehl Prof. Dr. Volker Schomerus Prof. Dr. Gleb Arutyunov Prof. Dr. Jörg Teschner Prof. Dr. Elisabetta Gallo
Vorsitzende/r der Prüfungskommission:	Prof. Dr. Bernd Kniehl
Datum der Disputation:	25.04.2022
Vorsitzender Fach-Promotionsausschusses PHYSIK	Prof. Dr. Wolfgang Parak
Leiter des Fachbereichs PHYSIK:	Prof. Dr. Günter H. W. Sigl
Dekan der Fakultät MIN:	Prof. Dr. Heinrich Graener

Abstract

A very powerful tool in Conformal Field Theories is the conformal block expansion, which plays a crucial role in the conformal bootstrap programme. The goal of this thesis is to improve the understanding and mathematical control over conformal block expansions for more than four external fields, studying the so-called multipoint conformal blocks from the perspective of the differential equations these satisfy. The results presented here stem from newly discovered relations between multipoint conformal blocks and Gaudin integrable models. These allow the introduction of special limits for multipoint conformal blocks which reduce them to some of their sub-components. Reduction to three-point blocks leads to a further novel connection between conformal blocks and integrable Calogero-Moser-Sutherland models. These results pave the way for future computations of multipoint conformal blocks, starting from certain well-behaved limits.

Zusammenfassung

Ein sehr wirkungsvolles Werkzeug in konformen Feldtheorien ist die konforme Blockentwicklung, die eine entscheidende Rolle im konformen Bootstrap-Programm spielt. Das Ziel dieser Arbeit ist es, das Verständnis und die mathematische Kontrolle über konforme Blockentwicklungen für mehr als vier externe Felder zu verbessern, indem die sogenannten konformen Mehrpunktblöcke aus der Perspektive der Differentialgleichungen, die diese erfüllen, untersucht werden. Die hier vorgestellten Ergebnisse stammen aus neu entdeckten Beziehungen zwischen konformen Mehrpunktblöcken und integrierbaren Gaudin-Modellen. Diese ermöglichen die Einführung spezieller Grenzwerte für konforme Mehrpunktblöcke, die sie auf einige ihrer Unterkomponenten reduzieren. Die Reduktion auf Dreipunktblöcke führt zu einer weiteren neuartigen Verbindung zwischen konformen Blöcken und integrierbaren Calogero-Moser-Sutherland-Modellen. Diese Ergebnisse ebnen den Weg für zukünftige Berechnungen von Mehrpunkt-konformen Blöcken, ausgehend von bestimmten gut gezogenen Grenzen.

Declaration on oath

I hereby declare under oath that I have written this dissertation myself and have not used any aids or sources other than those indicated.

Eidesstattliche Versicherung

Hiermit versichere ich an Eides statt, die vorliegende Dissertationsschrift selbst verfasst und keine anderen als die angegebenen Hilfsmittel und Quellen benutzt zu haben.

Hamburg, 2022

_____

Unterschrift des Doktoranden

This thesis is based on the publications:

- I. Buric, S. Lacroix, J. A. Mann, L. Quintavalle and V. Schomerus, *"From Gaudin Integrable Models to d-dimensional Multipoint Conformal Blocks"*, Phys. Rev. Lett. 126, 021602 (2021), arxiv:2009.11882
- I. Buric, S. Lacroix, J. A. Mann, L. Quintavalle and V. Schomerus, *"Gaudin Models and Multipoint Conformal Blocks: General Theory"*, JHEP 2110, 139 (2021), arxiv:2105.00021
- I. Buric, S. Lacroix, J. A. Mann, L. Quintavalle and V. Schomerus, *"Gaudin Models and Multipoint Conformal Blocks II: Comb channel vertices in 3D and 4D"*, JHEP 2111, 182 (2021), arxiv:2108.00023
- I. Buric, S. Lacroix, J. A. Mann, L. Quintavalle and V. Schomerus, *"Gaudin Models and Multipoint Conformal Blocks III: Comb channel coordinates and OPE factorisation"*, arxiv:2112.10827

Other publications by the author:

- S. Appella, A. Atayev, O. Bond, B. Collins, M. Dablander, N. Fadeev, A. Lacey, P. Morawiecki, H. Ockendon, D. Polvara, E. Powell, L. Quintavalle, E. Wilson, Y. Zhou, T. Wiles, *"Determining the conductance of networks created by randomly dispersed cylinders."*, Mathematics in Industry Reports (MIIR) 2021

Contents

Chapter 1

Introduction

It is safe to say that Quantum Field Theories (QFTs) are the most successful framework for fundamental physics: the use of QFTs in particle physics led to an unprecedented level of agreement between theoretical predictions and experimental data. Iconic in this sense is the determination, using quantum electrodynamics, of the anomalous magnetic moment $g_e - 2$ of the electron, representing the most accurate verified prediction in the history of physics. The extraordinary robustness of this type of results is suggestive that the view of the world painted by QFTs has deep roots in the quintessence of reality.

At the core of the QFT machinery lies the concept of symmetry. The basic symmetries of spacetime, often complemented with additional "gauge" symmetries, constitute the foundations of any such theory, and strongly constrain the space of possible Lagrangians that can be constructed. Most of the observables are then computed and understood from the Lagrangian in a perturbative regime, when an expansion for small values of certain physical parameters is possible. The prime example of this type of reasoning is the expansion of correlators and scattering amplitudes in Feynman diagrams, on which numerous phenomenological predictions have been built. One downside of the Feynman expansion, however, is that it is often only an asymptotic one, i.e. it can approximate the complete result up to a certain order, but it does not converge and can thus not be resummed to obtain results beyond perturbation theory. Many theories do not even grant a full, non-perturbative picture, but can only be fully made sense of as "effective" theories, which give a coarse-grained description of field interactions at certain energy scales, but break down above a certain cutoff energy at which one starts to probe finer-grained structures.

In a Wilsonian paradigm [1], these theories can be interpreted as intermediate outputs of a renormalization group (RG) flow, in which finer-grained degrees of freedom of an underlying, richer-in-detail theory are integrated out to produce an effective low-energy description. In this picture, a special role is played by those theories which are not modified by the action of the RG flow: these are the *Conformal Field Theories* (CFTs) [2], the main framework of this thesis.

CFTs are thus theories that do not change when acted upon with scale transformations, and are rather universal throughout different branches of physics. Scale invariance in these theories, combined with Poincaré symmetry of spacetime, is promoted to the broader group of conformal symmetries which, in addition to giving CFTs their name, supplies them with extremely powerful mathematical tools to compute their observables, even non-perturbatively. CFTs are in fact the main class of interacting theories for which a non-perturbative handle can be currently achieved and have thus been the prime example of theories that can be exactly solvable [3], at least in certain two-dimensional cases.

The usefulness of CFTs is however not limited to the construction of well-behaved toy models for particle physics, but is quite more far-reaching. For instance, any physical system that undergoes a second-order phase transition is scale-invariant, and the critical exponents that characterize the behavior of certain observables in these systems can be well understood and computed from a CFT approach. Furthermore, thanks to holographic approaches such as the well-known AdS/CFT correspondence or the more recent

Celestial Holography program, the study of CFTs can directly shed light on aspects of quantum gravity that are still not understood. Two-dimensional CFTs also appear in the context of string theory as the theories that describe the dynamics of the string worldsheet.

One of the first breakthroughs in the non-perturbative understanding of CFTs happened in the '70s, with the introduction of Polyakov's conformal bootstrap program [4]. This consisted in the exploitation of general features such as conformal symmetry, locality, and unitarity, to obtain systems of algebraic equations for anomalous dimensions and coupling constants that could then be solved. The strength of this approach was not only that it did not rely on any perturbative expansion, but it could even be used without any information on a possible underlying Lagrangian. This led to the impressive results in two dimensions we hinted to above, [3].

For years, however, this type of approach failed to extend beyond the realm of two-dimensional CFTs. This until 2008, when the program was revived in a paper by Rattazzi, Rychkov, Tonni, and Vichi [5], in which was shown that conformal consistency conditions can be used together with numerical methods to obtain bounds on the parameters of CFTs. Since then, numerous numerical and analytic approaches have been introduced and used [6–16], which allowed to gather an astounding amount of data on CFTs, among which surely stands out the incredibly precise numerical estimate of the critical exponents in the 3D Ising model [9, 17].

In its modern version, the conformal bootstrap mainly revolves around the Operator Product Expansion (OPE), which allows replacing the product of two fields in a correlator with an infinite sum over insertions of one single field. Repeated application of the OPE allows for a full decomposition of correlators in terms of kinematical functions, the *conformal blocks*, combined with some dynamical coefficients. The associativity of the OPE implies that regardless of the order of the operations, also known as OPE channel, the different conformal block expansions need to encode the same result and thus be equivalent. This is translated to formulas as the *crossing equations*, which can be used as consistency conditions to "bootstrap" non-perturbative data.

In the bootstrap approach is therefore of crucial importance to get good control over the conformal block expansion. A seminal contribution in this direction was that of Dolan and Osborn [18, 19], who introduced a technique based on Casimir operators and associated differential equations which allows efficient computation of certain four-point conformal blocks. This paved the way for many results concerning four-point conformal blocks [20–31], which themselves allowed to apply the bootstrap techniques for a wide variety of four-point functions.

For many years these were almost the only type of correlators that attracted the focus of the bootstrap community. This is because if one were to know all the possible four-point functions of a certain CFT, one would then be able to compute any correlator with any number of external legs, thanks to the OPE. In recent years, however, it has become more and more clear how the application of the bootstrap logic to *multipoint* correlators, i.e. correlators with more than four external fields, could grant much easier access to certain observables [32–35].

But, to reiterate, in order to do bootstrap it is crucial to have well under mathematical control the conformal block expansion. This is not yet the case for general correlators, as the approaches established for four points do not scale as easily to higher number of points, while new approaches targeted directly to multipoint correlators have only recently started to gain traction [36–40]. This is the context of this thesis, whose goal is to delve into the subject of multipoint conformal blocks from the point of view of the differential equations these satisfy, in an extended version of the Dolan-Osborn approach to a higher-point setting. The main results of this thesis have been published already in [41–44] by the author of this thesis and collaborators, with contributions equally distributed among all the authors.

We will now outline the structure of this thesis. Chapter 2 is a general review of Conformal Field Theory, which introduces most of the basic concepts and tools that are needed throughout the rest of the thesis.

Most of the results are rather standard and can be found in reviews such as [45]; the perspective with which these results are examined is however atypical, tailored towards the use that will be made of in later parts of this work. Particular focus is posed on the embedding space formalism – a tool which can be used to greatly simplify CFT computations – and the constraints that conformal invariance imposes on the correlators. This discussion leads to the introduction of the concept of conformal blocks, ubiquitous in this thesis.

Chapter 3 reports the new findings of [41, 42], in which we introduced a novel connection between the problem of (multipoint) conformal blocks and the integrable Gaudin models. This represents a natural extension of the Dolan-Osborn set of Casimir differential operators, which are complemented with newly introduced *vertex differential operators* to make the multipoint conformal block problem integrable.

Chapter 4, based on [44], targets the study of OPE limits for conformal blocks in the comb channel. A novel type of conformally invariant coordinates is introduced, which allows a simple analysis of the leading behaviour of blocks associated with a certain exchanged field. This leads to remarkable factorization formulas, which make explicit how, when taking OPE limits, the conformal blocks are reduced to products of its sub-components. This allows the reduction of the system of differential equations associated with a multipoint conformal block, to smaller systems that characterizes blocks with a lower number of external fields.

One such type of reduced system is then analyzed in chapter 5, where the focus is targeted towards three-point functions with one associated degree of freedom. These systems correspond to any three-point function that can be obtained from reduction of an N-point function in the comb channel. In particular, we report the results of [43], where the single vertex differential operator that characterizes these systems is analyzed, and is identified as the Hamiltonian of a crystallographic elliptic Calogero-Moser-Sutherland model.

We finally wrap up in chapter 6 with some closing remarks and an outlook on future research.

Chapter 2

Conformal Field Theory

Any theory compatible with Einstein's special theory of relativity must be invariant under the the Poincaré group of symmetry. This consists in all transformations that leave the flat metric of spacetime invariant:

$$\mathrm{d}s'^2 = g_{\mu\nu}\mathrm{d}x'^\mu \mathrm{d}x'^\nu = g_{\mu\nu}\mathrm{d}x^\mu \mathrm{d}x^\nu = \mathrm{d}s^2 \,, \tag{2.1}$$

with $g_{\mu\nu} = \eta_{\mu\nu} = \mathrm{diag}(-1, 1, \ldots, 1)$ for Lorentzian signatures and $g_{\mu\nu} = \delta_{\mu\nu}$ for Euclidean signature. The individual transformations that make up this group are the Lorentz transformations

$$e^{L^\mu{}_\nu} : x^\mu \to M^\mu{}_\nu\, x^\nu \,, \qquad M^T g M = g \qquad \Longrightarrow \qquad \mathrm{d}s'^2 = \left(g_{\mu\nu} M^\mu{}_\rho M^\nu{}_\sigma\right) \mathrm{d}x^\rho \mathrm{d}x^\sigma = g_{\mu\nu}\mathrm{d}x^\mu \mathrm{d}x^\nu \tag{2.2}$$

and the translations

$$e^{a^\mu P_\mu} : x^\mu \to x^\mu + a^\mu \qquad \Longrightarrow \qquad \mathrm{d}s'^2 = g_{\mu\nu}\, \mathrm{d}(x^\mu + a^\mu)\, \mathrm{d}(x^\nu + a^\nu) = g_{\mu\nu}\mathrm{d}x^\mu \mathrm{d}x^\nu \,. \tag{2.3}$$

Theories which enjoy *conformal* symmetry are invariant under a larger group of symmetry which extends the Poincaré transformations above; these are all transformations that leave angles invariant or, analogously, that leave the metric invariant up to an overall factor:

$$\mathrm{d}s'^2 = g_{\mu\nu}\mathrm{d}x'^\mu \mathrm{d}x'^\nu = \Lambda(x)^2 g_{\mu\nu}\mathrm{d}x^\mu \mathrm{d}x^\nu = \Lambda(x)^2 \mathrm{d}s^2 \,. \tag{2.4}$$

A generic conformal transformation is spanned by the Poincaré transformations defined above, for which $\Lambda(x)^2 = 1$, plus two additional types. These are the dilatations

$$e^{\lambda D} : x^\mu \to \lambda x^\mu \qquad \Longrightarrow \qquad \mathrm{d}s'^2 = \lambda^2 g_{\mu\nu}\mathrm{d}x^\mu \mathrm{d}x^\nu \tag{2.5}$$

and the conformal inversion

$$\mathcal{I} : x^\mu \to \frac{x^\mu}{x^2} \qquad \Longrightarrow \qquad \mathrm{d}s'^2 = (x^2)^{-2} g_{\mu\nu}\mathrm{d}x^\mu \mathrm{d}x^\nu \,, \tag{2.6}$$

which is a unipotent transformation $\mathcal{I}^2 = \mathbb{1}$. This last transformation, the conformal inversion, is the only one we introduced so far which is not connected to the identity. For many purposes it is often best to also introduce the *special conformal transformations*, connected to the identity, which are obtained by composing an inversion, a translation, and another inversion:

$$e^{a^\mu K_\mu} = e^{-a^\mu \mathcal{I} P_\mu \mathcal{I}} = \mathcal{I} e^{-a^\mu P_\mu} \mathcal{I} : x^\mu \to \frac{x^\mu - x^2 a^\mu}{1 - 2(a\cdot x) + x^2 a^2} \,. \tag{2.7}$$

The infinitesimal version of the conformal transformations connected to the identity can be studied by plugging $x'^\mu = x^\mu + \varepsilon^\mu(x)$ in (2.4), obtaining the Conformal Killing Equation (CKE)

$$\partial_\mu \varepsilon_\nu + \partial_\nu \varepsilon_\mu = \frac{2}{d}\left[\partial \cdot \varepsilon(x)\right] g_{\mu\nu} \,. \tag{2.8}$$

In $d > 2$, the solutions to this equation correspond precisely to the infinitesimal version of the transformations (2.2), (2.3), (2.5), (2.7), from which it is also straightforward to obtain the expressions for the generators:

- **Lorentz transformations**:

$$\varepsilon^\mu = \omega^{[\mu\nu]} x_\nu \qquad \Longrightarrow \qquad L_{\mu\nu} = -x_\mu \partial_\nu + x_\nu \partial_\mu \,; \tag{2.9}$$

- **Translations**:

$$\varepsilon^\mu = a^\mu \qquad \Longrightarrow \qquad P_\mu = \partial_\mu \,; \tag{2.10}$$

- **Dilatations**:

$$\varepsilon^\mu = \lambda x^\mu \qquad \Longrightarrow \qquad D = x^\mu \partial_\mu \tag{2.11}$$

- **Special conformal transformations**:

$$\varepsilon^\mu = 2x^\mu (b \cdot x) - b^\mu x^2 \qquad \Longrightarrow \qquad K_\mu = 2x_\mu (x \cdot \partial) - x^2 \partial_\mu \,. \tag{2.12}$$

These generators satisfy the following commutation relations

$$\begin{gathered}
[D, L_{\mu\nu}] = 0 \,, \qquad [P_\mu, P_\nu] = 0 \,, \qquad [K_\mu, K_\nu] = 0 \,, \\
[D, P_\mu] = P_\mu \,, \qquad [D, K_\mu] = -K_\mu \,, \\
[K_\mu, P_\nu] = 2 g_{\mu\nu} D - 2 L_{\mu\nu} \,, \\
[L_{\mu\nu}, P_\rho] = g_{\nu\rho} P_\mu - g_{\mu\rho} P_\nu \,, \\
[L_{\mu\nu}, K_\rho] = g_{\nu\rho} K_\mu - g_{\mu\rho} K_\nu \,, \\
[L_{\mu\nu}, L_{\rho\sigma}] = g_{\nu\rho} L_{\mu\sigma} - g_{\mu\rho} L_{\nu\sigma} + g_{\nu\sigma} L_{\rho\mu} - g_{\mu\sigma} L_{\rho\nu} \,,
\end{gathered} \tag{2.13}$$

which form an $\mathfrak{so}(d,2)$ algebra in Lorentzian signature, or an $\mathfrak{so}(d+1,1)$ algebra for the Euclidean case. To make this manifest, one can add the two null directions $+$ and $-$ to form a $(d+2)$-dimensional index $A = \{+, -, \mu\}$, with corresponding metric being

$$g_{AB} = \left(\begin{array}{cc|c} 0 & -\frac{1}{2} & \\ -\frac{1}{2} & 0 & \mathbb{O}_{2\times d} \\ \hline & \mathbb{O}_{d\times 2} & g_{\mu\nu} \end{array}\right) \tag{2.14}$$

and recombine generators in the following way

$$M_{-+} = 2D \,, \qquad M_{+\mu} = P_\mu \,, \qquad M_{-\mu} = -K_\mu \,, \qquad M_{\mu\nu} = L_{\mu\nu} \,, \tag{2.15}$$

from which it is simple to check that the commutation relations acquire the form of a (generalized) Lorentz algebra

$$[M_{AB}, M_{CD}] = g_{BC} M_{AD} - g_{AC} M_{BD} + g_{BD} M_{CA} - g_{AD} M_{CB} \,. \tag{2.16}$$

Quantum Field Theories which are invariant under the set of transformations described here are known as Conformal Field Theories (CFTs), and are the main focus of this thesis. From now on, we will be mainly working in Euclidean signature, referring back to Lorentzian signature only for some comments.

2.1 States and fields in Conformal Field Theory

The first important thing to describe in a quantum theory is its space of states, or in other words, its Hilbert space. In Euclidean CFTs it is natural to foliate space with S^{d-1} spheres, with leftover radial direction representing Euclidean time. As "zero time" slice one can consider the unit sphere, on which it is possible to construct the Hilbert space. This will admit a natural "time" evolution through the action of the dilatation generator, which for positive scale factor maps spheres into larger and larger ones, as schematically represented in Figure 2.1a. The dilatation operator assumes therefore the role of the Hamiltonian in this type of quantization, known as *radial quantization*. A completely equivalent visualization of this quantization, which also gives a perhaps more interpretation of the time coordinate,

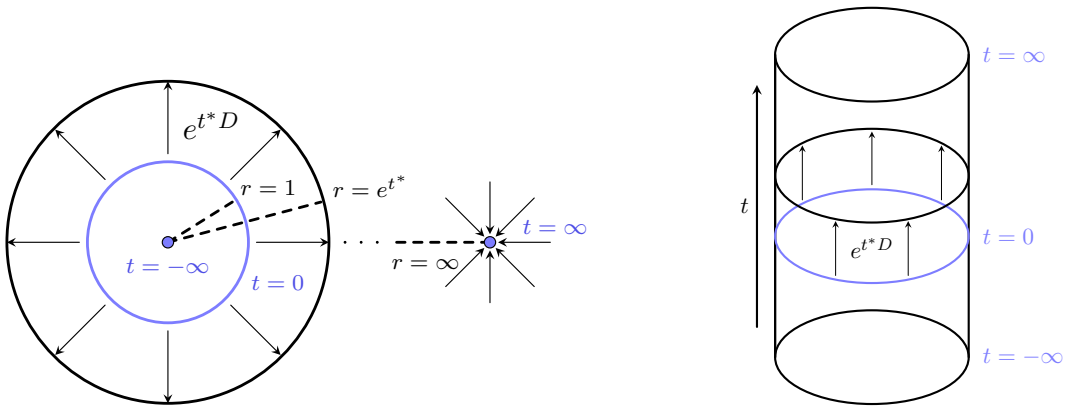

(a) Radial quantization in flat space **(b)** Mapping of radial quantization to a cylinder

Figure 2.1: (a) Radial quantization in Euclidean CFT, where equal time slices correspond to S^{d-1} spheres. Time evolution is implemented by the action of the dilatation generator D, which for past and future infinite times makes the S^{d-1} degenerate into the point at the origin or the point at infinity. The same configuration can be conformally mapped to a cylinder $\mathbb{R} \times S^{d-1}$ as in **(b)**, where the time direction is naturally interpreted as the $\mathbb{R}$ component of the cylinder.

is given by considering the conformal mapping from flat space to a cylinder – see Figure 2.1b – by which the radial coordinate is logarithmically mapped to a Euclidean time direction on the cylinder

$$r \to t = \log r \qquad \Longrightarrow \qquad \mathrm{d}s^2 = \mathrm{d}r^2 + r^2 \mathrm{d}s^2_{S^{d-1}} = r^2 \left(\mathrm{d}t^2 + \mathrm{d}s^2_{S^{d-1}}\right) = r^2 \mathrm{d}s^2_{\text{cyl}} \overset{\text{conf.}}{\simeq} \mathrm{d}s^2 \,. \tag{2.17}$$

In this type of quantization, Lorentzian conjugation corresponds to Euclidean time reflection:

$$\begin{gathered} \left(|\psi(t_L)\rangle\right)^\dagger = \left(e^{t_L D} |\psi(0)\rangle\right)^\dagger = \langle\psi(0)| e^{-t_L D} = \langle\psi(t_L)| \\ \Downarrow \\ \left(|\psi(t_E)\rangle\right)^\dagger = \left(|\psi(it_L)\rangle\right)^\dagger = \left(e^{it_L D} |\psi(0)\rangle\right)^\dagger = \langle\psi(0)| e^{it_L D} = \langle\psi(-it_L)| = \langle\psi(-t_E)| \,, \end{gathered} \tag{2.18}$$

which is actually the same operation as a conformal inversion:

$$x^\mu = r\hat{x}^\mu = e^t \hat{x}^\mu \qquad \xrightarrow{t \to -t} \qquad e^{-t}\hat{x}^\mu = r^{-1}\hat{x}^\mu = \frac{x^\mu}{|x|^2} = \mathcal{I}\, x^\mu \,, \tag{2.19}$$

under which we know from (2.7) that P^μ generators are mapped to K^μ and vice versa. This implies that in radial quantization we have the relation

$$P^\dagger_\mu = K_\mu \,, \tag{2.20}$$

while for Lorentz/rotation generators we have the usual relation

$$L^\dagger_{\mu\nu} = L^T_{\mu\nu} = L_{\nu\mu} = -L_{\mu\nu} \,. \tag{2.21}$$

In this thesis we will consider only the case of unitary CFTs, with therefore a unitary time evolution dictated by the Hamiltonian D, and with a positive semi-definite energy spectrum. It is therefore natural in this case to consider as basis of states one which diagonalizes the Hamiltonian

$$D\,|\Delta, \varrho\rangle = \Delta\,|\Delta, \varrho\rangle \ , \tag{2.22}$$

with eigenvalue Δ known as the *conformal dimension*, and ϱ being equal to a set of labels that fully specify the basis element being considered. Given the commutation relations of P^μ and K^μ with D, one can see that states obtained by action of these generators increase or respectively decrease the conformal dimension

$$D\left(P^\mu\,|\Delta, \varrho\rangle\right) = [D, P^\mu]\,|\Delta, \varrho\rangle + P^\mu\left(D\,|\Delta, \varrho\rangle\right) = (\Delta + 1)\left(P^\mu\,|\Delta, \varrho\rangle\right) \ , \tag{2.23}$$

$$D\left(K^\mu\,|\Delta, \varrho\rangle\right) = [D, K^\mu]\,|\Delta, \varrho\rangle + K^\mu\left(D\,|\Delta, \varrho\rangle\right) = (\Delta - 1)\left(K^\mu\,|\Delta, \varrho\rangle\right) \ . \tag{2.24}$$

To have a positive semi-definite spectrum in Δ, it is necessary that for some n:

$$(K^\mu)^n \, |\Delta, \varrho\rangle = 0 \, . \tag{2.25}$$

This implies the existence of a class of states which are highest-weight, namely that satisfy (2.25) with $n = 1$. These are known as *conformal primary states*, while all the other states – obtained by acting with P^μ on primaries – are known as their *descendants*. The set made by a primary state and all of its descendants is also known as a *conformal multiplet*.
Requiring to have a positive semi-definite scalar product and therefore a Hilbert space, imposes constraints on the Δ spectrum of the CFT; for example for a scalar primary state $|\Delta\rangle$ one has

$$0 \leq \|P_\mu \, |\Delta\rangle\|^2 = \langle \Delta | K_\mu P_\mu | \Delta \rangle = \Delta \, , \tag{2.26}$$

where in this case the repeated indices are not summed over. This instructs us on the fact that in a unitary CFT the conformal dimension of the states has to be non-negative; the state that saturates the bound, with $\Delta = 0$, can be naturally defined to be the vacuum state of the theory. A similar analysis with the action of two translation generators on a scalar state gives an independent bound

$$0 \leq \left\| P^2 \, |\Delta\rangle \right\|^2 = \langle \Delta | K^2 P^2 | \Delta \rangle = 8 \, d \, \Delta \left(\Delta + 1 - \frac{d}{2} \right) \, , \tag{2.27}$$

which instructs us that, if $\Delta > 0$, then

$$\Delta \geq \frac{d}{2} - 1 \, . \tag{2.28}$$

Acting with more than two translation generators turns out not to give independent inequalities, so scalar fields in unitary CFTs only need to satisfy the *unitarity bound* (2.28). A similar analysis can be done for states with non-trivial $\mathfrak{so}_d$ representation ϱ, obtaining bounds which depend on the additional labels of the state.
Having introduced the space of states we are interested in, we can now introduce a crucial tool that CFTs are equipped with: a one-to-one correspondence between states and fields (local operators) of the theory, known as the *state-operator map*.
The map from operators to states is easily obtained by taking the path integral within a S^d sphere of radius r^* that contains the insertion point of the operator. If no operator is inserted (or analogously, if only the identity operator is inserted), the path integral simply produces a unitary evolution from the vacuum state at time $t = -\infty$ to the vacuum state at time $t = t^*$. On the other hand, if we insert a local operator with definite scaling dimension $[D, \mathcal{O}_\Delta(0)] = \Delta$ inside a certain sphere, the path integral produces a different well defined state at time $t = t^*$. If the initial operator is inserted at the origin, the state that is produced is then an eigenstate of D

$$D \left(\mathcal{O}_\Delta(0) \, |0\rangle \right) = [D, \mathcal{O}_\Delta(0)] \, |0\rangle + \mathcal{O}_\Delta(0) D \, |0\rangle = \Delta \left(\mathcal{O}_\Delta(0) \, |0\rangle \right) \, , \tag{2.29}$$

which is no longer the case if the operator is inserted at another point $x^\mu \neq 0$. In this other case, the state can be however written as a linear combination of the eigenstates above:

$$\mathcal{O}_\Delta(x) \, |0\rangle = e^{x \cdot P} \mathcal{O}_\Delta(0) e^{-x \cdot P} \, |0\rangle = e^{x \cdot P} \left(\mathcal{O}_\Delta(0) \, |0\rangle \right) = \sum_n \frac{1}{n!} (x \cdot P)^n \left(\mathcal{O}_\Delta(0) \, |0\rangle \right) \, , \tag{2.30}$$

where we used the fact that the vacuum state is invariant under translations.
The map from states to operators can be obtained by defining the field $\mathcal{O}_{\Delta,\varrho}$ through the equation

$$\langle \mathcal{O}_1(x_1) \mathcal{O}_2(x_2) \ldots \mathcal{O}_{\Delta,\varrho}(0) \rangle = \langle 0 | \mathcal{O}_1(x_1) \mathcal{O}_2(x_2) \ldots | \Delta, \varrho \rangle \, . \tag{2.31}$$

In particular, states that are primary are mapped to operators which transform under conformal transformations as

$$\mathcal{O}_{\Delta,\varrho}(x) \to \widetilde{\mathcal{O}}_{\Delta,\varrho}(x') = \frac{1}{\Lambda(x)^\Delta} \, \varrho[L^\mu{}_\nu(x)] \mathcal{O}_{\Delta,\varrho}(x) \, , \tag{2.32}$$

where $\Lambda(x)$ is the scale factor that also appeared in (2.4) and $\varrho[L^{\mu}{}_{\nu}]$ is a rotation generator that acts in the representation ϱ.
Since the states that make up the CFT Hilbert space can be prepared by insertions of operators, the characterization of states is equivalent to discussing which local operators can appear in the theory. From this moment on we will therefore focus mainly on the field content of the CFT rather than the states. Fields in CFT are representations of the $\mathfrak{so}(d+1,1)$ algebra and can be labeled using an $\mathfrak{so}(1,1)$ weight Δ, corresponding to the eigenvalue of D, together with $n = \lfloor \frac{d}{2} \rfloor$ (half-)integer labels associated with Dynkin diagrams for the $\mathfrak{so}_d$ algebra, as in Figure 2.2.

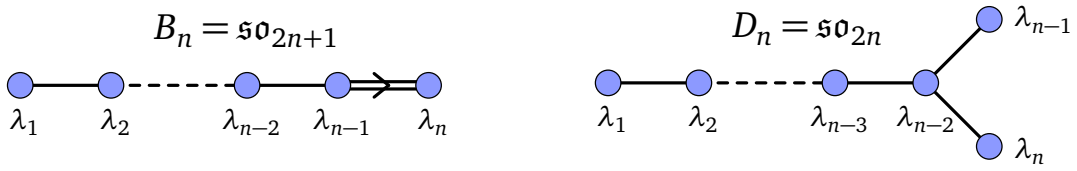

(a) Odd-dimensional case **(b)** Even-dimensional case

Figure 2.2: Dynkin diagrams for the rotation algebra $\mathfrak{so}_d$. The Lie algebra type depends on whether the spacetime dimension is even or odd. Finite-dimensional representations are labeled by these Dynkin diagrams, where a non-negative integer is assigned to every node.

For our purposes, it will be very convenient to introduce an analogous labeling system for $\mathfrak{so}_d$ with m_i as defined in Table 2.1.

$\mathbf{d = 2n+1}$	$\mathbf{d = 2n}$
$j_1 = \lambda_1 + \lambda_2 + \cdots + \frac{\lambda_n}{2}$	$j_1 = \lambda_1 + \lambda_2 + \cdots + \frac{\lambda_{n-1}+\lambda_n}{2}$
$j_2 = \lambda_2 + \cdots + \frac{\lambda_n}{2}$	$j_2 = \lambda_2 + \cdots + \frac{\lambda_{n-1}+\lambda_n}{2}$
$\vdots$	$\vdots$
$j_{n-1} = \lambda_{n-1} + \frac{\lambda_n}{2}$	$j_{n-1} = \frac{\lambda_{n-1}+\lambda_n}{2}$
$j_n = \frac{\lambda_n}{2}$	$j_n = \frac{\lambda_{n-1}-\lambda_n}{2}$

Table 2.1: Map from the Dynkin labels λ_i to the spins j_i of $\mathfrak{so}_d$ representations.

Given that the λ_i are non-negative integers, the labels j_i are therefore half-integers satisfying the inequalities

$$j_1 \geq j_2 \geq j_3 \geq \cdots \geq j_{n-1} \geq |j_n| \geq 0\,, \tag{2.33}$$

where the last equality becomes simply $j_n \geq 0$ in odd dimensions.
The results of this thesis concern mainly scalar and tensor representations, we will thus focus mostly on these. We will name the j_i labels the *spins* of the field $\mathcal{O}_{\Delta,j_1,\ldots,j_L}$, and we will name such a field with j_i integers a Mixed-Symmetry Tensor with L spins, in short MST_L. We will refer to the number of spins L as the *(spin) depth* of the $\mathfrak{so}_d$ representation. For the case of one single spin label – namely for depth $L = 1$ representations – we will use the standard terminology of Symmetric Traceless Tensor, or STT. When dealing with STTs or MST_2 fields we will also often rename the spin variables to

$$l \equiv j_1\,, \qquad \ell \equiv j_2\,, \tag{2.34}$$

such that indices become more manageable when dealing with more than one field.
For tensor representations, the j_i labeling has the advantage of making very manifest the symmetries in the index structure of the fields, as these can now be represented as

$$\mathcal{O}^{\left(\mu_1^{(1)}\ldots\mu_{j_1}^{(1)}\right)\left(\mu_1^{(2)}\ldots\mu_{j_2}^{(2)}\right)\ldots\left(\mu_1^{(L)}\ldots\mu_{j_L}^{(L)}\right)}(x) \tag{2.35}$$

with each $\mu^{(i)}$ group of indices being symmetrized, while exchanges of $\mu_k^{(i)} \leftrightarrow \mu_p^{(j)}$ with $(i) \neq (j)$ produce minus signs.

Note how the representation as (2.35) are not irreducible if d is even and $j_n \neq 0$, namely where the set of nodes with nonzero Dynkin labels has the same topology as Figure 2.2b. In this peculiar case, in fact, fields can be decomposed into self-dual part $\star\mathcal{O} = \mathcal{O}$ and anti-self dual part $\star\mathcal{O} = -\mathcal{O}$; we will review this case in more detail in section 2.3.2.

Having introduced the types of operators that our theories of interest are made of, we can now introduce tools which very powerful tools that greatly simplify computations of correlators in Conformal Field Theory: the *operator product expansion* and the *embedding space formalism*.

2.2 The Operator Product Expansion

In the previous section, we discussed how CFTs are supplied with a correspondence between local operators and states. A natural question to ask in this context is what happens if we act with a second operator $\mathcal{O}_i(x_1)$ on a state produced by the action of an operator on the vacuum, such as in $\mathcal{O}_j(x_2)\,|0\rangle$. This operation in general will not produce an eigenstate of the dilatation generator, but the result can be expanded on a basis of eigenstates, which we know are either primary or descendant:

$$\mathcal{O}_i(x_1)\mathcal{O}_j(x_2)\,|0\rangle = \sum_{\Psi \text{ primary}} c_\Psi\,|\Psi(\Delta_k, \varrho, P^n)\rangle \tag{2.36}$$

where Ψ is a state which for $n = 0$ is a primary and for $n > 0$ is a descendant, while c_Ψ is the coefficient that multiplies the state $|\Psi\rangle$. If we are radially quantizing around some point y, we know from the state-operator map that the state $|\Psi\rangle$ can be seen as being produced by the insertion of a single primary operator $\mathcal{O}_k(y)$, possibly acted upon with some translation generators in case the state is a descendant. In more explicit terms, this means that we can rewrite the product of two fields acting on the vacuum as

$$\mathcal{O}_i(x_1)\mathcal{O}_j(x_2)\,|0\rangle = \sum_{k \text{ primary}} \lambda_{ijk}\hat{f}_{ijk}(x_1, x_2, y, \partial_y)\mathcal{O}_k(y)\,|0\rangle\ , \tag{2.37}$$

which is valid in any S^{d-1} sphere centered in y that contains only the two fields $\mathcal{O}_i(x_1)$ and $\mathcal{O}_j(x_2)$. It is important to note that not all primaries can appear in this expansion, but rather only those that belong to the tensor product representation of $\mathcal{O}_i(x_1)$ and $\mathcal{O}_j(x_2)$. Stripping away the states from (2.37), this can be rewritten only in terms of fields as

$$\mathcal{O}_i(x_1)\mathcal{O}_j(x_2) = \sum_{k \text{ primary}} \lambda_{ijk}\hat{f}_{ijk}(x_1, x_2, y, \partial_y)\mathcal{O}_k(y) \tag{2.38}$$

which is known as the Operator Product Expansion, or OPE in short.

Expression (2.38) is understood to be valid inside of a correlator, and as long as there are no additional fields inserted within the sphere of radius $r^* = \max(|x_1 - y|, |x_2 - y|)$ centered at y, see Figure 2.3.

It can be checked that the form of the differential operators $\hat{f}_{ijk}(x_1, x_2, y, \partial_y)$ is completely fixed by conformal invariance. This means that the theory-dependent content in the OPE is therefore only the set of λ_{ijk}, known as the *OPE coefficients*.

Using iteratively the OPE it is possible to decompose any N-point function to a linear combination of two-point functions, whose form can be determined exactly. The coefficients that appear in this linear combination are simply products of the OPE coefficients; this implies that with full knowledge of the spectrum $\{\Delta, \varrho\}$ of a theory and all of its OPE coefficients, it is possible to fully determine any correlator and therefore any observable of the theory. For this reason the set of OPE coefficients and spectrum quantum numbers is known as the *CFT data*, which constitutes the only dynamical content of a CFT.

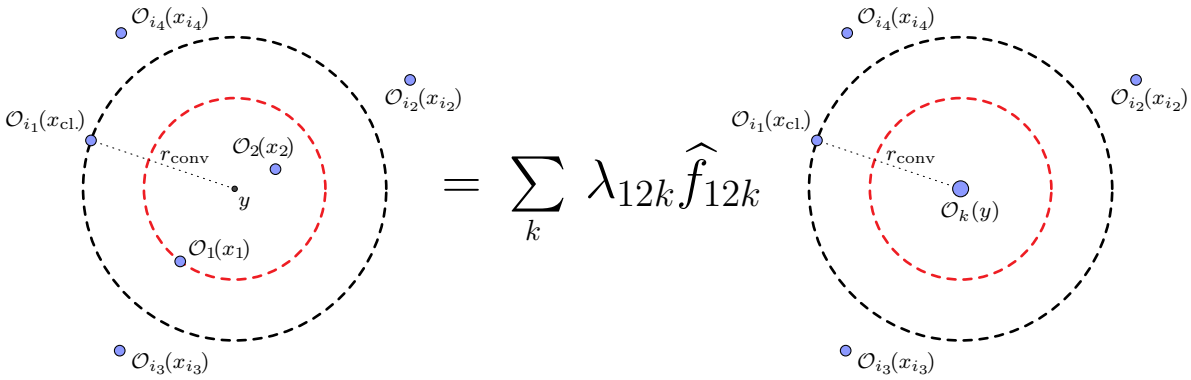

Figure 2.3: Schematic representation of an Operator Product Expansion between fields $\mathcal{O}_1(x_1)$ and $\mathcal{O}_2(x_2)$, centered at y. This operation is possible as long as there are no additional operators within a circle that encompasses both fields (the red circle in this figure is the smallest one). The radius of convergence corresponds to the distance between y and the closest operator to it which is not involved in the OPE (located at $x_{\text{cl.}}$ in this figure).

2.3 The Embedding Space Formalism

We saw with (2.15) that the conformal generators can be naturally lifted to Lorentz generators of a $(d+1,1)$-dimensional space. This is also known as the *embedding space*. In this section we would like to make this mapping concrete also for coordinates, constructing an invertible map that relates vectors in d dimensional Euclidean space to vectors in $d+2$ dimensional Lorentzian space subject to two constraints, such that the number of degrees of freedom match.
To do so, one can consider vectors X^A which are null and projective, such that the two constraints are compatible with Lorentz transformations. These, given an index $A = \{+, -, \mu\}$ and a metric

$$\mathrm{d}s^2 = \mathrm{d}X^A \mathrm{d}X_A = -\mathrm{d}X^+ \mathrm{d}X^- + \delta_{\mu\nu} \mathrm{d}X^\mu \mathrm{d}X^\nu \,, \tag{2.39}$$

are related to the vectors x^μ via

$$X^A = \lambda \left(1, x^2, x^\mu\right) \sim \left(1, x^2, x^\mu\right) \,, \tag{2.40}$$

where $\sim$ stands for projective equivalence of these vectors.
In (2.40) we have picked as a reference a particular section of the null cone, which corresponds to the RHS after the $\sim$ sign. This reference section, known as *Poincaré section* or *Poincaré patch*, is rather important, as every time we manipulate expressions with embedding space vectors X^A we always have to project back to a Poincaré section of the form (2.40) with $X^+ = 1$ to obtain meaningful results. This fact is also the key to recover conformal transformations from Lorentz transformations in embedding space: after transforming $X \to MX$ we have to rescale X by a factor $\lambda(X)$ such that $X^+ = 1$. This transforms the metric as

$$\begin{aligned} \mathrm{d}s'^2 = \mathrm{d}\left(\lambda(X) X^A\right) \mathrm{d}\left(\lambda(X) X_A\right) \\ = \left(\lambda(X)\mathrm{d}X^A + X^A \nabla\lambda \cdot \mathrm{d}X\right)\left(\lambda(X)\mathrm{d}X_A + X_A \nabla\lambda \cdot \mathrm{d}X\right) \\ = \lambda(X)^2 \mathrm{d}X^A \mathrm{d}X_A \end{aligned} \tag{2.41}$$

where we used the fact that X^A lives on the light-cone and thus $X^2 = X \cdot \mathrm{d}X = 0$. Upon restriction to $X^+ = 1$, which in turn implies $\mathrm{d}X^+ = 0$, we obtain

$$\mathrm{d}s'^2 = \lambda(X)^2 \mathrm{d}X^A \mathrm{d}X_A \xrightarrow{X^+=1} \lambda(x)^2 g_{\mu\nu} \mathrm{d}x^\mu \mathrm{d}x^\nu \tag{2.42}$$

which can be clearly interpreted as a conformal transformation of d-dimensional space with scale factor $\Lambda(x) \equiv \lambda(x)$.

2.3.1 Scalar fields in embedding space

We now would like to understand how fields look like when lifted to the embedding space, starting with the simplest case of scalar operators. A natural condition to require is that when the embedding space field $\phi(X)$ is restricted to the Poincaré patch (2.40) it has to coincide with the field in physical space

$$\phi(X)\big|_{X^+=1} \equiv \phi(x)\,. \tag{2.43}$$

Furthermore, the field is required to have homogeneous dependence on X

$$\phi(\lambda X) = \lambda^{-\Delta}\phi(X) \tag{2.44}$$

and the action of $\mathfrak{so}(d+1,1)$ transformations on it has to be implemented by usual Lorentz transformations

$$[M_{AB}, \phi(X)] = \mathcal{T}_{AB}\phi(X)\,, \qquad \mathcal{T}_{AB} = X_A\frac{\partial}{\partial X^B} - X_B\frac{\partial}{\partial X^A}\,. \tag{2.45}$$

The properties we just described imply that when taking a Lorentz transformation in embedding space, we have

$$\phi(x) \equiv \phi(X)\Big|_{X^+=1} \xrightarrow{M_{\mu\nu}} \phi(X') = (X'^+)^{-\Delta}\phi\left(X'\big|_{X'^+=1}\right) \equiv \left(X'^+\right)^{-\Delta}\phi(x) \tag{2.46}$$

where we recovered precisely the way primary operators transform, (2.32), with $\Lambda(X) \equiv X'^+$. The main advantage of working with the embedding space fields, is that the conformal generators become linear operators, and we can easily construct and manipulate the Lorentz invariant expressions, which will allow us to construct with ease the conformal correlators. In fact, due to (2.44) we have that correlators are homogeneous functions of all the X_i variables, with $i = 1, \dots, N$ being an index that runs through all external fields

$$\langle\phi_1(\lambda_1 X_1)\dots\phi_N(\lambda_N X_N)\rangle = \lambda_1^{-\Delta_1}\cdots\lambda_N^{-\Delta_N}\langle\phi_1(X_1)\dots\phi_N(X_N)\rangle\,. \tag{2.47}$$

This homogeneity degree can only be composed by the invariant building blocks we have at our disposal, which in this case are simply the scalar products

$$X_{ij} \equiv X_i\cdot X_j = -\frac{(x_i-x_j)^2}{2}\,, \tag{2.48}$$

where we also specified their relation with the physical space coordinates x_i. The simplicity of the condition (2.47) together with the limited number of invariant building blocks simplifies dramatically the construction of conformal correlators.

2.3.2 Tensor fields in embedding space

We saw in section 2.1 that spinning fields – those that have a non-trivial $\mathfrak{so}_d$ representation – are associated with L indices $j_1, \dots, j_L$ and, in case the j_i are all integers, these correspond to tensor representations MST_L. In this section we want to construct their lift to embedding space tensors and express them in a bosonic index-free formalism.

For these tensor representations, the index structure can usually be repackaged in a Young diagram as in Figure 2.4, where every box correspond to an index, every row to indices that are symmetrized, and every column to indices that are antisymmetrized. This Young diagram representation is not irreducible in the case d is even and the depth is maximal $L = d/2$, as fields can be further decomposed into a self-dual part $\star\mathcal{O} = \mathcal{O}$ and an anti-self-dual part $\star\mathcal{O} = -\mathcal{O}$. We will see the embedding space origin of this decomposition later in this section, and we will explicitly work with it in section 5.2.2, with particular focus on the $d = 4$ case.

When translating Young diagrams to explicit tensorial expressions with indices, one needs to focus either on the symmetries or on the antisymmetries of the indices. In this thesis we will conventionally choose the former, and express tensors as we did in (2.35):

$$\mathcal{O}^{\left(\mu_1^{(1)}\dots\mu_{j_1}^{(1)}\right)\left(\mu_1^{(2)}\dots\mu_{j_2}^{(2)}\right)\dots\left(\mu_1^{(L)}\dots\mu_{j_L}^{(L)}\right)}(x)\,. \tag{2.35}$$

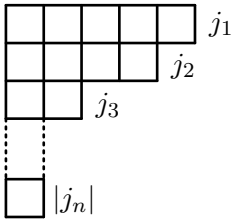

Figure 2.4: Young diagram representation of a tensor field. Rows represent indices that are symmetrized, and columns represent indices that are antisymmetrized.

The promotion to embedding space tensors follows a similar procedure as the previous subsection, where we lift the coordinate dependence to light-like vectors in embedding space

$$\mathcal{O}_{\Delta,\varrho}(x) \;\to\; \mathcal{O}_{\Delta,\varrho}(X)\,, \qquad\qquad \left\{X \in \mathbb{R}^{1,d+1} |\, X^2 = 0\right\}, \tag{2.49}$$

such that the tensor becomes a homogeneous function of X with degree $-\Delta$

$$\mathcal{O}_{\Delta,\varrho}(\lambda X) = \lambda^{-\Delta}\mathcal{O}_{\Delta,\varrho}(X)\,. \tag{2.50}$$

The index structure, trivial in the previous case of scalars, is now subject to a promotion from physical space indices μ_i to embedding space indices A_i, transforming (2.35) to

$$\mathcal{O}^{\left(A_1^{(1)}\ldots A_{j_1}^{(1)}\right)\left(A_1^{(2)}\ldots A_{j_2}^{(2)}\right)\ldots\left(A_1^{(L)}\ldots A_{j_L}^{(L)}\right)}(X) \tag{2.51}$$

with the added constraints of the tensor being transverse with respect to any index

$$X_{A_i^{(k)}}\mathcal{O}^{\left(A_1^{(1)}\ldots A_{j_1}^{(1)}\right)\ldots A_i^{(k)}\ldots\left(A_1^{(L)}\ldots A_{j_L}^{(L)}\right)}(X) = 0\,, \tag{2.52}$$

and traceless with respect to any pair of indices

$$\eta_{A_{i_1}^{(k_1)}A_{i_2}^{(k_2)}}\,\mathcal{O}^{A_1^{(1)}\ldots A_{i_1}^{(k_1)}\ldots A_{i_2}^{(k_2)}\ldots A_{j_L}^{(L)}}(X) = 0\,. \tag{2.53}$$

To avoid cluttering all expressions with many indices, it is often convenient to make use of an *index-free formalism*, which allows to repackage all the index information into a polynomial dependence on some auxiliary vectors. For STTs this has been known for a long time [46, 47], and has been restated in embedding space in [48]. For MST_L with $L \geq 2$, this can be obtained in two different ways, one which focuses on the antisymmetry properties of the columns of Young tableaux as in [49], and one which focuses on the symmetries of the rows as in [50]. In this thesis we will follow the latter convention and introduce one type of "polarization vector" $Z_p \in \mathbb{C}^{d+2}$ for every row and thus in a number equal to the depth L of the MST. A number j_p of copies of Z_p vectors are then contracted with the indices of the p-th row to construct an index-free function in the following way:

$$\mathcal{O}_{\Delta,\varrho}\left(X, Z_1, \ldots, Z_L\right) \equiv \mathcal{O}_{\Delta,\varrho}^{\left(A_1^{(1)}\ldots A_{j_1}^{(1)}\right)\ldots\left(A_1^{(L)}\ldots A_{j_L}^{(L)}\right)}(X)\,\left(Z_1^{A_1^{(1)}}\cdots Z_1^{A_{j_1}^{(1)}}\right)\cdots\left(Z_L^{A_1^{(L)}}\cdots Z_L^{A_{j_L}^{(L)}}\right). \tag{2.54}$$

The properties of tracelessness and transversality of the tensor $\mathcal{O}_{\Delta,\varrho}$ are translated into the conditions

$$X^2 = X\cdot Z_p = Z_p\cdot Z_q = 0 \tag{2.55}$$

for the coordinates, and due to (2.54) the tensor will have a polynomial dependence on the Z_p with homogeneous degree j_p, generalizing (2.50) to

$$\mathcal{O}_{\Delta,\varrho}(\lambda_0 X, \{\lambda_p Z_p\}) = \lambda_0^{-\Delta}\lambda_1^{j_1}\cdots\lambda_L^{j_L}\mathcal{O}_{\Delta,\varrho}(X, \{Z_p\})\,. \tag{2.56}$$

Furthermore, the dependence on the auxiliary vectors respects the following set of gauge invariance conditions

$$\mathcal{O}_{\Delta,\varrho}\left(X, \left\{Z_p + \beta_{p,0}X + \sum_{q<p}\beta_{p,q}Z_q\right\}\right) = \mathcal{O}_{\Delta,\varrho}(X, \{Z_p\})\,, \qquad \forall\beta_{p,q}\in\mathbb{C}\,. \tag{2.57}$$

In this formulation, the generators act on fields as Lorentz transformations both on the X and Z_p, extending (2.45) to

$$\mathcal{T}_{AB} = X_A \frac{\partial}{\partial X^B} + \sum_p Z_{p\,A} \frac{\partial}{\partial Z_p^B} - (A \leftrightarrow B)\,. \tag{2.58}$$

Before we conclude this brief presentation of embedding space for tensor fields, we want to add some comments. First, note that functions in the variables X, Z_p can be assigned a multi-degree that has $L+1$ components, one for the variable X and then one for each of the L polarizations Z_p. The assignment is such that a field $\mathcal{O}$ with weight Δ and spins j_p has degree $[-\Delta, j_1, \ldots, j_L]$. This degree is measured by the independent rescalings of the variables that we have introduced, and any equation must be such that this multi-degree is equal on both sides.

At this point, we have rephrased the concept of a tensor field of weight Δ and spin j_p in terms of functions $\mathcal{O}_{\Delta,\varrho}$ of the variables (X, Z_p) subject to the conditions (2.55). These functions must satisfy the homogeneity conditions (2.56), as well as the gauge invariance conditions (2.57). These two conditions ensure that the differential operators (2.58) give rise to an irreducible representation of the conformal algebra. Let us note that the homogeneity conditions (2.56) can also be continued to non-integer values of j_p in case one deals with representations with continuous spin.

It is important to notice how the gauge invariance conditions (2.57) constrain the way in which the variables Z_p can appear in expressions that involve the field $\mathcal{O}_{\Delta,\varrho}$. In fact, the only gauge invariant tensors that can be formed from $(X, \{Z_p\})$ are linear combinations or contractions of the wedge products

$$C^{(0)}_A = X_A\,, \qquad C^{(p)}_{A_1\ldots A_{p+1}} = \left(X \wedge \bigwedge_{q=1}^{p} Z_q\right)_{A_1\ldots A_{p+1}}\,. \tag{2.59}$$

Let us point out that the projective light ray contains d degrees of freedom. After imposing transversality $X \cdot Z_1 = 0$ and the gauge invariance (2.57), there remain $d-2$ degrees of freedom in the polarization Z_1. Similarly, Z_2 contains $d-4$ degrees of freedom, etc. This implies that the variable Z_L for tensor fields of maximal depth $L = \text{rank}_d - 1 = d/2$ in even dimensions has no continuous physical degrees of freedom. In the reduction from embedding space variables to gauge-invariant tensors, all $C^{(0)}, \ldots, C^{(L-1)}$ are fixed by $X, \ldots, Z_{L-1}$, while $C^{(L)} = C^{(L-1)} \wedge Z_L$. Up to gauge equivalence, this implies that $\text{Span}(Z_L)$ is fixed to be one of two unique null directions in the complex plane orthogonal to $\text{Span}(X, \ldots, Z_{L-1})$. To distinguish these two null directions, we can use the fact that $C^{(L)}$ is a $(L+1)$-form in $\mathbb{C}^{2(L+1)}$ given by the wedge product of $L+1$ mutually orthogonal null vectors, and must therefore be either self-dual or anti-self-dual with respect to the Hodge star,

$$\star\, C^{(L)}_{A_1\ldots A_{L+1}} = \frac{1}{(L+1)!}\epsilon_{A_1\ldots A_{2L+2}} C^{(L)A_{L+2}\ldots A_{2L+2}} = \pm\, C^{(L)}_{A_1\ldots A_{L+1}}\,. \tag{2.60}$$

The above condition separates the space of gauge equivalence classes of $(X, Z_1, \ldots, Z_L)$ into two distinct $\text{SO}(d+1,1)$ orbits: the *self-dual* orbit $\star C^{(L)} = C^{(L)}$ with L-th polarization vector Z_L and the *anti-self-dual* orbit $\star \overline{C}^{(L)} = -\overline{C}^{(L)}$ with L-th polarization vector $\overline{Z}_L$. When contracting a tensor with polarization vectors as in (2.54), we get that using vectors in the (anti-)self-dual orbit projects said tensor to its (anti-)self-dual part, such that the two projections $\mathcal{O}_{\Delta,\varrho}(X, Z_1, \ldots, Z_L)$ and $\mathcal{O}_{\Delta,\bar{\varrho}}(X, Z_1, \ldots, \overline{Z}_L)$ define an irreducible representation of $\mathfrak{so}(d+1,1)$. Tensors in the anti-self-dual representation $\mathcal{O}_{\Delta,\bar{\varrho}}$ will be conventionally chosen to be those with negative spin j_L.

Poincaré patches for polarization vectors

Let us conclude this subsection on embedding space tensors by having a more in-depth discussion on the Poincaré patches for the polarization vectors Z_p. Due to the orthogonality constraints (2.55), the homogeneity conditions (2.56) and the gauge invariances (2.57), we know that the embedding space tensors $\mathcal{O}_{\Delta,\varrho}(X, Z_1, \ldots, Z_L)$ are defined in a manifold which is more constrained than $(L+1)$ copies of

the embedding space for X. If we then wish to consider only polarizations Z_p that belong to the space where tensors are defined, we will be supplied with additional equivalences between these vectors, that translate into a more restrictive form of their Poincaré patches.
To make this less abstract and as a warm up for the general case, let us first consider the case of Z_1; the more restricted Poincaré patches for Z_p, $p > 1$ will be constructed iteratively starting from this. As before, the null and projectiveness constraints imply that we can write Z_1 in the form

$$Z_1 = \left(1, z_1^2, z_1^\mu\right) . \tag{2.61}$$

Using the gauge invariance

$$Z_1 \sim Z_1 + \alpha X$$

we can subtract X from (2.61) to get

$$Z_1 \sim \left(0, z_1^2 - x^2, z_1^\mu - x^\mu\right) . \tag{2.62}$$

Due to $Z_1 \cdot X = 0$ we know that $(z_1 - x)^2 = 0$, which allows to recast the last expression as

$$Z_1 \sim (0, 2x \cdot (z_1 - x), z_1^\mu - x^\mu) , \tag{2.63}$$

and shifting the definition of z_1^μ by x^μ, one can write the Poincaré patch as

$$Z_1 = (0, 2x \cdot z_1, z_1^\mu) . \tag{2.64}$$

The projectiveness of Z_1 is inherited by z_1, which means that if we express the d-dimensional metric in terms of complex coordinates

$$\mathrm{d}s_d^2 = \mathrm{d}x_+ \mathrm{d}x_- + \mathrm{d}s_{d-2}^2 \tag{2.65}$$

we can express z_1 in a way very similar to (2.40), but in two less dimensions in terms of a $(d-2)$-dimensional vector $z_{1,d-2}^{\mu'}$:

$$z_1^\mu = \left(1, -z_{1,d-2}^2, z_{1,d-2}^{\mu'}\right) .$$

Starting from Z_2, all the successive Z_p with $p \geq 2$ satisfy the same relations as Z_1, plus extra orthogonality and gauge invariances of the same type as above. This implies that the construction of the Poincaré patches can be iterated; if we define

$$Z_0 \equiv X , \qquad z_{p,d+2} \equiv Z_p , \qquad z_{p,d} \equiv z_p , \tag{2.66}$$

and we parametrize the $(d-2n)$-dimensional metric via complex coordinates by nesting the decomposition (2.65), we get the iterative definitions

$$z_{p,d-2n} = \begin{cases} (0, 2z_{n,d-2n} \cdot z_{p,d-2n}, z_{p,d-2n}) & n \in \{-1, 0, 1, \ldots, p-2\} , \\ \left(1, \zeta_{p,d+2-2p}^2, \zeta_{p,d+2-2p}\right) & n = p-1 , \end{cases} \tag{2.67}$$

where $p \in \left\{0, 1, \ldots, \left\lfloor \frac{d}{2} - 1 \right\rfloor\right\}$ and $\zeta_{p,m}$ is an unconstrained m-dimensional vector.
For $p = \left\lfloor \frac{d}{2} \right\rfloor$, the way the iteration stops depends on whether the dimension is even or odd. For odd dimensions we simply have

$$\zeta_{\left\lfloor \frac{d}{2} \right\rfloor, 3} = \left(1, -\zeta_1^2, \zeta_1\right) , \qquad \zeta_1 \in \mathbb{C} \tag{2.68}$$

while for even dimensions we end up with two possible two-dimensional projective null vectors:

$$\zeta_{\left\lfloor \frac{d}{2} \right\rfloor, 2} = (0, 1) \tag{2.69}$$

$$\overline{\zeta}_{\left\lfloor \frac{d}{2} \right\rfloor, 2} = (1, 0) . \tag{2.70}$$

These two inequivalent solutions to the null and gauge invariance constraints correspond precisely to the self-dual and anti-self-dual representations we discussed below (2.60), with (2.69) corresponding to the last two components of $Z_{\left\lfloor \frac{d}{2} \right\rfloor}$ and (2.70) to those of $\overline{Z}_{\left\lfloor \frac{d}{2} \right\rfloor}$.

2.4 Correlation functions in CFT

We will now address the construction of generic correlation functions in CFT using the tools that we introduced so far. Of great relevance are going to be the basic building blocks (2.59) as well as the homogeneity constraints (2.56). These tools can be used to fully encode the constraints coming from conformal symmetry and allow a simple determination of the structure of generic correlators.

2.4.1 One-point functions

One-point functions in CFT are extremely simple. Using the state-operator map we can write one-point functions as the overlap between two states

$$\langle 0|\mathcal{O}(X)|0\rangle = \langle 0|\Psi\rangle \ , \qquad \text{where} \qquad |\Psi\rangle \equiv \mathcal{O}(X)\,|0\rangle \ . \tag{2.71}$$

Since the state $|\Psi\rangle$ has the same degrees of homogeneity as the field $\mathcal{O}(X)$, but the vacuum $\langle 0|$ has all zero homogeneity degrees, the only way to have a nonzero overlap between the two states is if $|\Psi\rangle = |0\rangle$, which implies that the field we inserted is actually the identity $\mathbb{1}$. Since we consider states to be normalized to 1, we can summarize this as

$$\langle \mathcal{O}(X)\rangle = \begin{cases} 1 & \text{if} \quad \mathcal{O} \equiv \mathbb{1}\,, \\ 0 & \text{otherwise}\,. \end{cases} \tag{2.72}$$

2.4.2 Two-point functions

The construction of two-point functions in embedding space is rather trivial, as these are completely fixed by conformal invariance. In the scalar case the homogeneity constraint (2.47) is

$$\langle \phi_1(\lambda_1 X_1)\phi_2(\lambda_2 X_2)\rangle = \lambda_1^{-\Delta_1}\lambda_2^{-\Delta_2}\,\langle \phi_1(X_1)\phi_2(X_2)\rangle \tag{2.73}$$

and there is only one Lorentz invariant building block that can be used: X_{12}. The fact that X_1 and X_2 only appear paired together implies that, for them to be present, their homogeneity degree needs to be the same, i.e. $\Delta_1 = \Delta_2$. If instead the two fields have different conformal dimension, the only way to satisfy (2.73) is to have a vanishing two-point function. This is summarized in the expression

$$\langle \phi_1(X_1)\phi_2(X_2)\rangle = \begin{cases} \mathcal{N}_{12} X_{12}^{-\Delta} & \text{if} \quad \Delta_1 = \Delta_2 \equiv \Delta\,, \\ 0 & \text{if} \quad \Delta_1 \neq \Delta_2\,, \end{cases} \tag{2.74}$$

where we introduced the normalization factor $\mathcal{N}_{12}$, which in the rest of this thesis we will consider to be $\mathcal{N}_{12} = 1$. If we want to project the correlator (2.74) back to physical space, we can use (2.48), which gives us

$$\langle \phi_1(x_1)\phi_2(x_2)\rangle = \begin{cases} \mathcal{N}_{12}\left(\frac{x_1 - x_2}{2}\right)^{-2\Delta} & \text{if} \quad \Delta_1 = \Delta_2 \equiv \Delta\,, \\ 0 & \text{if} \quad \Delta_1 \neq \Delta_2\,. \end{cases} \tag{2.75}$$

Spinning case

For the more generic case of spinning fields $\mathcal{O}_{\Delta_1,\ell_1}$ and $\mathcal{O}_{\Delta_2,\ell_2}$, we know that we can construct the $C^{(p)} = C^{(p)}_{A_1\ldots A_{p+1}}$ building blocks introduced in (2.59) up to $p = L_i$ for both fields, and correlation functions need to be constructed out of Lorentz invariants obtained by contractions of these building blocks. It is easy to see that with only two points at disposal, the only non-zero invariants that can be constructed are contractions of C objects with the same amount of indices:

$$H^{(p)}_{ij} \equiv \frac{1}{(p+1)!} C^{(p)}_i \cdot C^{(p)}_j \ , \tag{2.76}$$

where we added a subscript $i = 1, 2$ to indicate which of the two fields' variables we are considering for the C objects. Note that, by our previous definition of $C^{(0)}_A = X_A$, we have $H^{(0)}_{ij} = X_{ij}$. Other combinations

of C tensors are bound to vanish, since if, assuming $p > q$, we take

$$\left(C_i^{(p)}\right)_{A_1\dots A_{p+1}}\left(C_j^{(q)}\right)^{A_1\dots A_{q+1}} = \left(C_i^{(p)}\cdot C_j^{(q)}\right)_{A_{q+2}\dots A_{p+1}}\,, \tag{2.77}$$

we have that contracting this with something that includes X_i (as all the $C_i^{(p)}$ do) will vanish due to (2.55), while contracting with something that includes X_j will vanish due to the presence of two X_j contracted with an antisymmetric tensor $C_i^{(p)}$.

In (2.76) we skipped over one special case, namely that for which we have maximal depth representations in even dimensions $p = \lfloor \frac{d}{2} \rfloor$. In this case, we can construct four different objects by taking contractions of C tensors in either self-dual or anti-self-dual representations

$$H_{ij}^{(d/2)} = \frac{1}{\left(\frac{d}{2}+1\right)!}C_i^{(d/2)}\cdot C_j^{(d/2)}\,, \qquad H_{\bar{\imath}\bar{\jmath}}^{(d/2)} = \frac{1}{\left(\frac{d}{2}+1\right)!}\overline{C}_i^{(d/2)}\cdot \overline{C}_j^{(d/2)}\,, \tag{2.78}$$

$$H_{\bar{\imath}j}^{(d/2)} = \frac{1}{\left(\frac{d}{2}+1\right)!}\overline{C}_i^{(d/2)}\cdot C_j^{(d/2)}\,, \qquad H_{i\bar{\jmath}}^{(d/2)} = \frac{1}{\left(\frac{d}{2}+1\right)!}C_i^{(d/2)}\cdot \overline{C}_j^{(d/2)}\,, \tag{2.79}$$

two of which are actually vanishing in a way that depends on whether d is a multiple of four or not:

$$\begin{aligned} H_{ij}^{(d/2)} &= H_{\bar{\imath}\bar{\jmath}}^{(d/2)} = 0\,, \qquad && (d = 4n)\,, \\ H_{\bar{\imath}j}^{(d/2)} &= H_{i\bar{\jmath}}^{(d/2)} = 0\,, \qquad && (d = 4n+2)\,. \end{aligned} \tag{2.80}$$

Since fields in (anti-)self-dual representation will only be contracted with the $(\overline{Z}_{d/2})$ $Z_{d/2}$ vectors and not their dual, we have that there is only one tensor structure H which can be used to make up the homogeneity in $(\overline{Z}_{d/2})$ $Z_{d/2}$. The same applies for the odd dimensional case, with only one H tensor structure that can make up the homogeneity in the lowest spin $j_{\lfloor d/2 \rfloor}$. Once the dependence on the maximal depth $H^{(L)}$ structure is fixed, there will be only one H structure that can be used to adjust the homogeneity in the j_{L-1} spin, and the same applies iteratively until one fixes the Δ_i, Δ_j homogeneity using $H_{ij}^{(0)}$. This means that in order to satisfy the homogeneity constraints (2.56) for both fields in the correlator, these need to have the same quantum numbers if $d \neq 0 \mod 4$, or need to have same quantum numbers up to the last spin, which has to be opposite, if $d = 4n$. A general two-point function in CFT can then be written as

$$\langle \mathcal{O}_{\Delta_1,\varrho_1}\mathcal{O}_{\Delta_2,\varrho_2}\rangle = \begin{cases} \prod_{p=0}^{\lfloor d/2 \rfloor}\left(H_{s_1 s_2}^{(p)}\right)^{|j_p|-|j_{p+1}|} & \text{if } \begin{cases} d\neq 4n\,, & \Delta_1=\Delta_2 \text{ and } \varrho_1=\varrho_2\,, \\ & \text{or} \\ d = 4n\,, & \Delta_1=\Delta_2 \text{ and } \varrho_1=\varrho_2^*\,, \end{cases} \\ 0 & \text{otherwise}\,, \end{cases} \tag{2.81}$$

where $j_p = 0$ for $p > \lfloor d/2 \rfloor$, the conjugate of a representation ϱ corresponds to

$$\varrho^* = (\Delta, j_1, \dots, j_{\lfloor d/2 \rfloor -1}, j_{\lfloor d/2 \rfloor})^* = (\Delta, j_1, \dots, j_{\lfloor d/2 \rfloor -1}, -j_{\lfloor d/2 \rfloor})\,,$$

the symbol s_i is defined as

$$s_i = \begin{cases} i & \text{if } \; j_{i,\lfloor d/2 \rfloor} \geq 0\,, \\ \bar{\imath} & \text{if } \; j_{i,\lfloor d/2 \rfloor} < 0\,, \end{cases} \tag{2.82}$$

and we redefine $H_{s_1 s_2}^{(p)}$ to be simply $H_{12}^{(p)}$ for $p < d/2$.

2.4.3 Three-point functions

Scalar three-point functions are also completely fixed by conformal symmetry up to a constant. This time the only conformal invariants that can be constructed in embedding space are

$$X_{12}\,, \qquad X_{23}\,, \qquad X_{13}\,. \tag{2.83}$$

This implies that scalar three-point functions have to be of the form

$$\langle \phi_1(X_1)\phi_2(X_2)\phi_3(X_3)\rangle = X_{12}^{\alpha_{12}} X_{23}^{\alpha_{23}} X_{13}^{\alpha_{13}} \,. \tag{2.84}$$

The homogeneity condition in this case is

$$\langle \phi_1(\lambda_1 X_1)\phi_2(\lambda_2 X_2)\phi_3(\lambda_3 X_3)\rangle = \lambda_1^{-\Delta_1}\lambda_2^{-\Delta_2}\lambda_3^{-\Delta_3}\,\langle \phi_1(X_1)\phi_2(X_2)\phi_3(X_3)\rangle \tag{2.85}$$

which leads to the system of equations

$$\alpha_{12}+\alpha_{13} = -\Delta_1\,, \qquad \alpha_{12}+\alpha_{23} = -\Delta_2\,, \qquad \alpha_{23}+\alpha_{13} = -\Delta_3\,, \tag{2.86}$$

that is solved by

$$\langle \phi_1(X_1)\phi_2(X_2)\phi_3(X_3)\rangle = \frac{\lambda_{123}}{X_{12}^{\frac{\Delta_1+\Delta_2-\Delta_3}{2}} X_{23}^{\frac{\Delta_2+\Delta_3-\Delta_1}{2}} X_{13}^{\frac{\Delta_1+\Delta_3-\Delta_2}{2}}}\,. \tag{2.87}$$

Note that we used here the same notation as the OPE coefficients that appeared in (2.38). This is not an accident, as requiring compatibility of the OPE with this form of the three-point function requires that these three-point coefficients and the OPE coefficients are actually the same objects.
As before, the conversion of the correlator (2.87) to physical space becomes trivial using (2.48), which gives

$$\langle \phi_1(x_1)\phi_2(x_2)\phi_3(x_3)\rangle = \frac{\lambda_{123}}{(x_1-x_2)^{\Delta_1+\Delta_2-\Delta_3}\,(x_2-x_3)^{\Delta_2+\Delta_3-\Delta_1}\,(x_1-x_3)^{\Delta_1+\Delta_3-\Delta_2}}\,. \tag{2.88}$$

Two scalars and one spinning operator

Three point functions start to be less and less trivial when introducing spinning fields. The simplest case of an insertion of just one spinning operator, however, is still fixed up to a constant, as we will now show. We know from (2.59) that the three-point function can only be made by Lorentz invariants constructed from the $C^{(L+1)}_{A_1\dots A_{L+1}}$ tensors. We have $L+1$ of these associated with the field $\mathcal{O}_{\Delta_1,\rho_1}(X_1, Z_{1,1},\dots Z_{1,L})$, while for the two scalar fields these correspond simply to the coordinates

$$\left(C_2^{(0)}\right)^A = X_2^A\,, \qquad \left(C_3^{(0)}\right)^A = X_3^A\,.$$

It is immediate to see that it is not possible to have a nonzero three-point function if we have $L>1$, as we do not have enough objects to contract with the $C^{(L)}_{A_1\dots A_{L+1}}$ tensors with more than two indices.
We here recovered the well-known fact that three-point function of two scalars and a spinning field are nonzero only if the field with spin is an STT. This statement is normally proved using the OPE and the fact that the tensor product representation of two scalars can only sit in an STT or a scalar representation itself.
If we then restrict to the only non-trivial case, that of an STT and two scalars, we can now construct an additional invariant compared to ones of the three-scalar case (2.83):

$$V_{1,32} = \frac{X_3\cdot(X_1\wedge Z_1)\cdot X_2}{X_{23}}\,. \tag{2.89}$$

The invariant $V_{1,32}$ is the only one that can carry the Z_1 homogeneity weight, and its presence in the three-point function is thus fully constrained by (2.56). Once the homogeneity constraint for Z_1 is taken care of, the three-point function can then be fully fixed in the same way as the scalar case, leading to the result

$$\langle \mathcal{O}_{\Delta_1,j_1}(X_1,Z_1)\phi_2(X_2)\phi_3(X_3)\rangle = \lambda_{123}\frac{V_{1,32}^{j_1}}{X_{12}^{\frac{\Delta_1-j_1+\Delta_2-\Delta_3}{2}} X_{23}^{\frac{\Delta_2+\Delta_3-\Delta_1+j_1}{2}} X_{13}^{\frac{\Delta_1-j_1+\Delta_3-\Delta_2}{2}}}\,. \tag{2.90}$$

General case: the space of three-point tensor structures

As soon as we add one second spinning operator, three-point functions are no longer fully constrained by conformal symmetry, and the expression depends very much on the specific case one is interested in.
For example, if we have two STTs and one scalar, it is easy to see that $\mathfrak{so}(d+1,1)$ invariance combined with the homogeneity constraints (2.56) is not enough to fix the correlator. We can in fact construct the zero-homogeneity variable

$$\mathcal{X} = \frac{H_{12}^{(1)}}{V_{1,32}V_{2,13}} \tag{2.91}$$

whose dependence on the correlator is not constrained by conformal invariance. In light of similarities with analogous objects we will construct for the four-point case, we will call variables such as the $\mathcal{X}$ we constructed here *cross ratios*. The presence of a cross ratio implies that by imposing conformal invariance and the homogeneity constraints we can only restrict such a correlator to a form of the type

$$\langle \mathcal{O}_1(X_1,Z_1)\mathcal{O}_2(X_2,Z_2)\phi_3(X_3)\rangle = \frac{V_{1,32}^{l_1}V_{2,13}^{l_2}}{X_{12}^{\frac{\Delta_1+\Delta_2-\Delta_3+l_1+l_2}{2}}X_{23}^{\frac{\Delta_2+\Delta_3-\Delta_1-l_1+l_2}{2}}X_{31}^{\frac{\Delta_3+\Delta_1-\Delta_2+l_1-l_2}{2}}} t(\mathcal{X})\,. \tag{2.92}$$

We know however that the Z dependence need to be polynomial, and that Z appears both in the $H_{12}^{(1)}$ and $V_{i,jk}$ objects. This implies that the function $t(\mathcal{X})$ has to be a polynomial of maximal order $n_{12} = \min(l_1, l_2)$, and can be thus expanded in any basis of polynomials up to that order, leading to an expression of the form

$$\langle \mathcal{O}_1(X_1,Z_1)\mathcal{O}_2(X_2,Z_2)\phi_3(X_3)\rangle = \frac{V_{1,32}^{l_1}V_{2,13}^{l_2}}{X_{12}^{\frac{\Delta_1+\Delta_2-\Delta_3+l_1+l_2}{2}}X_{23}^{\frac{\Delta_2+\Delta_3-\Delta_1-l_1+l_2}{2}}X_{31}^{\frac{\Delta_3+\Delta_1-\Delta_2+l_1-l_2}{2}}} \sum_{\mathfrak{t}=0}^{n_{12}} \lambda_{123}^{\mathfrak{t}}\, g_{\mathfrak{t}}(\mathcal{X})\,. \tag{2.93}$$

This last result instructs us on the fact that three-point function are in general not specified by one single OPE coefficient, but are parametrized by a finite number of coefficients that span the space of *independent three-point tensor structures*. Similarly, the OPE of two spinning fields or one scalar and one spinning field will produce a certain field in multiple terms with different tensor structures, which will have expansion coefficients $\lambda_{123}^{\mathfrak{t}}$ equal to the ones present in (2.93).
When dealing with three spinning fields, or with fields with more than one single spin, it will be possible to construct more and more cross ratios like $\mathcal{X}$ all of which will be associated with a discrete expansion of similar type to the one in (2.93). For this reason a general expression for spinning three-point functions would be rather heavy to set up, and we will only discuss in more detail the cases directly involved in our analysis of [43] in section 5.

2.4.4 Four-point functions

Starting from four-point functions on, correlators are no longer fixed by conformal symmetry up to a constant.
This can be easily understood by first introducing the concept of a *conformal frame*, which consists on a reference configuration of points which can be achieved by acting with conformal transformations on a generic configuration of points in physical space. This can be seen as some sort of gauge fixing for conformal transformations.
The conformal frame we will consider can be achieved by taking the following successive transformations

- a special conformal transformation that maps point x_3 to ∞, implemented by $\mathcal{I}e^{-x_3^\mu P_\mu/x_3^2}\mathcal{I}$, which successively transforms the point as

$$x_3^\mu \xrightarrow{\mathcal{I}} x_3^\mu \xrightarrow{e^{-x_3^\mu P_\mu/x_3^2}} 0 \xrightarrow{\mathcal{I}} \infty\,;$$

- a translation that maps the transformed x_2 point to the origin;

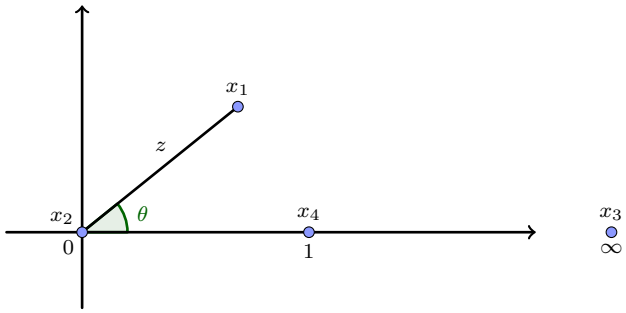

Figure 2.5: Conformal frame for four points in physical space. Any configuration of four points can be gauge fixed to a plane, with only two leftover degrees of freedom that can be encoded in a complex vector z.

- an SO(d) rotation that brings point x_4 to a reference coordinate direction $\vec{e}_1$;
- a dilatation that rescales x_4 to have unit norm;
- an SO($d-1$) rotation, orthogonal to the direction $\vec{e}_1$, that brings the point x_1 to the plane spanned by directions $\vec{e}_1$ and $\vec{e}_2$;

up to this point, we used all conformal transformations except for an SO($d-2$) subgroup, which acts as a stabilizer of the four-point configuration. We can therefore conclude that any configuration of four points is conformally equivalent to the one we constructed here, represented in Figure 2.5. At this point, it is rather easy to see that sets of two or three points do not have any conformally invariant degree of freedom, as these can always be mapped to 0, ∞, or to 0, 1 and ∞. This agrees with the results of the previous subsections. For four points, instead, we have a continuum of conformally inequivalent configurations parametrized by the possible locations of x_1 in the $(\vec{e}_1, \vec{e}_2)$ plane[1].
This can also be seen by the fact that, given the basic invariant building blocks

$$X_{12}\,, \qquad X_{13}\,, \qquad X_{14}\,, \qquad X_{23}\,, \qquad X_{24}\,, \qquad X_{34}\,, \tag{2.94}$$

it is possible to construct two independent conformally invariant *cross ratios*

$$u = \frac{X_{12}X_{34}}{X_{13}X_{24}}\,, \qquad v = \frac{X_{14}X_{23}}{X_{13}X_{24}} \tag{2.95}$$

whose dependence on the correlator cannot be fixed by the homogeneity conditions (2.47) as these have homogeneity degree zero with respect to all the X_i coordinates.
This implies that scalar four-point functions can therefore be written in the form

$$\langle \phi_1(X_1)\phi_2(X_2)\phi_3(X_3)\phi_4(X_4)\rangle = \Omega_4^{\{\Delta_i\}}(X_1, X_2, X_3, X_4)F(u, v) \tag{2.96}$$

where the prefactor $\Omega_4^{\{\Delta_i\}}$ is a function of the X_i that satisfies the correct homogeneity constraints (2.47). The precise form of $\Omega_4^{\{\Delta_i\}}$ is a matter of convention, as one can always multiply that prefactor by some function of the u and v cross ratios and it will still satisfy the homogeneity constraints[2]. In this thesis, we will consider the prefactor

$$\Omega_4^{\{\Delta_i\}} = \frac{1}{(X_{12})^{\Delta_1+\Delta_2}\,(X_{34})^{\Delta_3+\Delta_4}} \left(\frac{X_{24}}{X_{14}}\right)^{\frac{\Delta_1-\Delta_2}{2}} \left(\frac{X_{14}}{X_{13}}\right)^{\frac{\Delta_3-\Delta_4}{2}}\,, \tag{2.97}$$

which corresponds to the same conventions as [51].

[1] we are here assuming to be in $d > 1$ dimensions; in $d = 1$ the construction of the frame follows the same logic but is deprived of any rotation and $\vec{e}_2$ direction, leaving only one conformally invariant degree of freedom along $\vec{e}_1$
[2] the definition of the function $F(u, v)$ will of course change accordingly

The conformal block expansion

We have not yet used all the tools we have at our disposal to obtain information on the four-point correlators. We have seen in fact in section 2.2 that N-point functions in CFT can always be reduced to linear combinations of lower-point ones through the use of the OPE. We will therefore now try to understand what information this expansion can give us.
Let us start from the same four-point function as before. We can now imagine performing the OPE on the pairs of fields (12) and (34), to get

$$\Big\langle \underbrace{\phi_1(x_1)\phi_2}(x_2)\underbrace{\phi_3(x_3)\phi_4}(x_4)\Big\rangle = \sum_k \lambda_{12k}\lambda_{34k}\left[\hat{f}_{12k}(x_1,x_2,y_1,\partial_{y_1})\hat{f}_{34k}(x_1,x_2,y_2,\partial_{y_2})\,\langle \mathcal{O}_k(y_1)\mathcal{O}_k(y_2)\rangle\right]. \quad (2.98)$$

Where we used the fact that the two-point function is non-zero only if the "exchanged" fields produced in the two OPEs are the same. Alternatively, we could have also just taken one single OPE, e.g. (12), to get

$$\begin{aligned}\Big\langle \underbrace{\phi_1(x_1)\phi_2}(x_2)\phi_3(x_3)\phi_4(x_4)\Big\rangle &= \sum_k \lambda_{12k}\left[\hat{f}_{12k}(x_1,x_2,y,\partial_y)\,\langle \mathcal{O}_k(y)\phi_3(x_3)\phi_4(x_4)\rangle\right] \\ &= \sum_k \lambda_{12k}\lambda_{34k}\left[\hat{f}_{12k}(x_1,x_2,y,\partial_y)\,\frac{V_{y,34}^{l_k}}{X_{y4}^{\frac{\Delta_k-l_k+\Delta_4-\Delta_3}{2}}X_{43}^{\frac{\Delta_4+\Delta_3-\Delta_k+l_k}{2}}X_{y3}^{\frac{\Delta_k-l_k+\Delta_3-\Delta_4}{2}}}\Big|_{\text{phys.}}\right] \end{aligned} \quad (2.99)$$

which is bound to be the same expression as (2.98), but where we used the fact that three-point functions with two scalars are completely fixed by conformal symmetry to the form (2.90), which can then be reduced to physical space.
In both cases, the object in square brackets is completely fixed by conformal symmetry and is referred to as a *conformal partial wave*. The conformal partial wave expansion can be combined with the constrained form of the four-point correlator we had obtained in (2.96) to rewrite the expansion in terms of objects that depend on the cross ratios only, the *conformal blocks* $g_{\Delta_k,l_k}^{\Delta_{12},\Delta_{34}}$:

$$\langle\phi(x_1)\phi(x_2)\phi(x_3)\phi(x_4)\rangle = \Omega_4^{\{\Delta_i\}}(X_i)\sum_k \lambda_{12k}\lambda_{34k}\,g_{\Delta_k,l_k}^{\Delta_{12},\Delta_{34}}(u,v)\,. \quad (2.100)$$

The conformal blocks constitute thus a "basis" of functions on which one can expand the four-point correlators, and where every individual block repackages all the contributions to a correlator that come from a certain conformal multiplet (conformal primary operator plus all of its descendants). Note that this type of expansion is very similar to the one we had in (2.93) for three-points, with the main difference being that the expansion in four-point blocks comprises an infinite amount of terms. In light of this analogy, we will be calling the basis of functions $g_{\mathfrak{t}}(\mathcal{X})$ for three-point correlators *three-point blocks*.
The strength of the expansion (2.100) is that it provides a clear separation between dynamical theory-dependent quantities, represented by the OPE coefficients λ_{ijk}, and kinematical quantities which are universal for any CFT, the conformal blocks. It is thus clear that the determination of conformal blocks in CFT is of crucial importance to the writing of explicit expressions for four-point correlators.

OPE channels and crossing symmetry

There is nothing fundamental in the choice we made in (2.98) for how to decompose the correlator with the use of the OPE; we could have analogously picked the two pairs of fields of which we computed the OPE in a different way, and we would have obtained a different type of expansion for the same correlator. These inequivalent ways in which correlators can be OPE decomposed are known as *OPE channels*, which

are in one-to-one correspondence with trivalent tree diagrams that connect N points, as in Figure 2.6. The choice we made in (2.98) corresponds to the so-called *s-channel* expansion of Figure 2.6a, but there in total two more inequivalent ways to decompose that correlator: the *t-channel* of Figure 2.6b and the *u-channel* of Figure 2.6c.

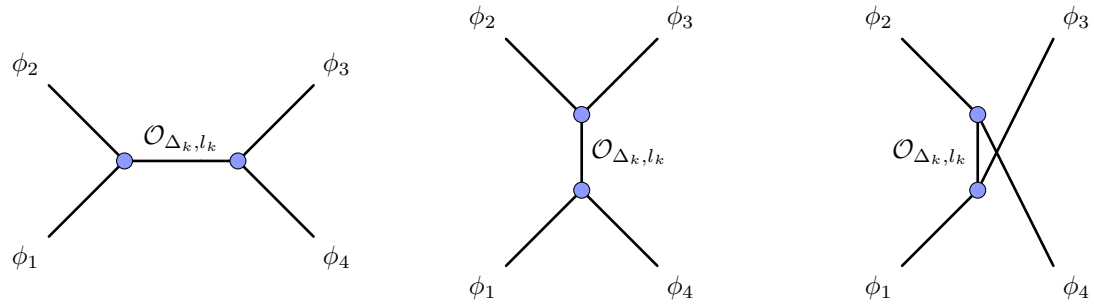

(a) s channel **(b)** t channel **(c)** u channel

Figure 2.6: All the possible OPE decompositions of four-point correlators. These are obtained by taking OPEs of pairs of fields until one has reduced the correlator to a sum over two-point functions of a certain "exchanged" operator $\mathcal{O}_{\Delta_k,l_k}$.

The fact that all these different expansions give rise to the same correlator can be seen as an exchange symmetry for the correlator, known as *crossing symmetry*, which gives rise to some non-trivial equalities. For example, exchanging the fields ϕ_2 and ϕ_4, an s-channel expansion gets transformed into a t-channel one, while the cross ratios u and v get exchanged. This translates into a *crossing equation* of the form:

$$v^{\frac{\Delta_2+\Delta_3}{2}} \sum_k \lambda_{12k}\lambda_{34k} g^{\Delta_{12},\Delta_{34}}_{\Delta_k,l_k}(u,v) = u^{\frac{\Delta_3+\Delta_4}{2}} \sum_{k'} \lambda_{23k'}\lambda_{41k'} g^{\Delta_{23}\Delta_{41}}_{\Delta_{k'},l_{k'}}(v,u)\,. \tag{2.101}$$

This type of equation is at the core of the *conformal bootstrap* program, an approach which reverses the logic of determining N-point functions from knowledge of lower-point ones using the OPE, to that of using symmetry constraints such as crossing on N-point functions to extract information on the allowed CFT data of a theory.

Four-point conformal blocks and the Casimir equations

Since the four-point functions are the simplest type of correlators for which one can write crossing equations, the focus of the CFT and bootstrap community has been mainly targeted towards these, which lead to a very strong insight on four-point blocks. First powerful results were obtained initially in [18], where the authors, Dolan and Osborn, directly analyzed the OPE expansion and found a recurrence relation which could be explicitly solved in $d = 2$ or $d = 4$ dimensions to determine four-point blocks with scalar external legs. It was however not until their later work [19], that a much more efficient way to determine blocks was found. In this paper, they used the fact that fields in CFT, including the primaries exchanged in the diagrams of Figure 2.6, satisfy eigenvalue equations associated with Casimir operators; this simple fact can actually be used to obtain differential equations for conformal blocks as we will now discuss.

Casimir operators are elements of the universal enveloping algebra of a Lie algebra that commute with all elements of the algebra. For this reason, Casimirs are used to label representations, and the number of independent Casimirs that can be constructed for our case of interest, $\mathfrak{so}(d+1,1)$, corresponds precisely to the number of labels we introduced in section 2.1: $\left\lfloor \frac{d}{2}+1 \right\rfloor$. These Casimir operators are constructed starting from tensors $\kappa_p^{\alpha_1\cdots\alpha_p}$, with α indices in the adjoint representation, which are invariant tensors under the action of the Lie algebra. These tensors are then contracted with the conformal generators to form the Casimirs. If we restrict our attention to STTs labeled by $(\Delta, l \equiv j_1)$, the two only relevant

Casimir operators are

$$\mathcal{C}as^2 = \kappa_2^{\alpha\beta} M_\alpha M_\beta = \frac{1}{2} M_{AB} M^{BA} \tag{2.102}$$

$$\mathcal{C}as^4 = \kappa_4^{\alpha_1\alpha_2\alpha_3\alpha_4} M_{\alpha_1} M_{\alpha_2} M_{\alpha_3} M_{\alpha_4} = \frac{1}{2} M_{AB} M^{BC} M_{CD} M^{DA} \tag{2.103}$$

which acting on irreps evaluate to

$$\mathcal{C}as^2 \left|\mathcal{O}_{\Delta,l}\right\rangle = \left[\Delta(\Delta - d) + l(l + d - 2)\right] \left|\mathcal{O}_{\Delta,l}\right\rangle \equiv c^{(2)}_{\Delta,l} \left|\mathcal{O}_{\Delta,l}\right\rangle \tag{2.104}$$

$$\begin{aligned} \mathcal{C}as^4 \left|\mathcal{O}_{\Delta,l}\right\rangle = \Bigg[& \frac{\Delta}{2} \left(d^2 (3\Delta + 1) - d^3 - d\Delta (4\Delta + 1) + 2\Delta^3\right) \\ & + \frac{l}{2} \left(2l^3 + 4(d-2)l^2 + \left(3d^2 - 13d + 12\right) l + d^3 - 7d^2 + 14d - 8\right) \Bigg] \left|\mathcal{O}_{\Delta,l}\right\rangle \equiv c^{(4)}_{\Delta,l} \left|\mathcal{O}_{\Delta,l}\right\rangle \,, \end{aligned} \tag{2.105}$$

where we introduced the constants $c^{(p)}_{\Delta,l}$.
Note that if we act on a state generated by two fields, we obtain

$$\mathcal{C}as^p \phi_1(X_1)\phi_2(X_2) \left|0\right\rangle = \mathcal{D}^p_{12} \phi_1(X_1)\phi_2(X_2) \left|0\right\rangle \tag{2.106}$$

with

$$\mathcal{D}^2_{12} = \frac{1}{2} \left(\mathcal{T}_{12}\right)^{AB} \left(\mathcal{T}_{12}\right)_{BA} \,, \qquad \mathcal{D}^4_{12} = \frac{1}{2} \left(\mathcal{T}_{12}\right)^{AB} \left(\mathcal{T}_{12}\right)_{BC} \left(\mathcal{T}_{12}\right)^{CD} \left(\mathcal{T}_{12}\right)_{DA} \,, \qquad \mathcal{T}_{12} = \mathcal{T}_1 + \mathcal{T}_2 \,, \tag{2.107}$$

and $\mathcal{T}_i$ being the action of conformal generators as differential operators on the i-th field.
Let us now consider a conformal partial wave expansion, e.g. in the s-channel. This can be seen as a summation of four-point correlators where certain projection operators $\mathcal{P}_{\Delta,l}$ are inserted in the middle:

$$\sum_{\Delta,l} \langle 0|\phi_1(X_1)\phi_2(X_2)\mathcal{P}_{\Delta,l}\phi_3(X_3)\phi_4(X_4)|0\rangle \,. \tag{2.108}$$

If we focus on one single term of the expansion and act on this with the differential operator $\mathcal{D}^p_{12}$, we can see this as a four-point function with an additional insertion of a Casimir operator

$$\mathcal{D}^p_{12} \langle 0|\phi_1(X_1)\phi_2(X_2)\mathcal{P}_{\Delta,l}\phi_3(X_3)\phi_4(X_4)|0\rangle = \langle 0|\phi_1(X_1)\phi_2(X_2)\mathcal{C}as^p\mathcal{P}_{\Delta,l}\phi_3(X_3)\phi_4(X_4)|0\rangle \,. \tag{2.109}$$

At this point, the Casimir operator can be made act on the projection on the right, obtaining the differential equation

$$\mathcal{D}^p_{12} \langle 0|\phi_1(X_1)\phi_2(X_2)\mathcal{P}_{\Delta,l}\phi_3(X_3)\phi_4(X_4)|0\rangle = c^{(p)}_{\Delta,l} \langle 0|\phi_1(X_1)\phi_2(X_2)\mathcal{P}_{\Delta,l}\phi_3(X_3)\phi_4(X_4)|0\rangle \,. \tag{2.110}$$

The expectation values in (2.110) are the conformal partial waves, which from (2.100) we know correspond to the conformal blocks multiplied by the prefactor $\Omega_4^{\{\Delta_i\}}(X_i)$. By extracting this, it is possible to rewrite this as a differential equation for conformal blocks, the so-called *Casimir equation*, which therefore depends only on the cross ratios:

$$\left(\Omega_4^{\{\Delta_i\}}(X_i)\right)^{-1} \mathcal{D}^p_{12} \left(\Omega_4^{\{\Delta_i\}}(X_i) g^{\Delta_{12},\Delta_{34}}_{\Delta,l}(u,v)\right) \equiv \mathcal{D}'^p_{12} g^{\Delta_{12},\Delta_{34}}_{\Delta,l}(u,v) = c^p_{\Delta,l} g^{\Delta_{12},\Delta_{34}}_{\Delta,l}(u,v) \,. \tag{2.111}$$

Later on in this thesis we will often abuse the notation and remove the prime symbol on the differential operators $\mathcal{D}'^p_{(ij)}$ that act in cross-ratio space. For more concrete expressions, we refer the reader to section 4.2.1 and, in particular, equation (4.8).
Note how by looking for solutions of (2.111) for $p = 1, 2$ we are looking for a basis of functions $g^{\Delta_{12},\Delta_{34}}_{\Delta,l}(u,v)$ in two variables which simultaneously diagonalizes two operators $\mathcal{D}^p_{12}$. In other words we could say that the number of "conserved charges" of the system equals the number of degrees of

freedom in it, which makes the determination of four-point conformal blocks an integrable problem. This instructs us on the fact that solving (2.111) is enough to fully determine four-point conformal blocks.
What we just exposed in this subsection is the type of approach introduced by Dolan and Osborn in [19], which requires the solution of the Casimir equations, in particular of the quadratic one, to efficiently determine four-point conformal blocks for scalar external legs. Thanks to this, scalar blocks are known in closed form for even dimension d, while they can be written as series expansions for odd dimensions. Stemming from this original idea, many efficient approaches have been established for general four-point blocks including those with spinning external legs, see e.g. [20–31].

2.4.5 Higher-point functions

Analogously to the four-point case, scalar conformal correlators for $N > 4$, known as multipoint correlation functions or higher-point functions, have a number of invariant degrees of freedom left unconstrained by conformal symmetry, the cross ratios. The number of cross ratios increases with N in a way that depends on the dimension d, and which is easy to understand starting from the four-point conformal frame picture we explained in the previous section. There, we understood that four-point configurations in Euclidean space are all conformally equivalent to the one where three points are at fixed positions $(x_2, x_3, x_4) = (0, \infty, \vec{e}_1)$ and x_1 is located in the $\vec{e}_1\vec{e}_2$ plane. Furthermore, an $\mathrm{SO}(d-2)$ subgroup acts as a stabilizer of the four-point configuration. Every time we introduce an i-th point, $4 < i \leq d+2$, we introduce a d-dimensional vector which can be acted upon with the stabilizer subgroup of $i-1$ points, $\mathrm{SO}(d+2-i)$. This reduces the number of degrees of freedom that are introduced at any step to $i-2$. This happens until the number i reaches $d+2$, after which with every additional point one introduces d unconstrained degrees of freedom. The total number of cross ratios for an N-th point function amounts therefore to

$$n_{cr}(N,d) = \begin{cases} \frac{1}{2}N(N-3) & N \leq d+2 \\ Nd - \frac{1}{2}(d+2)(d+1) & N > d+2 \end{cases} . \tag{2.112}$$

From conformal symmetry alone, using analogous statements as the lower-point cases, we can constrain the form of higher-point correlators to be

$$\langle \phi_1(X_1) \cdots \phi_N(X_N) \rangle = \Omega_N^{\{\Delta_i\}}(X_1, \ldots, X_N) F(u_1, \ldots, u_{n_{cr}}) \tag{2.113}$$

where $\Omega_N^{\{\Delta_i\}}$ is again a prefactor constructed out of scalar products X_{ij} such that it is homogeneous of degree $-\Delta_i$ with respect to all of the variables X_i.
Once more, the expression (2.113) can be further decomposed using the OPE, which allows writing down conformal block decompositions. The number of OPE channels/diagrams increases dramatically with N, as for N external points there are $(2N-5)!!$ possible trivalent diagrams that can connect them. The individual diagrams will also become more complex, see e.g. Figure 2.7.
In order be able to write formulas for multipoint blocks and to set up grounds for later parts of this thesis, let us first introduce some notation. Given an OPE channel we enumerate internal lines by indices $r = 1, \ldots, N-3$ and vertices by indices $\mathfrak{v} = 1, \ldots, N-2$. Any ordering will do, as there is no general rule on how to enumerate these. In addition to the labels associated with exchanged fields in an OPE diagram – the conformal dimensions Δ_r and $\mathfrak{so}_d$ representations ϱ_r – the multipoint OPE expansion is also labeled by integers $t_\mathfrak{v}$ that parametrize the space of independent tensor structures constructed around every non-trivial vertex $\mathfrak{v}$ of the diagram (i.e. vertices to which are attached two or three spinning fields). The use of the OPE allows in fact to write the general expression

$$\langle \phi_1(X_1) \cdots \phi_N(X_N) \rangle = \Omega_N^{\{\Delta_i\}}(X_1, \ldots, X_N) \sum_{\Delta_r, \varrho_r, \mathfrak{t}_\mathfrak{v}} \left(\prod_\mathfrak{v} \lambda^{\mathfrak{t}_\mathfrak{v}}_{\ldots} \right) g^{\Delta_i}_{\{\Delta_r, \varrho_r, \mathfrak{t}_\mathfrak{v}\}}(u_1, \ldots, u_{n_{cr}}) , \tag{2.114}$$

where the $g^{\Delta_i}_{\{\Delta_r, \varrho_r, \mathfrak{t}_\mathfrak{v}\}}$ functions are themselves the *multipoint conformal blocks*, which will be the main target of attention for the remaining part of this thesis.

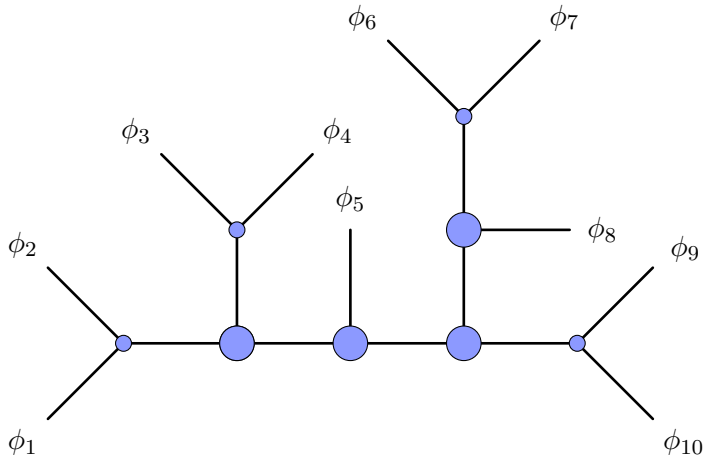

Figure 2.7: Choice of an OPE channel for a 10-point function. The bigger blue vertices are associated with non-trivial tensor structures.

The conformal block expansion (2.114) is much more complicated than the one we observed for four points in (2.100). However, despite the increased difficulty, the computation of multipoint blocks might be worth the cost, as a solid understanding of these blocks has the potential to bring in techniques and results that are much more efficient and powerful. This can be understood, for instance, from the following observations:

- a single multipoint correlator contains information equivalent to that of infinitely many four-point functions;
- OPE coefficients of spinning operators are accessible also when dealing only with external scalars in a multipoint setting;
- by understanding how to take OPE limits, it is possible to reduce multipoint correlators to spinning lower-point ones, and have an orthogonal perspective on how these can be computed;
- for the $N \geq 6$ case, light-cone limits of multipoint correlators are related to Wilson loops and scattering amplitudes of theories which enjoy dual conformal invariance such as $\mathcal{N} = 4$ super Yang-Mills; for these theories a nice interplay between conformal bootstrap and modern amplitudes techniques is therefore possible [32, 33].

It is not then surprising to know that in recent years more and more attention has been put in the understanding of multipoint conformal blocks [36, 37, 39, 40, 52–60], leading to concrete determination of many one- and two-dimensional multipoint conformal blocks, as well as determination of certain light-cone limits of $d \geq 3$ conformal blocks and recursion relations for five-point blocks. For long time, however, it has not been clear how to extend the differential equation approach of Dolan and Osborn we reviewed at the end of 2.4.4, to a multipoint setting in $d \geq 3$. This is due to an initial roadblock that we will now outline.

It is natural to expect that multipoint conformal blocks associated with a certain OPE diagram need to satisfy a number of Casimir equations for every internal leg of said diagram. However, the number of internal Casimir operators does not grow with the same rate as the number of degrees of freedom of the system $n_{cr}(N, d)$, counted in (2.112). This is already apparent from the case of $N = 5$ conformal blocks, whose 15 channels all have the same topology as that in Figure 2.8. In this case there are two internal legs which correspond to two exchanges of an STT, each labeled by a conformal dimension Δ_r and spin l_r, which can be measured by diagonalization of a quadratic and a quartic Casimir operator. The total number of Casimir operators is therefore four, which does not match the number of cross ratios

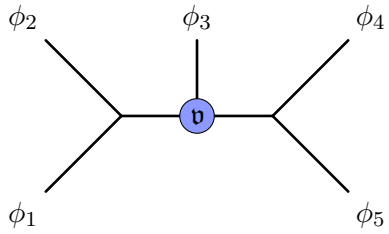

Figure 2.8: Choice of OPE diagram for 5-point correlator.

$n_{cr}(5, d \geq 3) = 5$. This implies that the problem is not yet integrable, as it requires the diagonalization of an additional operator to have equal number of conserved charges and degrees of freedom. The same type of problem manifests for correlators with more than five legs, as increasing the number of external fields by one adds, for N large enough, d degrees of freedom, while the extra internal leg that is formed can only account for a maximum of $\lfloor \frac{d}{2} \rfloor + 1$ additional Casimir operators.
This issue can be rephrased in the fact that the diagonalization of the exchanged Casimir operators does not specify a basis for the independent tensor structures at every non-trivial vertex of an OPE diagram. To make the determination of multipoint conformal blocks an integrable problem, it is therefore necessary to introduce a set of differential operators that are conformally invariant, that commute with the exchanged Casimir operators, and that allow a decomposition of the space of invariant tensor structures at every vertex. This is precisely the problem we addressed in [41] and completed in [42] with the help of Gaudin models; we will review this approach in the next chapter.

Chapter 3

Gaudin Models and Multipoint Conformal Blocks

The goal of this chapter is to report our results of [41, 42], where we discussed how to measure simultaneously a complete set of quantum numbers for multipoint conformal blocks through a sufficiently large set of commuting differential operators. This discussion applies to any d, any number N of external points and any OPE channel.

3.1 Setup and Summary of Results

As we highlighted already at the end of the previous chapter, when dealing with higher-point correlation functions is easy to see that the quantum numbers of fields exchanged in the intermediate channels are not sufficient to fully characterize the conformal blocks. The precise number of such intermediate field labels does depend on the channel topology, at least for $N > 5$, but it is always strictly smaller than the number n_{cr} of cross ratios. The quantum numbers we will discuss are measured by acting with differential operators in the cross ratios. The latter divide into two families. First, differential operators that measure the quantum numbers of intermediate fields are associated with the links of the OPE diagram and are referred to as *Casimir differential operators*, since they are straightforward generalizations of the Casimir differential operators constructed for $N = 4$ by Dolan and Osborn. Second, differential operators that measure choices of tensor structures, the first example of which was introduced in [41], are referred to as *vertex differential operators*. Let us note that for scalar blocks, the choice of tensor structures and hence the vertex differential operators are relevant as soon as multiple non-scalar exchanges are involved. These types of blocks have only been considered recently in [40] and [37, Appendix E] for five-point blocks, and in a certain limit in [32–34] for five or six scalar legs.

To enumerate elements of an OPE diagram $\mathcal{C}^N_{OPE}$ we will use the notation we introduced in section 2.4.4, with indices $r = 1, \dots, N-3$ for internal legs and $\mathfrak{v} = 1, \dots, N-2$ for internal vertices. OPE diagrams are (plane) trees and hence by cutting any internal line with label r we separate the diagram into two disconnected pieces. Hence, r is associated with a partition of the external fields into two disjoint sets,

$$\underline{N} = \{1, \dots, N\} = I_{r,1} \uplus I_{r,2} \ . \tag{3.1}$$

Similarly, any vertex $\mathfrak{v}$ gives rise to a partition of $\underline{N}$ into three disjoint sets

$$\underline{N} = I_{\mathfrak{v},1} \uplus I_{\mathfrak{v},2} \uplus I_{\mathfrak{v},3} \ . \tag{3.2}$$

Given any subset $I \subset \underline{N}$ we can define the following set of first order differential operators in the insertion points x_i,

$$\mathcal{T}^{(I)}_\alpha = \sum_{i \in I} \mathcal{T}^{(i)}_\alpha \ . \tag{3.3}$$

Let us note that for two disjoint sets $I_1, I_2 \subset \underline{N}$ we have

$$\mathcal{T}_\alpha^{(I_1 \uplus I_2)} = \mathcal{T}_\alpha^{(I_1)} + \mathcal{T}_\alpha^{(I_2)} \ , \quad [\, \mathcal{T}_\alpha^{(I_1)} \, , \, \mathcal{T}_\beta^{(I_2)} \,] = 0 \ . \tag{3.4}$$

Casimir differential operators. With this notation it is very easy to construct the differential operators that measure the quantum numbers of the intermediate fields,

$$\mathcal{C}as_r^p = \mathcal{D}_{r,1}^p = \kappa_p^{\alpha_1,\ldots,\alpha_p} \left[\mathcal{T}_{\alpha_1}^{(I_{r,1})} \cdots \mathcal{T}_{\alpha_p}^{(I_{r,1})} \right]_{|\mathcal{G}} = \mathcal{D}_{r,2}^p \ . \tag{3.5}$$

Here κ_p denotes *symmetric* conformally invariant tensors of order p and the superscript p runs through

$$p = 2, 4, \ldots \begin{cases} d+1 = 2r_d & \text{for } d \text{ odd} \\ d = 2r_d - 2 & \text{for } d \text{ even} \end{cases} \tag{3.6}$$

The number $r_d = [(d+2)/2]$ denotes the rank of the conformal Lie algebra. In even dimensions d, the symmetric invariant tensor κ_p of order $p = 2r_d = d+2$ actually possesses a square root of order $p = r_d$ that also commutes with all generators of the conformal algebra. This so-called *Pfaffian* differential operator has the same form as in (3.5), but with a symmetric invariant tensor κ_p of order $p = d/2+1$,

$$\mathcal{P}f_r = \mathcal{D}_{r,1}^{d/2+1} = \kappa_{d/2+1}^{\alpha_1,\ldots,\alpha_{d/2+1}} \left[\mathcal{T}_{\alpha_1}^{(I_{r,1})} \cdots \mathcal{T}_{\alpha_{d/2+1}}^{(I_{r,1})} \right]_{|\mathcal{G}} = -(-1)^{d/2} \mathcal{D}_{r,2}^{d/2+1} \ . \tag{3.7}$$

When $d = 4k+2$, the symmetric invariants of order $p = d/2+1$ are twofold degenerate and we should use two different symbols for these two invariants of order $d/2+1$. In order not to clutter notation too much, we decided to ignore this distinction. In other words, we will consider $\kappa_{d/2+1}$ as a pair of symmetric invariants when $d = 4k+2$.

In our formulas for the differential operators we have placed a subscript $|\mathcal{G}$ to stress that they are defined as operators acting on correlations functions, i.e. on functions $\mathcal{G}$ that satisfy the conformal Ward identities

$$\mathcal{G}_N(x_i, \Delta_i) := \langle 0 | \phi_1(x_1) \cdots \phi_N(x_N) | 0 \rangle \, , \qquad \mathcal{T}_\alpha^{(\underline{N})} \mathcal{G}_N(x_i, \Delta_i) = 0 \, . \tag{3.8}$$

In our construction of the differential operators we have favored the set $I_{r,1}$ over $I_{r,2}$. But from the conformal Ward identities we can conclude that

$$\mathcal{T}_\alpha^{(I_{r,1})} \mathcal{G}_N(x_i, \Delta_i) = -\mathcal{T}_\alpha^{(I_{r,2})} \mathcal{G}_N(x_i, \Delta_i) \ .$$

Though some caution is needed when we apply this relation to the evaluation of the Casimir differential operator, see Subsection 3.2.1 for details, it is not difficult to see that all differential operators of even order come out the same if we pick $I_{r,2}$ rather than $I_{r,1}$. There is only one family for which the set matters, namely for the Pfaffian operators when d is a multiple of four. In that case the operator flips sign when we change the set. Of course, overall factors are a matter of convention and hence of no concern. Therefore, we shall drop the reference to the set we use in the construction of Casimir differential operators, writing $\mathcal{D}_r^p$ instead of $\mathcal{D}_{r,1}^p$.

An important point to note is that the Casimir differential operators need not be independent. To illustrate this, consider the case $N = 4$ for $d > 2$. Since all external fields are assumed to be scalar, the single intermediate field is a symmetric traceless tensor and is hence characterized by two numbers only, its weight Δ and spin l. These can be measured by the Casimir differential operators $\mathcal{D}^2$ and $\mathcal{D}^4$. But starting from $d = 4$, the conformal algebra possesses Casimir elements of higher order which are independent in general, but become dependent on the lower order ones when evaluated on symmetric traceless tensors. More generally, the number of independent Casimir differential operators at a given internal line r is given by

$$\mathfrak{d}_r(\mathcal{C}_{OPE}^N, d) = \mathfrak{d}(I_{r,1}, d), \quad \text{where} \quad \mathfrak{d}(I, d) = \min(|I|, N - |I|, r_d), \tag{3.9}$$

and $|I|$ denotes the order of the set I. In this chapter we shall refer to the number $\mathfrak{d}(I,d)$ as the *depth* of the index set I and to $\mathfrak{d}_r$ as the depth of the link r. This is not to be confused with the *spin depth* L of MST_L fields we introduced in section 2.1, which we will not be using in this chapter[1]. Note that $\mathfrak{d}_r = \mathfrak{d}(I_{r,1},d) = \mathfrak{d}(I_{r,2},d)$ is independent of which of the two index sets we choose to compute it with. By summing the depths of all internal links, we can determine the total number of independent Casimir differential operators to be

$$n_{cdo}(\mathcal{C}^N_{OPE},d) = \sum_{r=1}^{N-3} \mathfrak{d}_r(\mathcal{C}^N_{OPE},d)\ . \tag{3.10}$$

Let us note that the total number of Casimir differential operators does depend on the topology of the OPE channel, not just on the number N of points. In the case of $N=6$ and $d\geq 4$, for example, there are $n_{cdo}(\mathcal{C}^{N=6}_{comb},d)=7$ Casimir differential operators in the comb channel, while the snowflake channel admits only $n_{cdo}(\mathcal{C}^{N=6}_{snowflake},d)=6$ of such operators.

Vertex differential operators. What we have described so far is nothing new, and can be established by elementary means. But as we have explained, starting from $N=5$ the Casimir differential operators do not suffice to resolve all quantum numbers of the conformal blocks, i.e. n_{cdo} is strictly smaller that n_{cr} for all OPE channels. Our main task is to construct additional differential operators that can measure the choice of tensor structures at the vertices independently of the weights and spins of the intermediate fields, i.e. we need to find a complete set of vertex differential operators that commute with the Casimir differential operators and among themselves. In this chapter we describe how to accomplish this task, for any number N of external scalar fields and any OPE topology. One central claim is that these vertex differential operators take the form

$$\mathcal{D}^{p,\nu}_{\mathfrak{v},12} = \kappa_p^{\alpha_1,\dots,\alpha_\nu,\alpha_{\nu+1},\dots,\alpha_p}\left[\mathcal{T}^{(I_{\mathfrak{v},1})}_{\alpha_1}\dots\mathcal{T}^{(I_{\mathfrak{v},1})}_{\alpha_\nu}\mathcal{T}^{(I_{\mathfrak{v},2})}_{\alpha_{\nu+1}}\dots\mathcal{T}^{(I_{\mathfrak{v},2})}_{\alpha_p}\right]_{|\mathcal{G}} \tag{3.11}$$

where $\nu=1,\dots,p-1$ and $p=2,4,\dots,2r_d=d+1$ when d is odd. For even d, we let p run through even integers until we reach d and add a set of Pfaffian vertex operators $\mathcal{P}f^{\nu}_{\mathfrak{v},12},\nu=1,2,\dots d/2$ which are constructed with a symmetric invariant tensor κ_p of order $p=d/2+1$. Let us note that the definition of all these vertex differential operators also makes sense for $\nu=0$ and $\nu=p$. The corresponding objects coincide with Casimir differential operators for the links that enter the first and second leg of the vertex. This is why we have excluded them from our list. The remaining operators still allow us to reconstruct the Casimir operators for the link that enters the third leg. Therefore, there is one linear relation for each value that p can assume, i.e. we have r_d linear relations in total. One may use these relations to eliminate e.g. the operator with $\nu=p/2$.

Let us note that the definition of the vertex operators $\mathcal{D}^{p,\nu}_{\mathfrak{v},ij}$ depends on the choice of labeling of the subsets $I_{\mathfrak{v},j}$ forming the partition $\underline{N}=I_{\mathfrak{v},1}\cup I_{\mathfrak{v},2}\cup I_{\mathfrak{v},3}$ associated with the vertex $\mathfrak{v}$, which is arbitrary. However, the algebra generated by the vertex operators $\mathcal{D}^{p,\nu}_{\mathfrak{v}}$ is in fact independent of this choice: more precisely, the vertex operators constructed from another choice of labeling of the $I_{\mathfrak{v},j}$'s are linear combinations of the operators $\mathcal{D}^{p,\nu}_{\mathfrak{v},12}$, modulo the use of the conformal Ward identities (3.8), see section 3.2.2.

The number of vertex differential operators at a given vertex is now easy to count. Taking into account that one additional linear relation among the operators listed in eq. (3.11), one finds

$$n_v(d) = \begin{cases} \frac{1}{4}(d^2-4) & \text{for } d \text{ even} \\ \frac{1}{4}(d^2-1) & \text{for } d \text{ odd} \end{cases} \tag{3.12}$$

The first key result of [42] is that these vertex differential operators commute among themselves and with the Casimir differential operators. Commutation between Casimir and vertex differential operators is obvious. Similarly, it is easy to show that two vertex operators commute if they are associated with different vertices $\mathfrak{v}\neq\mathfrak{v}'$. The deepest part of our claim concerns the fact that also vertex operators

[1] the two quantities are very much related, as $\mathfrak{d}_r = L_r+1$. In this chapter, however, we find more useful to use the definition of depth as the $\mathfrak{d}_r$ above, which here allows to often avoid shifts by one unit in formulas.

associated with the same vertex commute. It does not seem straightforward to prove this statement by elementary manipulations. Below we shall use an indirect strategy in which we identify these vertex differential operators with Hamiltonians of some Gaudin integrable system defined on a 3-punctured sphere. For the latter, commutativity has already been established.

Of course the vertex differential operators we listed may not all be independent, as for the Casimir operators, see discussion above. In order to count the number of independent vertex differential operators, we shall employ the depth function $\mathfrak{d}(I,d)$ we introduced in eq. (3.9). For a given vertex $\mathfrak{v}$ inside an OPE channel $\mathcal{C}^N_{OPE}$, the number of independent vertex differential operators is expected to be equal to the degrees of freedom associated with this vertex

$$n_{vdo,\mathfrak{v}}(\mathcal{C}^N_{OPE},d) = n_{cr}(\sum_{i=1}^{3}\mathfrak{d}_{\mathfrak{v},i},d) - \sum_{i=1}^{3}\mathfrak{d}_{\mathfrak{v},i}(\mathfrak{d}_{\mathfrak{v},i}-1) \leq n_v(d) \tag{3.13}$$

where $\mathfrak{d}_{\mathfrak{v},i} = \mathfrak{d}(I_{\mathfrak{v},i},d)$ with $i=1,2,3$. The inequality is saturated for vertices $\mathfrak{v}$ with $\mathfrak{d}_{\mathfrak{v},i} = r_d$. For the special vertices that can appear in the comb channel and in which one of the legs is scalar, the formula becomes

$$n_{vdo,\mathfrak{v}_m} = m-1\ , \quad n_{vdo,\mathfrak{v}_{r_d}} = r_d - 1 - \delta_{d,even}$$

for $m=1,\ldots,r_d-1$. Here $\mathfrak{v}_m$ is a vertex with $\mathfrak{d}_{\mathfrak{v}_m,1}=m, \mathfrak{d}_{\mathfrak{v}_m,2}=1$ and $\mathfrak{d}_{\mathfrak{v}_m,3}=m+1$, see Figure 3.1, and $\mathfrak{v}_d$ is the maximal comb channel vertex with $\mathfrak{d}_{\mathfrak{v}_{r_d},1} = r_d = \mathfrak{d}_{\mathfrak{v}_{r_d},3}$. The total number $n_{vdo}(\mathcal{C}^N_{OPE},d)$ of vertex differential operators is obtained by summing over all $N-2$ vertices, i.e.

$$n_{vdo}(\mathcal{C}^N_{OPE},d) = \sum_{\mathfrak{v}=1}^{N-2} n_{vdo,\mathfrak{v}}(\mathcal{C}^N_{OPE},d)\ .$$

At least for the comb channel, it is easy to verify that the number of independent Casimir and vertex differential operators coincides with the number of cross ratios,

$$n_{cdo}(\mathcal{C}^N_{OPE},d) + n_{vdo}(\mathcal{C}^N_{OPE},d) = n_{cr}(N,d)\ .$$

The formula holds of course for all OPE channels. Below we shall exhibit the relations among vertex

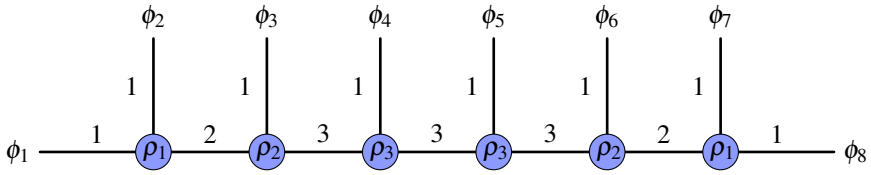

Figure 3.1: OPE diagram in the comb channel for a scalar eight-point function in $d=4$. The edge labels correspond to the depth $\mathfrak{d}$ of the associated links. When taking an OPE with a scalar field, the depth always increases by one until the maximal allowed depth $\mathfrak{d}=r_d$ is reached.

differential operators that are responsible for the reduction from the $n_v(d)$ operators in our list (3.11) (with $\nu=p/2$ removed) to the $n_{vdo,\mathfrak{v}}(\mathcal{C}^N_{OPE},d)$ independent vertex differential operators that are needed to characterize the vertex $\mathfrak{v}$. This is the second key result of this chapter. It will allow us in particular to determine the precise order of each independent vertex differential operator.

While Gaudin models for the 3-punctured sphere only enter the discussion as a convenient tool to construct commuting vertex differential operators at the individual vertices, the relation between conformal blocks and Gaudin models turns out to reach much further. In fact, is is possible to embed the whole set of Casimir and vertex differential operators for arbitrary scalar N-point functions into Gaudin models on the N-punctured sphere. The latter contains N additional complex parameters that are not present in correlation functions. In the Gaudin integrable model these parameters correspond to the poles of the Lax matrix and they enter all Gaudin Hamiltonians. By considering different limiting configurations of

these parameters is is possible to recover the full set of Casimir and vertex differential operators for scalar N-point functions in all the OPE channels. This construction not only embeds our differential operators into a unique Gaudin integrable model, but also shows that operators in different channels are related by a smooth deformation.

Let us finally outline the content of the following sections. Section 3.2 is mostly devoted to the study of the individual vertices. After a brief discussion of commutativity for Casimir differential operators and also vertex differential operators assigned to different vertices, we shall zoom into the individual vertices for most of section 3.2. In section 3.2.2 we construct the vertex differential operators in terms of the commuting Hamiltonians of a 3-site Gaudin integrable system. Section 3.2.3 addresses the relations between these operators for restricted vertices. The main purpose of section 3.3 is to embed the whole set of Casimir and vertex differential operators for arbitrary scalar N-point functions into Gaudin models on the N-punctured sphere. In section 3.4 we discuss one concrete example, namely we construct all five differential operators that characterize the blocks of a scalar 5-point function in any $d \geq 3$. Two of these operators are of order two while the other three are of fourth order.

3.2 The Vertex Integrable System

The aim of this section is to address the key new element in the construction of multi-point conformal blocks for $d \geq 3$: the vertices. In the first subsection we shall show that the construction of commuting differential operators for scalar N-point blocks can be reduced by rather elementary arguments to the construction of commuting differential operators for 3-point functions of spinning fields. Recall that the dependence on spin degrees of freedom can be encoded in auxiliary variables from which one is often able to construct non-trivial cross ratios, even in the case of a 3-point function. Constructing sufficiently many commuting vertex differential operators that act on such cross ratios of the 3-point function requires more powerful technology from integrability which we shall turn to in the second subsection. There we construct commuting differential operators for vertices from the Gaudin integrable model for the 3-punctured sphere. The basic construction provides $n_v(d)$ of such commuting operators and hence sufficiently many even for the most generic vertices. For special vertices, such as those appearing in the comb channel with external scalars, there exist linear relations between these operators. These are the subject of the third subsection.

3.2.1 Reduction to the vertex systems

Our goal here is to prove that Casimir and vertex operators constructed around different vertices of an OPE diagram commute. More precisely we shall show that

$$[\,\mathcal{D}^{p}_{r}\,,\,\mathcal{D}^{q}_{r'}\,]=0 \quad , \quad [\,\mathcal{D}^{p}_{r}\,,\,\mathcal{D}^{q,\nu}_{\mathfrak{v},a}\,]=0 \tag{3.14}$$

for every pair $(r,p),(r',q)$ of Casimir operators and any choice $(\mathfrak{v},q,\nu)$ of a vertex operator, including the Pfaffian Casimir and vertex operators that appear at order $p,q=d/2+1$ when the dimension d is even. Note that the individual vertex differential operators also depend on the choice $a\in\{12,23,13\}$ of a pair of legs. In addition, we shall also establish that vertex operators associated with different vertices commute,

$$[\,\mathcal{D}^{p,\nu}_{\mathfrak{v},a}\,,\,\mathcal{D}^{q,\mu}_{\mathfrak{v}',b}\,]=0 \quad \textit{for } \mathfrak{v}\neq\mathfrak{v}' \tag{3.15}$$

and all triples (p,ν,a) and (q,μ,b). This leaves only the commutativity of operators attached to the same vertex which is deferred to the next subsection.

The properties (3.14) and (3.15) are in fact elementary. They require global conformal invariance, the tree structure of OPE diagrams and the commutativity property (3.4). To begin with, let us recall that we associated two disjoint sets $I_{r,1}$ and $I_{r,2}$ to every link. As we pointed out before, the Casimir differential operators (3.5) do not depend on whether we used the generators $\mathcal{T}_\alpha^{(I_{r,1})}$ or $\mathcal{T}_\alpha^{(I_{r,2})}$ to construct them. Let

us briefly discuss the details of the proof. Note that we think of $\mathcal{D}$ as an operator acting on correlation functions $\mathcal{G}$. This is signaled by the subscript $|\mathcal{G}$ in the definition of the Casimir differential operators. In evaluating products of first order differential operators, one can only apply the Ward identity (3.8) to the rightmost operator, which acts directly on the correlation function, and not on some derivative thereof. But once we have converted the rightmost operators $\mathcal{T}^{(I_{r,1})}$ into $-\mathcal{T}^{(I_{r,2})}$, they will commute with all operators to their left, such that we can freely move them all the way to the left and proceed to apply the Ward identity to the next set of first order operators, and so on. If we finally take into account that the invariants κ of the conformal Lie algebra are symmetric, we arrive at an expression for the Casimir differential operators in terms of $\mathcal{T}^{(I_{r,2})}$.
A similar analysis can be carried out for vertex operators, see also Subsection 3.2.2. Without loss of generality we can assume that we have constructed our vertex operators in terms of the generators $\mathcal{T}^{(I_{\mathfrak{v},1})}$ and $\mathcal{T}^{(I_{\mathfrak{v},2})}$ and want to switch to constructing them from $\mathcal{T}^{(I_{\mathfrak{v},1})}$ and $\mathcal{T}^{(I_{\mathfrak{v},3})}$ instead. To do so we make use of the invariance condition

$$\left[\mathcal{T}_\alpha^{(I_{\mathfrak{v},2})}\right]_{|\mathcal{G}} = -\left[\mathcal{T}_\alpha^{(I_{\mathfrak{v},1})} - \mathcal{T}_\alpha^{(I_{\mathfrak{v},3})}\right]_{|\mathcal{G}} \tag{3.16}$$

that follows from relations (3.2) and (3.8). After we apply this to the rightmost operator in the vertex differential operator, we use the commutativity property (3.4) to move the generators $\mathcal{T}^{(I_{\mathfrak{v},1})}$ and $\mathcal{T}^{(I_{\mathfrak{v},3})}$ to the left of $\mathcal{T}^{(I_{\mathfrak{v},2})}$. We continue this replacement process until all the generators $\mathcal{T}^{(I_{\mathfrak{v},2})}$ are removed and using symmetry of the tensor κ we find

$$\mathcal{D}^{p,\nu}_{\mathfrak{v},12} = (-1)^{p-\nu} \sum_{\mu=0}^{p-\nu} \binom{p-\nu}{\mu} \mathcal{D}^{p,\nu+\mu}_{\mathfrak{v},13} \tag{3.17}$$

along with a similar relation for the Pfaffian vertex operators for $p = d/2+1$ and d even. Since the last term in this sum with $\mu = p-\nu$ is just a Casimir operator, we have managed to express all vertex differential operators that are constructed from the generators associated with $I_{\mathfrak{v},1}$ and $I_{\mathfrak{v},2}$ as a linear combination of the vertex operators associated with the pair $I_{\mathfrak{v},1}$ and $I_{\mathfrak{v},3}$ and a Casimir operator. This is the main input in proving the commutativity statements (3.14) and (3.15).

Let us start with a pair of links r, r'. Each of these links divides the set of external points into the two disjoint sets $I_{r,1}, I_{r,2}$ and $I_{r',1}, I_{r',2}$ respectively. Since the OPE diagram is a tree, it is always possible to find a pair $i,j = 1,2$ such that $I_{r,i} \cap I_{r',j} = \emptyset$. For this choice

$$[\,\mathcal{D}^p_r\,,\,\mathcal{D}^q_{r'}\,] = [\,\mathcal{D}^p_{r,i}\,,\,\mathcal{D}^q_{r',j}\,] = 0 \tag{3.18}$$

because of the commutativity property (3.4). This proves our first claim. Note that the same arguments also apply to the case in which $r = r'$ and also if one or both operators are Pfaffian, i.e. if d is even and $p, q = d/2+1$.

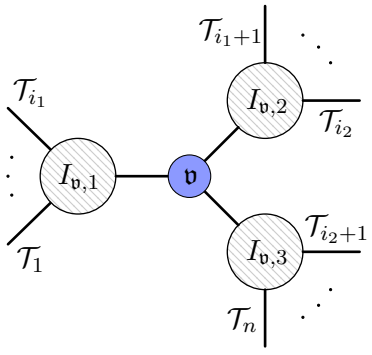

Figure 3.2: Schematic representation of a generic OPE diagram with focus on one vertex. The choice of a vertex automatically divides the diagram into three branches.

Let us now extend this argument to include vertex differential operators. In order to prove that the Casimir operators associated to a link r commute with the vertex operators associated to any vertex $\mathfrak{v}$ we recall that any choice of a vertex $\mathfrak{v}$ on an OPE diagram divides the diagram into the three distinct branches that are glued to the vertex, and we denote these by $I_{\mathfrak{v},j}$ as in Figure 3.2. A quick glance at Figure 3.2 suffices to conclude that given r and $\mathfrak{v}$ it is possible to find a pair $i \in 1,2$ and $j \in 1,2,3$ such that $I_{r,i} \subset I_{\mathfrak{v},j}$, since the link r must be in one of the three branches. It follows that $I_{r,i} \cap (I_{\mathfrak{v},j_1} \cup I_{\mathfrak{v},j_2}) = \emptyset$ for $j_1 \neq j \neq j_2$. Commutativity of Casimir and vertex differential operators then follows since we can construct the Casimir differential operators in terms of the generators for $I_{r,i}$ while using the generators for $I_{\mathfrak{v},j_1}$ and $I_{\mathfrak{v},j_2}$ for the vertex differential operators.

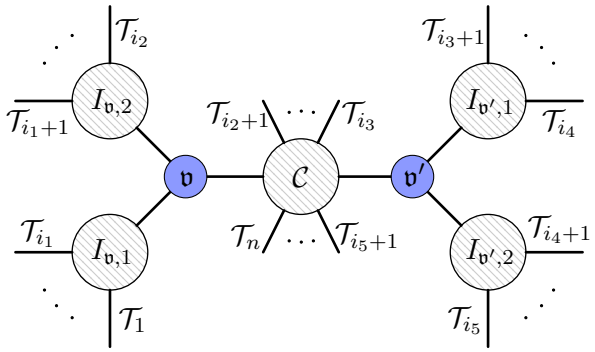

Figure 3.3: Schematic representation of a generic OPE diagram with focus on two internal vertices. Operators supported around distinct vertices trivially commute, as they can be written in terms of generators that belong to different branches.

Let us finally consider any two distinct vertices $\mathfrak{v}$ and $\mathfrak{v}'$ on an OPE diagram. As we highlight in Figure 3.3, any configuration of two vertices divides the diagram into five parts: four external branches $I_{\mathfrak{v},j}$, $I_{\mathfrak{v}',j}$, $j = 1,2$, attached to only one vertex, and the central part $\mathcal{C}$ of the diagram that is attached to both vertices $\mathfrak{v}$ and $\mathfrak{v}'$. Following what we just claimed with focus on one vertex, we can use diagonal conformal symmetry to rewrite the operators around $\mathfrak{v}$ and $\mathfrak{v}'$ to depend on disjoint sets of legs $I_{\mathfrak{v},j}$, $I_{\mathfrak{v}',j}$ with $j = 1,2$. Since generators associated to these sets commute (3.4), it follows automatically that operators constructed around different vertices must commute as well.
This implies that to prove commutativity of our set of operators, we can just focus on operators that live around one single vertex. To prove the commutativity of these vertex operators we will now make use of the integrability technology that is provided by Gaudin models.

3.2.2 The vertex system and Gaudin models

In this section, we will explain how the operators (3.11) associated with a vertex $\mathfrak{v}$ in the OPE diagram naturally arise from a specific Gaudin model, which in particular will provide us with a proof of their commutativity. Let us start by reviewing briefly how Gaudin models are defined [61, 62]. They are integrable systems naturally constructed from a choice of a simple Lie algebra $\mathfrak{g}$. Having in mind applications of these systems to conformal field theories, we will choose $\mathfrak{g}$ to be the conformal Lie algebra $\mathfrak{so}(d+1,1)$ of the Euclidean space $\mathbb{R}^d$, with basis M_α as in the previous section. The Gaudin model depends in general on m complex numbers w_j, called its sites, to which are attached m independent representations of the algebra $\mathfrak{g}$. To obtain the vertex system we address in this section, we restrict our attention here to the case $m = 3$ and associate with these three sites the representations of $\mathfrak{g}$ corresponding to the three fields attached to the vertex $\mathfrak{v}$. More precisely, using the notation defined in section 3.1 and in particular the partition $\underline{N} = I_{\mathfrak{v},1} \cup I_{\mathfrak{v},2} \cup I_{\mathfrak{v},3}$ constructed from the vertex $\mathfrak{v}$, we will attach to the three sites w_j, $j = 1,2,3$, of the Gaudin model the generators $\mathcal{T}_\alpha^{(I_{\mathfrak{v},j})}$ which define representations of $\mathfrak{g}$ in terms of first-order differential operators in the insertion points x_i.

A key ingredient in the construction of the Gaudin model is its so-called Lax matrix, whose components in the basis M^α are defined here as

$$\mathcal{L}^{\mathfrak{v}}_\alpha(z) = \sum_{j=1}^{3} \frac{\mathcal{T}_\alpha^{(I_{\mathfrak{v},j})}}{z - w_j}, \tag{3.19}$$

where z is an auxiliary complex variable called the spectral parameter. In the above equation, we have denoted the Lax matrix as $\mathcal{L}^{\mathfrak{v}}_\alpha(z)$ to emphasize that this is the matrix corresponding to the vertex $\mathfrak{v}$. For any elementary symmetric invariant tensor κ_p of degree p on $\mathfrak{g}$, there is a corresponding z-dependent Gaudin Hamiltonian of the form

$$\mathcal{H}^{(p)}_{\mathfrak{v}}(z) \quad = \quad \kappa_p^{\alpha_1\cdots\alpha_p}\mathcal{L}^{\mathfrak{v}}_{\alpha_1}(z)\cdots\mathcal{L}^{\mathfrak{v}}_{\alpha_p}(z) + \ldots, \tag{3.20}$$

where $\ldots$ represent quantum corrections, involving a smaller number of components of the Lax matrix $\mathcal{L}^{\mathfrak{v}}_\alpha$ and their derivatives with respect to z. These corrections are chosen specifically to ensure that the Gaudin Hamiltonians commute for all values of the spectral parameter and all degrees:

$$\big[\mathcal{H}^{(p)}_{\mathfrak{v}}(z), \mathcal{H}^{(q)}_{\mathfrak{v}}(w)\big] = 0, \qquad \forall\, z, w \in \mathbb{C}, \quad \forall\, p, q\ . \tag{3.21}$$

The existence of such commuting Hamiltonians was first proven in [63], using some previously established results [64] on the so-called Feigin-Frenkel center of affine algebras at the critical level. The explicit expression for the quantum corrections was obtained in [65, 66] for Lie algebras of type A and in [67] for types B, C, D, which is the case we are concerned with here (indeed, $\mathfrak{g} = \mathfrak{so}(d+1,1)$ is of type B for d odd and of type D for d even). We refer to [68] for a summary of these results. The properties of the Feigin-Frenkel center were further studied in the recent work [69], the results of which imply that the quantum corrections in $\mathcal{H}^{(p)}_{\mathfrak{v}}(z)$ are sums of terms of the form

$$\tau^{\alpha_1\cdots\alpha_q}\,\partial_z^{r_1-1}\mathcal{L}^{\mathfrak{v}}_{\alpha_1}(z)\cdots\partial_z^{r_q-1}\mathcal{L}^{\mathfrak{v}}_{\alpha_q}(z), \tag{3.22}$$

where $q < p$, $\tau^{\alpha_1\cdots\alpha_q}$ is a completely symmetric invariant tensor of degree q on $\mathfrak{g}$ and $r_1, \cdots, r_q$ are positive integers such that $r_1 + \cdots + r_q = p$. For what follows, it will be useful to consider the leading part of the Hamiltonian (3.20) alone, without quantum corrections, which we will denote as

$$\widehat{\mathcal{H}}^{(p)}_{\mathfrak{v}}(z) = \kappa^{\alpha_1\cdots\alpha_p}\mathcal{L}^{\mathfrak{v}}_{\alpha_1}(z)\cdots\mathcal{L}^{\mathfrak{v}}_{\alpha_p}(z)\ . \tag{3.23}$$

Let us finally note that the quantum corrections are absent for both the quadratic Hamiltonian $\mathcal{H}^{(2)}_{\mathfrak{v}}(z)$ and the Pfaffian Hamiltonian $\mathcal{H}^{(d/2+1)}_{\mathfrak{v}}(z)$ that exists for d even, such that these two Hamiltonians coincide with their leading parts.

To make the link with the vertex operators defined in section 3.1, we will make a specific choice of the parameters w_j of the Gaudin model. More precisely, we set

$$w_1 = 0, \qquad w_2 = 1 \qquad \text{and} \qquad w_3 = \infty\ . \tag{3.24}$$

In particular, the Lax matrix (3.19) reduces to

$$\mathcal{L}^{\mathfrak{v}}_\alpha(z) = \frac{\mathcal{T}_\alpha^{(I_{\mathfrak{v},1})}}{z} + \frac{\mathcal{T}_\alpha^{(I_{\mathfrak{v},2})}}{z-1}\ . \tag{3.25}$$

Let us now study the Gaudin Hamiltonians $\mathcal{H}^{(p)}_{\mathfrak{v}}(z)$ for this particular choice of parameters. We will first focus on their leading part $\widehat{\mathcal{H}}^{(p)}_{\mathfrak{v}}(z)$. Reinserting the above expression of the Lax matrix in eq. (3.23), we simply find

$$\widehat{\mathcal{H}}^{(p)}_{\mathfrak{v}}(z) = \sum_{\nu=0}^{p}\binom{p}{\nu}\frac{\mathcal{D}^{p,\nu}_{\mathfrak{v},12}}{z^\nu(z-1)^{p-\nu}}, \tag{3.26}$$

where $\mathcal{D}^{p,\nu}_{\mathfrak{v},12}$ is the vertex operator defined in eq. (3.11). To obtain this expression, we have used the fact that $\mathcal{T}_\alpha^{(I_{\mathfrak{v},1})}$ and $\mathcal{T}_\beta^{(I_{\mathfrak{v},2})}$ commute to bring all $\mathcal{T}_\alpha^{(I_{\mathfrak{v},1})}$'s to the left, as well as the symmetry of the tensor

$\kappa_p^{\alpha_1\cdots\alpha_p}$ to relabel the Lie algebra indices as in eq. (3.11). Noting that the fractions $z^{-\nu}(z-1)^{\nu-p}$ for $\nu = 0, \cdots, p$ are linearly independent functions of z, it is then clear that one can extract all the vertex operators $\mathcal{D}^{p,\nu}_{\mathfrak{v},12}$ from $\widehat{\mathcal{H}}^{(p)}_{\mathfrak{v}}(z)$. Note that the "extremal" operators $\mathcal{D}^{p,0}_{\mathfrak{v},12}$ and $\mathcal{D}^{p,p}_{\mathfrak{v},12}$ coincide with the Casimir operators of the fields at the branches $I_{\mathfrak{v},1}$ and $I_{\mathfrak{v},2}$ of the vertex. The same equation also holds for the Pfaffian operators $\mathcal{H}^{(d/2+1)}_{\mathfrak{v}}(z)$.

Our goal in this section is to prove the commutativity of the vertex operators $\mathcal{D}^{p,\nu}_{\mathfrak{v},12}$ using known results on Gaudin models. This would follow automatically from the commutativity (3.21) of the Gaudin Hamiltonians $\mathcal{H}^{(p)}_{\mathfrak{v}}(z)$ if these Hamiltonians contained the operators $\mathcal{D}^{p,\nu}_{\mathfrak{v},12}$. But we have already proven above that the latter are naturally extracted from the leading parts $\widehat{\mathcal{H}}^{(p)}_{\mathfrak{v}}(z)$ of the Gaudin Hamiltonians, without the quantum corrections. These quantum corrections are in general crucial for the commutativity of the Hamiltonians. However, we shall prove below that the quantum corrections of the specific Gaudin model considered here can always be expressed in terms of lower-degree Hamiltonians, and can thus be discarded without breaking the commutativity property. In this case, the non-corrected Hamiltonians $\widehat{\mathcal{H}}^{(p)}_{\mathfrak{v}}(z)$ pairwise commute for all values of the spectral parameter and all degrees, thus demonstrating the desired commutativity of the vertex operators $\mathcal{D}^{p,\nu}_{\mathfrak{v},12}$.

Let us then analyze these quantum corrections. Recall that they are composed of terms of the form (3.22). Reinserting the expression (3.25) of the Lax matrix for the present choice of parameters w_j in this equation, we find that the quantum corrections contain only terms of the form

$$\tau^{\alpha_1\cdots\alpha_q}\,\mathcal{T}^{(I_{\mathfrak{v},1})}_{\alpha_1}\cdots\mathcal{T}^{(I_{\mathfrak{v},1})}_{\alpha_\nu}\mathcal{T}^{(I_{\mathfrak{v},2})}_{\alpha_{\nu+1}}\cdots\mathcal{T}^{(I_{\mathfrak{v},2})}_{\alpha_q}, \tag{3.27}$$

with prefactors composed of powers of z and $z-1$, and where $\tau^{\alpha_1\cdots\alpha_q}$ is a completely symmetric invariant tensor on $\mathfrak{g}$ of degree $q < p$, as in eq. (3.22). In particular, $\tau^{\alpha_1\cdots\alpha_q}$ decomposes as a product of elementary symmetric invariant tensors κ_k, symmetrized over the indices α_i, with $k \leq q < p$. The correction in the above equation can thus be re-expressed as an algebraic combination of lower-degree vertex operators $\mathcal{D}^{k,\nu}_{\mathfrak{v},12}$. Since these are the coefficients of the non-corrected Hamiltonian $\widehat{\mathcal{H}}^{(k)}_{\mathfrak{v}}(z)$, recursion on the degrees shows that the quantum corrections can indeed be expressed in terms of lower-degree Hamiltonians, as anticipated.

Let us end this subsection with a brief discussion on the role played by the choice of labeling of the branches $I_{\mathfrak{v},1}$, $I_{\mathfrak{v},2}$ and $I_{\mathfrak{v},3}$ attached to the vertex $\mathfrak{v}$. As mentioned in section 3.1, this choice is arbitrary but enters the definition (3.11) of the vertex operators $\mathcal{D}^{p,\nu}_{\mathfrak{v},12}$, which in this case contain only the generators $\mathcal{T}^{(I_{\mathfrak{v},1})}_{\alpha}$ and $\mathcal{T}^{(I_{\mathfrak{v},2})}_{\alpha}$. In the context of the 3-sites Gaudin model considered in this subsection, this is related to the choice of positions w_j of the sites made in eq. (3.24). In particular, the absence of generators $\mathcal{T}^{(I_{\mathfrak{v},3})}_{\alpha}$ in the Gaudin Hamiltonians $\mathcal{H}^{(p)}(z)$ is due to the fact that we sent the site w_3 to infinity. One could have made another choice of labeling and constructed vertex operators $\mathcal{D}^{p,\nu}_{\mathfrak{v},23}$ from the generators $\mathcal{T}^{(I_{\mathfrak{v},3})}_{\alpha}$ and $\mathcal{T}^{(I_{\mathfrak{v},2})}_{\alpha}$, for instance. The corresponding choice of positions of the sites would then be related to the initial one by the Möbius transformation that exchanges 0 and ∞ and fixes 1, i.e. the inversion $z \mapsto \frac{1}{z}$. More precisely, under such a transformation of the spectral parameter, the Lax matrix of the Gaudin model behaves as a 1-form on the Riemann sphere and satisfies

$$-\frac{1}{z^2}\mathcal{L}^{\mathfrak{v}}_{\alpha}\left(\frac{1}{z}\right) = -\frac{\mathcal{T}^{(I_{\mathfrak{v},1})}_{\alpha}+\mathcal{T}^{(I_{\mathfrak{v},2})}_{\alpha}}{z} + \frac{\mathcal{T}^{(I_{\mathfrak{v},2})}_{\alpha}}{z-1}\,. \tag{3.28}$$

Acting on the correlation function $\mathcal{G}_N$, which satisfies the Ward identities (3.8), this Lax matrix then becomes

$$-\frac{1}{z^2}\mathcal{L}^{\mathfrak{v}}_{\alpha}\left(\frac{1}{z}\right)_{|\mathcal{G}} = \left[\frac{\mathcal{T}^{(I_{\mathfrak{v},3})}_{\alpha}}{z} + \frac{\mathcal{T}^{(I_{\mathfrak{v},2})}_{\alpha}}{z-1}\right]_{|\mathcal{G}}, \tag{3.29}$$

and thus coincides with the Lax matrix from which one would build the vertex operators $\mathcal{D}^{p,\nu}_{\mathfrak{v},23}$ with generators $\mathcal{T}^{(I_{\mathfrak{v},3})}_{\alpha}$ and $\mathcal{T}^{(I_{\mathfrak{v},2})}_{\alpha}$. This proves that the operators $\mathcal{D}^{p,\nu}_{\mathfrak{v},23}$ can naturally be extracted from the

generating functions

$$\frac{(-1)^p}{z^{2p}}\widehat{\mathcal{H}}_{\mathfrak{v}}^{(p)}\left(\frac{1}{z}\right)_{|\mathcal{G}} \ . \tag{3.30}$$

Using the expression (3.26) of $\widehat{\mathcal{H}}_{\mathfrak{v}}^{(p)}(z)$ in terms of the initial vertex operators $\mathcal{D}_{\mathfrak{v},12}^{p,\nu}$, we thus get that the $\mathcal{D}_{\mathfrak{v},23}^{p,\nu}$'s are linear combinations of the $\mathcal{D}_{\mathfrak{v},12}^{p,\nu}$'s, as was demonstrated by direct computation in the previous subsection. Let us note that the use of the Ward identities was a crucial step in the above reasoning, as highlighted for instance by the subscript $\mathcal{G}$ in eq. (3.30). This step should be performed with care, in particular when using the Ward identities to replace $-\mathcal{T}_\alpha^{(I_{\mathfrak{v},1})} - \mathcal{T}_\alpha^{(I_{\mathfrak{v},2})}$ by $\mathcal{T}_\alpha^{(I_{\mathfrak{v},3})}$ in the Hamiltonians (3.30). Indeed, one can use the Ward identities only for generators on the right. In order to do so, one thus has to commute generators to bring them to the right, replace them through the Ward identities and commute them back to their original place. Although this procedure can in general create non-trivial corrections, it can in fact be done freely in the case at hand: indeed, commuting operators $\mathcal{T}_{\alpha_k}^{(I_{\mathfrak{v},j})}$ and $\mathcal{T}_{\alpha_l}^{(I_{\mathfrak{v},j})}$ within the Hamiltonian $\widehat{\mathcal{H}}_{\mathfrak{v}}^{(p)}$ creates a term proportional to the structure constant $f_{\alpha_k\alpha_l}{}^{\beta}$, which vanishes when contracted with the symmetric tensor $\kappa_p^{\alpha_1\cdots\alpha_p}$. This ensures that the Hamiltonian (3.30) indeed serves as a generating function of the operators $\mathcal{D}_{\mathfrak{v},23}^{p,\nu}$ built from $\mathcal{T}_\alpha^{(I_{\mathfrak{v},3})}$ and $\mathcal{T}_\alpha^{(I_{\mathfrak{v},2})}$. A similar reasoning applies for the other choices of labeling, by considering the appropriate Möbius transformations that permute the sites 0, 1 and ∞ of our 3-site Gaudin model.

3.2.3 Restricted vertices and relations between vertex operators

In the previous subsection we have shown that all of the operators listed in eq. (3.11) commute with each other. As we have pointed out before, we did not include operators with $\nu = 0$ and $\nu = p$ in the list since these coincide with Casimir differential operators,

$$\mathcal{D}_{\mathfrak{v},12}^{p,0} = \mathcal{D}_{r_1}^p \quad , \quad \mathcal{D}_{\mathfrak{v},12}^{p,p} = \mathcal{D}_{r_2}^p \ . \tag{3.31}$$

Here r_i denotes the link that is attached to the i^{th} leg of the vertex $\mathfrak{v}$, i.e. for which $I_{r_i,j} = I_{\mathfrak{v},i}$ with either $j = 1$ or $j = 2$. The remaining $p-1$ operators satisfy one more linear relation since

$$\sum_{\nu=0}^{p}\binom{p}{\nu}\mathcal{D}_{\mathfrak{v}}^{p,\nu} = \mathcal{D}_{r_3}^p \ . \tag{3.32}$$

Let us note that this relation also applies to the Pfaffian vertex operators that exist for $p = d/2+1$ when d is even. We have used this relation to drop one of the vertex differential operators. Once these obvious relations are taken care of, the total number of commuting vertex differential operators is given by eq. (3.12) and matches precisely the maximal number of cross ratios that can be associated to a single (generic) vertex, see upper bound of eq. (3.13) in the introduction. But restricted vertices carry fewer variables, so their corresponding differential operators (constructed in the previous section) must obey further relations. It is the main goal of this subsection to discuss these relations. We will also check that, once these are taken into account, the number of remaining vertex differential operators matches the number (3.13) of cross ratios at restricted vertices.

Our arguments are based on an important auxiliary result concerning the differential operators $\mathcal{T}_\alpha^{(I)}$ that are associated to some subset $I \subset \underline{N}$ of order $|I| \leq N/2$. To present this requires a bit of preparation. Up to this point there was no need to spell out the precise form of the symmetric invariant tensors κ_p that we used to construct our differential operators. Now we need to be a bit more specific. As is well known, such tensors can be realized as symmetrized traces,

$$\kappa_p^{\alpha_1\cdots\alpha_p} = tr\Big(M^{(\alpha_1}\cdots M^{\alpha_p)}\Big) = str\big(M^{\alpha_1}\cdots M^{\alpha_p}\big) \ . \tag{3.33}$$

Here M^α denote the generators of the conformal Lie algebra and $(\dots)$ signal symmetrization with respect to the indices. In the following we shall use the symbol *str* to denote this symmetrized trace. The

trace can be taken in any faithful representation. The simplest of such choices is to use the fundamental representation. In order to construct the associated symmetric invariants more explicitly, we shall replace the index α that enumerates the basis of the conformal algebra by a pair $\alpha = [AB]$ where A, B are embedding space indices such as those we introduced in section 2.3 and $M^{[AB]} = -M^{[BA]}$. In the fundamental representation, the matrix elements of these generators take the form

$$\left(M_f^{[AB]}\right)^C{}_D = \eta^{AC}\,\delta^B_D - \eta^{BC}\,\delta^A_D\ ,$$

where η_{AB} is the Minkowski metric with signature $(d+1,1)$ and η^{AB} is its inverse. This makes it now easy to compute κ_p explicitly. The only issue arises in even d. In this case the symmetrized traces in the fundamental representation do not generate all the invariants. In order to obtain the missing invariant, one has to include the trace in a chiral representation. The standard construction employs the spinor representation in which generators $M^{[AB]}$ are represented as

$$\left(M_s^{[AB]}\right)^\sigma{}_\tau = \frac{1}{4}\,[\,\gamma^A\,,\,\gamma^B\,]^\sigma{}_\tau\ ,$$

where γ^A are the $d+2$-dimensional γ matrices and the matrix indices are $\sigma, \tau = 1, \ldots, 2^{d/2+1}$. One can then project to a chiral spinor representation with the help of $\gamma_c \sim \gamma^0 \cdots \gamma^{d+1}$.

Let us now introduce the symbol $\mathcal{T}^{(I)}$ to denote the following Lie-algebra valued differential operators

$$\mathcal{T}^{(I)} = M^\alpha \cdot \mathcal{T}^{(I)}_\alpha = \frac{1}{2} M^{[AB]} \cdot \mathcal{T}^{(I)}_{[AB]}\ .$$

Upon evaluation in some finite-dimensional representation, such as the fundamental or the spinor representation, these become matrix valued differential operators. With this notation we write our set (3.11) as

$$\mathcal{D}^{p,\nu}_{\mathfrak{v},12} = str_f\left(\underbrace{\mathcal{T}^{(I_{\mathfrak{v},1})}\ldots\mathcal{T}^{(I_{\mathfrak{v},1})}}_{\nu}\underbrace{\mathcal{T}^{(I_{\mathfrak{v},2})}\ldots\mathcal{T}^{(I_{\mathfrak{v},2})}}_{p-\nu}\right)_{|\mathcal{G}} \tag{3.34}$$

when d is odd and the parameters p and ν assume the values $p = 2, 4, \ldots, d+1$ and $\nu = 1, \ldots, p-1$, as usual. For even dimension d, on the other hand, we use the symmetrized trace in the fundamental representation for $p = 2, 4, \ldots, d$ and construct the missing Pfaffian vertex differential operators as

$$\mathcal{D}^{d/2+1,\nu}_{\mathfrak{v},12} = str_s\left(\underbrace{\mathcal{T}^{(I_{\mathfrak{v},1})}\ldots\mathcal{T}^{(I_{\mathfrak{v},1})}}_{\nu}\underbrace{\mathcal{T}^{(I_{\mathfrak{v},2})}\ldots\mathcal{T}^{(I_{\mathfrak{v},2})}}_{d/2+1-\nu}\gamma_c\right)_{|\mathcal{G}} \tag{3.35}$$

where we take the trace in the spinor representation and include the factor γ_c in the argument.

In finding relations between the vertex differential operators for restricted vertices we actually work with the total symbols of the differential operators rather than the operators themselves. This means that we replace the partial derivatives $\partial^{(i)}_\mu$ with commuting coordinates p^i_μ. The associated matrices of functions of x^μ_i and p^i_μ will be denoted by $\bar{\mathcal{T}}^{(I)}$. As before we shall add a subscript f, s to denote the matrices in the fundamental and the spinor representation. After passing to the total symbol the entries of the matrices commute and we can drop the symmetrization prescription when taking traces. As a result, the total symbols of the vertex differential operators are simply traces of powers of the matrices $\bar{\mathcal{T}}^{(I)}$.

We are now ready to state the main result needed to elucidate the relations between vertex differential operators. It concerns the matrix elements of the n^{th} power of the matrices $\bar{\mathcal{T}}^{(I)}_{f,s}$ for the fundamental and the spinor representations. In both cases, these matrix elements are functions of x^μ_i and p^i_μ with $i \in I$. Our main claim is that these matrix elements can be expressed in terms of lower order ones of the same form whenever $n > 2\mathfrak{d}_I$, where $\mathfrak{d}_I = \mathfrak{d}(I,d)$ is the integer defined in eq. (3.9). More precisely, for each matrix element AB there exist coefficients $\varrho^{(n,m)}_{AB}$ such that

$$\left(\bar{\mathcal{T}}^{(I)\,n}_f\right)^A{}_B = \sum_{m=0}^{2\mathfrak{d}_I} \varrho^{(n,m)}_{f;AB}\left(\bar{\mathcal{T}}^{(I)\,m}_f\right)^A{}_B\ . \tag{3.36}$$

Note that there is no summation over A, B on the right hand side. The coefficients ϱ_{AB} depend only on the external conformal weights Δ_i and the total symbols $\bar{\mathcal{D}}^p_{(I)}$ of the Casimir operators associated with the index set I. If the index set I has depth $\mathfrak{d}_I = 1$, for example, i.e. if the $\bar{\mathcal{T}}^{(I)}$ describe the action of the conformal algebra on a single scalar primary, then starting from $n = 3$ all matrix elements can be expressed in terms of lower order ones. In the case of the spinor representation one has a very similar relation

$$\big(\bar{\mathcal{T}}_s^{(I)\,n}\big)^\sigma{}_\tau = \sum_{m=0}^{\mathfrak{d}_I} \varrho_{s;\sigma,\tau}^{(n,m)} \big(\bar{\mathcal{T}}_s^{(I)\,m}\big)^\sigma{}_\tau \,. \tag{3.37}$$

which now applies for $n > \mathfrak{d}_I$ and involves a summation over m that ends at $\mathfrak{d}_I = \mathfrak{d}(I, d)$, see definition (3.9). So if $\mathfrak{d}_I = 1$, for example, the matrix elements of the square are expressible in terms of the matrix elements of $\bar{\mathcal{T}}_s^{(I)}$. We verify both statements (3.36) and (3.37) in Appendix A.3 using embedding space formalism.

We are now prepared to discuss relations between vertex differential operators. Let us consider a vertex $\mathfrak{v}$ inside our OPE diagram. As we have explained before, $\mathfrak{v}$ splits the set $\underline{N}$ into three subsets $I_{\mathfrak{v},i}$ with $i = 1, 2, 3$. Each of these sets determines an integer $\mathfrak{d}_i = \mathfrak{d}(I_{\mathfrak{v},i}, d)$. Let us suppose that we construct the vertex differential operators using $\mathcal{T}^{(I_{\mathfrak{v},i})}$ for $i = 1, 2$ as in eq. (3.34). If one of the integers $\mathfrak{d}_1$ or $\mathfrak{d}_2$ is smaller than r_d we immediately obtain relations among the vertex differential operators. In fact, when applied to the matrices $\bar{\mathcal{T}}^{(I_{\mathfrak{v}},1)}$, our claim (3.36) implies that all operators we obtain when $\nu > 2\mathfrak{d}_1$ can be expressed in terms of Casimir and vertex differential operators of lower order. The same is true when $p - \nu > 2\mathfrak{d}_2$, as follows again from eq. (3.36), but this time applied to $\bar{\mathcal{T}}^{(I_{\mathfrak{v}},2)}$. Consequently, for any $p \geq 2\mathfrak{d}_1, 2\mathfrak{d}_2$, we can restrict the range of the index ν to be $p - 2\mathfrak{d}_2 \leq \nu \leq 2\mathfrak{d}_1$, with $\nu = 0, p$ excluded as before.

But this does not yet include the full set of relations that appears whenever $\mathfrak{d}_3$ is smaller than $\min(\mathfrak{d}_1 + \mathfrak{d}_2, r_d)$. One of the simplest examples of this occurs in the 6-point snowflake channel in $d > 3$, see Figure 3.4, where two symmetric traceless tensor operators on two branches are combined at the central vertex $\mathfrak{v}$ to form another symmetric traceless tensor on the third branch.

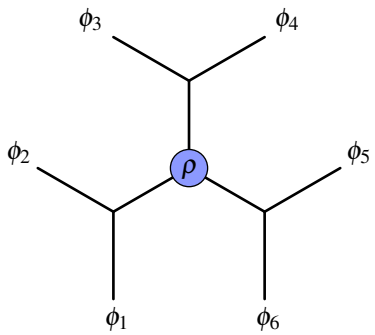

Figure 3.4: Snowflake OPE diagram. Here the tensor product of any two branches around the vertex $\mathfrak{v}$ would allow a mixed symmetry tensor of depth $\mathfrak{d} = 4$ to appear in $d \geq 6$, but diagonal conformal symmetry constrains this to match with the symmetric traceless tensor produced on the third branch.

To take restrictions from the third branch I_3 into account, it is sufficient to use the total symbol of eq. (3.16) and impose once more our dependence statement (3.36) for product matrices, this time for $\mathcal{T}^{(I_{\mathfrak{v},3})}$. This tells us that the matrix elements of powers

$$\Big(\bar{\mathcal{T}}^{(I_{\mathfrak{v},1})} + \bar{\mathcal{T}}^{(I_{\mathfrak{v},2})}\Big)^{n\ A}{}_{B} \tag{3.38}$$

with $n > 2\mathfrak{d}_3$ can be written in terms of lower order terms. In order to convert this observation into relations among the vertex differential operators of order p, we can multiply the expression (3.38) with

some appropriate powers of $\bar{\mathcal{T}}^{(I_{\mathfrak{v},i})}$, $i=1,2$, and consider the matrix elements of the products

$$\left(\bar{\mathcal{T}}^{(I_{\mathfrak{v},1})}+\bar{\mathcal{T}}^{(I_{\mathfrak{v},2})}\right)^{n}\left(\bar{\mathcal{T}}^{(I_{\mathfrak{v},2})}\right)^{\nu}\left(\bar{\mathcal{T}}^{(I_{\mathfrak{v},1})}\right)^{p-n-\nu} \tag{3.39}$$

for $n>2\mathfrak{d}_3$, any allowed value of $p>n$ and $\nu=0,\dots,p-n$. By binomial expansion, we can write the expression (3.39) as a linear combination of our basic vertex differential operators. After taking relations on the branches $I_{\mathfrak{v},1}$ and $I_{\mathfrak{v},2}$ into account, we obtain an additional nontrivial relation from the third branch $I_{\mathfrak{v},3}$. For example, in the cases where n is odd, contracting (3.38) with $\left(\mathcal{T}^{(I_{\mathfrak{v},2})}\right)^{B}{}_{A}$ leads to a relation between vertex and Casimir operators of order $n+1$ and further lower order operators. This effectively reduces the amount of vertex operators at order p by up to $p-2\mathfrak{d}_3-1$, though the actual number can be lower in case there are less than $p-2\mathfrak{d}_3-1$ vertex operators at order p left after imposing the constraints from the first two branches. If we are interested in counting the number of vertex operators at a given even order p, the procedure we just outlined is summarized in the following counting formula

$$n^{(p)}_{vdo,\mathfrak{v}}=\max\left[\left((p-2)-\sum_{i=1}^{3}\Theta_0(p-2\mathfrak{d}_i)(p-2\mathfrak{d}_i-1)\right),0\right], \tag{3.40}$$

where Θ_0 is the Heaviside step function with $\Theta_0(0)=0$, the factor $(p-2)$ gives the maximal amount of vertex operators at order p, the factor $(p-2\mathfrak{d}_i-1)$ corresponds to the number of relations introduced for every $\mathfrak{d}_i<p/2$, and the maximum enforces the number to be 0 if there are more than $(p-2)$ relations in total.

Our description of relations between vertex differential operators exploited the auxiliary statement (3.36) and did not include the Pfaffian vertex differential operators. It is clear, however, that precisely the same reasoning also applies to the latter using eq. (3.37) instead of eq. (3.36). The counting formula (3.40) gets also slightly modified for this Pfaffian case

$$n^{(p=d/2+1)}_{vdo,\mathfrak{v}}=\max\left[\left((p-2)-\sum_{i=1}^{3}\Theta_0(p-\mathfrak{d}_i)(p-\mathfrak{d}_i-1)\right),0\right]. \tag{3.41}$$

Note that the arguments we have outlined here exhibit relations between vertex operators, but we have not shown that these relations are complete, i.e. that the remaining vertex differential operators are in fact independent. A priori, it could in fact happen that the exceeding relations we get from here, or additional relations obtained from a different reasoning, could provide additional dependencies. We checked however that summing the counting formulas (3.40) and (3.41) for all allowed orders p in a given dimension d, gives rise to a number of vertex differential operators equal to the number of cross ratios (3.13) associated with every allowed vertex. This provides strong evidence in favor of the independence of our vertex differential operators. In some particularly relevant cases in lower dimensions we can also prove independence.

Example: The $N=6$ snowflake channel for $d=7$. Let us see how all of this works in the example of a snowflake channel in $d=7$, presented in Figure 3.4. We enumerate the internal links by $r=1,2,3$. The associated index sets $I_{r,i}$ are $I_{1,1}=\{1,2\}, I_{2,1}=\{3,4\},\dots$. Here we have two symmetric traceless tensors associated with $r=1,2$. In a more general OPE diagram these could produce a mixed symmetry tensor with maximal depth $\mathfrak{d}=r_d=4$, but in the snowflake diagram the field on the third link must also be a symmetric traceless tensor of depth $\mathfrak{d}(I_3,d=7)=2$. Our prescription tells us to consider operators (3.34) up to $p=8$. Eliminating powers of $\mathcal{T}_1=\mathcal{T}^{(12)}$ and $\mathcal{T}_2=\mathcal{T}^{(34)}$ higher than 4, it immediately follows that there are no vertex operators of order 8

$$\cancel{\mathcal{T}_1^{7}\mathcal{T}_2},\quad \cancel{\mathcal{T}_1^{6}\mathcal{T}_2^{2}},\quad \cancel{\mathcal{T}_1^{5}\mathcal{T}_2^{3}},\quad \cancel{\mathcal{T}_1^{3}\mathcal{T}_2^{5}},\quad \cancel{\mathcal{T}_1^{2}\mathcal{T}_2^{6}},\quad \cancel{\mathcal{T}_1\mathcal{T}_2^{7}}, \tag{3.42}$$

while there could be up to two operators of order 6

$$\cancel{\mathcal{T}_1^{5}\mathcal{T}_2},\quad \mathcal{T}_1^{4}\mathcal{T}_2^{2},\quad \mathcal{T}_1^{2}\mathcal{T}_2^{4},\quad \cancel{\mathcal{T}_1\mathcal{T}_2^{5}}, \tag{3.43}$$

and two operators of order 4

$$\mathcal{T}_1^3\mathcal{T}_2\,, \quad \mathcal{T}_1\mathcal{T}_2^3\,. \tag{3.44}$$

Here and in the following steps we are using notation for which stroked terms are dependent on lower order operators. Let us also recall that the operators with $\nu = p/2$ have been omitted to account for the relation between the vertex and Casimir differential operators for the third leg. The reduction of $\mathcal{T}_3 = \mathcal{T}^{(56)}$ to a symmetric traceless tensor implies the existence of $p - 2\mathfrak{d}_3 - 1$ relations between p order monomials. The only useful relation in this case is the one produced for $p = 6$, coming from the expansion

$$\cancel{(\mathcal{T}_1+\mathcal{T}_2)^5} = \mathcal{T}_1^5 + 5\mathcal{T}_1^4\mathcal{T}_2 + 10\mathcal{T}_1^3\mathcal{T}_2^2 + 10\mathcal{T}_1^2\mathcal{T}_2^3 + 5\mathcal{T}_1\mathcal{T}_2^4 + \mathcal{T}_2^5\,, \tag{3.45}$$

which can be contracted with either $\mathcal{T}_1$ or $\mathcal{T}_2$ and traced over to get a relation between the sixth order monomials (including the one associated to the Casimir of the third leg):

$$\cancel{(\mathcal{T}_1+\mathcal{T}_2)^5\,\mathcal{T}_2} = \cancel{\mathcal{T}_1^5\mathcal{T}_2} + 5\mathcal{T}_1^4\mathcal{T}_2^2 + 10\mathcal{T}_1^3\mathcal{T}_2^3 + 10\mathcal{T}_1^2\mathcal{T}_2^4 + 5\cancel{\mathcal{T}_1\mathcal{T}_2^5} + \cancel{\mathcal{T}_2^6}\,. \tag{3.46}$$

This reduces the amount of independent vertex operators by one, bringing us to a total of three independent operators, which matches with the number of associated cross ratios.

3.3 OPE channels and limits of Gaudin models

At this point we have defined a set of differential operators associated with the intermediate fields and the individual vertices of a given OPE diagram with N external fields. The new vertex operators were constructed in Subsection 3.2.2 from a Gaudin model with three sites, which was crucial in proving their commutativity. Our construction of the vertex operators has been *local* in its focus on a particular building block, namely a single vertex that is associated to a local element of the OPE diagram. The purpose of this section is to adopt a more *global* perspective by showing that the whole set of Casimir and vertex differential operators for any N-point OPE channel can be obtained by taking an appropriate limit of an N-site Gaudin model. The N-site Gaudin model itself makes no reference to the choice of OPE channel. The latter enters only through the choice of limit. We will therefore refer to these limits as OPE limits of the N-site Gaudin model. These OPE limits are generalizations of the so-called bending flow and caterpillar limits that have been considered in the mathematical literature, see e.g. [70–72]. The same limit of a 4-site Gaudin model - which may be identified with the elliptic Inozemtsev model [73] - has also appeared in the physics literature recently [74]. Eberhardt, Komatsu and Mizera have shown that the limit theory coincides with the hyperbolic Calogero-Sutherland model, which is known to describe the Casimir equations of 4-point conformal blocks.

3.3.1 N sites Gaudin model and OPE limits

Let us first define the Gaudin model that we will use in this section. Since this construction is similar to the one of the 3-sites Gaudin model considered in section 3.2.2, we refer to that section for details and references. As before, we consider a Gaudin model based on the conformal Lie algebra $\mathfrak{g} = \mathfrak{so}(d+1,1)$ but now with N sites, whose positions $w_1, \cdots, w_N \in \mathbb{C}$ are for the moment arbitrary. We naturally associate these sites with the N external fields in the correlation function under consideration and more precisely attach to each site $i \in \{1, \cdots, N\}$ the representation of $\mathfrak{g}$ defined by the generators $\mathcal{T}_\alpha^{(i)}$, which describe the action of the conformal transformations on the scalar field $\phi_i(x_i)$ in terms of first-order differential operators. Then we define the (components of the) Lax matrix of the model as

$$\mathcal{L}_\alpha(z, w_i) = \sum_{i=1}^{N} \frac{\mathcal{T}_\alpha^{(i)}}{z - w_i}\,. \tag{3.47}$$

The associated Gaudin Hamiltonians $\mathcal{H}^{(p)}(z, w_i)$ of degree p are given by the same equation (3.20) that we used for the 3-site case. Recall that κ_p denotes the conformally invariant symmetric tensor of degree p

and ... represent quantum corrections. The latter have the same form as in the 3-site case, see eq. (3.22). It is well known that these N-site Gaudin Hamiltonians commute, just as their three site analogues, i.e. they satisfy eq. (3.21). At the same time, it is easy to verify that they are invariant under diagonal conformal transformations,

$$\left[\mathcal{H}^{(p)}(z,w_i),\mathcal{T}_\alpha^{(\underline{N})}\right]=0,\qquad \forall\, z\in\mathbb{C},\quad \forall\, p, \tag{3.48}$$

where $\mathcal{T}_\alpha^{(\underline{N})}=\sum_{i=1}^N\mathcal{T}_\alpha^{(i)}$ are the diagonal conformal generators that also appear in the Ward identities (3.8). This means that Gaudin Hamiltonians descend to correlation functions $\mathcal{G}$.
The Hamiltonian $\mathcal{H}^{(p)}(z,w_i)$ of the N-site Gaudin model depends on the N complex parameters w_i that specify the poles of the Lax matrix. These parameters have no a priori interpretation in the context of correlation functions. Note that we can always apply Möbius transformations on the z-variable to fix three of the w_i. This is what allowed us in the previous section to set the parameters of the 3-site Gaudin model to the specific values (3.24), in which case the Lax matrix (3.25) and its corresponding differential operators contain no extra parameters. Our main claim is that we can reconstruct the entire set of 3-site Lax matrices $\mathcal{L}_\alpha^{\mathfrak{v}}(z)$, as well as the associated vertex Hamiltonians $\mathcal{H}_{\mathfrak{v}}^{(p)}(z)$, one set for each vertex $\mathfrak{v}$, from the N-site Lax matrix and the associated Gaudin Hamiltonians $\mathcal{H}^{(p)}(z)=\mathcal{H}^{(p)}(z,w_i)$ by taking appropriate scaled limits of the complex parameters w_i.

In order to make a precise statement, we need a bit of preparation. The limits we are about to discuss must depend on the choice of the OPE channel. So let us assume we are given such a channel $\mathcal{C}$. In order to define the limits we pick an (arbitrary) external edge in the diagram, which will serve as a reference point and which, up to reordering, we can suppose to have label N. As this edge is external, it is attached to a unique vertex, which we will denote by $\mathfrak{v}_*$. Such a choice of reference vertex defines a so-called rooted tree representation of the diagram. We then draw the OPE diagram on a plane, with the vertex $\mathfrak{v}_*$ situated at the top and with each vertex having two downward edges attached. Such a representation on a plane forces us to make a choice of which edges are pointing towards the left and which edges are pointing towards the right: this choice is arbitrary, and gives rise to what is called a plane (or ordered) representation of the underlying rooted tree. We give an example of such a plane rooted tree representation for an 8-point OPE diagram in Figure 3.5 below.

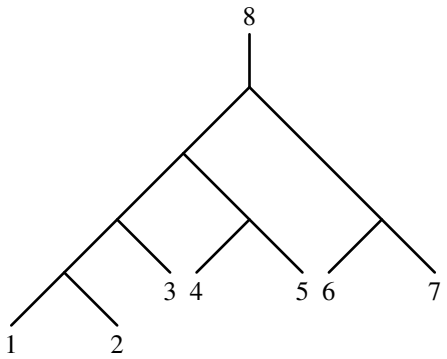

Figure 3.5: Plane rooted tree representation of an OPE diagram with 8 external fields.

Recall from section 3.1 that each vertex $\mathfrak{v}$ of the OPE diagram defines a partition $\underline{N}=I_{\mathfrak{v},1}\cup I_{\mathfrak{v},2}\cup I_{\mathfrak{v},3}$, with the sets $I_{\mathfrak{v},j}$ formed by the labels of the external fields attached to the three branches of the vertex. Although the choice of labeling of these branches was arbitrary in section 3.1, we will now fix it using the plane rooted tree representation of the diagram picked above: choose the branch $I_{\mathfrak{v},1}$ to be the one pointing to the bottom left and the branch $I_{\mathfrak{v},2}$ to be the one pointing to the bottom right. By construction, the last branch $I_{\mathfrak{v},3}$ then always points to the top and contains the reference point N.

Each vertex $\mathfrak{v}$ in the diagram is thereby associated with a sequence $s^{\mathfrak{v}} = (s_1^{\mathfrak{v}}, s_2^{\mathfrak{v}}, \dots, s_{n_{\mathfrak{v}}}^{\mathfrak{v}})$ of elements $s_a^{\mathfrak{v}} \in \{1, 2\}$. This sequence $s^{\mathfrak{v}}$ encodes the path from $\mathfrak{v}_*$ to $\mathfrak{v}$. It tells us whether we have to move to the left (for $s_a^{\mathfrak{v}} = 1$) or right (for $s_a^{\mathfrak{v}} = 2$) every time we reach a new vertex until we arrive at $\mathfrak{v}$ after $n_{\mathfrak{v}}$ steps. We shall also refer to the length $n_{\mathfrak{v}}$ of the sequence as the depth of the vertex and to $s^{\mathfrak{v}}$ as the *binary sequence* of $\mathfrak{v}$. Note that the top vertex $\mathfrak{v}_*$ has depth $n_{\mathfrak{v}_*} = 0$. Let us point out that the notion of depth used in this section refers to the distance from the root $\mathfrak{v}_*$ and is very different from the depth $\mathfrak{d}$ introduced in eq. (3.9) of the introduction.
In order to construct the limit of the Gaudin model that we are interested in, we will need to assign a polynomial $g_{\mathfrak{v}}(\varpi)$ to each vertex $\mathfrak{v}$. If $s^{\mathfrak{v}}$ is the binary sequence associated with the vertex $\mathfrak{v}$, the polynomial $g_{\mathfrak{v}}$ is defined as

$$g_{\mathfrak{v}}(\varpi) = \sum_{a=1}^{n_{\mathfrak{v}}} \varpi^{a-1} \delta_{s_a^{\mathfrak{v}},2} \ . \tag{3.49}$$

Obviously the top vertex $\mathfrak{v}_*$ is assigned to $g_{\mathfrak{v}_*}(\varpi) = 0$. The vertices of depth $n_{\mathfrak{v}} = 1$ are associated with $g_{\mathfrak{v}_1}(\varpi) = 0$ or $g_{\mathfrak{v}_2}(\varpi) = 1$, depending on whether they are reached from $\mathfrak{v}_*$ by going down to the left ($\mathfrak{v}_1$) or to the right ($\mathfrak{v}_2$).
Similarly, we can assign polynomials $f_i(\varpi)$ to each external edge $1 \leq i < N$ at the bottom of the plane rooted tree. Once again, we can encode the path from $\mathfrak{v}_*$ down to the edge i by a binary sequence $s^i = (s_1^i, s_2^i, \dots, s_{n_i}^i)$. The length n_i of the sequence s^i is also referred to as the depth of the edge i. Now we introduce

$$f_i(\varpi) = \sum_{a=1}^{n_i} \varpi^{a-1} \delta_{s_a^i,2} + \varpi^{n_i} \delta_{s_{n_i}^i,1} \ . \tag{3.50}$$

and set

$$f_N(\varpi) = \varpi^{-1} \tag{3.51}$$

for the external edge of the reference field at the top of the plane rooted tree. Thereby we have now set up all the necessary notation that is needed to construct the relevant scaling limits of the N-site Gaudin model.

We can now move on to the main result of this section, namely how to reconstruct the vertex Hamiltonians $\mathcal{H}_{\mathfrak{v}}^{(p)}(z)$ of the 3-site Gaudin model of the previous section from the N-site Hamiltonians $\mathcal{H}^{(p)}(z) = \mathcal{H}^{(p)}(z, w_i)$. To this end, we will first construct the vertex Lax matrices (3.25) from the Lax matrix (3.47) before studying the associated Hamiltonians (3.20) in the limit. As it turns out, we can recover the parameter free Lax matrix $\mathcal{L}^{\mathfrak{v}}$ that is associated with the vertex $\mathfrak{v}$ as

$$\mathcal{L}_\alpha^{\mathfrak{v}}(z) = \frac{\mathcal{T}_\alpha^{(I_{\mathfrak{v},1})}}{z} + \frac{\mathcal{T}_\alpha^{(I_{\mathfrak{v},2})}}{z-1} = \lim_{\varpi \to 0} \ \varpi^{n_{\mathfrak{v}}} \mathcal{L}_\alpha\big(\varpi^{n_{\mathfrak{v}}} z + g_{\mathfrak{v}}(\varpi), w_i = f_i(\varpi)\big) \ . \tag{3.52}$$

Let us note that in the limit, the site $w_N = \varpi^{-1}$ associated with the reference field N goes to infinity, while the sites of the other external fields approach $z = 0$ or $z = 1$ depending on whether they are located at the right or left branch of the the plane rooted tree, i.e. whether their binary sequence $s^{\mathfrak{v}}$ starts with $s_1^{\mathfrak{v}} = 1$ or $s_1^{\mathfrak{v}} = 2$. We shall prove eq. (3.52) in the third Subsection 3.3.3 through a recursive procedure that will also offer insight into the construction of the polynomials $g_{\mathfrak{v}}$ and f_i.

Let us now turn to the limit construction for the Gaudin Hamiltonians. We claim that the Hamiltonians $\mathcal{H}^{(p)}(z, w_i)$ of the N-sites Gaudin model give rise to the Hamiltonians $\mathcal{H}_{\mathfrak{v}}^{(p)}(z)$ of the different 3-sites vertex Gaudin models defined in section 3.2.2 as

$$\mathcal{H}_{\mathfrak{v}}^{(p)}(z) = \lim_{\varpi \to 0} \varpi^{p n_{\mathfrak{v}}} \mathcal{H}^{(p)}\big(\varpi^{n_{\mathfrak{v}}} z + g_{\mathfrak{v}}(\varpi), w_i = f_i(\varpi)\big) \ . \tag{3.53}$$

The fact that this statement holds for the leading part of the Hamiltonians, without quantum corrections, follows directly from the corresponding limit (3.52) of the Lax matrix

$$\varpi^{p n_{\mathfrak{v}}} \kappa_p^{\alpha_1 \cdots \alpha_p} \mathcal{L}_{\alpha_1}\big(\varpi^{n_{\mathfrak{v}}} z + g_{\mathfrak{v}}(\varpi)\big) \cdots \mathcal{L}_{\alpha_p}\big(\varpi^{n_{\mathfrak{v}}} z + g_{\mathfrak{v}}(\varpi)\big) \xrightarrow{\varpi \to 0} \kappa^{\alpha_1 \cdots \alpha_p} \mathcal{L}_{\alpha_1}^{\mathfrak{v}}(z) \cdots \mathcal{L}_{\alpha_p}^{\mathfrak{v}}(z) \ .$$

But it requires a bit of work to argue that the quantum corrections also have the required behaviour under the limit. Consider a term of the form (3.22) in the correction: by appropriately distributing the powers $\varpi^{pn_\mathfrak{v}}$, using the fact that $r_1 + \cdots + r_q = p$, and performing the change of spectral parameter $z \mapsto z'_\mathfrak{v}(\varpi) = \varpi^{n_\mathfrak{v}} z + g_\mathfrak{v}(\varpi)$ in the derivatives, we find that

$$\begin{aligned}
&\varpi^{pn_\mathfrak{v}} \tau^{\alpha_1 \cdots \alpha_q}\, \partial^{r_1-1}_{z'_\mathfrak{v}(\varpi)} \mathcal{L}_{\alpha_1}\big(z'_\mathfrak{v}(\varpi)\big) \cdots \partial^{r_q-1}_{z'_\mathfrak{v}(\varpi)} \mathcal{L}_{\alpha_q}\big(z'_\mathfrak{v}(\varpi)\big) \\
&\quad = \quad \tau^{\alpha_1 \cdots \alpha_q} \partial_z^{r_1-1}\Big(\omega^{n_\mathfrak{v}}\, \mathcal{L}_{\alpha_1}\big(\varpi^{n_\mathfrak{v}} z + g_\mathfrak{v}(\varpi)\big)\Big) \cdots \partial_z^{r_q-1}\Big(\omega^{n_\mathfrak{v}}\, \mathcal{L}_{\alpha_q}\big(\varpi^{n_\mathfrak{v}} z + g_\mathfrak{v}(\varpi)\big)\Big) \\
&\quad \xrightarrow{\varpi \to 0} \quad \tau^{\alpha_1 \cdots \alpha_q}\, \partial_z^{r_1-1} \mathcal{L}^\mathfrak{v}_{\alpha_1}(z) \cdots \partial_z^{r_q-1} \mathcal{L}^\mathfrak{v}_{\alpha_q}(z),
\end{aligned}$$

such that this correction term reduces in the OPE limit to the corresponding correction in $\mathcal{H}^{(p)}_\mathfrak{v}(z)$. As the vertex operators $\mathcal{D}^{p,\nu}_\mathfrak{v}$ and the Casimir operators $\mathcal{D}^p_r$ of the intermediate fields attached to the vertex $\mathfrak{v}$ are naturally extracted from the Hamiltonian $\mathcal{H}^{(p)}_\mathfrak{v}(z)$, the property (3.53) shows that the full set of operators defined in section 3.1 can be obtained from the limit of the N-sites Gaudin model considered here. Before the limit $\varpi \to 0$, The commutativity property (3.21) of the N-site Gaudin Hamiltonians can be written as

$$\Big[\mathcal{H}^{(p)}\big(\varpi^{n_\mathfrak{v}} z + g_\mathfrak{v}(\varpi)\big), \mathcal{H}^{(q)}\big(\varpi^{n_\mathfrak{v}} w + g_\mathfrak{v}(\varpi)\big)\Big] = 0, \qquad \forall\, z, w \in \mathbb{C}, \quad \forall\, p, q, \quad \forall\, \mathfrak{v}, \mathfrak{v}'. \tag{3.54}$$

for arbitrary ϖ, and is therefore preserved in the limit $\varpi \to 0$,

$$\big[\mathcal{H}^{(p)}_\mathfrak{v}(z), \mathcal{H}^{(q)}_{\mathfrak{v}'}(w)\big] = 0, \qquad \forall\, z, w \in \mathbb{C}, \quad \forall\, p, q, \quad \forall\, \mathfrak{v}, \mathfrak{v}'. \tag{3.55}$$

This provides an alternative proof of the commutativity of all Casimir operators $\mathcal{D}^p_r$ and vertex operators $\mathcal{D}^{p,\nu}_\mathfrak{v}$. Moreover, this statement now holds without needing to use conformal Ward identities. The proof relies on a specific choice of labeling of the edges at vertices, given by a plane rooted tree representation of the OPE diagram. Different such representations of the diagram correspond to different limits of the same underlying N-sites Gaudin model and give rise to different sets of commuting operators, which however generate the same algebra when acting on solutions of the conformal Ward identities. Finally, let us note that the above construction automatically ensures the compatibility of these operators with the conformal Ward identities, since taking appropriate limits of eq. (3.48) demonstrates that they commute with the diagonal conformal generators $\mathcal{T}^{(N)}_\alpha$.

3.3.2 Examples

Before we prove our main result, let us illustrate the construction of the operators from limits of Gaudin models with two examples. The first one addresses the so-called comb channel OPE diagrams for which we have already outlined the limit in [41]. The second example deals with the snowflake OPE channel of the $N = 6$-point function.

Comb channel. Let us consider the comb channel OPE diagram with N external fields. To apply the construction of the present section, we first need to pick a plane rooted tree representation of this diagram. We will choose to represent it with all internal edges pointing towards the bottom left. We then label the external edges of the tree as follows: we let N be the top edge of the tree, 1 be edge furthest to the left and label by $2, \cdots, N-1$ the external edges pointing to the bottom right at each vertex, from the bottom to the top. Moreover, we enumerate the vertices $\mathfrak{v} = [r]$ by an integer $r = 1, \ldots, N-2$, from bottom to top. We represent this plane rooted tree in Figure 3.6, with external edges indicated in black and vertices in blue. One can compute the limit of the Gaudin model associated with this tree using the construction outlined in the previous subsection. For the polynomials f_i that determine the parameters w_i of the Gaudin model, one finds from eq. (3.50) that

$$w_i = f_i(\varpi) = \varpi^{N-1-i}, \qquad \forall\, i \in \{1, \cdots, N\}\,. \tag{3.56}$$

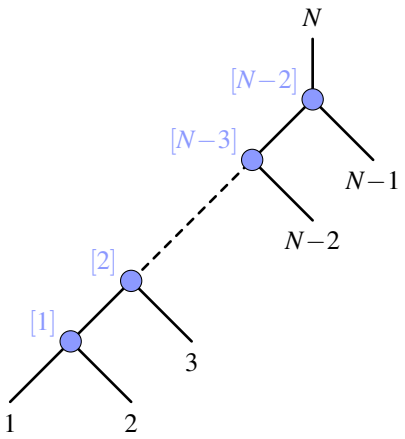

Figure 3.6: Choice of plane rooted tree representation of the comb channel OPE diagram with N points.

Let us now consider the vertices $\mathfrak{v} = [r]$, with $r = 1, \dots, N-2$. From the general construction, and formula (3.49) in particular, we find

$$n_{[r]} = N - 2 - r \qquad \text{and} \qquad g_{[r]}(\varpi) = 0, \qquad \forall\, r \in \{1, \cdots, N-2\}\ . \tag{3.57}$$

Note in particular that for this choice of plane rooted tree, the polynomial functions $g_{\mathfrak{v}}$ are all zero, since all vertices $\mathfrak{v} = [r]$ sit on the leftmost branch of the tree. The limit of the Gaudin Lax matrix

$$\mathcal{L}_\alpha(z, w_i = f_i(\varpi)) = \sum_{i=1}^{N} \frac{\mathcal{T}_\alpha^{(i)}}{z - \varpi^{N-1-i}} \tag{3.58}$$

associated with the vertex $[r]$ then reads

$$\varpi^{N-2-r} \mathcal{L}_\alpha\big(\varpi^{N-2-r} z\big) \xrightarrow{\varpi \to 0} \mathcal{L}_\alpha^{[r]}(z) = \frac{\mathcal{T}_\alpha^{(1)} + \cdots + \mathcal{T}_\alpha^{(r)}}{z} + \frac{\mathcal{T}^{(r+1)}}{z-1}. \tag{3.59}$$

In sum, the vertex Gaudin Hamiltonians of the comb channel OPE limit are

$$\varpi^{p(N-2-r)} \mathcal{H}^{(p)}\big(\varpi^{N-2-r} z\big) \xrightarrow{\varpi \to 0} \mathcal{H}_{[r]}^{(p)}(z). \tag{3.60}$$

Snowflake channel. The results of the present section allow us to discuss more general topologies of OPE diagrams than the comb channel. The first example of such a topology is the snowflake channel of 6-point functions. We represent this OPE diagram as a plane rooted tree following the conventions of Figure 3.7, where the external edges are labeled in black from 1 to 6 and the vertices are labeled in blue from [1] to [4]. Note in particular that the internal vertex of the diagram corresponds here to the label [3].

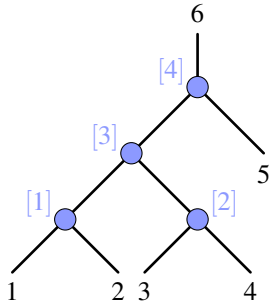

Figure 3.7: Choice of plane rooted tree representation of the snowflake OPE diagram.

We can immediately read off the depth of the four vertices as

$$n_{[1]} = n_{[2]} = 2, \qquad n_{[3]} = 1, \qquad n_{[4]} = 0. \tag{3.61}$$

We can now encode the positions of all four vertices in a binary sequence and apply the formulas (3.49) to construct the polynomials $g_{\mathfrak{v}}$, yielding

$$g_{[1]}(\varpi) = g_{[3]}(\varpi) = g_{[4]}(\varpi) = 0 \qquad \text{and} \qquad g_{[2]}(\varpi) = \varpi. \tag{3.62}$$

Similarly, one can encode the five external edges at the bottom of the diagram in binary sequences and apply eq. (3.50) to determine the positions of the $N = 6$ sites,

$$w_1 = \varpi^3, \qquad w_2 = \varpi^2, \qquad w_3 = \varpi + \varpi^3, \qquad w_4 = \varpi + \varpi^2, \qquad w_5 = 1, \qquad w_6 = \frac{1}{\varpi}. \tag{3.63}$$

Inserting this parameterization of the complex parameters w_i in terms of ϖ back into the Lax matrix of the 6-sites Gaudin model, we obtain

$$\mathcal{L}_\alpha(z) = \frac{\mathcal{T}_\alpha^{(1)}}{z-\varpi^3} + \frac{\mathcal{T}_\alpha^{(2)}}{z-\varpi^2} + \frac{\mathcal{T}_\alpha^{(3)}}{z-\varpi-\varpi^3} + \frac{\mathcal{T}_\alpha^{(4)}}{z-\varpi-\varpi^2} + \frac{\mathcal{T}_\alpha^{(5)}}{z-1} + \frac{\varpi\,\mathcal{T}_\alpha^{(6)}}{\varpi\, z-1}. \tag{3.64}$$

Given this expression and our formulas for $n_{\mathfrak{v}}$ and $g_{\mathfrak{v}}$, it is now straightforward to check the limits (3.52) for all four vertices,

$$\varpi^2\mathcal{L}_\alpha(\varpi^2 z) \xrightarrow{\varpi\to 0} \frac{\mathcal{T}_\alpha^{(1)}}{z} + \frac{\mathcal{T}_\alpha^{(2)}}{z-1}, \qquad \varpi^2\mathcal{L}_\alpha(\varpi^2 z+\varpi) \xrightarrow{\varpi\to 0} \frac{\mathcal{T}_\alpha^{(3)}}{z} + \frac{\mathcal{T}_\alpha^{(4)}}{z-1}, \tag{3.65}$$

$$\varpi\mathcal{L}_\alpha(\varpi z) \xrightarrow{\varpi\to 0} \frac{\mathcal{T}_\alpha^{(1)}+\mathcal{T}_\alpha^{(2)}}{z} + \frac{\mathcal{T}_\alpha^{(3)}+\mathcal{T}_\alpha^{(4)}}{z-1}, \qquad \mathcal{L}_\alpha(z) \xrightarrow{\varpi\to 0} \frac{\mathcal{T}_\alpha^{(1)}+\mathcal{T}_\alpha^{(2)}+\mathcal{T}_\alpha^{(3)}+\mathcal{T}_\alpha^{(4)}}{z} + \frac{\mathcal{T}_\alpha^{(5)}}{z-1}.$$

These indeed give the expected vertex Lax matrices $\mathcal{L}_\alpha^{\mathfrak{v}} = \mathcal{L}_\alpha^{[r]}$ for the vertices labeled by $r = 1, 2, 3, 4$. These two examples suffice to gain a first intuition into how we take limits of Gaudin models and thereby manage to embed the vertex Lax matrices into the full N-sites model. We will now explain the derivation of our results for general OPE diagrams.

3.3.3 Recursive proof of the limits

Subtrees. Our goal in this subsection is to prove that our limit construction is indeed able to recover all vertex Lax matrices, as we have claimed. Let us consider some OPE channel $\mathcal{C}$ represented by a plane rooted tree T. The approach that we follow is recursive. Let us consider the top vertex $\mathfrak{v}_*$ of the tree, which is by construction attached to the external edge N. We denote by e' and e'' the left and right downward edges attached to $\mathfrak{v}_*$ (which can correspond to either external or intermediate fields depending on the topology of the diagram). We can then see the tree T as being composed of the vertex $\mathfrak{v}_*$ and of two (plane rooted) subtrees with reference edges e' and e'', which we will call T' and T'' respectively. In Figure 3.8 below, we illustrate the two subtrees obtained in the example of Figure 3.5.

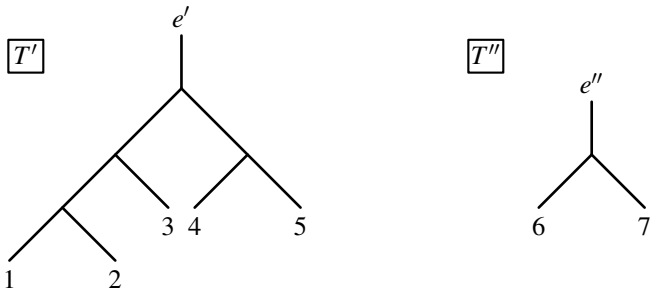

Figure 3.8: Subtrees of the tree 3.5.

We will now prove that if the limit construction of Subsection 3.3.1 holds for the subtrees T' and T'', then it also holds for the initial tree T, thus proving that it holds for any tree by induction. Let us first introduce some useful notation. We will denote by E' and E'' the external edges of T that belong to the subtrees T' and T'' respectively. Note that if T' is not trivial, i.e. if e' is not an external edge of the initial tree T, then the full set of external edges of T' is $E' \cup \{e'\}$ (since e' is external in T' but not in T). On the other hand, if e' is external in T, then we simply have $E' = \{e'\}$ and the subtree T' is trivial. Let us also denote by V, V' and V'' the set of vertices of T, T' and T'', such that $V = V' \cup V'' \cup \{\mathfrak{v}_*\}$.

Recursion relations. Recall the polynomial $g_\mathfrak{v}(\varpi)$ defined in eq. (3.49) for any vertex $\mathfrak{v} \in V$ of T in terms of the binary sequence $s^\mathfrak{v} = (s_1^\mathfrak{v}, \cdots, s_{n_\mathfrak{v}}^\mathfrak{v})$. Let us suppose that this vertex is contained in the subtree T' and thus belongs to V': it is then associated with a binary sequence $s'^\mathfrak{v} = (s_1'^\mathfrak{v}, \cdots, s_{n'_\mathfrak{v}}'^\mathfrak{v})$ in T'. By construction, the depth $n'_\mathfrak{v}$ of $\mathfrak{v}$ in T' is given by $n_\mathfrak{v} - 1$. Moreover, it is clear that the binary sequence of $\mathfrak{v}$ in T is related to that in T' by $s^\mathfrak{v} = (1, s_1'^\mathfrak{v}, \cdots, s_{n_\mathfrak{v}-1}'^\mathfrak{v})$. Indeed, since $\mathfrak{v}$ belongs to T', the path from $\mathfrak{v}_*$ to $\mathfrak{v}$ starts by going to the bottom left ($s_1^\mathfrak{v} = 1$), and is then given by the path from e' to $\mathfrak{v}$, encoded by $s'^\mathfrak{v}$. It is then clear that the polynomial $g_\mathfrak{v}(\varpi)$ defined by eq. (3.49) is related to the corresponding polynomial $g'_\mathfrak{v}(\varpi)$ defined for T' by $g_\mathfrak{v}(\varpi) = \varpi\, g'_\mathfrak{v}(\varpi)$. Similarly, if $\mathfrak{v}$ belongs to V'', we have $s^\mathfrak{v} = (2, s_1''^\mathfrak{v}, \cdots, s''^\mathfrak{v}_{n_\mathfrak{v}-1})$ and thus $g_\mathfrak{v}(\varpi) = 1 + \varpi\, g''_\mathfrak{v}(\varpi)$. In conclusion, the polynomials $g_\mathfrak{v}(\varpi)$ satisfy the recursion relation

$$g_\mathfrak{v}(\varpi) = \begin{cases} \varpi g'_\mathfrak{v}(\varpi) & \text{if } \mathfrak{v} \in V', \\ 1 + \varpi g''_\mathfrak{v}(\varpi) & \text{if } \mathfrak{v} \in V'', \\ 0 & \text{if } \mathfrak{v} = \mathfrak{v}_*. \end{cases} \tag{3.66}$$

A similar analysis can be performed for the sites $w_i = f_i(\varpi)$ associated with the external edges $i \in \underline{N}$ through eq. (3.50), distinguishing three cases. If $i = N$ is the top reference edge, then we recall that $w_N = f_N(\varpi) = \varpi^{-1}$. If $i \in E'$ is an edge belonging to the subtree T', then one can relate the binary sequences s^i and s'^i describing i in T and T' in a similar way as for the vertices in the paragraph above. We then find that the polynomial $f_i(\varpi)$ satisfy the recursion relation

$$f_i(\varpi) = \begin{cases} \varpi & \text{if } e' \text{ is external in } T, \\ \varpi f'_i(\varpi) & \text{else.} \end{cases} \tag{3.67}$$

Note that in the first case, the subtree T' is trivial and the index i is then necessarily equal to e', while in the second case i is different from e' and the subtree T' is therefore non-trivial. Finally, if $i \in E''$ belongs to the subtree T'', then we similarly find

$$f_i(\varpi) = \begin{cases} 1 & \text{if } e'' \text{ is external in } T, \\ 1 + \varpi f''_i(\varpi) & \text{else.} \end{cases} \tag{3.68}$$

Here, $i = e''$ in the first case and $i \neq e''$ in the second one.

Induction hypotheses. We will now suppose that the limit procedure defined in Subsection 3.3.1 holds for the subtrees T' and T''. To phrase these induction hypotheses more precisely, let us focus first on the subtree T'. If it is non-trivial, i.e. if e' is not external in T, the external edges of T' are $E' \cup \{e'\}$. We then introduce the Gaudin Lax matrix associated with T' as

$$\mathcal{L}'_\alpha(z) = \sum_{i \in E' \cup \{e'\}} \frac{\mathcal{T}_\alpha^{(i)}}{z - f'_i(\varpi)}, \tag{3.69}$$

where the sites associated with the external edges $E' \cup \{e'\}$ are set to the positions $f'_i(\varpi)$ prescribed by the limit procedure of Subsection 3.3.1. Here, the generators $\mathcal{T}_\alpha^{(i)}$ associated with external fields $i \in E'$ are defined by their expression in the initial tree T, while the generators associated with e' are defined by $\mathcal{T}_\alpha^{(e')} = \mathcal{T}_\alpha^{(\underline{N} \setminus E')}$. By construction, the latter satisfy the commutation relations of $\mathfrak{g}$ and commute with the other generators $\mathcal{T}_\alpha^{(i)}$, $i \in E'$, as required. Moreover, this definition ensures that the diagonal

conformal generators $\sum_{i\in\underline{N}}\mathcal{T}_\alpha^{(i)}$ of the tree T coincides with the ones $\sum_{i\in E'\cup\{e'\}}\mathcal{T}_\alpha^{(i)}$ of T' (however, as we will see, the definition of $\mathcal{T}_\alpha^{(e')}$ is in fact irrelevant for the recursive proof).
As T' is assumed to be non-trivial here, its vertex set V' is non-empty. The induction hypothesis that we make in this subsection is then that eq. (3.52) holds for the subtree T', that is to say

$$\mathcal{L}_\alpha^{\mathfrak{v}}(z)=\frac{\mathcal{T}_\alpha^{(I_{\mathfrak{v},1})}}{z}+\frac{\mathcal{T}_\alpha^{(I_{\mathfrak{v},2})}}{z-1}=\lim_{\varpi\to 0}\ \varpi^{n'_{\mathfrak{v}}}\mathcal{L}'_\alpha\big(\varpi^{n'_{\mathfrak{v}}}z+g'_{\mathfrak{v}}(\varpi)\big),\qquad\forall\mathfrak{v}\in V'. \tag{3.70}$$

In this equation, we used the Lax matrix $\mathcal{L}_\alpha^{\mathfrak{v}}(z)$ associated with the vertex $\mathfrak{v}$ as defined in the initial tree T: indeed, it is clear that this vertex Lax matrix coincides with the one associated with $\mathfrak{v}$ in the subtree T' (in particular, the subsets of external edges $I_{\mathfrak{v},1}$ and $I_{\mathfrak{v},2}$ associated with the left and right branches of $\mathfrak{v}$ are the same when defined for T as when defined for T').
Similarly, if T'' is non-trivial, we consider the associated Lax matrix

$$\mathcal{L}''_\alpha(z)=\sum_{i\in E''\cup\{e''\}}\frac{\mathcal{T}_\alpha^{(i)}}{z-f''_i(\varpi)}, \tag{3.71}$$

and suppose that it satisfies the induction hypothesis

$$\mathcal{L}_\alpha^{\mathfrak{v}}(z)=\frac{\mathcal{T}_\alpha^{(I_{\mathfrak{v},1})}}{z}+\frac{\mathcal{T}_\alpha^{(I_{\mathfrak{v},2})}}{z-1}=\lim_{\varpi\to 0}\ \varpi^{n''_{\mathfrak{v}}}\mathcal{L}''_\alpha\big(\varpi^{n''_{\mathfrak{v}}}z+g''_{\mathfrak{v}}(\varpi)\big),\qquad\forall\mathfrak{v}\in V''. \tag{3.72}$$

Proof of the induction. We are now in a position to prove that the induction carries from the subtrees T' and T'' to T. For that, we will show that the limit (3.52) holds for every vertex $\mathfrak{v}\in V$, with three cases to distinguish. If $\mathfrak{v}\in V'$ belongs to the subtree T', we will use the induction hypothesis (3.70) and the recursion relations (3.66), first case, and (3.67). Similarly, if $\mathfrak{v}\in V''$ belongs to T'', we will use the induction hypothesis (3.72) and the recursion relations (3.66), second case, and (3.68). Finally, if $\mathfrak{v}$ is the reference vertex $\mathfrak{v}_*$, then the limit will follow without having to use any induction hypothesis. As these proofs are rather technical, we gather them in Appendix A.1.

3.4 Example: 5-point conformal blocks

As an example of our construction of commuting differential operators, let us consider a correlator of five scalar fields

$$\langle\phi_1\phi_2\phi_3\phi_4\phi_5\rangle \tag{3.73}$$

and fix the OPE decomposition as in Figure 2.8.
This correlator can be be written schematically using (2.113), which for the five-point case becomes

$$\langle\phi_1\phi_2\phi_3\phi_4\phi_5\rangle=\Omega_5^{(\Delta_i)}(x_i)F^{(\Delta_i)}(u_1,\dots,u_5)\,. \tag{3.74}$$

As usual, $\Omega_5^{(\Delta_i)}(x_i)$ is a prefactor that takes into account the covariance of the correlator with respect to conformal transformations, while $F^{(\Delta_i)}(u_1,\dots,u_5)$ is a conformally invariant function which depends on five cross ratios and admits a conformal block decomposition. In order to obtain differential equations for 5-point conformal blocks, one first needs to determine which Casimir and vertex operators characterize these blocks, and then compute their action on the space of cross ratios u_i.
For the OPE decomposition of Figure 2.8, the recipe of section 3.2 instructs us to construct four Casimir operators, two for each internal leg

$$\mathcal{D}^2_{(12)}=(\mathcal{T}_1+\mathcal{T}_2)_{[AB]}\,(\mathcal{T}_1+\mathcal{T}_2)^{[BA]}\,, \tag{3.75}$$

$$\mathcal{D}^2_{(45)}=(\mathcal{T}_4+\mathcal{T}_5)_{[AB]}\,(\mathcal{T}_4+\mathcal{T}_5)^{[BA]}\,, \tag{3.76}$$

$$\mathcal{D}^4_{(12)}=(\mathcal{T}_1+\mathcal{T}_2)_{[AB]}\,(\mathcal{T}_1+\mathcal{T}_2)^{[BC]}\,(\mathcal{T}_1+\mathcal{T}_2)_{[CD]}\,(\mathcal{T}_1+\mathcal{T}_2)^{[DA]}\,, \tag{3.77}$$

$$\mathcal{D}^4_{(45)}=(\mathcal{T}_4+\mathcal{T}_5)_{[AB]}\,(\mathcal{T}_4+\mathcal{T}_5)^{[BC]}\,(\mathcal{T}_4+\mathcal{T}_5)_{[CD]}\,(\mathcal{T}_4+\mathcal{T}_5)^{[DA]}\,, \tag{3.78}$$

and one vertex operator

$$\mathcal{D}^{4,3}_{\mathfrak{v},(12)3} = (\mathcal{T}_1+\mathcal{T}_2)_{[AB]}\,(\mathcal{T}_1+\mathcal{T}_2)^{[BC]}\,(\mathcal{T}_1+\mathcal{T}_2)_{[CD]}\,(\mathcal{T}_3)^{[DA]}\,. \tag{3.79}$$

Note that – in agreement with the general recipe – the vertex operator is not uniquely defined and (3.79) can be shifted by terms proportional to $(\mathcal{T}_1+\mathcal{T}_2)^2(\mathcal{T}_3)^2$ or to the Casimir operators.

To make explicit computations, we will use the embedding space formalism we introduced in section 2.3, which allows for much faster computations given the simple form of conformal generators in this setting. Note here that the dimension of spacetime only appears in our computations as a parameter when contracting Kronecker deltas $\delta^A_A = d+2$, and can be therefore kept generic.

The first step is the choice of prefactor $\Omega_5^{(\Delta_i)}$ and cross ratios u_i. We chose to use the same conventions as [36], where the author computed 5-point blocks in the case of scalar exchange; the expression for $\Omega_5^{(\Delta_i)}$ in physical space coordinates can be easily translated into one in embedding space through the simple relation

$$X_{ij} \equiv X_i \cdot X_j = -\frac{(x_i-x_j)^2}{2}\,, \tag{2.48}$$

and one obtains (up to an overall normalization) the prefactor

$$\Omega_5^{(\Delta_i)} = \frac{\left(\frac{X_{23}}{X_{13}}\right)^{\frac{\Delta_1-\Delta_2}{2}}\left(\frac{X_{24}}{X_{23}}\right)^{\frac{\Delta_3}{2}}\left(\frac{X_{35}}{X_{34}}\right)^{\frac{\Delta_4-\Delta_5}{2}}}{(X_{12})^{\frac{\Delta_1+\Delta_2}{2}}(X_{34})^{\frac{\Delta_3}{2}}(X_{45})^{\frac{\Delta_4+\Delta_5}{2}}}\,. \tag{3.80}$$

Regarding the cross ratios, it is natural to build four of these using the same construction of the standard 4-point cross ratios (u,v) introduced in [18], but supported on two different sets of points

$$\begin{aligned} u_1 &= \frac{X_{12}X_{34}}{X_{13}X_{24}}\,, \qquad & v_1 &= \frac{X_{14}X_{23}}{X_{13}X_{24}}\,,\\ u_2 &= \frac{X_{23}X_{45}}{X_{24}X_{35}}\,, \qquad & v_2 &= \frac{X_{25}X_{34}}{X_{24}X_{35}}\,, \end{aligned} \tag{3.81}$$

while an interesting choice for the fifth cross ratio is

$$U_1^{(5)} = \frac{X_{15}X_{23}X_{34}}{X_{24}X_{13}X_{35}}\,. \tag{3.82}$$

In comparison with a potentially more natural parameterization using five independent 4-point cross ratios, as in e.g. [32, 54], this parameterization of cross ratio space has the advantage of presenting all of our differential operators with polynomial coefficients in the u_i. We will discuss this feature of polynomiality more in detail in section 4.2.2.

Using the scalar representation for generators in the embedding space (2.45), the operators (3.75)–(3.79) can be easily expressed as objects $D_{(X_i)}$ acting on the coordinates X_i^A. To obtain their action on the space of cross ratios $\mathcal{D}_{(u_i)}$, one simply conjugates the $D_{(X_i)}$ by the prefactor as in (2.111), which for the five-point case becomes

$$\mathcal{D}_{(u_i)} g^{(\Delta_i)}_{\Delta_r,l_r,\mathfrak{t}}\left(u_1,v_1,u_2,v_2,U_1^{(5)}\right) = \frac{1}{\Omega_5^{(\Delta_i)}} D_{(X_i)}\left(\Omega_5^{(\Delta_i)} g^{(\Delta_i)}_{\Delta_r,l_r,\mathfrak{t}}\left(u_1,v_1,u_2,v_2,U_1^{(5)}\right)\right)\,. \tag{3.83}$$

In practical terms, the RHS above is expressed in terms of the generators (2.45) and the expressions (3.80)–(3.82) of $\Omega_5^{(\Delta_i)}$ and the u_i's in terms of scalar products. The LHS is then obtained by solving (3.81–3.82) for five different scalar products and substituting them in the RHS after the conjugation has been done; the remaining scalar products will drop out and the final answer for the LHS will be expressed only in terms of the cross ratios.

As an attempt to simplify the analytic expressions for the differential equations, it is natural to try to extend the 4-point change of coordinates of Dolan and Osborn [19, 51]

$$u = z\bar{z}\,, \qquad v = (1-z)(1-\bar{z}) \tag{3.84}$$

to the 5-point case. A very good candidate for this purpose is the change of coordinates

$$\begin{aligned} u_1 &= z_1\bar{z}_1\,, \qquad v_1 = (1-z_1)(1-\bar{z}_1)\,, \\ u_2 &= z_2\bar{z}_2\,, \qquad v_2 = (1-z_2)(1-\bar{z}_2)\,, \\ U_1^{(5)} &= w(z_1-\bar{z}_1)(z_2-\bar{z}_2)+(1-z_1-z_2)(1-\bar{z}_1-\bar{z}_2)\,, \end{aligned} \tag{3.85}$$

which leads to the simplest expressions for the quadratic Casimirs that we could find. Indeed, by introducing the notation

$$\epsilon = \frac{d-2}{2}\,, \tag{3.86}$$

$$a = \frac{\Delta_1-\Delta_2}{2}\,, \qquad \tilde{a} = \frac{\Delta_5-\Delta_4}{2}\,, \qquad b = -\frac{\Delta_3}{2}\,, \tag{3.87}$$

$$\mathcal{U}_i^{(k)} = z_i^k\partial_{z_i} - \bar{z}_i^k\partial_{\bar{z}_i} \tag{3.88}$$

$$\mathcal{V}_{i,j} = \frac{z_i\bar{z}_i}{z_i-\bar{z}_i}\left(\mathcal{U}_i^{(0)} - \mathcal{U}_i^{(1)} + \frac{1}{z_i-\bar{z}_i}\left(1+w(z_i+\bar{z}_i-2)+\frac{z_i\bar{z}_j-z_j\bar{z}_i}{z_j-\bar{z}_j}\right)\partial_w\right) \tag{3.89}$$

$$\mathcal{W}_{i,j} = \frac{z_j+\bar{z}_j}{z_j-\bar{z}_j}\mathcal{U}_i^{(2)} + \frac{2z_i\bar{z}_i}{z_i-\bar{z}_i}\mathcal{U}_j^{(1)} + \frac{2z_i\bar{z}_i}{z_i-\bar{z}_i}\left(\frac{1}{z_i-\bar{z}_i} - w\frac{z_j+\bar{z}_j}{z_j-\bar{z}_j} + \frac{z_i\bar{z}_j-z_j\bar{z}_i}{(z_i-\bar{z}_i)(z_j-\bar{z}_j)}\right)\partial_w \tag{3.90}$$

and the expression for the $d=1$ quadratic Casimirs

$$D^{(a,b)}_{z_1,z_2} = z_1^2(1-z_1)\partial_{z_1}^2 - (a+b+1)z_1^2\partial_{z_1} - abz_1 - z_1^2z_2\partial_{z_1}\partial_{z_2} - az_1z_2\partial_{z_2} \tag{3.91}$$

one obtains the following compact expressions for the quadratic Casimirs in arbitrary dimension[2]

$$\mathcal{D}^2_{(12)} = D^{(a,b)}_{z_1,z_2} + D^{(a,b)}_{\bar{z}_1,\bar{z}_2} + 2\epsilon\mathcal{V}_{1,2} + w(1-w)\frac{(z_2-\bar{z}_2)^{1+a}}{(z_1-\bar{z}_1)^a}\mathcal{W}_{1,2}\frac{(z_1-\bar{z}_1)^a}{(z_2-\bar{z}_2)^{1+a}}\partial_w + \frac{w}{(z_1\bar{z}_1)^a}\mathcal{U}_1^{(2)}(z_1\bar{z}_1)^a\mathcal{U}_2^{(1)}\,, \tag{3.92}$$

$$\mathcal{D}^2_{(45)} = D^{(\tilde{a},b)}_{z_2,z_1} + D^{(\tilde{a},b)}_{\bar{z}_2,\bar{z}_1} + 2\epsilon\mathcal{V}_{2,1} + w(1-w)\frac{(z_1-\bar{z}_1)^{1+\tilde{a}}}{(z_2-\bar{z}_2)^{\tilde{a}}}\mathcal{W}_{2,1}\frac{(z_2-\bar{z}_2)^{\tilde{a}}}{(z_1-\bar{z}_1)^{1+\tilde{a}}}\partial_w + \frac{w}{(z_2\bar{z}_2)^{\tilde{a}}}\mathcal{U}_2^{(2)}(z_2\bar{z}_2)^{\tilde{a}}\mathcal{U}_1^{(1)}\,. \tag{3.93}$$

We have also attempted similar types of factorizations for the quartic Casimirs and the vertex operator, in the spirit of the decomposition in equation (4.14) of [51]; so far to no great avail.

[2] these expressions differ with what one would get from (3.75) and (3.76) by an overall factor of (-2).

Chapter 4

Limits of multipoint conformal blocks and OPE factorization

The goal of this chapter is to report our results of [44], where we discussed the construction of multipoint cross ratios and managed to obtain a set of cross ratios for N-point functions in the comb channel that is perfectly adapted to OPE factorizations into lower point blocks. The explicit formulas are developed for $d \leq 4$ dimensions but the ideas are more general and should admit an extension to higher d.

4.1 Setup and Summary of Results

To set up some notation we consider the comb channel for M fields in $d = 4$, see Figure 4.1.[1]

Figure 4.1: Schematic representation of an M-point comb channel OPE diagram in $d = 4$. All the external legs at the interior of the comb are scalars, while we allow fields ϕ_1 and ϕ_M to sit in a generic representation.

In general, we can insert arbitrary spinning fields at the external legs, but we shall assume that the fields ϕ_j on the external legs $j = 2, \ldots, M-1$ in the interior of the comb are scalar fields of conformal weight Δ_j. Here we introduced a dot inside the Δ symbol to distinguish external conformal dimensions from the ones that can appear in the internal legs of the comb. The two fields ϕ_1 and ϕ_M at the two sides of the comb are allowed to carry any spin, i.e. they can be symmetric traceless tensors (STTs) or even mixed symmetry tensors (MSTs). We denote the quantum numbers of these fields by $\varphi_1 = [\Delta_L, l_L, \ell_L]$ and $\varphi_M = [\Delta_R, l_R, \ell_R]$. Here the subscripts L and R stand for 'left' and 'right', respectively, corresponding to the position in the OPE diagram. Note that STTs correspond to fields with $\ell = 0$ and scalar fields are obtained if we also set $l = 0$. The intermediate fields that appear along the horizontal lines of the comb are labeled by $[s]$ with $s = 1, \ldots, M-3$. We may think of $[s] = \{s+1, s+2\}$ as a pair of consecutive integers that enumerate the two external scalar fields we attach on the two sides of the internal link. The associated intermediate fields $\mathcal{O}_{[s]}$ possess quantum numbers $\varphi_{[s]} = [\Delta_s, l_s, \ell_s]$ with non-vanishing ℓ_s in generic cases. Only ϕ_1 being scalar enforces $\ell_1 = 0$ at the first internal leg and similarly we have $\ell_{M-3} = 0$ in case ϕ_M is scalar. When $M > 4$ the total number of cross ratios for M-point functions with

[1] The following discussion is later applied to subdiagrams of an N-point comb channel OPE diagram which is why we do not set $M = N$ and will also allow for two of the external fields to carry spin.

$M-2$ scalar and two spinning insertions is given by

$$n_{cr}^{M} = 4(M-3) + 1 - 2\delta_{l_L=0=\ell_L} - 2\delta_{l_R=0=\ell_R} \ . \tag{4.1}$$

The subtractions correspond to the cases in which either one or both of the fields ϕ_1, ϕ_M are scalar. An $M=3$-point function (vertex) with one scalar external field has no cross ratios unless the other two fields are both spinning in which case there is a unique cross ratio, see the discussion in section 5.2. For $M=4$ points with at least two scalar insertions one has

$$n_{cr}^{M=4} = 5 - 2\delta_{l_L=0=\ell_L} - 2\delta_{l_R=0=\ell_R} + \delta_{l_L=0=\ell_L}\delta_{l_R=0=\ell_R} \ . \tag{4.2}$$

Note that the application to a four-point function of four scalar fields gives $n_{cr}^{M=4} = 5-4+1 = 2$, i.e. there are two cross ratios in this case as we saw in section 2.4.4.

The comb channel Hamiltonians are relatively easy to construct, at least in principle. In order to do so, we employ the first order differential operators $\mathcal{T}_{j,\alpha}, j = 1, \dots M$, that describe the behaviour of a primary field $\phi_j(x_j)$ under the conformal transformation generated by the generators M_α of the conformal algebra. In addition, let us also define

$$\mathcal{T}_{[s],\alpha} \equiv \mathcal{T}_{\alpha}^{(I_{[s],1})} = \sum_{k=1}^{s+1} \mathcal{T}_{k,\alpha} \ . \tag{4.3}$$

The Casimir differential operators $\mathcal{D}_s^p, s = 1, \dots, M-3$ are given by the p^{th}-order Casimir element in terms of the first-order operators $\mathcal{T}_{[s],\alpha}$. For generic comb channel links in $d=4$, the integer p assumes the values $p = 2, 3, 4$. In case the field ϕ_1 is a scalar, the first link only carries two quantum numbers and hence there must be one relation between the three Casimir elements so that one can restrict to $p = 2, 4$. A similar statement holds in case the field ϕ_M is scalar. In addition, we also have fourth order vertex differential operators which can be written in the form

$$\mathcal{V}_s^4 = \kappa_4^{\alpha_1 \dots \alpha_4} \mathcal{S}_{s,\alpha_1} \cdots \mathcal{S}_{s,\alpha_4}, \qquad \mathcal{S}_{s,\alpha} = \mathcal{T}_{s+1,\alpha} - \mathcal{T}_{[s-1],\alpha} \tag{4.4}$$

for $s = 1, \dots, M-2$. The operators $\mathcal{V}_1^4$ and $\mathcal{V}_{M-2}^4$ can be expressed in terms of the Casimir differential operators whenever ϕ_1 and ϕ_M are both scalar. So the number of differential operators we have constructed here coincides with the number n_{cr}^M of cross ratios, in accordance with what we discussed in Chapter 3, whose arguments instruct us that these operators are all independent and mutually commuting. In our discussion of the 6-point function we will work with a set that is slightly different from the one we described here, maximizing efficient computations over symmetry of formal expressions.

The joint eigenfunctions of these operators depend on the weights $\Delta_j, j = 2, \dots, M-1$ of the external scalar fields as well as the quantum numbers $\varphi_1 = [\Delta_L, l_L, \ell_L]$ and $\varphi_M = [\Delta_R, l_R, \ell_R]$ of the two fields ϕ_1 and ϕ_M, respectively. Of course, they also depend on the eigenvalues of the differential operators. We parametrize these eigenvalues through the quantum numbers $\varphi_{[s]} = [\Delta_s, l_s, \ell_s], s = 1, \dots, M-3$ of the internal primaries as well as the eigenvalues $\mathfrak{t}_s, s = 1, \dots, M-2$, of the vertex differential operators $\mathcal{V}_4^s$. The latter correspond to a choice of tensor structures at the vertices. These wave functions are denoted by

$$g^{\varphi_1, \Delta_j, \varphi_M}_{[\Delta_s, l_s, \ell_s; \mathfrak{t}_s]} = g^{\varphi_1, \Delta_j, \varphi_M}_{[\Delta_s, l_s, \ell_s; \mathfrak{t}_s]}(u) \tag{4.5}$$

where u denotes any set of n_{cr}^M independent cross ratios. While the construction of the n_{cr} differential equations these functions satisfy is fully algorithmic, see previous paragraph, the resulting expressions are rather lengthy in general. On the other hand, there are a few cases for which one obtains well-known differential operators. For $M=3$ with two spinning fields ϕ_1, ϕ_3, the unique vertex differential operator was shown in [43] to coincide with the lemniscatic elliptic Calogero-Moser-Sutherland Hamiltonian discovered by Etingof, Felder, Ma and Veselov in [75], see the discussion in Chapter 5. The most well-known system appears for $M=4$ when all the fields ϕ_i are scalar. In this case the resulting Hamiltonians famously coincide with those of a 2-particle hyperbolic Calogero-Sutherland model of type BC_2, [76]. The associated

eigenvalue equations turn out to be equivalent to the Casimir equations for scalar four-point blocks that were calculated and analyzed by Dolan and Osborn [19]. The corresponding eigenfunctions have been studied extensively. In mathematics this was initiated by the work of Heckman and Opdam [77]. The most relevant mathematical results were later re-derived independently in physics, starting with the work of Dolan and Osborn [18, 19, 51]. Continuing with $M = 4$ the next step is to include cases in which one or both of the fields ϕ_1 and ϕ_4 carry spin. Systems of this type have been studied in the physics literature by [20, 48, 78]. In particular so-called seed conformal blocks in $d = 4$ dimensions have been characterized through a set of Casimir differential equations. The solution for these special blocks was developed in the same papers and extensions to more general blocks in [28]. Alternatively, it is also possible to derive Casimir differential equations within the context of harmonic analysis of the conformal group [79–81]. More universally, it is also possible to construct spinning 2-particle Calogero-Sutherland Hamiltonians for any choice of spin representations of ϕ_1 and ϕ_4, using Harish-Chandra's radial component map [82] as will be discussed in [83]. The radial component map provides Casimir equations for spinning four-point blocks with external fields of arbitrary spin and in any dimension, thereby generalising vastly the current status in the physics literature. In spite of being so general, the resulting expressions for the universal spinning Casimir operators turn out to be surprisingly compact. Nevertheless, a universal solution theory has not yet been developed.

After this preparation we are now able to state the main results of [44]. These concern conformal blocks for correlation functions of N scalar fields. Obviously, the explicit form of the differential operators depends very much on the coordinates/cross ratios that are being used. Below we shall start with one relatively simple choice that consists of $2(N-3)$ four-point cross ratios, $N-4$ five-point cross ratios and $N-5$ six-point cross ratios. The total number is $4N-15$ which coincides with the number of cross ratios of a scalar N-point function in $d = 4$ when $N > 4$. These initial cross ratios are depicted in Figures 4.2a and 4.3. They turn out to be relatively well adapted to performing explicit computations. In particular, one can verify that all the coefficients of the differential operators are polynomials in these cross ratios. For this reason we shall refer to them as 'polynomial' cross ratios.

The key to the work of this Chapter is contained in subsection 4.2.4 where we introduce a new set of independent conformal invariants, first for $N = 6$ and then more generally for any number N of insertions. The $2(N-3)$ four-point cross ratios mentioned above give rise to $N-3$ pairs $(z_r, \bar{z}_r), r = 1, \ldots, N-3$, of invariants, one for each internal edge. These are direct generalisations of the usual invariants $z, \bar{z}$ that are used to parametrize four-point cross ratios. The five-point cross ratios are then employed to build $N-4$ invariants $w_r, r = 2, \ldots, N-3$, one for each non-trivial vertex. The construction of the w_r is an immediate extension of the variable w that we introduced in (3.85) to complement the variables $z_1, \bar{z}_1, z_2, \bar{z}_2$. But starting with $N = 6$, there exists $N-5$ additional independent invariants that involve the six-point cross ratios we described above. From these we define new conformal invariants $\Upsilon_r, r = 2, \ldots, N-4$, one for each internal edge in which an MST can propagate. This invariant is first constructed for the unique intermediate MST exchange in a six-point comb channel diagram for scalar external fields, see eq. (4.29), and then extended to higher numbers $N \geq 6$ of insertions at the end of section 4.2.4. In the same subsection we also provide a nice geometrical interpretation for all the new conformal invariants which we shall refer to as comb channel OPE coordinates.

The association of these invariants with specific links and vertices is much more than mere counting. Consider a link $r \in \{2, \ldots, N-4\}$ in which an MST propagates. This link comes with a set of three invariants $z_r, \bar{z}_r, \Upsilon_r$. Our central claim concerning OPE factorization of multipoint blocks can now be formulated after rewriting the blocks g in terms of the OPE coordinates $g = g(z_r, \bar{z}_r, \Upsilon_r; w_s)$. When these functions are expanded around $z_b = \bar{z}_b = 0 = \Upsilon_b$[2] for one particular value of $b \in \{2, \ldots, N-4\}$ the

[2]Note that the three limits do not commute. We take the limit $\bar{z}_b \to 0$ first before taking z_b and Υ_b to zero. Once taken the first limit, the order of limits for the last two two variables does not matter.

leading term is claimed to be of the form

$$g^{\Delta_i}_{[\Delta_r,l_r,\ell_r;\mathfrak{t}_r]}(z_r,\bar{z}_r,\Upsilon_r;w_s) = z_b^{\frac{1}{2}(\Delta_b+l_b+\ell_b)}\bar{z}_b^{\frac{1}{2}(\Delta_b-l_b-\ell_b)}\Upsilon_b^{\ell_b}\times \tag{4.6}$$
$$\times\left(g^{\Delta_{i\leq b+1},[\Delta_b,l_b,\ell_b]}_{[\Delta_r,l_r,\ell_r;\mathfrak{t}_s]}(z_r,\bar{z}_r,\Upsilon_r;w_s)^{r<b}_{s<b}\times g^{[\Delta_b,l_b,\ell_b],\Delta_{i>b+1}}_{[\Delta_r,l_r,\ell_r;\mathfrak{t}_s]}(z_r,\bar{z}_r,\Upsilon_r;w_s)^{r>b}_{s\geq b}+O(z_b,\bar{z}_b,\Upsilon_b)\right)\,.$$

In the first line we have displayed the leading exponents in any of the three variables. Note that these are determined by the quantum numbers of the exchanged intermediate field $\phi_{[b]}$. In case the latter is an STT, i.e. iff $\ell_b = 0$, this leading term is familiar from the theory of blocks for four-point functions of scalars. Once this term in the first line of the expression is factored out, the remaining function admits a power series expansion in the three variables $z_b, \bar{z}_b$ and Υ_b. The constant term in this power series expansion turns out to factorize into a product of two eigenfunctions of Gaudin Hamiltonians with $M_1 = b+2$ and $M_2 = N-b$ sites, respectively. The sub- and superscripts we have placed on the eigenfunctions apply to both the dependence of quantum numbers and conformal invariants. Let us note that this OPE factorization also holds for $b = 1$ and $b = N-3$ except that in these two cases the quantum number $\ell_b = 0$ so that the prefactor in the first line only contains powers of z_b and $\bar{z}_b$. In addition, one of the two blocks in the second line is simply a constant. One can actually verify such factorization formulas whenever explicit formulas for the blocks are available, e.g. for $d = 1$ comb-channel blocks which have been constructed in [36]. We have included one such explicit check for a six-point function in Appendix B.4. To prove the remarkable result (4.6) beyond those cases in which the blocks are known, the differential operators play a decisive role. Strictly speaking, our central claim remains somewhat conjectural for $N > 6$. But in the case of $N = 6$ we are able to establish it rigorously. A scalar six-point function in $d = 4$ dimensions depends on nine cross ratios. We parametrize these through the variables $z_r, \bar{z}_r, r = 1,2,3$, $\Upsilon = \Upsilon_2$ and $w_s, s = 1,2$. When we perform the limit on the variables $(z_2, \bar{z}_2, \Upsilon)$ that are associated with the internal MST exchange along the central link, the block factorizes into a product of two spinning $M = 4$-point blocks with a single spinning field and three scalars in each of them. Such spinning four-point blocks depend on three variables each. In our special parametrization these are given by $(z_1, \bar{z}_1; w_1)$ and $(z_3, \bar{z}_3; w_2)$, respectively. As we recalled above, spinning four-point blocks may be characterized as solutions of a specific set of differential equations that has been worked out at least for some examples in the CFT literature, see in particular [78]. The full set of these differential equations can been obtained with the help of Harish-Chandra's radial component map [83]. The strategy to prove our factorization result is to evaluate the limit of the six-site Gaudin Hamiltonians as $z_2, \bar{z}_2, \Upsilon$ are sent to zero and to map the resulting operators to the differential operators for spinning four-point blocks through an appropriate change of variables. Similarly, one can also consider the limit in which the pairs $(z_1, \bar{z}_1)$ and $(z_3, \bar{z}_3)$ are both sent to zero. Our OPE factorization states that the leading term in the resulting expansion is given by a spinning four-point block for two scalar and two spinning fields. Once again, it is possible to verify this claim by mapping the relevant differential operators onto each other.

Let us now briefly outline the content of each section. The next section is entirely devoted to a discussion of cross ratios. After a brief review of the two most commonly used sets of cross ratios for four-point functions, we will extend both of them to multipoint functions. The usual cross ratios u, v can be generalised to higher numbers N of insertion points in such a way that the Casimir differential operators for comb channel blocks have polynomial coefficients, at least for $N \leq 10$. The relevant *polynomial cross ratios* for multipoint functions are defined in section 4.2.2. While these cross ratios have some nice features, they are not well adapted to taking OPE limits. For this reason we shall introduce a second set of conformal invariants which we dub *OPE cross ratios*. We do so for $N = 5$ and $N = 6$ points first before discussing the case $N > 6$, using a nice geometric/group theoretic interpretation of these variables. Section 4.3 is devoted to a study of the OPE limits. The discussion focuses on $N = 6$-point functions. After a brief review of the Gaudin Hamiltonians that characterize comb channel blocks, we derive the asymptotic behaviour in the first line of eq. (4.6) and show that the leading term indeed factorizes into

a product of functions of the respective variables. These functions may be characterized through certain differential operators which can be obtained by studying the limiting behaviour of the original Gaudin Hamiltonians. In particular, it turns out that the Gaudin Hamiltonians split into two sets of operators that act on a disjoint subset of cross ratios. In section 4.4 we will identify these limiting differential operators with the Casimir operators of spinning four-point blocks. To this end we briefly sketch the results of [83] on the universal spinning Casimir operators. We cast these results in the form of universal spinning Calogero-Sutherland Hamiltonians before we compare these operators with those we obtained in section 4.3 when taking the OPE limit of multipoint functions. It turns out that the two sets of operators coincide. This establishes our result (4.6), including the identification of the leading term with a product of lower point conformal blocks.

4.2 Cross ratios for multipoint correlation functions

As we have explained in the introduction, there is much freedom in introducing sets of independent conformally invariant variables. In this section we introduce two such sets for multipoint correlation functions. The first one is referred to as polynomial cross ratios and it is a direct generalisation of the common four-point cross ratios u and v to scalar correlators with $N > 4$ field insertions. When written in these cross ratios, all the $N-3$ quadratic Casimir differential operators that characterize the comb channel multipoint blocks in sufficiently large dimension d turn out to possess polynomial coefficients, at least for $N \leq 10$. The second set of conformal invariants we introduce in this section is fundamental to all of our subsequent discussion. These new coordinates are akin to the variables z and $\bar{z}$ that are widely used for four-point functions. They possess a large number of remarkable properties. Most importantly for us, they behave well under dimensional reductions and when taking OPE limits, which is why we shall also refer to them as *OPE cross ratios*. In addition, these variables possess a nice geometric interpretation.
In the first subsection, the case of $N = 4$ will be briefly reviewed to highlight some of the properties of the cross ratios u, v and $z, \bar{z}$ that make them so useful and are desirable to maintain as we go to higher number N of insertions. The polynomial cross ratios are then introduced in the second subsection. Next, in the third subsection, we discuss the OPE coordinates for $N = 5$ where there is a single qualitatively new invariant that was introduced in [43] already. The fourth subsection contains the construction of a new invariant that is attached to the central link of the six-point comb channel diagram. We introduce this invariant and provide a geometrical interpretation. The latter is then used to extend the construction of comb channel invariants in $d = 4$ to $N > 6$ insertion points.

4.2.1 Prologue: Cross ratios for four-point blocks

In order to enter the discussion of cross ratios for correlation functions of scalar fields, we will begin with the well known case of $N = 4$ operators. As we saw in section 2.4.4, there exist two cross ratios one can build from the four insertions points $x_i, i = 1, \ldots, 4$,

$$u = \frac{X_{12}X_{34}}{X_{13}X_{24}}\,, \qquad v = \frac{X_{14}X_{23}}{X_{13}X_{24}}\,, \tag{4.7}$$

where we used the embedding space vectors X_i associated with the x_i coordinates, see section 2.3. These cross ratios can be represented schematically as in Figure 4.2a, where we disposed the four points along a square and every colored edge corresponds to a scalar product present in the associated cross ratio, with lines that intersect being present in the denominator. When written in these four-point cross ratios u, v, the second order Casimir operator takes the form, see eq. (2.10) in [51],

$$\frac{1}{2}\mathcal{D}^2_{(12)} = (1-u-v)\partial_v\left(v\partial_v + a + b\right) + u\partial_u\left(2u\partial_u - d\right) - (1+u-v)\left(u\partial_u + v\partial_v + a\right)\left(u\partial_u + v\partial_v + b\right), \tag{4.8}$$

with the two parameters $2a = \Delta_2 - \Delta_1$ and $2b = \Delta_3 - \Delta_4$ determined by the conformal weights Δ_i of the four external scalar fields. We observe that in these coordinates, the Casimir operator takes a

relatively simple form in which all the coefficient functions possess a polynomial dependence on the two cross ratios u and v. But it also has some less pleasant features. In particular, it is not directly amenable to a power series solution in the variables u, v. In order to formalize this a bit more, let us introduce the notion of a *grade* in some variable w. We say that a differential operator of the form $cw^n\partial_w^m$ has w-grade $\mathrm{gr}_w(cw^n\partial_w^m) = n - m$. When the grade is applied to some linear combination of such simple 'monomial' differential operators it returns a set of grades, one element for each term. For the grades of the Casimir operator (4.8) we find

$$\mathrm{gr}_u\left(\mathcal{D}^2_{(12)}\right) = \{0, 1\} \quad , \quad \mathrm{gr}_v\left(\mathcal{D}^2_{(12)}\right) = \{-1, 0, 1\} \ . \tag{4.9}$$

While the u-grade of the individual terms is non-negative, this is not the case for the v-grade. In other words, when written in the variables u, v, the quadratic Casimir operator contains simultaneously terms that lower and terms that raise the degree of a polynomial in v.

In order to analyze the eigenfunctions of four-point Casimir operators, Dolan and Osborn switched to another parametrization of the cross ratios through the complex variables z and $\bar{z}$,

$$u = z\bar{z} \quad , \quad v = (1 - z)(1 - \bar{z}) \ . \tag{4.10}$$

We point out that the change of variables is not one-to-one since u and v are invariant under the action of $\mathbb{Z}_2$ whose non-trivial element exchanges z with $\bar{z}$. Hence, functions of the cross ratios u and v correspond to $\mathbb{Z}_2$ invariant functions of $z, \bar{z}$. The invariants $z, \bar{z}$ possess a nice geometric interpretation. As we saw in the discussion around Figure 2.5, conformal transformations can be used to move the insertion points to the special positions $x_2 = 0$, $x_4 = \vec{e}_1$, $x_3 = \infty$ where $\vec{e}_1$ denotes the unit vector along the first coordinate direction of the d-dimensional Euclidean space. This choice of a conformal frame is stabilised by a subgroup $SO(d-1) \subset SO(d)$ of the rotation group that describes rotations around the first coordinate axis. These rotations can be used to move x_1 into the plane spanned by $\vec{e}_1$ and $\vec{e}_2$. The invariants $z, \bar{z}$ are the complex coordinates of x_1 in this plane. Let us note that in these coordinates it is very easy to implement the restriction to $d = 1$ for which there exists only one cross ratio, namely $z = \bar{z}$.

The geometric interpretation of the $z, \bar{z}$ coordinates, and in particular the simplicity of the reduction to $d = 1$, also manifests itself in another property. It turns out that the so-called Gram determinant of N insertion points takes a particularly simple form when written in $z, \bar{z}$. This is constructed starting from the embedding space coordinates $X_i \in \mathbb{R}^{1,d+1}$ associated with the N insertion points x_i. The determinant of the matrix of scalar products $X_{ij} = \langle X_i, X_j \rangle$ is then what is usually called the Gram determinant, which encodes information on independence of the x_i. These vectors are in fact linearly dependent if and only if the associated Gram determinant is zero. For $N = 4$ points $x_i \in \mathbb{R}^d$ the associated Gram determinant takes the form

$$\det(X_{ij})\big|_4 = (z - \bar{z})^2 X_{13}^2 X_{24}^2 \, . \tag{4.11}$$

We see that this expression is rather simple when written in terms of the cross ratios $z, \bar{z}$, much simpler than its expression in terms of u, v. Since any four vectors $X_i \in \mathbb{R}^{1,2}$ are linearly dependent, the four-point Gram determinant must vanish in $d = 1$. This is achieved by setting $z = \bar{z}$ so that all four points lie on a single line, in agreement with our discussion in the previous paragraph. The simplicity of the Gram determinant in the $z, \bar{z}$ coordinates means that these are very well suited to implement the dimensional reduction.

Next we turn to a discussion of the Casimir operator. When the expression we spelled out in eq. (4.8) is rewritten in terms of z and $\bar{z}$ it acquires the form

$$\begin{aligned}\mathcal{D}^2_{(12)} = {} & 2z^2(1-z)\frac{\partial^2}{\partial z^2} + 2\bar{z}^2(1-\bar{z})\frac{\partial^2}{\partial \bar{z}^2} - 2(a+b+1)\left(z^2\frac{\partial}{\partial z} + \bar{z}^2\frac{\partial}{\partial \bar{z}}\right) \\ & - 2ab(z+\bar{z}) + 2\varepsilon\frac{z\bar{z}}{z-\bar{z}}\left((1-z)\frac{\partial}{\partial z} - (1-\bar{z})\frac{\partial}{\partial \bar{z}}\right)\end{aligned} \tag{4.12}$$

with $\varepsilon = d-2$. We note that the resulting expression is slightly longer than for the original set u, v of four-point cross ratios, and its coefficients are no longer polynomial. However, the main advantage of the $z, \bar{z}$ coordinates is that they admit a rather simple implementation of the OPE limit in which we send $\bar{z} \to 0$ first, followed by the limit $z \to 0$. When $|\bar{z}| < |z|$ we can actually expand the last term in the expression for $\mathcal{D}^2_{(12)}$ in a power series. In the resulting expression, all terms possess non-negative $\bar{z}$ grade, i.e.

$$\mathrm{gr}_{\bar{z}}\left(\mathcal{D}^2_{(12)}\right) \in \{0, 1, 2, \dots\} \ . \tag{4.13}$$

In particular, there is no term in which the derivatives with respect to $\partial_{\bar{z}}$ outnumber the multiplications with $\bar{z}$. Keeping only terms of vanishing $\bar{z}$-grade we have

$$\mathcal{D}^2_{(12)} \sim 2z^2(1-z)\frac{\partial^2}{\partial z^2} + 2\bar{z}^2\frac{\partial^2}{\partial \bar{z}^2} - 2(a+b+1)z^2\frac{\partial}{\partial z} - 2abz - 2\varepsilon\bar{z}\frac{\partial}{\partial \bar{z}} + \dots \tag{4.14}$$

where $\dots$ stand for terms of positive $\bar{z}$ grade. We can now continue and analyze the z grade of the leading term in the previous formula. Obviously, the leading terms have non-negative z grade with the terms of vanishing grade given by

$$\mathcal{D}^2_{(12)} \sim 2z^2\frac{\partial^2}{\partial z^2} + 2\bar{z}^2\frac{\partial^2}{\partial \bar{z}^2} - 2\varepsilon\bar{z}\frac{\partial}{\partial \bar{z}} + \dots \tag{4.15}$$

where now the $\dots$ contain also terms of positive z grade. Now let us apply this discussion to the problem of finding eigenfunctions of the Casimir operator

$$\mathcal{D}^2_{(12)} g_{\Delta,l}(z,\bar{z}) = \left[\Delta(\Delta-d) + l(l+d-2)\right] g_{\Delta,l}(z,\bar{z}) \ . \tag{4.16}$$

For the limiting regime in which we replace the Casimir operator by the expression in eq. (4.15) the eigenvalue problem is very easy to solve,

$$g_{\Delta,l}(z,\bar{z}) \sim z^{\frac{\Delta+l}{2}}\bar{z}^{\frac{\Delta-l}{2}} c_{\Delta,l} + \dots \tag{4.17}$$

where $c_{\Delta,l}$ is a non-vanishing constant factor that is not determined by the eigenvalue equation and depends on the normalisation. Since all the terms we have omitted from our original Casimir operator have positive grade, we conclude that it possesses an eigenfunction of the form

$$g_{\Delta,l}(z,\bar{z}) \ = \ z^{\frac{\Delta+l}{2}}\bar{z}^{\frac{\Delta-l}{2}} f_{\Delta,l}(z,\bar{z}) = z^{\frac{\Delta+l}{2}}\bar{z}^{\frac{\Delta-l}{2}}\left(c_{\Delta,l} + O(z,\bar{z})\right) \tag{4.18}$$

where the function f possesses a power series expansion in z and $\bar{z}$ with non-vanishing constant term $c_{\Delta,l}$.

Before we turn to higher number $N > 4$ of insertion points we want to summarise a few of the desirable properties of the coordinates $z, \bar{z}$ that seem relevant. To begin with, when working with multipoint correlators it is certainly very desirable to have simple expressions for the Gram determinant. Note that N points $X_i \in \mathbb{R}^{1,d+1}$ are linearly dependent for $N > d+2$. So if we keep the dimension d fixed, going to larger values of N will inevitably lead to vanishing Gram determinants. Consequently, an N-point function in dimension $d < N-2$ lives on a subspace within the larger space of cross ratios for $d \geq N-2$. The explicit description of this subspace is easiest when we work with coordinates in which the Gram determinant factorizes into simple functions of the cross ratios. More importantly, we would like to find coordinates that are well adapted to the OPE limit in the sense we outlined above. For higher multipoint functions this means to find coordinates and association of subsets thereof with the internal links of the OPE diagram such that eigenfunctions admit a power series expansion in all these link variables. For $N > 4$ the leading term of these expansions will no longer be constant, of course, but it should factorize into a product of functions that are associated with the two subdiagrams that are connected by the link. We will indeed be able to construct such variables for all N-point comb channel diagrams, at least in $d = 4$ dimensions.

4.2.2 Polynomial cross ratios for comb channel multipoint blocks

In this subsection we address the construction of sets of cross ratios which make all coefficients of comb channel differential operators polynomial. Because of this property, we dub this set *polynomial cross ratios*. We have seen this feature before when we wrote the Casimir operator for four-point functions in the coordinates u, v, see eq. (4.8). In this sense, the polynomial cross ratios we are about to construct are natural extensions of the four-point cross ratios u, v.

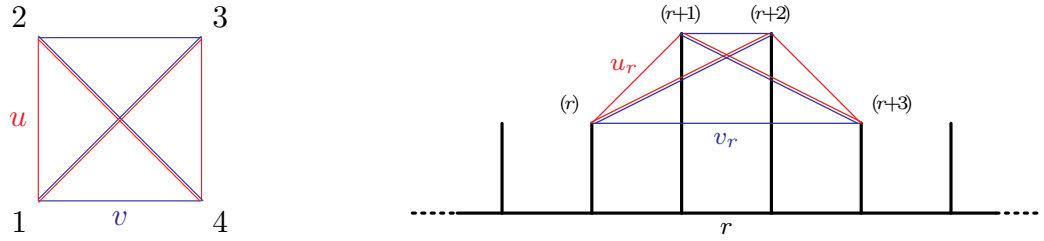

(a) Four-point cross ratios **(b)** Construction of four-point cross ratios around internal leg r

Figure 4.2: Schematic representation of the four-point cross ratios u and v, where intersecting lines correspond to terms in the denominator. The same type of cross ratios can be constructed around every internal leg by focusing on the closest four points.

It is possible to construct the four-point cross ratios of the same type for each internal link of the comb channel OPE diagram. Consider the link with label $r = 1, \dots, N-3$. Then the four nearest neighbor insertion points are x_i with $i = r, r+1, r+2, r+3$, see Figure 4.2b. From these we can build two four-point cross ratios u_r, v_r using the same expressions as in the case of four-point functions, i.e. for an N-point comb channel diagram we can construct $(N-3)$ sets of u, v type cross ratios through

$$u_r = \frac{X_{r(r+1)}X_{(r+2)(r+3)}}{X_{r(r+2)}X_{(r+1)(r+3)}}\,, \qquad v_r = \frac{X_{r(r+3)}X_{(r+1)(r+2)}}{X_{r(r+2)}X_{(r+1)(r+3)}}\,, \qquad r = 1, \dots, N-3\,. \tag{4.19}$$

Here we have used the construction in terms of the embedding space variables X_i, see previous subsection. The $2(N-3)$ cross ratios we have introduced so far do not suffice to generate all conformal invariants as soon as $d > 2$ and $N > 4$. We conjecture that a set of cross ratios that makes all coefficients of the N-point comb channel Casimir operators polynomial in $d \geq 2$ is obtained if we complement the four-point cross ratios (u_r, v_r) introduced above by the following set of m-point cross ratios

$$U_s^{(m)} = \frac{X_{s(s+m-1)}\prod_{j=1}^{m-3} X_{(s+j)(s+j+1)}}{\prod_{j=0}^{m-3} X_{(s+j)(s+j+2)}}\,, \qquad s = 1, \dots, (N-m+1)\,, \qquad m = 5, \dots, N. \tag{4.20}$$

The total number of cross ratios we have introduced is $N(N-3)/2$ which coincides with the number of independent cross ratios as long as $d \geq N-2$. We checked our claim of polynomial dependence explicitly by verifying that all comb channel quadratic Casimir operators that appear for up to $N = 10$ external scalar fields indeed have polynomial coefficients in the cross ratios we have introduced. In addition, we also verified the claim for vertex differential operators with $N \leq 6$. We shall often refer to the variables (4.20) as the *m-point polynomial cross ratios*, since they are constructed around every set of m adjacent points in an N-point function. The first few examples of these type of cross ratios with low values of m are represented schematically in Figure 4.3.

If the dimension d drops below its lower bound or alternatively, if for fixed dimension d the number N of insertion points satisfies $N > d+2$, there are additional relations between the cross ratios we have introduced. These can be found by computing the Gram determinant for the scalar products X_{ij}. Given d, the relations allow to express our m-point cross ratios $U^{(m)}$ with $m > d+2$ through cross ratios involving a lower number of insertion points. In other words, in dimension d the space of N-point conformal invariants is generated by the cross ratios $U_s^{(m)}$ with $m \leq d+2$. It is easy to verify that the number of such cross ratios indeed coincides with the expected number n_{cr}, see eq. (4.1).

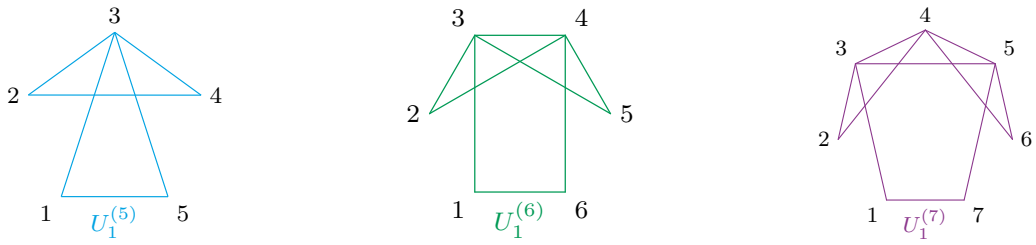

(a) Five-point cross ratio **(b)** Six-point cross ratio **(c)** Seven-point cross ratio

Figure 4.3: Polynomial cross ratios for five, six, and seven point functions. The colored lines correspond to scalar products present in the expression of the cross ratio, with lines that intersect outside vertices corresponding to terms in the denominator.

In d dimensions, there are $N-d-1$ of these m-point cross ratios with maximal value $m=d+2$. In particular, the first time one of these cross ratios is needed is for $(d+2)$-point functions. For example, to construct the conformal invariants of an N-point function in $d=3$ we need m-point cross ratios with $m=4,5$ only and the first time a five-point cross ratio appears is for $N=5$. Similarly, in $d=4$ dimensions we work with m-point cross ratios for $m=4,5,6$ and all these invariants actually appear starting with $N=6$ insertion points. Since we are mostly interested in $d=3,4$, it will be sufficient for us to analyze Casimir operators for correlation functions of $N=5$ and $N=6$ scalar fields.
The set of polynomial cross ratios we have introduced in this subsection leads to relatively simple expressions of Casimir operators, but it does not behave nicely when taking OPE limits of fields, i.e. the OPE limit cannot simply be obtained by taking a limit for a subset of cross ratios to specific values. We will now turn to the construction of new variables that are more suitable for OPE limits.

4.2.3 Five-point OPE cross ratios

We begin our discussion of the new OPE cross ratios with $N=5$. As we reviewed above, five insertion points give rise to five independent cross whenever $d\geq 3$. Our recipe for the construction of polynomial cross ratios in the previous subsection provides us with the following set

$$u_1=\frac{X_{12}X_{34}}{X_{13}X_{24}}\,,\qquad v_1=\frac{X_{14}X_{23}}{X_{13}X_{24}}\,,\qquad U_1^{(5)}=\frac{X_{15}X_{23}X_{34}}{X_{24}X_{13}X_{35}}\,,\tag{4.21}$$
$$u_2=\frac{X_{23}X_{45}}{X_{24}X_{35}}\,,\qquad v_2=\frac{X_{25}X_{34}}{X_{24}X_{35}}\,,$$

that corresponds precisely to the set we used in (3.81) and (3.82).
For this case we did introduce a new parametrization already in (3.85) through the following set of relations

$$\begin{aligned}u_1&=z_1\bar{z}_1\,,\qquad v_1=(1-z_1)(1-\bar{z}_1)\,,\\ u_2&=z_2\bar{z}_2\,,\qquad v_2=(1-z_2)(1-\bar{z}_2)\,,\\ U_1^{(5)}&=w_1(z_1-\bar{z}_1)(z_2-\bar{z}_2)+(1-z_1-z_2)(1-\bar{z}_1-\bar{z}_2)\,.\end{aligned}\tag{4.22}$$

Note that the $\mathbb{Z}_2$ symmetry one introduces when passing from u,v to $z,\bar{z}$ in the case of four-point functions is now enhanced to $\mathbb{Z}_2\times\mathbb{Z}_2$. In the case of five-point functions the two non-trivial generators of this symmetry act by $z_r\leftrightarrow\bar{z}_r, w_1\to(1-w_1)$ for $r=1,2$. When written in the conformal invariant coordinates $z_r,\bar{z}_r$ and $w=w_1$, the complexity of the differential operators remains roughly on the same level as for the polynomial cross ratios, in the same way as the quadratic Casimir operators for $N=4$ which have similar complexity in the two sets of variables, c.f. eqs. (4.8) and (4.12). But our OPE coordinates for five-point functions have a number of additional properties that are worth pointing out.
To begin with, they possess a rather nice geometric interpretation that requires going to a certain conformal frame. We already saw that using conformal transformations it is possible to move three points,

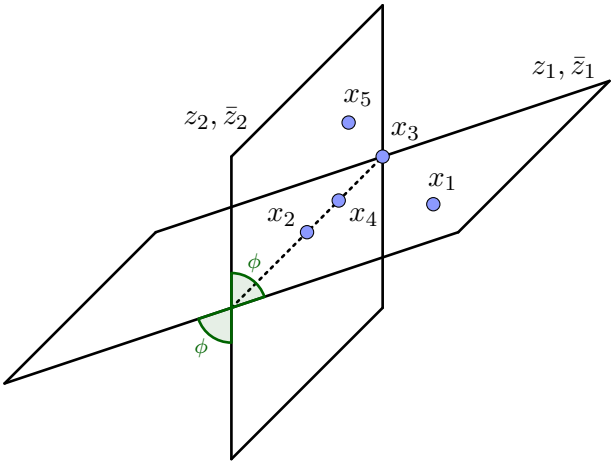

Figure 4.4: Conformal frame for five points

let's say x_2, x_3 and x_4, onto a single line to positions $0, 1, \infty$. Then we can use the remaining rotations transverse to that line in order to move x_1 into a plane and finally rotations transverse to that plane in order to move x_5 into some 3-dimensional subspace, i.e. there exists a conformal transformation $f^{(5)}$ such that

$$\begin{aligned} f^{(5)}(x_1) &= \rho_1(\cos\theta_1, \sin\theta_1, 0, \vec{0}) \,, \qquad f^{(5)}(x_2) = (0, 0, 0, \vec{0}) \,, \\ f^{(5)}(x_3) &= (\infty, 0, 0, \vec{0}) \,, \qquad f^{(5)}(x_4) = \vec{e}_1 = (1, 0, 0, \vec{0}) \,, \\ f^{(5)}(x_5) &= e_1 - \rho_2(\cos\theta_2, \sin\theta_2\cos\phi, \sin\theta_2\sin\phi, \vec{0}) \,. \end{aligned} \tag{4.23}$$

Here we have parametrized the image point $f^{(5)}(x_1)$ in the plane through an angle θ_1 and a distance ρ_1, as usual. Similarly, we have also parametrized the point $f^{(5)}(x_5)$ in a 3-dimensional space through two angles θ_2, ϕ and one distance ρ_2, using $f^{(5)}(x_4) = \vec{e}_1$ as reference point. In all these expressions, $\vec{0}$ denotes a vector with $d-3$ vanishing components. We note that in $d = 4$ dimensions, the conformal transformation $f^{(5)}$ is uniquely fixed by our choice of frame. It is now easy to compute our new variables $z_r, \bar{z}_r$ and w_1 in terms of θ_r, ρ_r and ϕ,

$$z_1 = \rho_1 e^{\mathrm{i}\theta_1} \,, \qquad \bar{z}_1 = \rho_1 e^{-\mathrm{i}\theta_1} \,, \qquad z_2 = \rho_2 e^{\mathrm{i}\theta_2} \,, \qquad \bar{z}_2 = \rho_2 e^{-\mathrm{i}\theta_2} \,, \qquad w_1 = \sin^2\frac{\phi}{2} \,. \tag{4.24}$$

This is illustrated in Figure 4.4. In particular we see that z_1, $\bar{z}_1$ and z_2, $\bar{z}_2$ describe the two planes $x_1x_2x_3x_4$ and $x_2x_3x_4x_5$ respectively, while w_1 is directly related to the angle ϕ between those planes. As we can read off from this picture the domain of w_1 for Euclidean signature is given by

$$w_1 \in [0, 1] \,. \tag{4.25}$$

The description we provided is valid for $d \geq 3$. As we go down to $d = 2$, there are no longer enough dimensions in order to have a non-vanishing angle ϕ between two 2-planes, i.e. we must set $\phi = 0$ or $\phi = \pi$ and hence $w_1 = 0$ or $w_1 = 1$. As in our review of four-point functions, we expect to recover these values of w_1 as zeroes of the Gram determinant. And indeed, the Gram determinant for the five coordinates X_i can be shown to acquire the following form

$$\det(X_{ij})\big|_5 = 2\frac{w_1\,(1-w_1)\,(z_1-\bar{z}_1)^2\,(z_2-\bar{z}_2)^2\,X_{13}^2X_{24}^2X_{35}^2}{X_{23}X_{34}} \,. \tag{4.26}$$

In addition to the two factors w_1 and $w_1 - 1$ we also notice the zeros that appear for $z_r = \bar{z}_r$, i.e. when the four points $x_1x_2x_3x_4$ or $x_2x_3x_3x_5$ lie on a line.

In section 5.3.2 we use these same coordinates to analyze the OPE limit of our Gaudin differential operators. This analysis shows clearly how the variable w_1 is naturally associated with the degree of freedom that described the choice of tensor structures at the internal vertex of a five-point OPE diagram.

More specifically, we take the OPE limit for the two sets $z_1, \bar{z}_1$ and $z_2, \bar{z}_2$ of variables that are associated with the two internal links of the OPE diagram. In the limit where we take $\bar{z}_r \to 0$ first, followed by $z_r \to 0$, the joint eigenfunctions of the five differential operators behave as

$$g_{\Delta_r,l_r;\mathfrak{t}}(z_r,\bar{z}_r,w_1) \sim \prod_{r=1}^{2} z_r^{\frac{\Delta_r+l_r}{2}} \bar{z}_r^{\frac{\Delta_r-l_r}{2}} \left(\gamma_{\Delta_r,l_r;\mathfrak{t}}(w_1) + O(z_r,\bar{z}_r)\right) \ . \tag{4.27}$$

The derivation follows the same steps we outlined in the discussion of four-point blocks in the first subsection. But in contrast to the case of $N = 4$, the leading term γ of the power series expansion in $z_r, \bar{z}_r$ is no longer constant but rather an eigenfunction of a single variable vertex differential operator for an STT-STT-scalar three-point function which we construct and analyze in Chapter 5.

4.2.4 Six-point OPE cross ratios

After reviewing our parametrization of five-point cross ratios we now turn to a discussion of $N = 6$. As long as $d \geq 4$ our set of independent polynomial cross ratios consists of

$$u_3 = \frac{X_{34}X_{56}}{X_{35}X_{46}}\,, \qquad v_3 = \frac{X_{45}X_{36}}{X_{35}X_{46}}\,, \qquad U_2^{(5)} = \frac{X_{26}X_{34}X_{45}}{X_{35}X_{24}X_{46}}\,, \tag{4.28}$$

$$U_1^{(6)} = \frac{X_{16}X_{23}X_{34}X_{45}}{X_{13}X_{24}X_{35}X_{46}}\,. \tag{4.29}$$

in addition to the five cross ratios already introduced in eq. (4.21). While the three cross ratios in the first line are of the same type as those we met in our discussion of $N = 5$, the six-point cross ratio in the second line is fundamentally new. In passing to our OPE coordinates it is natural to make use of the map (4.22) to transform the cross ratios shared with the previously discussed five-point function, while analogously mapping the cross ratios in eq. (4.28) to

$$\begin{aligned} u_3 &= z_3\bar{z}_3\,, \qquad v_3 = (1-z_3)(1-\bar{z}_3)\,, \\ U_2^{(5)} &= w_2(z_2-\bar{z}_2)(z_3-\bar{z}_3) + (1-z_2-z_3)(1-\bar{z}_2-\bar{z}_3)\,. \end{aligned} \tag{4.30}$$

For the six-point variable (4.29), a new type of mapping is necessary. In the same way as the variables z_r, $\bar{z}_r$ are associated with exchanges of STTs, and the w_s variables are associated with specific non-trivial tensor structures sitting at internal vertices of OPE diagrams, the new variable we want to introduce should be associated with exchanges of Mixed-Symmetry Tensors with two spins, and it should naturally combine with the z_2, $\bar{z}_2$ cross ratios to make up the three exchanged degrees of freedom of the middle link. We propose to introduce this conformal invariant $\Upsilon = \Upsilon_2$ through the relation

$$\begin{aligned} U_1^{(6)} = {} & \Upsilon\,(z_1-\bar{z}_1)\,(z_2-\bar{z}_2)\,(z_3-\bar{z}_3)\,\sqrt{w_1(1-w_1)w_2(1-w_2)} - w_1w_2\,(z_1-\bar{z}_1)\,(\bar{z}_2+z_2)\,(z_3-\bar{z}_3) \\ & + w_1\,(z_1-\bar{z}_1)\,[z_2\,(1-\bar{z}_3) - \bar{z}_2(1-z_3)] + w_2\,(z_3-\bar{z}_3)\,[z_2\,(1-\bar{z}_1) - \bar{z}_2(1-z_1)] \\ & + [z_2-(1-z_1)(1-z_3)]\,[\bar{z}_2-(1-\bar{z}_1)(1-\bar{z}_3)]\ . \end{aligned} \tag{4.31}$$

The new variables $z_r, \bar{z}_r, w_s$ and Υ admit an action of $\mathbb{Z}_2^3$ that leaves the original cross ratios invariant. The nontrivial elements σ_r of the three $\mathbb{Z}_2$ factors each exchange one of the pairs $z_r \leftrightarrow \bar{z}_r$, map $w_s \to (1-w_s)$ for $r = s, s+1$ and send Υ to $-\Upsilon$.

As a first quick test of our proposal, we can compute the six-point Gram determinant. When expressed in the OPE coordinates it reads

$$\det(X_{ij})\big|_6 = \frac{(1-w_1)\,w_1(1-w_2)\,w_2\,(z_1-\bar{z}_1)^2(z_2-\bar{z}_2)^2(z_3-\bar{z}_3)^2\left(4z_2\bar{z}_2 - \Upsilon^2\,(z_2-\bar{z}_2)^{\,2}\right)}{z_2^2\bar{z}_2^2} \frac{\prod_{i=1}^{4} X_{i,i+1}^2}{X_{34}^2}. \tag{4.32}$$

Given the lengthy relation between the six-point cross ratio $U^{(6)}$ and Υ it is very reassuring to see that the Gram determinant now fits into a single line. In addition, the new conformal invariant Υ appears

in a single factor, combined only with the cross ratios $z_2, \bar{z}_2$. If we reduce the dimension to $d = 3$, the number of cross ratios drops by one. In our new set of conformal invariants we see that Υ can then be expressed in terms of $z_2, \bar{z}_2$ as

$$\Upsilon^2 = \frac{4 z_2 \bar{z}_2}{(z_2 - \bar{z}_2)^2} \qquad \textit{for} \qquad d = 3. \tag{4.33}$$

All these simple relations are quite remarkable. On the other hand they are not yet sufficient to fully appreciate our definition of Υ. Given what we have seen one may for example still wonder why we did not rescale Υ to make the last bracket in the Gram determinant equal to $(\Upsilon^2 - 1)$. While that is certainly possible and leads to a nicer geometrical interpretation, the rescaled variable would result in more complicated expressions for the asymptotics of comb channel blocks in OPE limits, see our discussion in the next section.

The interpretation of our coordinates proceeds as in the previous subsection. In that case, each of the two internal links was associated with a complex plane. We used the coordinates $z_1, \bar{z}_1$ and $z_2, \bar{z}_2$ to specify two positions on these two planes and related the variable w_1 to the relative angle between the two planes within a 3-dimensional subspace. As we go to $N = 6$, the same picture applies, but with dimensions raised by one. Instead of the 2-planes in 3-space, we now have two 3-spaces that are associated with the points $x_1, \ldots, x_5$ and $x_2, \ldots, x_6$, respectively. These are embedded in a 4-dimensional subspace with the relative angle being measured by a new angle φ. Each of the two 3-spaces contains the configuration of two planes depicted in Figure 4.4. For the first five points $x_1, \ldots, x_5$ this defines the coordinates $\rho_1, \theta_1, \rho_2, \theta_2$ and ϕ as before. We obtain a similar set of coordinates for the second set $x_2, \ldots, x_6$. Now it is easy to see that one pair of coordinates coincides with the ones from the first quintuple of insertion points so that in total we need eight coordinates $\rho_r, \theta_r, \phi_1, \phi_2$ with $r = 1, 2, 3$ to parametrize the configurations within each of the 3-spaces. With these coordinates introduced one finds that

$$z_r := \rho_r e^{\mathrm{i}\theta_r}, \quad w_s := \sin^2 \frac{\phi_s}{2}, \quad \Upsilon := \pm \mathrm{i} \frac{\cos\varphi}{\sin\theta_2}, \tag{4.34}$$

where $r = 1, 2, 3$ and $s = 1, 2$. The sign in Υ is conventional, and can be absorbed in a shift of the angle φ. A more formal definition of the various geometric parameters on the right hand side will be given in the next subsection as part of a more general construction that applies to any number N of points in $d = 4$ dimensions.

4.2.5 Generalisation to higher number of points

In order to extend our choice of coordinates to higher number N of insertion points in $d = 4$ dimensions, it is useful to formalize the construction we have described at the end of the previous section. As described in subsection 4.2.3, each quintuple of consecutive points $x_s, x_{s+1}, \ldots, x_{s+4}$ defines a conformal transformation $f_s^{(5)}$ as in eq. (4.23)

$$\begin{aligned}
&f_s^{(5)}(x_s) =: \rho_s \vec{n}(\theta_s, 0)\ , \quad f_s^{(5)}(x_{s+1}) =: (0,0,0,0), \\
&f_s^{(5)}(x_{s+2}) =: (\infty,0,0,0)\ , \quad f_s^{(5)}(x_{s+3}) =: \vec{e}_1 = (1,0,0,0), \\
&f_s^{(5)}(x_{s+4}) =: \vec{e}_1 - \rho_{s+1} \vec{n}(\theta_{s+1}, \phi_s),
\end{aligned} \tag{4.35}$$

where $s = 1, \ldots, N-4$ and we defined the unit vectors $\vec{n}$ as

$$\vec{n}(\theta, \phi) := (\cos\theta, \sin\theta\cos\phi, \sin\theta\sin\phi, 0). \tag{4.36}$$

Thus, to compute x_6 in the conformal frame where $f_1^{(5)}(x_1), \ldots, f_1^{(5)}(x_5)$ are of the form (4.23), we express the sixth point as

$$f_1^{(5)}(x_6) = f_1^{(5)} \circ f_2^{(5)-1}(\vec{e}_1 - \rho_3\, \vec{n}(\theta_3, \phi_2)) \equiv h_{12}^{(5)}(\vec{e}_1 - \rho_3\, \vec{n}(\theta_3, \phi_2)). \tag{4.37}$$

By construction, $h_{12}^{(5)}$ is a conformal group element parametrized by the cross ratios of the six-point function. In Appendix B.2, we compute this conformal transformation and find

$$h_{12}^{(5)-1} = \rho_2^{-D}\mathcal{I}\sigma_1 e^{-\varphi M_{34}} e^{-\theta_2 M_{12}} e^{-\phi_1 M_{23}} e^{P_1}, \tag{4.38}$$

where $\mathcal{I}$ is conformal inversion and $\sigma_1 : (x^1, x^2, x^3, x^4) \mapsto (-x^1, x^2, x^3, x^4)$ is a reflection along the hyperplane orthogonal to the first coordinate direction. The explicit action of the element (4.38) on spacetime points x is given by

$$h_{12}^{(5)-1}(x) = \rho_2\sigma_1 e^{-\varphi M_{34}} e^{-\theta_2 M_{12}} e^{-\phi_1 M_{23}} \frac{x - \vec{e}_1}{(x-\vec{e}_1)^2}. \tag{4.39}$$

In particular we read off that the angle φ described the relative angle between two 3-spaces. It is obvious how to continue these constructions beyond $N = 6$ points in $d = 4$. We continue to introduce comb channel cross ratios $z_r, \bar{z}_r$ and w_s in terms of the polynomial cross ratios through relations (4.22) with indices running over $r = 1, \dots, N-3$ and $s = 1, \dots N-4$, respectively. Similarly, we introduce Υ_r with $r = 2, \dots N-4$ through relations of the form (4.31). After extending our relations (4.34) to a higher number of comb channel OPE coordinates we introduce the geometric coordinates as

$$z_r := \rho_r e^{\mathrm{i}\theta_r}, \quad w_s := \sin^2\frac{\phi_s}{2}, \quad \Upsilon_r := \pm\mathrm{i}\frac{\cos\varphi_r}{\sin\theta_{r+1}}, \tag{4.40}$$

and define in direct analogy to eq. (4.38) the conformal transformations

$$h_{s(s+1)}^{(5)} := f_s^{(5)} \circ f_{s+1}^{(5)-1} = \rho_{s+1}^{-D}\,\mathcal{I}\sigma_1 e^{-\varphi_s M_{34}} e^{-\theta_{s+1} M_{12}} e^{-\phi_s M_{23}} e^{-\varphi_{s-1} M_{34}} e^{P_1}, \tag{4.41}$$

for $s = 1, \dots, N-4$. We can thus supplement eqs. (4.35) by the relations

$$\begin{aligned}
&f_1^{(5)}(x_6) = h_{12}^{(5)}(\vec{e}_1 - \rho_3\vec{n}(\theta_3,\phi_2)) \ , \qquad f_1^{(5)}(x_7) = h_{23}^{(5)} \circ h_{12}^{(5)}(\vec{e}_1 - \rho_4\vec{n}(\theta_4,\phi_3)) \\
&\dots \\
&f_1^{(5)}(x_N) = h_{(N-5)(N-4)}^{(5)} \circ h_{(N-6)(N-5)}^{(5)} \circ \dots \circ h_{23}^{(5)} \circ h_{12}^{(5)}(\vec{e}_1 - \rho_{N-3}\vec{n}(\theta_{N-3},\phi_{N-4})).
\end{aligned}$$

These formulas allow us to compute the location of the insertion points in the conformal frame defined by the first five points $x_1, \dots, x_5$, see eq. (4.35), in terms of the geometric parameters ρ_r, θ_r, ϕ_s and φ_r. The latter possess a very simple relation with the OPE cross ratios that we spelled out in eq. (4.40).

4.3 OPE limits and factorization for six-point blocks

In the previous section we have introduced new conformally invariant coordinates for multipoint blocks in $d = 4$ dimensions that were naturally attached to the links and vertices of a comb channel OPE diagram, see e.g. Figure 4.5 for the example $N = 6$. To support our choice we provided a nice geometric interpretation and, closely related, showed that the Gram determinant for $N = 6$ points admits a simple factorized expression, see eq. (4.32). Recall that the six-point function in $d \leq 4$ is the first correlator for which the new link variable Υ appears. This makes $N = 6$ the decisive case when it comes to testing our cross ratios for comb channel blocks in $d = 4$. The next two sections are devoted to the most important test.

As we have reviewed in subsection 4.2.1, what makes the cross ratios $z, \bar{z}$ for 4-point function so useful is the fact that they provide power series expansions in the OPE limit where $z, \bar{z}$ go to zero. One can deduce this important feature from the expressions of the Casimir differential operators. Here we want to extend this type of analysis to the OPE limits of six-point functions and in particular to the limit in which the coordinates $z_2, \bar{z}_2$ and Υ attached to the central link of the comb channel diagram are sent to zero. Our goal is to show that in this limit the six-point comb channel blocks possess a power series expansion and that the leading term of this expansion factorizes into a product of two functions, one depending on $z_1, \bar{z}_1, w_1$, the other on $z_3, \bar{z}_3, w_2$.

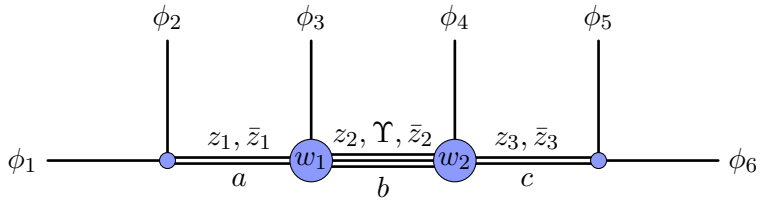

Figure 4.5: Six point function with external scalars in the comb channel. The z_i, $\bar{z}_i$, w_i and Υ type of cross ratios are naturally associated with one particular internal leg or vertex of the OPE diagram.

In our approach we characterize multipoint blocks as eigenfunctions of a complete set of commuting differential operators. For $N = 6$ comb channel blocks, these operators are briefly reviewed in the first subsection. Then we show that the OPE limit we are interested in does indeed correspond to sending $z_2, \bar{z}_2$ and Υ to zero. In the final subsection we then perform the OPE limit on the differential operators and show that these operators decouple into two independent sets associated with the left and right side of the diagram. We also provide concrete expressions for the limiting differential operators. These will be further analyzed in the next section.

4.3.1 Preliminaries on comb channel six-point blocks

In this subsection we shall specify all of our conventions concerning six-point blocks and the differential operators we use to characterize them. As usual, any six-point correlation function of scalar fields can be split into a product of some homogeneous prefactor Ω, which depends on the scaling weights Δ_i and insertion points x_i of the external scalar fields, and a function F of the nine cross ratios,

$$\langle \phi_1\phi_2\phi_3\phi_4\phi_5\phi_6\rangle = \Omega_6^{(\Delta_i)}(X_i)\, F^{(\Delta_i)}\Big(u_1, v_1, u_2, v_2, u_3, v_3, U_1^{(5)}, U_2^{(5)}, U_1^{(6)}\Big)\,. \tag{4.42}$$

The prefactor is not unique. Here we shall adopt the following choice:

$$\Omega_6^{(\Delta_i)}(X_i) = \frac{1}{X_{12}^{\frac{\Delta_1+\Delta_2}{2}} X_{34}^{\frac{\Delta_3+\Delta_4}{2}} X_{56}^{\frac{\Delta_5+\Delta_6}{2}}} \left(\frac{X_{23}}{X_{13}}\right)^{\frac{\Delta_1-\Delta_2}{2}} \left(\frac{X_{24}}{X_{23}}\right)^{\frac{\Delta_3}{2}} \left(\frac{X_{35}}{X_{45}}\right)^{\frac{\Delta_4}{2}} \left(\frac{X_{45}}{X_{46}}\right)^{\frac{\Delta_6-\Delta_5}{2}}\,. \tag{4.43}$$

The function $F^{(\Delta_i)}$ admits a conformal block decomposition of the form

$$F^{(\Delta_i)} = \sum_{\Xi} \lambda_\Xi\, g_\Xi^{(\Delta_i)}\Big(u_r, v_r, U_1^{(5)}, U_2^{(5)}, U_1^{(6)}\Big)\,, \quad \textit{where} \quad \Xi = \{\Delta_a, l_a, \Delta_b, l_b, \ell_b, \Delta_c, l_c, \mathfrak{t}_L, \mathfrak{t}_R\} \tag{4.44}$$

is a complete set of quantum numbers that includes the weights $\Delta_a, \Delta_b, \Delta_c$ and spins l_a, l_b, ℓ_b, l_c of the internal fields in the comb channel decomposition, as well as two quantum numbers $\mathfrak{t}_L$ and $\mathfrak{t}_R$ that label the choice of tensor structure at the two central vertices of the diagram in Figure 4.5. We have also split each summand into a product of OPE coefficients $\lambda = \lambda_\Xi$ and a conformal block g_Ξ. From now on we will drop the labels on g unless it is not clear from the context which ones they are.

According to our discussion of Chapter 3, the six-point comb channel conformal blocks in eq. (4.44) are joint eigenfunctions of nine differential operators. These include three quadratic Casimir operators, which are constructed for each of the three internal links of the OPE diagram as

$$\mathcal{D}^2_{(12)} = (\mathcal{T}_1 + \mathcal{T}_2)_{[AB]}(\mathcal{T}_1 + \mathcal{T}_2)^{[BA]} = \mathcal{D}^2_{(3456)}\,, \tag{4.45}$$

$$\mathcal{D}^2_{(123)} = (\mathcal{T}_1 + \mathcal{T}_2 + \mathcal{T}_3)_{[AB]}(\mathcal{T}_1 + \mathcal{T}_2 + \mathcal{T}_3)^{[BA]} = \mathcal{D}^2_{(456)}\,, \tag{4.46}$$

$$\mathcal{D}^2_{(56)} = (\mathcal{T}_5 + \mathcal{T}_6)_{[AB]}(\mathcal{T}_5 + \mathcal{T}_6)^{[BA]} = \mathcal{D}^2_{(1234)}\,. \tag{4.47}$$

The three quadratic Casimir operators are joined by three quartic ones which take the following form

$$\mathcal{D}^4_{(12)} = (\mathcal{T}_1+\mathcal{T}_2)_{[AB]}(\mathcal{T}_1+\mathcal{T}_2)^{[BC]}(\mathcal{T}_1+\mathcal{T}_2)_{[CD]}(\mathcal{T}_1+\mathcal{T}_2)^{[DA]} = \mathcal{D}^4_{(3456)}\,, \tag{4.48}$$

$$\mathcal{D}^4_{(123)} = (\mathcal{T}_1+\mathcal{T}_2+\mathcal{T}_3)_{[AB]}(\mathcal{T}_1+\mathcal{T}_2+\mathcal{T}_3)^{[BC]}(\mathcal{T}_1+\mathcal{T}_2+\mathcal{T}_3)_{[CD]}(\mathcal{T}_1+\mathcal{T}_2+\mathcal{T}_3)^{[DA]} = \mathcal{D}^4_{(456)}\,, \tag{4.49}$$

$$\mathcal{D}^4_{(56)} = (\mathcal{T}_5+\mathcal{T}_6)_{[AB]}(\mathcal{T}_5+\mathcal{T}_6)^{[BC]}(\mathcal{T}_5+\mathcal{T}_6)_{[CD]}(\mathcal{T}_5+\mathcal{T}_6)^{[DA]} = \mathcal{D}^4_{(1234)}\,. \tag{4.50}$$

In addition, there is one third-order Pfaffian operator that is assigned to the central link,

$$\mathcal{D}^3_{(123)} = \epsilon^{ABCDEF}(\mathcal{T}_1+\mathcal{T}_2+\mathcal{T}_3)_{[AB]}(\mathcal{T}_1+\mathcal{T}_2+\mathcal{T}_3)_{[CD]}(\mathcal{T}_1+\mathcal{T}_2+\mathcal{T}_3)_{[EF]}\,. \tag{4.51}$$

To complete the list of differential operators we finally spell out the two fourth order vertex operators,

$$\mathcal{D}^{4,3}_{L,(12)3} = (\mathcal{T}_1+\mathcal{T}_2)_{[AB]}(\mathcal{T}_1+\mathcal{T}_2)^{[BC]}(\mathcal{T}_1+\mathcal{T}_2)_{[CD]}(\mathcal{T}_3)^{[DA]}\,, \tag{4.52}$$

$$\mathcal{D}^{4,3}_{R,(56)4} = (\mathcal{T}_5+\mathcal{T}_6)_{[AB]}(\mathcal{T}_5+\mathcal{T}_6)^{[BC]}(\mathcal{T}_5+\mathcal{T}_6)_{[CD]}(\mathcal{T}_4)^{[DA]}\,. \tag{4.53}$$

In the following we will mostly focus on the quadratic Casimir operators. It is rather easy to compute the expression of these Casimir operators in the polynomial cross ratios with the aid of computer algebra software and verify that all their coefficients are indeed polynomial, as we had claimed in the previous section. The resulting expressions for Casimir operators are actually the simplest we have been able to find, simpler than for any other set of coordinates. On the other hand, the polynomial cross ratios are not well adapted to taking OPE limits, as we will argue in section 4.3.3. Taking the OPE limit will require passing to the new OPE coordinates introduced in the previous section.

4.3.2 The OPE limit from embedding space

Our goal now is to motivate why we expect the sum over descendants in the central intermediate link to be encoded in a power series expansion in the variables $z_2, \bar{z}_2, \Upsilon$. The idea here is to prepare the intermediate fields through an operator product expansion of either the three fields on the left or the three fields on the right of the central link. For the left hand side this amounts to making x_1, x_2 and x_3 collide.

It is a little more tricky to understand how the OPE limit is performed once we pass to the cross ratios. As an example, let us briefly look at the limit in which x_1 and x_2 come together. In the process we expect to go from a six-point function of scalar fields to a five-point function with one STT insertion and four scalars. While the former has nine cross ratios, the latter has only seven, i.e. we expect that two cross ratios are fixed in the OPE limit. On the other hand, if we apply the limit to the nine polynomial cross ratios we find

$$u_1 \to 0\,, \qquad v_1 \to 1\,, \qquad U_1^{(5)} \to v_2\,, \qquad U_1^{(6)} \to U_2^{(5)}\,. \tag{4.54}$$

Of course, this simply means that one needs to consider subleading terms in the limiting behaviour of the cross ratios to parametrize the seven cross ratios of the resulting five-point function, but it still illustrates how subtle OPE limits are in the space of cross ratios.

In order to analyze the triple OPE limits of our new cross ratios it is advantageous to work in embedding space. In the next few paragraphs we will review how to take double limits into STTs and triple limits into MSTs. A generic MST_2 has three associated vectors X, $Z \equiv Z_1$, and $W \equiv Z_2$; we will work with vectors in the Poincaré patches we discussed in section 2.3.2. Using the metric

$$\mathrm{d}s^2 = \mathrm{d}X^A \mathrm{d}X_A = -\mathrm{d}X^+\mathrm{d}X^- + \delta_{\mu\nu}\mathrm{d}X^\mu \mathrm{d}X^\nu\,, \tag{2.39}$$

these vectors acquire the form

$$X = \big(1, x^2, x\big)\,, \tag{4.55}$$

$$Z = (0, 2x\cdot z, z)\,, \qquad z = (\frac{1-\zeta^2}{2}, \mathrm{i}\frac{1+\zeta^2}{2}, \zeta) \in \mathbb{C}^d \tag{4.56}$$

$$W = (0, 2x\cdot w, w)\,, \qquad w = (\zeta\cdot\omega, -i\zeta\cdot\omega, \omega) \in \mathbb{C}^d\,, \tag{4.57}$$

where $\omega \in \mathbb{C}^{d-2}$ satisfies $\omega^2 = 0$ and is normalised such that $\omega_1 + \mathrm{i}\omega_2 \equiv 1$. By construction, these satisfy the null relations

$$X^2 = Z^2 = W^2 = X \cdot Z = X \cdot W = Z \cdot W = 0\,. \tag{4.58}$$

To discuss the OPE limit of a pair of scalars inserted at x_1 and x_2 we use their embedding space coordinates X_1 and X_2. Projecting to the STTs that are produced by the OPE of those two scalar fields requires to construct the embedding space coordinate X_{STT} and polarisation Z_{STT} of said fields from the coordinates of the two scalars. This can be achieved by taking a lightcone limit $X_1 \cdot X_2 = 0$ first. Once the lightcone condition is satisfied we introduce

$$X_{\mathrm{STT}} = \frac{1}{2}(X_1 + X_2)\,, \qquad Z_{\mathrm{STT}} = \frac{1}{(X_2 - X_1)_1 + \mathrm{i}(X_2 - X_1)_2}(X_2 - X_1)\,. \tag{4.59}$$

Note that the prefactor in the definition of Z_{STT} ensures that the polarisation is normalised such that $z_1 + \mathrm{i}z_2 = 1$, as in (4.56). Thanks to the condition $X_1 \cdot X_2 = 0$, the two vectors we have built from X_1 and X_2 satisfy the usual relations for STT variables, namely they both square to zero, $X_{\mathrm{STT}}^2 = 0 = Z_{\mathrm{STT}}^2$, and they are transverse to each other, i.e. $X_{\mathrm{STT}} \cdot Z_{\mathrm{STT}} = 0$. So far, we have only assumed that the two scalar fields are light-like separated so that $X_1 \cdot X_2 = 0$. To complete the OPE limit we can now set $X_2 = X_1 + \epsilon\, Z_{\mathrm{STT}}$ and compute the $\epsilon \to 0$ limit.

In order to address the triple OPE limit, it remains to discuss the operator product of an STT with a scalar field. Let us consider an STT with associated coordinates X_1, Z_1 and a scalar at position X_2. If we want to project to the exchange of an MST_2 produced by the OPE of those two fields, we need to be able to construct embedding space coordinates X_{MST_2} and polarisations $Z_{\mathrm{MST}_2}, W_{\mathrm{MST}_2}$ for an MST_2 field starting from the degrees of freedom of the two initial fields. To do so, we will follow a nested procedure with two limits of the type described above. As before, we start by first taking the lightcone limit $X_1 \cdot X_2 = 0$ and construct the expressions

$$X_{\mathrm{MST}_2} = \frac{1}{2}(X_1 + X_2)\,, \qquad Z' = \frac{1}{(X_2 - X_1)_1 + \mathrm{i}(X_2 - X_1)_2}(X_2 - X_1)\,. \tag{4.60}$$

From here, one can take $X_2 = X_1 + \epsilon\, Z'$ and compute the $\epsilon \to 0$ limit. This leads temporarily to something described by one coordinate X_{MST_2} and two auxiliary vectors of STT type Z_1 and Z'. To make this set suitable to describe an MST_2, we need to further reduce the degrees of freedom of the system and construct a variable W. This can be achieved by taking the lightcone limit $Z' \cdot Z_1 = X_2 \cdot Z_1 = 0$ and constructing

$$Z_{\mathrm{MST}_2} = \frac{1}{2}(Z' + Z_1)\,, \qquad W_{\mathrm{MST}_2} = \frac{1}{(Z' - Z_1)_3 + \mathrm{i}(Z' - Z_1)_4}(Z' - Z_1)\,. \tag{4.61}$$

These two vectors indeed satisfy the appropriate conditions for variables associated with an MST_2, and the normalisation is such that it matches the reference one we spelled out above. At this point we can complete the OPE limit by writing $Z' = Z + \epsilon W$ and taking $\epsilon \to 0$.

Let us now come back to the cross ratios and analyze their behaviour when we take the OPE limit. This is particularly simple if we take the OPE limit for the two scalar fields ϕ_1 and ϕ_2 in which case one find that $\bar{z}_1$ and z_1 both tend to zero while all other cross ratios remain finite. A similar statement holds for the OPE limit of the two scalar field ϕ_5 and ϕ_6. It is less straightforward to understand the leading behaviour for exchanges of a certain MST_2 for the internal leg in the middle. To study this, let us start by taking first the OPE limit on the left of side of the OPE diagram and reducing to a five-point function of fields $\mathcal{O}_a$, $\phi_3, \ldots, \phi_6$. Here, the OPE limit for leg b can simply be cast as a limit for one STT with coordinates X_a, Z_a and one scalar with coordinate X_3, of the form described in section 4.3.2. Following that, it is possible to check that

$$w_1 \xrightarrow{((12)3)\ \mathrm{OPE}} \begin{cases} 1 & \text{if} \quad (X_a \wedge X_3) \cdot (X_4 \wedge X_5) > 0\,, \\ 0 & \text{else}\,, \end{cases} \tag{4.62}$$

while the cross ratios z_2, $\bar{z}_2$ and Υ all tend to zero. On the other hand, if we were to take the limit from the right side in the ((65)4) order, we would end up with

$$w_2 \xrightarrow{((65)4)\ \text{OPE}} \begin{cases} 1 & \text{if} \quad (X_2 \wedge X_3)\cdot(X_4 \wedge X_c) > 0\,, \\ 0 & \text{else}\,, \end{cases} \tag{4.63}$$

while once again $z_2, \bar{z}_2$ and Υ vanish in the limit. This instructs us on the fact that the relevant regime to study the projection on exchanges of specific operators in the leg b of the six-point function is the part in common for both OPE limits we took above, namely $(z_2, \bar{z}_2, \Upsilon) \to 0$. Taking only these three cross ratios to zero, while leaving all others finite, corresponds to a regime in which the two triples (x_1, x_2, x_3) and (x_4, x_5, x_6) can each be enclosed in a sphere of radius r which is parametrically smaller than the distance R between any two points of the two triples. In this limiting regime, we need the six remaining cross ratios to parametrize the configuration of insertion points in the two small spheres, see Appendix B.3 for some more details.

4.3.3 OPE limits of six-point blocks

Our main goal in this subsection is to analyze the asymptotics of the six-points comb channel blocks in the limit where we send $\bar{z}_2, z_2$ and Υ to zero. We will first study the limiting behaviour of the Casimir equation for $\mathcal{D}^2_{(123)}$ under the assumption of a leading power-law behaviour of the form

$$g(z_s, \bar{z}_s, w_r, \Upsilon) \sim \bar{z}_2^{p_1} z_2^{p_2} \Upsilon^{p_3} \left(\psi(z_1, \bar{z}_1, z_3, \bar{z}_3, w_1, w_2) + O(z_2, \bar{z}_2, \Upsilon)\right) \tag{4.64}$$

in the three variables for the middle leg. In a similar way to what happens for exchanges of STTs, see our review in subsection 4.3.1, the precise powers depend on the order in which the limits are taken. Taking the limit $\Upsilon \to 0$ first turns out to be inconsistent, as it produces divergences in the Casimir equation. Instead we first take the $\bar{z}_2 \to 0$ limit followed by the one in z_2, in direct analogy to the $N = 4, 5$-point functions. Alternatively, we could also send z_2 to zero first, but given the symmetry of the cross ratios under $z \leftrightarrow \bar{z}$ and $w \leftrightarrow (1-w)$ this is a mere issue of convention. Once this limit is performed, the order in which the remaining two are performed turns out to be irrelevant and one finds

$$\bar{z}_2^{-p_1} z_2^{-p_2} \Upsilon^{-p_3} \mathcal{D}^2_{(123)} \bar{z}_2^{p_1} z_2^{p_2} \Upsilon^{p_3} \underset{z_2, \Upsilon \to 0}{\overset{\bar{z}_2 \to 0}{\longrightarrow}} -2\left(d\, p_1 - p_1^2 - p_2^2 + (p_3+1)(p_2 - p_1) - p_3(p_3-1)\right) + \dots \tag{4.65}$$

where we indicated the order of limits by placing the first one above the arrow and the remaining two below. As before, the $\dots$ correspond to higher order terms in $z_2, \bar{z}_2$ and Υ. This behaviour, in which the leading term of the second order Casimir differential operator for the central link is a constant was what we were going for when we introduced the OPE coordinates. Now we see that we have indeed achieved a first important goal.

Of course, we expect the constant term we just computed to match the eigenvalue of the quadratic Casimir element in the MST_2 representation of the exchanged intermediate field. The latter is related to the weight and spin labels of said fields as

$$c^{(2)}_{\Delta_b, l_b, \ell_b} = \Delta_b(\Delta_b - d) + l_b(l_b + d - 2) + \ell_b(\ell_b + d - 4)\,. \tag{4.66}$$

Equating this with the constant we computed in eq. (4.65) we can only match the coefficients in front of the dimension d provided that

$$p_1 = \frac{\Delta_b - l_b - \ell_b}{2}\,.$$

It is then natural to set the exponent p_2 of the variable z_2 to be

$$p_2 = \frac{\Delta_b + l_b + \ell_b}{2}\,. \tag{4.67}$$

This also ensures that for $\ell_b = 0$ one recovers the usual leading behaviour for intermediate STT exchange, see subsection 4.3.1. Requiring finally a full match with the Casimir eigenvalue leaves us with two possible solutions for the leading behaviour in Υ

$$p_3 = \ell_b \qquad \text{or} \qquad p_3 = l_b + 1\,. \tag{4.68}$$

This freedom, which cannot be eliminated by considering higher Casimir differential operators, is associated with the invariance of the Casimir elements under the action of Weyl transformations. Let us note that the two possible solutions correspond to the two possible behaviours in $(1-v)$ for the four-point s-channel OPE that distinguish between Euclidean and Minkowski conformal blocks [84]

$$(1-v)^l\,, \qquad \text{or} \qquad (1-v)^{1-\Delta}\,, \tag{4.69}$$

modulo an exchange of $-\Delta \leftrightarrow l$ and $l \leftrightarrow \ell$. Along with the interpretation of Υ as a degree of freedom associated with MST_2 fields, the first solution with $p_3 = \ell_b$ seems to be more natural. This choice will later be validated when we compare the limiting behaviour of the remaining non-trivial Casimir operators to those of spinning four-point blocks.

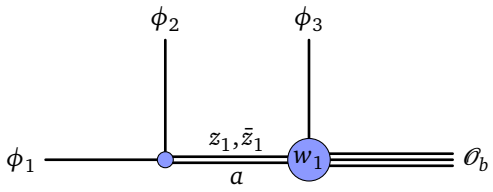

Figure 4.6: One of the four-point functions obtained in the OPE limit for the middle leg in a six-point function in comb channel. The rightmost field is a Mixed-Symmetry Tensor with two spin indices and the exchanged field is a Symmetric Traceless Tensor.

Now let us address the second part of our claims. As stated in the introduction we want to show that expansion of the conformal block (4.64) takes the more specific form

$$g(z_r, \bar{z}_r, w_1, w_2, \Upsilon) \overset{\bar{z}_2, z_2, \Upsilon \to 0}{\sim} \bar{z}_2^{\frac{\Delta_b - l_b - \ell_b}{2}} z_2^{\frac{\Delta_b + l_b + \ell_b}{2}} \Upsilon^{\ell_b} \left(g_a(z_1, \bar{z}_1, w_1) g_c(z_3, \bar{z}_3, w_2) + \dots\right)\,, \tag{4.70}$$

in which the leading term splits into a product of two functions of three variables each, and to characterize the two factors, one for the left side of the OPE diagram, see Figure 4.6, the other for the right. The proof is a nice application of Gaudin integrability, i.e. our characterisation of multipoint conformal blocks through differential equations. Having seen that the differential operators $\mathcal{D}^p_{(123)}, p = 2, 3, 4$, simply acts as multiplication with the value of the associated Casimir elements, we now need to study the limiting behaviour of the remaining six differential operators. These include two quadratic and two fourth order Casimir operators as well as two vertex operators. We will focus our discussion on the quadratic Casimir operators. Very remarkably, it turns out that the two quadratic Casimirs $\mathcal{D}^2_{(12)}$ and $\mathcal{D}^2_{(56)}$ decouple completely upon taking the OPE limit in the central link,

$$\mathcal{D}^2_{(12)} \xrightarrow{b\,\text{OPE}} \mathcal{D}^2_a(z_1, \bar{z}_1, w_1)\,, \qquad \mathcal{D}^2_{(123)} \xrightarrow{b\,\text{OPE}} c^{(2)}_{\Delta_b, l_b, \ell_b}\,, \qquad \mathcal{D}^2_{(56)} \xrightarrow{b\,\text{OPE}} \mathcal{D}^2_c(z_3, \bar{z}_3, w_2)\,. \tag{4.71}$$

Here b OPE denotes the limit in which we take $\bar{z}_2$ to zero followed by z_2 and Υ, as discussed before. Obviously, the expression for $\mathcal{D}^2_a$ and $\mathcal{D}^2_c$ are identical, given the symmetry of the OPE diagram and the limiting procedure. Hence it suffices to spell out an expression for $\mathcal{D}^2_a$ which takes the relatively simple

form

$$\begin{aligned}\mathcal{D}_a^2 = &-2\left(z_1-1\right)z_1^2\partial_{z_1}^2 - 2\left(\bar{z}_1-1\right)\bar{z}_1^2\partial_{\bar{z}_1}^2 + \frac{4\left(w_1-1\right)w_1 z_1\bar{z}_1\left(w_1\left(z_1-\bar{z}_1\right)+\bar{z}_1-1\right)}{\left(z_1-\bar{z}_1\right)^2}\partial_{w_1}^2 \\ &+2\left(1-w_1\right)w_1 z_1^2\partial_{z_1}\partial_{w_1} - 2\left(1-w_1\right)w_1\bar{z}_1^2\partial_{\bar{z}_1}\partial_{w_1} \\ &+2\left[z_1^2\left(a+b-1+\left(w_1-\frac{1}{2}\right)l_b\right)+\frac{z_1\bar{z}_1}{z_1-\bar{z}_1}(1-z_1)(d-2)\right]\partial_{z_1} \\ &+2\left[\bar{z}_1^2\left(a+b-1-\left(w_1-\frac{1}{2}\right)l_b\right)-\frac{z_1\bar{z}_1}{z_1-\bar{z}_1}\left(1-\bar{z}_1\right)(d-2)\right]\partial_{\bar{z}_1} \\ &+2\Bigg[a\left(w_1-1\right)w_1\left(z_1-\bar{z}_1\right)-\frac{2\left(w_1-1\right)w_1 z_1\bar{z}_1\left(l_b-1\right)}{z_1-\bar{z}_1} \\ &\qquad+\frac{z_1\bar{z}_1(d-2)\left(w_1\left(\bar{z}_1+z_1-2\right)-\bar{z}_1+1\right)}{\left(z_1-\bar{z}_1\right)^2}\Bigg]\partial_{w_1} \\ &-a\left[\left(2w_1-1\right)\left(z_1-\bar{z}_1\right)l_b+2b\left(\bar{z}_1+z_1\right)\right]-\frac{z_1\bar{z}_1\left(w_1\left(z_1-\bar{z}_1\right)+\bar{z}_1-1\right)}{\left(w_1-1\right)w_1\left(z_1-\bar{z}_1\right)^2}\ell_b\left(\ell_b+d-4\right)\ . \end{aligned} \tag{4.72}$$

Here the constants a, b are determined by the conformal weights of the external scalars and Δ_b through $2a = \Delta_2 - \Delta_1$ and $2b = \Delta_3 - \Delta_b$. The expression for $\mathcal{D}_c^2$ looks the same, but with variables $z_3, \bar{z}_3, w_2$ instead of $z_1, \bar{z}_2, w_1$ and parameters $2a = \Delta_4 - \Delta_b$ and $2b = \Delta_3 - \Delta_4$. We have also analyzed the fourth order Casimir operators as well as the vertex operators and shown that they display the same decoupling. We refrain from spelling out explicit expressions here.

For the time being, all we can do with the explicit expression for $\mathcal{D}_a^2$ is to appreciate that the formula looks relatively simple. In the next section we will analyze it further and show that it can be mapped to the quadratic Casimir operator for a spinning four-point function with three scalar and one MST_2 external field. Let us note that the blocks for such spinning four-point functions indeed depend on three variables, the two 4-point cross ratios and one additional variable associated with the choice of tensor structure at the scalar-STT-MST_2 vertex. Notice that our analysis implies in particular that conformal partial waves in the limit are polynomials of a bounded degree in a variable closely related to w_1, given in (4.114), a fact that is already non-trivial from the mere definition of OPE cross ratios.

Before we conclude this section we briefly want to discuss a second OPE limit that we have also worked out explicitly. It concerns a setup in which we take two OPE limits on the links a and c so that we end up with a four-point function of two STT fields and two scalars, see Figure 4.7. As explained before, we

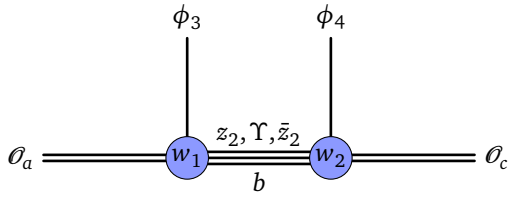

Figure 4.7: Four-point function obtained from OPE limit on legs a and c of a six-point function in comb channel. Fields at legs a and c are Symmetric Traceless Tensors, while the exchanged field is a Mixed-Symmetry Tensor with two spin indices.

perform this limit by first sending $\bar{z}_1$ and $\bar{z}_2$ to zero before taking the limits $z_1, z_2 \to 0$. In the limit, five of the nine cross ratios survive and one finds

$$g(z_1,\bar{z}_1,z_2,\bar{z}_2,z_3,\bar{z}_3,w_1,w_2,\Upsilon) \overset{\bar{z}_1,z_1,\bar{z}_3,z_3\to 0}{\sim} \bar{z}_1^{\frac{\Delta_a-l_a}{2}} z_1^{\frac{\Delta_a+l_a}{2}} \bar{z}_3^{\frac{\Delta_c-l_c}{2}} z_3^{\frac{\Delta_c+l_c}{2}} \left(g_b(z_2,\bar{z}_2,w_1,w_2,\Upsilon)+\dots\right). \tag{4.73}$$

The derivation of this limit follows the same steps we carried out in the discussion of the OPE limit on the link b above. In particular, one can show that upon taking the combined a and c OPE limit, the

second order Casimir operators behave as

$$\mathcal{D}^2_{(12)}, \mathcal{D}^2_{(56)} \xrightarrow{(a+c)\,\text{OPE}} \text{const}\,, \qquad \mathcal{D}^2_{(123)} \xrightarrow{(a+c)\,\text{OPE}} \mathcal{D}^2_b(z_2, \bar{z}_2, w_1, w_2, \Upsilon)\,. \tag{4.74}$$

Here 'const' denotes the value of the quadratic Casimir element in the STT representations of the intermediate fields that are exchanged in the channels a and c, respectively. The second order Casimir element for the link b reduces to an operator in the five remaining variables that can be worked out explicitly, even though the expression is a bit longer than in our discussion above. It can be found in the Mathematica notebook attached to [44]. In the next section we will argue that this 5-variable Casimir operator can be mapped to the Casimir operator of a spinning four-point function with two scalars and two STTs attached on either side of the OPE diagram.

4.4 Spinning Calogero-Sutherland models

In the previous section we have computed the six-point comb channel Casimir differential equations in two OPE limits. In the first case, we performed the OPE limit on the central link of the OPE diagram and obtained two sets of Casimir operators that act on three cross ratios each. The second order Casimir operators were spelled out in eq. (4.72). The second setup involved a combined OPE limit on the left and the right link and it resulted in a set of Casimir operators acting on a 5-variable system. In both cases, the resulting limiting system is expected to correspond to a spinning four-point correlator, either one involving three scalars and one MST or one with two scalars and two STT external fields. The Casimir operators for such four-point blocks have been constructed in some examples, see e.g. [25, 78–80]. Here we shall report on a very recent observation that all these Casimir operators can be constructed from Harish-Chandra's radial component map [83]. The construction actually works for arbitrary spinning four-point functions in any dimension.

We shall provide a short review of the previous work on the relation between spinning conformal blocks and harmonic analysis of spherical functions in the first subsection before we spell out the universal spinning Casimir operators in the second. The general construction will be worked out explicitly in a number of examples, including the two cases we mentioned in the previous paragraph. In the third subsection we then construct an explicit map between the OPE limits of Casimir operators obtained in the previous section with the spinning Casimir operators to be discussed below, thereby confirming the expectation that e.g. the Casimir operator spelled out in eq. (4.72) is identical to the Casimir operator for a spinning four-point function.

4.4.1 Spherical functions and the radial part of the Laplacian

As was shown in [79, 80, 85], conformal four-point functions admit a realisation as covariant vector-valued functions on the conformal group $G \sim SO(d+1,1)$[3] itself. More precisely, there is a bijective correspondence between solutions to conformal Ward identities and K-spherical functions on G, where $K \sim SO(1,1) \times SO(d)$ is the group of rotations and dilatations. Given two finite-dimensional irreducible representations ρ_L and ρ_R of K, with carrier spaces $W_{L,R}$, respectively, the space of K-spherical functions is defined as

$$\Gamma_{\rho_L,\rho_R} = \{f : G \to \text{Hom}(W_R, W_L) \mid f(k_L g k_R) = \rho_L(k_L) f(g) \rho_R(k_R)\}, \quad g \in G,\ k_{L,R} \in K\,. \tag{4.75}$$

We may, and occasionally will, identify $\text{Hom}(W_R, W_L) \cong W_L \otimes W_R^*$. Covariance properties of f are then written as

$$f(k_L g k_R) = (\rho_L(k_L) \otimes \rho_R^*(k_R^{-1})) f(g)\,. \tag{4.76}$$

The explicit map between K-spherical functions and conformal correlators may be found in [81, 86].

[3] We write $G \sim H$ to mean that Lie groups G and H are locally isomorphic, i.e. $Lie(G) \cong Lie(H)$.

Through the reinterpretation of conformal correlators as K-spherical functions on the conformal group, conformal blocks are carried to eigenfunctions of the group Laplacian, thus becoming a subject of harmonic analysis. By definition, spherical harmonics are eigenfunctions of the *radial part* of the Laplacian. The latter may be thought of as a differential operator in two variables with matrix coefficients. To explain this, we recall that the conformal group G admits a Cartan decomposition

$$G = KA_pK \ . \tag{4.77}$$

In other words, almost every[4] element of G can be factorized as $g = k_L a k_R$, with $k_L, k_R \in K$ and $a \in A_p$. The factor A_p is the two-dimensional abelian group generated by elements $H_1 = \frac{1}{2}(P_1 + K_1)$ and $H_2 = -\frac{i}{2}(P_2 - K_2)$, where P_μ, K_μ denote generators or translations and special conformal transformations, respectively. Clearly, spherical functions are uniquely determined by their restrictions to A_p. Furthermore, such restrictions are not arbitrary. Let $M \sim SO(d-2)$ be the centraliser of A_p in K. For any $m \in M$, given one decomposition $g = k_L a k_R$, we can form another $g = (k_L m)a(m^{-1}k_R)$ (one can fix the ambiguity by requiring that either k_L or k_R belongs to a particular section of K/M). When restricted to A_p, spherical functions take values in the space of M-invariants inside $\mathrm{Hom}(W_R, W_L)$. Indeed

$$f(a) = f(mam^{-1}) = \rho_L(m) f(a) \rho_R(m^{-1}) \ . \tag{4.78}$$

Because it commutes with left and right regular representations, the Laplacian Δ preserves the space Γ_{ρ_L,ρ_R}. The above comments allow us to regard its restriction to this space as a differential operator that acts on vector-valued functions in two variables.

4.4.2 Spinning blocks and Calogero-Sutherland models

We will now explain how radial parts of the Laplacian are related to spinning Calogero-Sutherland models. Let $h = \exp(t_i H_i)$ be an element of A_p and write $X' = h^{-1}Xh$ for any $X \in \mathfrak{g}$[5]. The quadratic Casimir of $\mathfrak{g}$ can be written as

$$\begin{aligned}\mathcal{C}as^2 &= H_1^2 + H_2^2 + \coth(t_1+t_2)(H_1+H_2) + \coth(t_1-t_2)(H_1-H_2) + (d-2)(\coth t_1 H_1 + \coth t_2 H_2) \\ &- \frac{D_+'^2 - 2\cosh(t_1+t_2)D_+'D_+ + D_+^2}{2\sinh^2(t_1+t_2)} - \frac{D_-'^2 - 2\cosh(t_1-t_2)D_-'D_- + D_-^2}{2\sinh^2(t_1-t_2)} \\ &+ \sum_{a=3}^{d}\left(\frac{M_{1a}'^2 - 2\cosh t_1 M_{1a}'M_{1a} + M_{1a}^2}{\sinh^2 t_1} + \frac{M_{2a}'^2 - 2\cosh t_2 M_{2a}'M_{2a} + M_{2a}^2}{\sinh^2 t_2}\right) - \frac{1}{2}M^{ab}M_{ab},\end{aligned} \tag{4.79}$$

where we have introduced $D_\pm = D \pm \mathrm{i}M_{12}$ and indices a, b to run over the set $\{3, 4, ..., d\}$. In the remainder of this section, Latin indices will always be assumed to be in this range. The validity of the last equation can be readily checked and we provide a short derivation in Appendix B.1. We call the above equation the radial decomposition of $\mathcal{C}as^2$. More generally, the radial decomposition of elements in $U(\mathfrak{g}_c)$ may be thought of as an infinitesimal version of the Cartan decomposition. Significance of the radial decomposition of $\mathcal{C}as^2$ lies in the fact that it allows to directly reduce the Laplacian to any space of K-spherical functions. All one needs to do is substitute the generators H_i by partial derivatives ∂_{t_i}, the primed generators x', with $x \in \mathfrak{k}_c$, by representation operators $\rho_L(x)$ and the unprimed generators $y \in \mathfrak{k}_c$ by $\rho_R^*(-y)$. The fact that the same prescription can be applied for all choices of ρ_L and ρ_R can be captured by defining a universal map

$$\Pi : U(\mathfrak{g}_c) \to \mathcal{D}(A_p) \otimes (U(\mathfrak{k}_c) \otimes_{U(\mathfrak{m}_c)} U(\mathfrak{k}_c)), \tag{4.80}$$

that assigns to any element of $U(\mathfrak{g}_c)$ a (class of a) differential operator on A_p with coefficients in two copies of $U(\mathfrak{k}_c)$ (here $\mathcal{D}(A_p)$ denotes the algebra of differential operators on A_p). The latter is called

[4] The set of elements that cannot be factorized has Haar measure zero.

[5] We use the notation $\mathfrak{g} = Lie(G)$ and $\mathfrak{g}_c = \mathfrak{g} \otimes \mathbb{C}$ and similarly for Lie algebras of all other groups under consideration.

Harish-Chandra's radial component map. In practice, for any $u \in U(\mathfrak{g}_c)$, $\Pi(u)$ is computed by radially decomposing u[6] and then replacing elements x', with $x \in U(\mathfrak{k}_c)$, by $x \otimes 1$ and elements y, with $y \in \mathfrak{k}_c$, by $1 \otimes y$. The replacements here belong to the product of two *commuting* copies of $U(\mathfrak{k}_c)$.

The universal Calogero-Sutherland Hamiltonian is a close cousin of the universal radial part of the Laplacian $\Pi(\mathcal{C}as^2)$ (see [87, 88] for a recent discussion). The two are related by conjugation, $H = \delta\Pi(\mathcal{C}as^2)\delta^{-1}$, by the factor

$$\delta(t_i) = \sqrt{\sinh^{d-2} t_1 \sinh^{d-2} t_2 \sinh(t_1+t_2)\sinh(t_1-t_2)}\ . \tag{4.81}$$

This is the essentially unique factor that gives an operator in a Schrödinger from, i.e. without first order derivatives in t_i. Explicitly, the universal Hamiltonian reads

$$\begin{aligned} H = {} & \partial_{t_1}^2 + \partial_{t_2}^2 + \frac{1 - D_+'^2 + 2\cosh(t_1+t_2) D_+' D_+ - D_+^2}{2\sinh^2(t_1+t_2)} + \frac{1 - D_-'^2 + 2\cosh(t_1-t_2) D_-' D_- - D_-^2}{2\sinh^2(t_1-t_2)} \\ & + \frac{M_{1a}' M_{1a}' - 2\cosh t_1 M_{1a}' M_{1a} + M_{1a} M_{1a} - \frac{1}{4}(d-2)(d-4)}{\sinh^2 t_1} \\ & + \frac{M_{2a}' M_{2a}' - 2\cosh t_2 M_{2a}' M_{2a} + M_{2a} M_{2a} - \frac{1}{4}(d-2)(d-4)}{\sinh^2 t_2} - \frac{1}{2} M^{ab} M_{ab} - \frac{d^2-2d+2}{2}\ . \end{aligned} \tag{4.82}$$

We have slightly abused the notation here: in eq. (4.79) both M_{1a} and M_{1a}' are elements of $U(\mathfrak{g}_c)$ and $M_{1a}' = h^{-1} M_{1a} h$, whereas in eq. (4.82), they are elements of $U(\mathfrak{k}_c) \otimes U(\mathfrak{k}_c)$. In accordance with the prescription spelled out above, spinning Calogero-Sutherland Hamiltonians, denoted H_{ρ_L,ρ_R}, are obtained from H by substitutions $x' \to \rho_L(x)$ and $y \to \rho_R^*(-y)$, with $x, y \in U(\mathfrak{k}_c)$. Equation (4.82) is the central one of this section and all applications below emerge from its special cases. Compared to the previous works [79, 80], which computed H_{ρ_L,ρ_R} for some particular representations $\rho_{L,R}$, the new observation of [83] concerns the universal spin dependence of these Schrödinger operators.[7]

As a first simple illustration of this universal formula let us briefly discuss the case of scalar functions on G. These correspond to four-point functions of scalar fields. For K-K invariant functions, i.e. trivial representations $\rho_L = \rho_R = 1$ the Hamiltonian we get reads

$$H_0 = \partial_{t_1}^2 + \partial_{t_2}^2 + \frac{1}{2}\left(\frac{1}{\sinh^2(t_1+t_2)} + \frac{1}{\sinh^2(t_1-t_2)}\right) - \frac{(d-2)(d-4)}{4}\left(\frac{1}{\sinh^2 t_1} + \frac{1}{\sinh^2 t_2}\right) - \frac{d^2-2d+2}{2}\ .$$

To make our coordinates on A_p agree with [79, 80], we introduce $u_1 = t_1 + t_2$ and $u_2 = t_1 - t_2$. The Hamiltonian then can be written as

$$H_0 = -2\left(H_{PT}^{(0,0)}(u_1) + H_{PT}^{(0,0)}(u_2) + \frac{(d-2)(d-4)}{8}\left(\frac{1}{\sinh^2\frac{u_1+u_2}{2}} + \frac{1}{\sinh^2\frac{u_1-u_2}{2}}\right)\right) - \frac{d^2-2d+2}{2}, \tag{4.83}$$

where $H_{PT}^{(a,b)}$ denotes the quantum mechanical Pöschl-Teller Schrödinger operator. The H_0 is the Hamiltonian of the hyperbolic BC_2 Calogero-Sutherland model with parameters $a = 0$, $b = 0$ and $\epsilon = d-2$, justifying our terminology. More precisely

$$H_0 = -2H_{cs}^{(0,0,d-2)} - \frac{d^2-2d+2}{2}\ . \tag{4.84}$$

[6] Almost any element $h \in A_p$ provides an isomorphism of vector spaces $U(\mathfrak{g}_c) \cong U(\mathfrak{a}_{p_c}) \otimes (U(\mathfrak{k}_c) \otimes_{U(\mathfrak{m}_c)} U(\mathfrak{k}_c))$

$$\Gamma_h : U(\mathfrak{a}_{p_c}) \otimes U(\mathfrak{k}_c) \otimes U(\mathfrak{k}_c) \to U(\mathfrak{g}_c), \quad \Gamma_h(H \otimes x \otimes y) = h^{-1} x h\ H\ y\ .$$

The element of $U(\mathfrak{g}_c)$ on the right hand side is said to be in a radially-decomposed form with respect to h. Notice that $U(\mathfrak{a}_{p_c})$ is naturally represented by differential operators on A_p with constant coefficients, i.e. $U(\mathfrak{a}_{p_c}) \cong \mathbb{C}[\partial_{t_1}, \partial_{t_2}]$.

[7] In the most direct way to derive Casimir equations for spinning conformal blocks, one would introduce spin by modifying generators of conformal transformations that act on individual fields. Upon reduction to the cross ratio space, this produces additional terms in the Casimir operator. Our procedure circumvents the reduction of spinning degrees of freedom and adds their contribution to the reduced operator directly.

For non-identical scalar fields, ρ_L and ρ_R are characters of the dilatation group $SO(1,1)$ and trivial representations of $SO(d)$. Writing $\rho_L(D) = 2a$ and $\rho_R^*(D) = 2b$, we obtain the potential

$$V_{\rho_L,\rho_R} = -\frac{2a^2 - 4\cosh(t_1+t_2)ab + 2b^2}{\sinh^2(t_1+t_2)} - \frac{2a^2 - 4\cosh(t_1-t_2)ab + 2b^2}{\sinh^2(t_1-t_2)} \ . \tag{4.85}$$

The full Hamiltonian is then that of the BC_2 Calogero-Sutherland model with parameters a, b and $\epsilon = d-2$

$$H_{\rho_L,\rho_R} = H_0 + V_{\rho_L,\rho_R} = -2H_{cs}^{(a,b,d-2)} - \frac{d^2-2d+2}{2} \ . \tag{4.86}$$

Wave functions of this operator were constructed in the seminal work of Heckman and Opdam [77]. Finally, assume that ρ_L and ρ_R arbitrary finite-dimensional representations. Due to the invariance condition (4.78), the Hamiltonian H_{ρ_L,ρ_R} is restricted to act on functions $F : A_p \to W_L \otimes W_R^*$ that satisfy $(\rho_L(M_{ab}) + \rho_R^*(M_{ab}))F = 0$. It is not difficult to see from the expression (4.82) that H_{ρ_L,ρ_R} is indeed a well-defined operator on this space. By writing $\rho_L(x)$ and $\rho_R^*(-y)$ as matrices one ends up with a certain matrix Schrödinger operator. Here we will follow a slightly different path: representations ρ_L and ρ_R of $\mathfrak{t}_c$ will be written in terms of differential operators that act on finite-dimensional spaces of polynomials. This allows to elegantly impose the M-invariance conditions - "spin cross ratios" of previous sections will arise as generators of M-invariants in $\mathrm{Hom}(W_R, W_L)$. When prepared in this way, the spinning Hamiltonians may be compared to those obtained through the OPE limit construction.

We will consider two examples in particular: 1) the representation ρ_L is trivial and ρ_R is a mixed symmetry tensor of depth two, and 2) both ρ_L and ρ_R are symmetric traceless tensors. Here, we are referring to the $SO(d)$ content of these representations. By the dictionary of [79, 81], the two cases correspond in conformal field theory to a four-point function of an MST_2 field and three scalars, and two STTs and two scalars, respectively, and hence they are directly relevant for the discussion of the two OPE limits we analyzed in the previous section.

One MST_2 and three scalars

We consider spinning Calogero-Sutherland Hamiltonians that arise when one of the representations ρ_L, ρ_R is trivial. For concreteness, let ρ_L be the trivial representation. The potential in the Schrödinger operator the simplifies to

$$V = -\frac{D_+^2}{2\sinh^2(t_1+t_2)} - \frac{D_-^2}{2\sinh^2(t_1-t_2)} + \sum_{a=3}^{d}\left(\frac{M_{1a}^2}{\sinh^2 t_1} + \frac{M_{2a}^2}{\sinh^2 t_2}\right) - \frac{1}{2}M^{ab}M_{ab} \ . \tag{4.87}$$

We assume that ρ_R is a mixed symmetry tensor (l,ℓ) of depth two of the rotation group. Thus, the generators may be realised as differential operators

$$iM_{12} \to \rho_R^*(-iM_{12}) = z^a\partial_a - l, \quad M_{ab} \to z_b\partial_{z^a} - z_a\partial_{z^b} + w_b\partial_{w^a} - w_a\partial_{w^b}, \tag{4.88}$$

$$iM_{1a} \to \frac{1}{2}\left((1+z^2)\partial_{z^a} - 2z_a(z^b\partial_{z^b} - l) + 2z^b(w_b\partial_{w^a} - w_a\partial_{w^b})\right), \tag{4.89}$$

$$M_{2a} \to \frac{1}{2}\left((1-z^2)\partial_{z^a} + 2z_a(z^b\partial_{z^b} - l) - 2z^b(w_b\partial_{w^a} - w_a\partial_{w^b})\right), \tag{4.90}$$

that act on polynomial functions of z^a and w^a. In the following, to simplify notation, we will write the differential operators $\rho_R^*(-M_{ab})$ simply as M_{ab}. The invariance condition (4.78) reads $M_{ab}f = 0$ and is solved by functions of the variables

$$X = z^a z_a, \quad W = w^a w_a, \quad Y = z^a w_a \ . \tag{4.91}$$

To get to the carrier space of ρ_R^*, we are further required to impose the homogeneity $Y\partial_Y f = \ell f$ and restrict to the lightcone $\{W = 0\}$. Individual pieces of the Hamiltonian (4.82) restrict to well-defined

operators on such functions. Introducing the operator

$$L_{l,\ell}(X) = -X(1-X)^2\partial_X^2 - \left(\ell(1-X) - 2(1-l)X + \frac{d-2}{2}(1+X)\right)(1-X)\partial_X + \left(1-l-\frac{d-2}{2}\right)(\ell(1-X)+lX) - \frac{l(d-2)}{2}, \tag{4.92}$$

we have

$$D = 2b, \quad iM_{12} = 2X\partial_X + \ell - l, \quad M_{1a}M_{1a} = L(X), \quad M_{2a}M_{2a} = L(-X)\ . \tag{4.93}$$

Therefore, the Hamiltonian reads

$$H_{l,\ell}^{(b)} = \partial_{t_1}^2 + \partial_{t_2}^2 + \frac{1-(2b+\ell-l+2X\partial_X)^2}{2\sinh^2(t_1+t_2)} + \frac{1-(2b-\ell+l-2X\partial_X)^2}{2\sinh^2(t_1-t_2)} + \frac{L_{l,\ell}(X) - \frac{1}{4}(d-2)(d-4)}{\sinh^2 t_1} + \frac{L_{l,\ell}(-X) - \frac{1}{4}(d-2)(d-4)}{\sinh^2 t_2} - \frac{d^2-2d+2}{2}\ . \tag{4.94}$$

Note that the Hamiltonian acts on three variables, t_1, t_2 and X. We will compare it to the second order differential operator (4.72) we obtained in the previous section when studying the OPE limit in the central intermediate link of the six-point function.

Two STTs and two scalars

Let us now address the second case in which the left and right representations of the rotation group are both symmetric traceless tensors. This leads to the Calogero-Sutherland Hamiltonian as a differential operator in five variables. In the universal Calogero-Sutherland Hamiltonian, we are required to make substitutions

$$iM'_{12} \to \rho_L(iM_{12}) = -z'^a\partial'_a + l', \quad M'_{ab} \to z'_a\partial'_b - z'_b\partial'_a, \tag{4.95}$$

$$iM'_{1a} \to -\frac{1}{2}\left((1+z'^2)\partial'_a - 2z'_a(z'^b\partial'_b - l')\right), \quad M'_{2a} \to -\frac{1}{2}\left((1-z'^2)\partial'_a + 2z'_a(z'^b\partial'_b - l')\right), \tag{4.96}$$

$$iM_{12} \to \rho_R^*(-iM_{12}) = z^a\partial_a - l, \quad M_{ab} \to z_b\partial_a - z_a\partial_b, \tag{4.97}$$

$$iM_{1a} \to \frac{1}{2}\left((1+z^2)\partial_a - 2z_a(z^b\partial_b - l)\right), \quad M_{2a} \to \frac{1}{2}\left((1-z^2)\partial_a + 2z_a(z^b\partial_b - l)\right)\ . \tag{4.98}$$

The invariance condition $(M'_{ab} - M_{ab})f = 0$ then means that f depends only on the scalar products

$$X_R = z^a z_a, \quad X_L = z'^a z'_a, \quad Y = z^a z'_a\ . \tag{4.99}$$

Individual pieces of the Hamiltonian commute with the constraints, so they reduce to operators in the variables (X_R, X_L, Y). To write them down, we introduce

$$L_1(X_R,X_L,Y) = \frac{1}{4}\Big(-4X_R(1-X_R)^2\partial_{X_R}^2 - 4Y(1-X_R)^2\partial_{X_R}\partial_Y + (4Y^2-(1+X_R)^2X_L)\partial_Y^2 + 2(1-X_R)(4(1-l)X_R - (d-2)(1+X_R))\partial_{X_R} - 2Y((-2l-d+4)X_R + 2l - d + 2)\partial_Y + 2l(2(1-l)X_R - (d-2)(1+X_R))\Big), \tag{4.100}$$

and

$$L_2(X_R,X_L,Y) = -\frac{1}{4}\Big(-4Y(1-X_R)(1-X_L)\partial_{X_R}\partial_{X_L} - 2(1-X_R)(X_R(1+X_L)-2Y^2)\partial_{X_R}\partial_Y - 2(1-X_L)(X_L(1+X_R)-2Y^2)\partial_{X_L}\partial_Y + (-4Y^3 + Y(-1+X_R+X_L+3X_RX_L))\partial_Y^2 + \big((2-d)(1+X_R)(1+X_L) + 2(1-l)X_R(1+X_L) + 2(1-l')X_L(1+X_R) - 4(1-l-l')Y^2\big)\partial_Y - 4lY(1-X_L)\partial_{X_L} - 4l'Y(1-X_R)\partial_{X_R} - 4ll'Y\Big)\ . \tag{4.101}$$

Then we have

$$M_{1a}M_{1a} = L_1(X_R, X_L, Y), \quad M_{2a}M_{2a} = L_1(-X_R, -X_L, -Y), \tag{4.102}$$

$$M'_{1a}M_{1a} = L_2(X_R, X_L, Y), \quad M'_{2a}M_{2a} = L_2(-X_R, -X_L, -Y)\ . \tag{4.103}$$

Clearly, the operators $M'_{1a}M'_{1a}$ and $M'_{2a}M'_{2a}$ are obtained from $M_{1a}M_{1a}$ and $M_{2a}M_{2a}$ by exchanging X_R and X_L. Together with

$$iM_{12} = 2X\partial_{X_R} + Y\partial_Y - l, \quad iM'_{12} = -2X_L\partial_{X_L} - Y\partial_Y + l', \tag{4.104}$$

$$\frac{1}{2}M^{ab}M_{ab} = \left(X_R X_L - Y^2\right)\partial_Y^2 - (d-3)Y\partial_Y\ . \tag{4.105}$$

these expressions are substituted in the formula (4.82) for the universal Hamiltonian to give the appropriate Calogero-Sutherland model that characterizes four-point blocks with two scalars and two STTs. It will be compared with the Hamiltonian we obtained in the previous section when we studied the double sided OPE limit of the six-point function.

4.4.3 Mapping between OPE-reduced operators and Calogero-Sutherland form

In this section we will see how, using the leading behaviours of six-point blocks spelled out in section 4.3 under the various OPE limits, it is possible to recover the spinning four-point Casimir equations from the previous subsection. Our strategy is to map the differential equations we obtained when discussing OPE limits into a certain "standard form" of a quantum mechanical Hamiltonian, which can then be identified with one of the spinning Calogero-Sutherland Hamiltonians constructed above. As a rule of thumb, we will modify the second-order derivatives by performing a change of variables; all first-order derivatives can instead be modified without affecting the second-order ones by "extracting" a certain function of the cross ratios from the target function. After this second operation, the new differential operator $\mathcal{D}'$ is related to the original one by conjugation by the factor ω

$$\psi = \omega\psi' \qquad \Longrightarrow \qquad \mathcal{D}' = \omega^{-1}\mathcal{D}\omega\ . \tag{4.106}$$

Let us now describe these steps in some more detail for the two cases we have analyzed in the previous section.

One MST$_2$ and three scalars

As a first step, it is possible to employ the change of variables used in [76] in order to map the second-order derivatives of $\mathcal{D}_a^2$ in z_1 and $\bar{z}_1$ to one-dimensional kinetic terms. More precisely, we make the following change of variables

$$z_1, \bar{z}_1 \qquad \longrightarrow \qquad \begin{cases} t_1 = \mathrm{i}\left[\arcsin\left(\frac{1}{\sqrt{z_1}}\right) + \arcsin\left(\frac{1}{\sqrt{\bar{z}_1}}\right)\right], \\ t_2 = \mathrm{i}\left[\arcsin\left(\frac{1}{\sqrt{z_1}}\right) - \arcsin\left(\frac{1}{\sqrt{\bar{z}_1}}\right)\right], \end{cases} \tag{4.107}$$

which leads to the anticipated transformation in the quadratic Casimir

$$2z_1^2(1-z_1)\partial_{z_1}^2 + 2\bar{z}_1^2(1-\bar{z}_1)\partial_{z_1}^2 \qquad \longrightarrow \qquad \partial_{t_1}^2 + \partial_{t_2}^2\,. \tag{4.108}$$

Secondly, we wish to eliminate first order derivatives with respect to t_1 and t_2. We can do so through conjugation of the type in eq. (4.106), with the factor

$$\omega(t_1, t_2, w_1) = (\sinh t_1 \sinh t_2)^{\,1-\frac{d}{2}}\,(\cosh t_1 - \cosh t_2)^{\,-a-b-\frac{1}{2}}\,(\cosh t_1 + \cosh t_2)^{\,a+b-\frac{1}{2}}$$
$$\left(\frac{\sinh t_1 + \sinh t_2}{\sinh t_1 - \sinh t_2}\,(1-w_1)^{\,2}\right)^{\frac{l_b-\ell_b}{2}}\ . \tag{4.109}$$

We now wish to eliminate the mixed derivatives $\partial_{t_i}\partial_{w_1}$, providing this way a partial decoupling of the internal leg and vertex degrees of freedom. This can be achieved by the change of variables

$$w_1 \qquad \longrightarrow \qquad X = \frac{\sinh t_1 - \sinh t_2}{\sinh t_1 + \sinh t_2}\frac{w_1}{1-w_1}\,. \tag{4.110}$$

The operator produced at the end of this procedure is of the spinning Calogero-Sutherland form, and corresponds precisely to the operator we spelled out in the previous subsection 4.4.2, see eq. (4.94).

Two STTs and two scalars

As we did in the previous subsection, the first step to map this operator to a quantum mechanical Hamiltonian is to make two derivatives become one-dimensional kinetic terms, which is done by transforming

$$z_2, \bar{z}_2 \qquad \longrightarrow \qquad \begin{cases} t_1 = \mathrm{i}\left[\arcsin\left(\frac{1}{\sqrt{z_2}}\right) + \arcsin\left(\frac{1}{\sqrt{\bar{z}_2}}\right)\right], \\ t_2 = \mathrm{i}\left[\arcsin\left(\frac{1}{\sqrt{z_2}}\right) - \arcsin\left(\frac{1}{\sqrt{\bar{z}_2}}\right)\right], \end{cases} \tag{4.111}$$

which leads to

$$2z_2^2(1-z_2)\partial_{z_2}^2 + 2\bar{z}_2^2(1-\bar{z}_2)\partial_{z_2}^2 \qquad \longrightarrow \qquad \partial_{t_1}^2 + \partial_{t_2}^2\,. \tag{4.112}$$

As a second step, it is possible to remove the first order derivatives in t_1 and t_2 by conjugating with

$$\begin{aligned}\omega(t_1,t_2,w_1,w_2,\Upsilon) = (\sinh t_1 \sinh t_2)^{1-\frac{d}{2}}\,(\cosh t_1 - \cosh t_2)^{-a-b-\frac{1}{2}}\,(\cosh t_1 + \cosh t_2)^{\,a+b-\frac{1}{2}} \\ \left(\frac{\sinh t_1 - \sinh t_2}{\sinh t_1 + \sinh t_2} w_1^2\right)^{\frac{l_a}{2}} \left(\frac{\sinh t_1 + \sinh t_2}{\sinh t_1 - \sinh t_2}\,(1-w_2)^2\right)^{\frac{l_b}{2}}\,.\end{aligned} \tag{4.113}$$

Finally, we can eliminate all mixed derivatives that involve the t_i coordinates by taking the change of variables

$$\begin{gathered} X_L = \frac{\sinh t_1 + \sinh t_2}{\sinh t_1 - \sinh t_2}\frac{1-w_1}{w_1}\,, \qquad X_R = \frac{\sinh t_1 - \sinh t_2}{\sinh t_1 + \sinh t_2}\frac{w_2}{1-w_2}\,, \\ Y = -\sqrt{\frac{(1-w_1)w_2}{(1-w_2)w_1}}\,\frac{\sinh t_1 \sinh t_2}{\cosh t_1 - \cosh t_2}\Upsilon\,. \end{gathered} \tag{4.114}$$

The operator obtained at the end of this procedure corresponds precisely to the one we constructed in subsection 4.4.2. This concludes the mappings between the differential operators obtained from the OPE limits and the Calogero-Sutherland Hamiltonians, confirming that the leading behaviors in section 4.3.3 are extracted properly.

Chapter 5

Vertex systems

The goal of this chapter is to report our results of [43], where we analyzed the simplest cases of vertex differential operators that appear in CFT, namely the case of three-point functions with an associated one-dimensional space of independent tensor structures. These corresponds to all the possible vertices that can appear in comb-channel correlation functions in 3D and 4D. We start by expanding the discussion of section 2.4.3 by spelling out the construction of all these one-dimensional systems, and we then shift our attention to the vertex differential operators one can construct in those cases. These correspond to the reduction of certain 3-site Gaudin models to the space of cross-ratios for 3-point functions. The main claim we review in this chapter is that for all these one-dimensional systems, we can map the vertex operators to Hamiltonians of a crystallographic elliptic Calogero-Moser-Sutherland (CMS) model that was first discovered by Etingof, Felder, Ma, and Veselov in [75].

5.1 Setup and Summary of Results

Let us start by providing all the basic knowledge and notation that is required to spell out the main results of [43]. We proceed in three steps. In the first subsection we review the counting of cross ratios for scalar correlation functions in general, and for spinning vertex systems in particular cases. Next we sketch a group theoretic interpretation of the cross ratios for the spinning vertex system. This will provide the link to the Gaudin integrable model and the construction of vertex operators which we outline in the third subsection.

5.1.1 Cross ratios and single parameter vertices

Let us consider an OPE channel $\mathcal{C}^N_{OPE}$ for an N-point correlation function of scalars. As before, we enumerate external lines by indices $i = 1, \dots, N$, internal lines by $r = 1, \dots N-3$, and vertices by $\mathfrak{v} = 1, \dots N-2$. The number of degrees of freedom associated with a single vertex depends on the spin of the three fields involved, i.e. whether they are scalars, symmetric traceless tensors, or fields with higher spin depth. The depth of the intermediate fields grows with the number of operator products that are required to construct them from scalars. More precisely, given the relation $L = \mathfrak{d} - 1$ between the spin depth L, and the shifted definition of depth of chapter 3, we have from (3.9) that the depth L_r of a link r in an OPE diagram is given by

$$L_r(\mathcal{C}^N_{OPE}, d) = L(I_{r,1}, d), \quad \textit{where} \quad L(I, d) = \min(|I|, N - |I|, \text{rank}_d) - 1 \ . \tag{5.1}$$

Here, rank_d denotes the rank of the d-dimensional conformal algebra, i.e. the dimension of its Cartan subalgebra. Let us now look at a particular vertex $\mathfrak{v}$ in an OPE diagram in a d-dimensional conformal field theory. We call the ordered set $(L_{\mathfrak{v},1}, L_{\mathfrak{v},2}, L_{\mathfrak{v},3})$ of depths $L_{\mathfrak{v},k}$ of the three adjacent legs with $L_{\mathfrak{v},1} \geq L_{\mathfrak{v},2} \geq L_{\mathfrak{v},3}$ the *type* of the vertex. This type determines the number of degrees of freedom that

are associated with $\mathfrak{v}$ according to the formula

$$n_{vdo,\mathfrak{v}}(\mathcal{C}^N_{OPE}, d) = n_{cr}\left(\sum_{k=1}^{3} L_{\mathfrak{v},k} + 3, d\right) - \sum_{k=1}^{3} L_{\mathfrak{v},k}(L_{\mathfrak{v},k}+1)\ . \tag{5.2}$$

Here, $n_{cr}(M,d)$ counts the total number of independent cross ratios of a scalar M-point function in d dimensions we expressed in (2.112). As we showed in section 2.4.3, vertices $\mathfrak{v}$ with two scalar legs are completely fixed by conformal symmetry and do not contribute any degree of freedom, i.e. $n_{vdo,\mathfrak{v}} = 0$ for $L_{\mathfrak{v},1} = 0 = L_{\mathfrak{v},2}$. Vertices for which none of the legs are scalar are easily seen to have at least two degrees of freedom. Hence, vertices that possess a single degree of freedom must necessarily have one scalar leg. These are the three cases

$$(L_{\mathfrak{v},1}, L_{\mathfrak{v},2}, L_{\mathfrak{v},3}) = \begin{cases} \text{I}: & (1,1,0) & \textit{for} & d \geq 3 \\ \text{II}: & (2,1,0) & \textit{for} & d \geq 4 \\ \text{III}: & (2,2,0) & \textit{for} & d = 4 \end{cases}\ . \tag{5.3}$$

Let us note that in $d > 4$ the vertex of type III possesses two degrees of freedom. The reduction to a

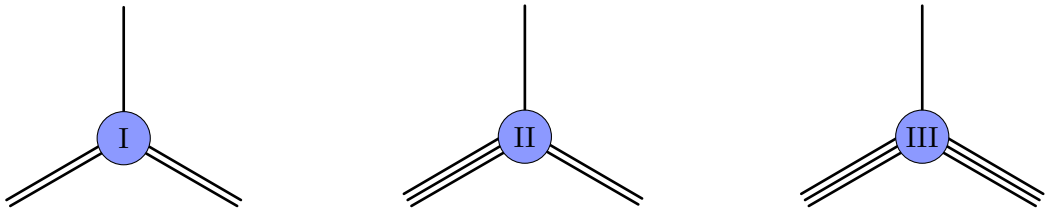

(a) STT-STT-scalar **(b)** MST_2-STT-scalar **(c)** MST_2-MST_2-scalar

Figure 5.1: Vertices with an associated one-dimensional space of tensor structures. Single-lined legs are scalars; double or triple lines correspond respectively to STT and MST_2 representations. For the type III vertex in Figure 5.1c, the space is two-dimensional and reduces to one dimension only in $d = 4$.

single degree of freedom in $d = 4$ is exceptional. In standard terms, type I vertices involve one scalar and two STTs, type II occur for one scalar, one STT and one MST of depth $L = 2$ while type III contain one scalar and two MSTs of depth $L = 2$. These three different types, depicted in Figure 5.1, exhaust all those vertices that can appear in the comb channel of scalar N-point functions in $d = 3$ and $d = 4$ dimensions. By definition, all vertices in the comb channel have at least one external leg which is scalar, i.e. has $L = 0$. Let us also note that for 5-point functions in any d the only non-trivial vertex is of type I, which is included in our list. Similarly, for 6-point functions in the comb channel one only needs vertices of type II. In this sense, the theory we are about to describe addresses some of the vertices that are most relevant for applications, and constitutes all the possible vertices that can be recovered from the OPE limits of chapter 4.

The construction of the single conformal invariant $\mathcal{X}$ that describes the vertices in our list (5.3) from the coordinates and polarizations of the three individual fields, as well as the parameterization of 3-point functions of the three types in terms of this cross ratio, will be reviewed in the next section 5.2, see eqs. (5.13), (5.14) and (5.18). The precise embedding of individual (single variable) vertex systems into a multi-point function is illustrated in subsection 5.3.2 for the example of the type I vertex system and its relation with the vertex in a scalar 5-point function.

5.1.2 Group theoretic reformulation of the vertex system

The main goal of this chapter is to characterize the three different types of vertices listed in eq. (5.3) through some differential equation of fourth order. As we reviewed in chapter 3, scalar N-point blocks can be characterized as joint eigenfunctions of $n_{cr}(N,d)$ commuting Gaudin Hamiltonians. In an appropriate limit of parameters of the Gaudin model, the Hamiltonians were shown to include all the Dolan-Osborn

Casimir operators that measure the weight and spin of intermediate fields. The embedding of these operators into an N-site Gaudin model guarantees that the Casimir operators can be complemented into a full set commuting differential operators, one for each cross ratio, and it provides explicit expressions for the additional differential operators which can be associated with the vertices of the OPE diagram and are thereby referred to as vertex differential operators. The Gaudin model allows us to prepare the individual vertex systems, see section 3.3. In the context of the present work, this is most easily described for the vertex of type III. The 4-dimensional conformal group $G = \mathrm{SO}(1,5)$ possesses 15 generators. It has a number of interesting subgroups. In our discussion, two of them play a particular role. The first one is the parabolic subgroup $P = (\mathrm{SO}(1,1) \times \mathrm{SO}(4)) \ltimes \mathbb{R}^4$ that is generated by dilatations, rotations and special conformal transformations. The quotient G/P admits a transitive action of translations and is therefore 4-dimensional. The representations that are associated with scalar fields, i.e. representations of depth $L = 0$, can be realized on the sections of line bundles over G/P. Another closely related realization of this representation is obtained on the space of holomorphic sections in a bundle over the complexification $G_{\mathbb{C}}/P_{\mathbb{C}}$. It is the latter version we shall adopt here. The second subgroup we need is the 9-dimensional Borel subgroup $B_{\mathbb{C}} \subset G_{\mathbb{C}}$. In this case, the quotient $G_{\mathbb{C}}/B_{\mathbb{C}}$ is a flag manifold and we can realize any representation (of depth $L = 2$) on a space of holomorphic sections in a line bundle over it. Given a vertex of type I, it is now natural to assign the following coset space,

$$\mathcal{M}(2,2,0;d=4) = \left(G_{\mathbb{C}}/B_{\mathbb{C}} \times G_{\mathbb{C}}/B_{\mathbb{C}} \times G_{\mathbb{C}}/P_{\mathbb{C}}\right)/G_{\mathbb{C}} \ . \tag{5.4}$$

Here, the complexified conformal group $G_{\mathbb{C}}$ in the denominator acts diagonally from the left on the three factors in the numerator. Note that the numerator has dimension $6+6+4=16$. So, once we divide by the 15-dimensional conformal group we end up with a 1-dimensional quotient space. The coordinate $\mathcal{X}$ of this space is the unique degree of freedom that the vertex of type III contributes. A triple product of coset spaces, such as the one in equation (5.4), may be regarded as the configuration space of a 3-site Gaudin integrable system.

To treat other vertices we introduce the following family of subgroups $P_{d,L}$, $L = 0, \ldots, \mathrm{rank}_d - 1$, of the complexified d-dimensional conformal group $G_{\mathbb{C}}$,

$$P_{d,L} = \mathcal{S}_{1,1}^{(d)}\left(\mathcal{S}_2^{(d-2)}\left(\cdots \mathcal{S}_2^{(d+2-2L)}\left(\mathcal{S}_2^{(d-2L)}(\mathrm{SO}_{\mathbb{C}}(d-2L))\right)\cdots\right)\right) \subset G_{\mathbb{C}} = \mathrm{SO}_{\mathbb{C}}(1,d+1) \ . \tag{5.5}$$

Here, $\mathcal{S}_2^{(M)}(H) \subset \mathrm{SO}_{\mathbb{C}}(M+2)$ denotes a subgroup that is defined for any positive integer M and any subgroup $H \subset \mathrm{SO}_{\mathbb{C}}(M)$ as

$$\mathcal{S}_2^{(M)}(H) = (\mathrm{SO}_{\mathbb{C}}(2) \times H) \ltimes \mathbb{C}^M \subset \mathrm{SO}_{\mathbb{C}}(M+2)$$

where the carrier space $\mathbb{C}^M$ of the fundamental representation of $H \subset \mathrm{SO}_{\mathbb{C}}(M)$ is extended to a representation of $\mathrm{SO}_{\mathbb{C}}(2) \times H$ by requiring that the elements of $\mathbb{C}^M$ carry one unit of $\mathfrak{so}(2)$ charge. This also ensures that $\mathcal{S}_2^{(M)}(H)$ becomes a subgroup of $\mathrm{SO}_{\mathbb{C}}(M+2)$. We use a very similar construction to build

$$\mathcal{S}_{1,1}^{(d)}(H) = (\mathrm{SO}_{\mathbb{C}}(1,1) \times H) \ltimes \mathbb{C}^d$$

for any subgroup $H \subset \mathrm{SO}_{\mathbb{C}}(d)$. With $P_{d,L}$ fully defined we note that the first member $P_{d,0}$ of this family is the parabolic subgroup $P_{d,0} = P_{\mathbb{C}}$ while the last one with $L = \mathrm{rank}_d - 1$ coincides with the Borel subgroup $P_{d,\mathrm{rank}_d-1} = B_{\mathbb{C}}$. One can thus realize the representation of the conformal group that is associated to a tensor field of depth L on a line bundle over the quotient $G_{\mathbb{C}}/P_{d,L}$. The choice of the line bundle is determined by the weight and spin of the field. With this notation, we can now define

$$\mathcal{M}(L_1,L_2,L_3;d) = \left(G_{\mathbb{C}}/P_{d,L_1} \times G_{\mathbb{C}}/P_{d,L_2} \times G_{\mathbb{C}}/P_{d,L_3}\right)/G_{\mathbb{C}} \ . \tag{5.6}$$

Is is easy to see that the dimension of this space coincides with the number of independent conformal invariants that can be constructed from the insertion points and polarizations of three fields of depth L_k,

i.e.

$$dim_{\mathbb{C}}\left(\mathcal{M}(L_1,L_2,L_3;d)\right) = n_{cr}(\sum_{k=1}^{3} L_k + 3, d) - \sum_{k=1}^{3} L_k(L_k+1)\ . \tag{5.7}$$

The space $\mathcal{M}$ is the configuration space of the integrable Gaudin model on the 3-punctured sphere with punctures of depth L_k.

5.1.3 From Gaudin Hamiltonians to Lemniscatic CMS models

The Gaudin Hamiltonians provide a complete set of commuting higher order differential operators on $\mathcal{M}$. Here we shall content ourselves with a very brief review of the vertex system, for more detail see section 3.2.2. A key ingredient in the construction of the Gaudin model is its Lax matrix, whose components in the basis M^α of the conformal Lie algebra are defined as

$$\mathcal{L}^{\mathfrak{v}}_{\alpha}(w) = \sum_{k=1}^{3} \frac{\mathcal{T}^{(k)}_{\alpha}}{w-w_k}\ , \tag{5.8}$$

where w is an auxiliary complex variable called the spectral parameter and we can fix the three complex parameters w_k to be $w_1 = 0$, $w_2 = 1$ and $w_3 = \infty$. The symbols $\mathcal{T}^{(k)}_{\alpha}$ here denote the first order differential operators that describe the action of the conformal algebra on the three spinning primaries at the vertex or, equivalently, on the flag manifolds $G_{\mathbb{C}}/P_{d,L_k}$ we introduced above. The superscript $\mathfrak{v}$ on the Lax matrix emphasizes that this is the matrix corresponding to the vertex $\mathfrak{v}$.
For any elementary symmetric invariant tensor κ_p of degree p on the conformal Lie algebra, there is a corresponding w-dependent Gaudin Hamiltonian. As in chapter 3, we choose κ_p such that the Hamiltonian takes the form

$$\mathcal{H}^{(p)}_{\mathfrak{v}}(w) \quad = \quad str\left(\mathcal{L}^{\mathfrak{v}}_{\alpha_1}(w)\cdots\mathcal{L}^{\mathfrak{v}}_{\alpha_p}(z)\right) + \ldots\,, \tag{5.9}$$

where $\ldots$ represent quantum corrections, involving a smaller number of components of the Lax matrix. Our analysis in subsection 3.2.3 shows that for the vertex systems in our list (5.3) there is only one such independent Hamiltonian and it is of order $p = 4$. Indeed we have argued there that the lower order operators are trivial while the higher order ones can be rewritten in terms of lower order operators. A non-trivial operator can be extracted from the family (5.9) with $p = 4$ as

$$\mathcal{D}_{\mathfrak{v}} \equiv \mathcal{D}^{4,3}_{\mathfrak{v},13} = \mathrm{str}\left(\mathcal{T}^{(1)}\mathcal{T}^{(1)}\mathcal{T}^{(1)}\mathcal{T}^{(3)}\right)\ . \tag{5.10}$$

For the single variable vertices listed in (5.3) the Gaudin model provides the single differential operator of order four which depends on the conformal weights and spins of the three fields. We will work it out explicitly for all three cases, see section 5.3. The results are a bit cumbersome to spell out at first.
In section 5.4 we will massage the answer and thereby pass to a much more compact algebraic formulation where we construct the Hamiltonian from the generators of a deformation of some generalized Weyl algebra. The commutation relations of its three generators $A, A^\dagger$ and N depend on the spins of the fields, see eqs. (5.91) - (5.94). In the limit of $d = 3$ this algebra is actually well known in the literature on quiver varieties where it appears as a generalized Weyl algebra or deformed/quantized Kleinian singularity of affine type $\tilde{A}_3$. Our deformation to $d \neq 3$ can be seen to possess finite dimensional representations whenever the spin quantum numbers are integers, and the dimension of these representations coincides with the number of 3-point tensor structures. Once the algebra generated by $A, A^\dagger$ and N is introduced, the expression for the Hamiltonian can be stated in a single line, see (5.96). Obviously, this Hamiltonian does depend on the choice of conformal weights, unlike the algebra it is a part of. In some sense, the formulas of section 5.4 provide the most compact formulation of our vertex operators and we believe that similar formulations are likely to exist for higher dimensional vertex systems.
Section 5.5 contains the main result we anticipated in the introduction of this chapter: there we show that the vertex operators for all three vertex systems listed in eq. (5.3) can be mapped to a CMS

Hamiltonian, namely the Hamiltonian for a crystallographic elliptic model that was originally discovered by Etingof, Felder, Ma and Veselov about a decade ago, see [75]. This lemniscatic CMS Hamiltonian is spelled out in equation (5.132). It is a fourth-order differential operator in a single variable z. The relation between the cross ratio $\mathcal{X}$ of the vertex system and the new elliptic variable z is stated in eq. (5.146). The map involves Weierstrass' elliptic function $\wp(z)$. The lemniscatic Hamiltonian contains three non-trivial coefficient functions $c_p(z)$ which are defined in eqs. (5.133)-(5.135). These coefficient functions depend on 12 multiplicities $m_{i,\nu}$ with $i = 1, \ldots, 4$, and $\nu = 0, 1, 2$, subject to the five constraints given in eq. (5.125), such that there are only seven remaining independent parameters. These determine the coupling constants in the coefficient functions $c_p(z)$ through eq. (5.152) and eqs. (5.136)-(5.138). For each of the three single variable vertex systems we determine the parameters $m_{i,\nu}$ in equations (5.152) and (5.153)-(5.160) (type I, II; for type II one sets $\ell_2 = 0$) and (5.164)-(5.171) (type III). We note that in cases I and II, the vertex Hamiltonians do not exhaust the entire seven parameter family of lemniscatic models. In fact, for these two cases the multiplicities satisfy the additional constraint (5.163) that reduces the number of independent parameters to six. Only for vertices of type III are the parameters of the lemniscatic model unrestricted.

5.2 Three-Point Functions in Embedding Space

The scope of this section is to construct all the vertex systems we listed in (5.3), which have an associated one-dimensional space of tensor structures. We divide the analysis into two subsections. Vertices of type I and II, which exist for all sufficiently high dimensions, are treated in the first subsection. The case of type III which is restricted to $d = 4$ dimensions requires special treatment and is presented in the second subsection. The use of embedding space formalism and polarization variables gives rise to an elegant reformulation that allows us to construct 3-point correlators easily, up to a function t of conformal invariant variables that is not determined by conformal symmetry, as we saw in (2.92).

5.2.1 Spinning 3-point functions in embedding space

We are now interested in those 3-point functions for which conformal symmetry leaves one free parameter, i.e. the three configurations of spinning fields listed in eq. (5.3). These correspond to the vertices for STT-STT-scalar in $d \geq 3$, MST_2-STT-scalar in $d \geq 4$, and MST_2-MST_2-scalar in $d = 4$, respectively. In section 5.3 we will actually address the computation of the vertex operators for these three cases through a single computation by passing through the 3-point function for MST_2-MST_2-scalar in $d > 4$. From there, we can then descend to the three cases we are interested in. As one can easily see, the vertex of type $(2, 2, 0)$ in $d > 4$ comes with two cross ratios and carries seven quantum numbers: three conformal weights and four spin labels. In order to descend to the three types in the list (5.3), we need to specialize the quantum numbers and restrict to a single cross ratio, see below.
To simplify notation and avoid multiple indices, we will use the notation of section 4.3.2 with

$$Z \equiv Z_1 \,, \quad W \equiv Z_2 \,, \tag{5.11}$$

and use Latin indices $i, j, k = 1, 2, 3$ to run over the three points. The first two spin labels will be as usual be indicated by the letters l and ℓ. With this notation, correlation functions are expressed in terms of the field $\phi_{\Delta_1, l_1, \ell_1}(X_1, Z_1, W_1)$, which therefore has spins $l_1 \geq \ell_1 \geq 0$ and depends on the coordinate X_1 and the two polarization vectors Z_1 and W_1, as well as the fields $\phi_{\Delta_2, l_2, \ell_2}(X_2, Z_2, W_2)$ and $\phi_{\Delta_3}(X_3)$.
From what we saw in section 2.4.3, we know that three-point functions with auxiliary variables such as Z and W need to be constructed out of gauge invariant quantities (2.59). The first task now is therefore to find which non-vanishing independent tensor structures can be constructed out of these. This means building a set of conformal invariants from the position variables X_i and the polarizations Z_i, W_i that generate functions of any degree in all of the seven variables, along with the two cross ratios. The latter

are conformal invariants of vanishing degree. To begin with, we have the scalar products of position vectors

$$X_{12} = X_1 \cdot X_2\,, \qquad X_{23} = X_2 \cdot X_3\,, \qquad X_{31} = X_3 \cdot X_1\,. \tag{5.12}$$

If we denote the multi-degree of a MST_2-MST_2-scalar vertex by $[-\Delta_1, l_1, \ell_1; -\Delta_2, l_2, \ell_2; -\Delta_3]$, these scalar products have degree $deg X_{12} = [1,0,0;1,0,0;0]$ etc. Next, it is customary to introduce the following contractions of the two-forms with two position vectors

$$V_1 = V_{1,32} = \frac{X_3 \cdot (X_1 \wedge Z_1) \cdot X_2}{X_{23}}\,, \qquad V_2 = V_{2,13} = \frac{X_1 \cdot (X_2 \wedge Z_2) \cdot X_3}{X_{31}}\,. \tag{5.13}$$

The two objects V_1 and V_2 have degree $deg\, V_1 = [1,1,0;0,0,0;0]$ and $deg\, V_2 = [0,0,0;1,1,0;0]$. Another simple tensor structure is given by the the contractions of the two-forms, see (2.76),

$$H_{12} \equiv H_{12}^{(1)} = \frac{1}{2}(X_1 \wedge Z_1) \cdot (X_2 \wedge Z_2)\,. \tag{5.14}$$

It has degree $deg\, H_{12} = [1,1,0;1,1,0;0]$. The tensor structures we have introduced so far do not depend on the polarizations W_i, in contrast to the remaining three variables that we will introduce now. These include the following contractions of a three-form with a two-form and a vector,

$$U_{123} = \frac{1}{2}(X_1 \wedge Z_1 \wedge W_1)_{ABC}(X_2 \wedge Z_2)^{AB} X_3^C\,, \qquad U_{213} = \frac{1}{2}(X_2 \wedge Z_2 \wedge W_2)_{ABC}(X_1 \wedge Z_1)^{AB} X_3^C\,, \tag{5.15}$$

and, finally, the contraction of the two three-forms

$$K_{12} \equiv H_{12}^{(2)} = \frac{1}{3!}(X_1 \wedge Z_1 \wedge W_1) \cdot (X_2 \wedge Z_2 \wedge W_2)\,. \tag{5.16}$$

In the notation of [50], these MST_2 tensor structures correspond to $U_{ijk} = T_{i,jk}^{3,21}$ and $K_{ij} = T_{i,j}^{3,3}$. The degrees of these three tensor structures are $deg\, U_{123} = [1,1,1;1,1,0;1]$, $deg\, U_{213} = [1,1,0;1,1,1;1]$ and $deg\, K_{12} = [1,1,1;1,1,1;0]$. This concludes our list of building blocks of tensor structures for the MST_2-MST_2-scalar vertex in $d > 4$. For the reader's convenience we listed the tensor structures and their degrees in Tab. 5.1.

As one can easily count, we have written nine independent tensor structures, the degrees of which span the entire 7-dimensional space of multi-degrees. Since we know that the MST_2-MST_2-scalar vertex admits two cross ratios, the tensor structures we introduced indeed suffice to decompose the 3-point function in the following way

$$\Phi_{123}(X_i; Z_i, W_i) := \langle \phi_{\Delta_1,l_1,\ell_1}(X_1, Z_1, W_1)\phi_{\Delta_2,l_2,\ell_2}(X_2, Z_2, W_2)\phi_{\Delta_3}(X_3)\rangle = \Omega_{l_1,l_2;\ell_1,\ell_2}^{\Delta_1,\Delta_2,\Delta_3}\, t(\mathcal{X},\mathcal{Y})\,, \tag{5.17}$$

where $\Omega_{l_1,l_2;\ell_1,\ell_2}^{\Delta_1,\Delta_2,\Delta_3}$ is a prefactor that takes care of all homogeneity conditions (2.56), i.e. it is a product of powers of tensor structures that matches the degree of the correlation function on the left hand side. The function $t(\mathcal{X},\mathcal{Y})$ is a conformal invariant that depends on two variables of vanishing degree,

$$\mathcal{X} = \frac{H_{12}}{V_1 V_2}\,, \qquad \mathcal{Y} = \frac{X_{13}X_{23}V_1V_2K_{12}}{X_{12}U_{123}U_{213}}\,. \tag{5.18}$$

Of course, the prefactor Ω is not uniquely fixed by the homogeneity condition simply because it is possible to form objects of vanishing degree from the nine tensor structures. The remaining freedom can be fixed by choosing not to employ H_{12} and K_{12} in the construction of Ω. This leaves us with a unique prefactor satisfying all of the required homogeneities in (X_i, Z_i, W_i),

$$\Omega_{l_1,l_2;\ell_1,\ell_2}^{\Delta_1,\Delta_2,\Delta_3} = \frac{V_1^{l_1-\ell_1-\ell_2}V_2^{l_2-\ell_1-\ell_2}U_{123}^{\ell_1}U_{213}^{\ell_2}}{X_{12}^{\frac{\Delta_1+\Delta_2-\Delta_3+l_1+l_2-\ell_1-\ell_2}{2}}X_{23}^{\frac{\Delta_2+\Delta_3-\Delta_1-l_1+l_2+\ell_1+\ell_2}{2}}X_{31}^{\frac{\Delta_3+\Delta_1-\Delta_2+l_1-l_2+\ell_1+\ell_2}{2}}}\,. \tag{5.19}$$

After one has fixed Ω, the remaining freedom in the 3-point function is normally taken into account by expanding in a discrete set of 3-point tensor structures with vanishing multi-degree. These are then

combined with OPE coefficients to make up the full correlator. The standard tensor structures, once homogenized, represent a basis for the space of $t(\mathcal{X},\mathcal{Y})$, but this basis is of course not unique. As we have recalled in chapter 3, a distinguished basis arises naturally from the study of higher-point conformal blocks as eigenfunctions of the vertex differential operators.

Now that we have parametrized the MST_2-MST_2-scalar vertex in terms of the function $t(\mathcal{X},\mathcal{Y})$ of two cross ratios, we need to explain how to descend to the three types of vertices we are interested in. We will postpone the reduction to type III to subsection 5.2.2, and we will address here types I and II that are the simplest to discuss. In these two cases, the variable W_2 does not appear because the spinning field $\phi_{\Delta_2,l_2,\ell_2}$ is in an STT representation. Therefore, we only have seven tensor structures whose degrees span a 6-dimensional space of degrees. Consequently, there can be only one non-trivial cross ratio which is $\mathcal{X}$. Since it is impossible to construct the cross ratio $\mathcal{Y}$, the function $t(\mathcal{X},\mathcal{Y})$ cannot depend on it, and therefore reduces to $t(\mathcal{X})$.
Going to type I does not impose any further constraint on the remaining variable $\mathcal{X}$. Indeed, without a variable W_1 it is not possible to construct the tensor structure U_{123} so that we remain with six tensor structures whose degrees span a 5-dimensional space of degrees. The construction of $\mathcal{X}$ is not affected.
The upshot of all this discussion is very simple: for vertices of type I and II in our list (5.3) the 3-point function assumes the form spelled out in eq. (5.17), but with a function t that depends only on $\mathcal{X}$ and not on $\mathcal{Y}$,

$$\langle\phi_{\Delta_1,l_1,\ell_1}(X_1,Z_1,W_1)\phi_{\Delta_2,l_2,\ell_2=0}(X_2,Z_2)\phi_{\Delta_3}(X_3)\rangle = \Omega^{\Delta_1,\Delta_2,\Delta_3}_{l_1,l_2;\ell_1,\ell_2=0}t(\mathcal{X})\,, \tag{5.20}$$

where the prefactor Ω is given in eq. (5.19) and for vertices of type I one imposes $\ell_1 = 0$, recovering (2.92).

Before we conclude this section, we want to carry our discussion of the function $t(\mathcal{X})$ one step further. So far we have not enforced spin labels to be integers so that our general form (5.20) still applies to 3-point functions of objects with continuous spin. Now we would like to explore the additional conditions that arise from the restriction to spins with integer values. This discussion is completely analogous to the one we reviewed around equation (2.93). Since MSTs depend polynomially on the auxiliary variables Z_i, the function $t(\mathcal{X})$ is constrained to live in a finite-dimensional space, as one can infer from the definition (5.18) of the cross ratio $\mathcal{X}$. The tensor structures V_i that appear in its denominator each contain factors of Z_i. Therefore, the highest power of V_i from the denominators of $t(\mathcal{X})$ must not exceed the power of V_i that appears in the numerator of the prefactor (5.19) in order to ensure polynomial dependence on the Z variables. This provides an upper bound on the exponent M of $\mathcal{X}^M$ in a series expansion of $t(\mathcal{X})$. Negative powers of $\mathcal{X}$ are not possible either, as these would produce the tensor structure H_{12} in the denominator, which itself contains both Z_1 and Z_2 but cannot be compensated by the prefactor Ω that does not contain H_{12}. In conclusion, $t(\mathcal{X})$ must be a polynomial of order up to $n_t = \min(l_1-\ell_1, l_2-\ell_1)$ if $n_t \geq 0$, and it must vanish if $n_t < 0$. The set of all allowed functions $t(\mathcal{X})$ therefore spans an (n_t+1)-dimensional space of tensor structures. For type III vertices, we will be able to write 3-point functions in the same form as (5.20) with $\ell_2 \neq 0$. However, this last discussion on the polynomiality of $t(\mathcal{X})$ and the space of tensor structures will be substantially different.
There is a slight twist to this story that is relevant for the STT-STT-scalar vertex in $d = 3$. Note that all the tensor structures we have introduced so far are even under parity. So all of the 3-point tensor structures that they generate are also parity even. But for the type I vertex in $d = 3$, it is also possible to construct a parity-odd tensor structure given by

$$O^{(3)}_{123} = \epsilon_{ABCDE}X_1^A X_2^B X_3^C Z_1^D Z_2^E\ . \tag{5.21}$$

Its degree in the 5-dimensional space of degrees for type I vertices is $deg\, O_{123} = [1,1;1,1;1]$. The square of this parity-odd tensor structure must be parity-even, and it can be expressed in terms of tensor structures

	$-\Delta_1$	$-\Delta_2$	$-\Delta_3$	l_1	l_2	ℓ_1	ℓ_2
H_{12}	1	1	0	1	1	0	0
K_{12}	1	1	0	1	1	1	1
V_1	1	0	0	1	0	0	0
V_2	0	1	0	0	1	0	0
U_{123}	1	1	1	1	1	1	0
U_{213}	1	1	1	1	1	0	1

Table 5.1: Degrees of tensor structures of the MST_2-MST_2-scalar 3-point function in $d > 4$.

constructed above as

$$\left(O^{(3)}_{123}\right)^2 \propto (1-\mathcal{X})\mathcal{X}V_1^2V_2^2\frac{X_{13}X_{23}}{X_{12}}\,. \tag{5.22}$$

We infer from this equation that parity-odd 3-point tensor structures contain factors of $\sqrt{(1-\mathcal{X})\mathcal{X}}$, generalizing the polynomial space of $t(\mathcal{X})$ to also include these half-integer powers. A similar analysis can be done for the type II vertex in $d = 4$. However one finds no extension of the space of polynomials; we will describe this in the following subsection.

5.2.2 Embedding space construction in $d = 4$ dimensions

We now address the restriction of the 3-point function (5.17) to $d = 4$, thereby describing vertices of type III. In going from $d > 4$ to $d = 4$, the number of independent cross-ratios reduces from two to just one. One may think of this reduction in terms of a constraint that is imposed on the variable $\mathcal{Y}$. The simplest way to understand the need of a reduction in cross-ratio space is by observing that the embedding space for a theory in $d = 4$ dimensions is 6-dimensional, while the MST_2-MST_2-scalar 3-point function described in the previous subsection depends on seven vectors $(X_1, Z_1, W_1, X_2, Z_2, W_2, X_3)$. Seven vectors in a six-dimensional space must be linearly dependent, which is equivalent to the vanishing of the determinant of their Gram matrix. For the case at hand, the Gram determinant is easily computed in terms of our tensor structures, and the vanishing condition becomes

$$\frac{X_{12}}{X_{13}X_{23}}\frac{U_{213}U_{123}}{V_1V_2}\frac{\mathcal{Y}^2(-1+\mathcal{X})+\mathcal{Y}}{\mathcal{X}} = 0\,, \tag{5.23}$$

with two solutions in cross-ratio space: $\mathcal{Y} = 0$ and $\mathcal{Y} = 1/(1-\mathcal{X})$. To understand the reason why two different solutions appear and what each one means, we first need to explain in more detail some properties of the embedding space representation of mixed-symmetry tensors in $d = 4$.

As we already reviewed in section 2.3.2, the representations labeled by Young diagrams that we consider for generic d are actually reducible in even dimensions when $L = d/2$, and further decompose into irreducible self-dual and anti-self-dual representations. To see this more concretely, let us specialize our discussion of section 2.3.2 on Poincaré patches to the $d = 4$ case. Following the same conventions as there, we can write the X and Z vectors as

$$\begin{aligned} X &= \left(1, x^2, x^\mu\right)\,, \\ Z = (0, 2x\cdot z, z^\mu) \qquad z^\mu &= (1, -\zeta_+\zeta_-, \zeta_+, \zeta_-)\,, \end{aligned} \tag{5.24}$$

where we use three pairs of coordinates $(X_{+\,1}, X_{-\,1}, X_{+\,2}, X_{-\,2}, X_{+\,3}, X_{-\,3})$ in which metric given by $ds^2 = -dX_{+\,1}dX_{-\,1} + dX_{+\,2}dX_{-\,2} + dX_{+\,3}dX_{-\,3}$. The variable W, introduced to parametrize the space of solutions to $X\cdot W = Z\cdot W = W^2 = 0$ quotiented by the gauge and projective equivalence $W \sim \lambda W + \alpha Z + \beta X$, has instead two possible solutions in $d = 4$, see the discussion that lead to equations (2.69) and (2.70). The two possibilities can be spelled out as:

$$W = (0, 2x\cdot w, w^\mu) \qquad w^\mu = (0, -\zeta_+, 0, 1) \quad or \tag{5.25}$$

$$\overline{W} = (0, 2x\cdot \overline{w}, \overline{w}^\mu) \qquad \overline{w}^\mu = (0, -\zeta_-, 1, 0)\,. \tag{5.26}$$

It is easy to check that $\star(X \wedge Z \wedge W) = X \wedge Z \wedge W$, and $\star(X \wedge Z \wedge W) = -X \wedge Z \wedge \overline{W}$. As a result, W and $\overline{W}$ define two distinct orbits of the conformal group in embedding space, and the restriction to the W or $\overline{W}$ orbit projects a spinning representation to its self-dual or anti-self-dual part. To make the choice of orbit and duality explicit, we now slightly modify the homogeneity conditions of (2.56): we redefine W and $\overline{W}$ to have opposite homogeneity degree, such that $\ell > 0$ denotes self-dual representations encoded by polynomials of order $|\ell|$ in W, and $\ell < 0$ denotes anti-self-dual representations encoded by polynomials of order $|\ell|$ in $\overline{W}$. To motivate this prescription, recall that the double cover of the Lorentzian conformal group $\mathrm{SO}(2,4)$ by $\mathrm{SU}(2,2)$ defines a map from $\mathbb{C}^4$ twistor fields to $\mathbb{R}^{2,4}$ embedding space fields. In the twistor formalism, it is customary to label representations by the Dynkin labels $(J, \bar{J}) \equiv (\lambda_1, \lambda_2)$, cf. Table 2.1, that respectively count the number of indices transforming in the chiral and anti-chiral representation of the $\mathrm{SL}_{\mathbb{C}}(2)$ Lorentz subgroup[1]. In Appendix C.1 we construct an explicit map from gauge invariant embedding space tensors to twistor space variables. Using this, one can readily verify that our prescription to label self-dual and anti-self-dual representations is equivalent to the identification

$$l = \frac{J + \bar{J}}{2}\,, \qquad \ell = \frac{J - \bar{J}}{2}\,, \tag{5.27}$$

which corresponds precisely to the relations of Table 2.1 specialized to $d = 4$, and is standard in the CFT_4 literature.

With the introduction of these two vectors W and $\overline{W}$, the space of tensor structures that one can construct changes dramatically. To see this, we begin by evaluating our expression for the tensor structure K with W_i, respectively $\overline{W}_i$, $i = 1, 2$, taken from the same Poincaré patch (5.25), respectively (5.26),

$$K_{12} = \frac{1}{3!}\,(X_1 \wedge Z_1 \wedge W_1) \cdot (X_2 \wedge Z_2 \wedge W_2) = 0 = \frac{1}{3!}\,\big(X_1 \wedge Z_1 \wedge \overline{W}_1\big) \cdot \big(X_2 \wedge Z_2 \wedge \overline{W}_2\big) = K_{\bar{1}\bar{2}}\,, \tag{5.28}$$

which corresponds precisely to the specialization of (2.80) to the $d = 4$ case. On the right hand side, we introduced the notation that barred indices $\bar{\imath}$ in tensors correspond to occurrences of the variable $\overline{W}_i$, as opposed to W_i. The vanishing of the tensor structures K_{12} and $K_{\bar{1}\bar{2}}$ in $d = 4$, however, is accompanied by the possibility of constructing two more tensor structures combining the self-dual and the anti-self-dual vectors, cf. (2.79). It turns out that the resulting tensor structures are perfect squares, we can thus define the following tensor structures in place of $K_{\bar{1}2}$ and $K_{1\bar{2}}$:

$$k_{1\bar{2}} = \sqrt{\frac{1}{3!}\,(X_1 \wedge Z_1 \wedge W_1) \cdot \big(X_2 \wedge Z_2 \wedge \overline{W}_2\big)}\,, \qquad k_{\bar{1}2} = \sqrt{\frac{1}{3!}\,\big(X_1 \wedge Z_1 \wedge \overline{W}_1\big) \cdot (X_2 \wedge Z_2 \wedge W_2)}\,. \tag{5.29}$$

Despite the presence of square roots, the fact that the radicand is a perfect square implies that $k_{1\bar{2}}$ and $k_{\bar{1}2}$ are both polynomials in the d-dimensional variables x_i, z_i. These two structures satisfy the following relation

$$H_{12} = 2k_{1\bar{2}}k_{\bar{1}2}\,. \tag{5.30}$$

Let us also spell out the degrees of the two new tensor structures,

$$deg\, k_{1\bar{2}} = \left[\frac{1}{2}, \frac{1}{2}, \frac{1}{2}; \frac{1}{2}, \frac{1}{2}, -\frac{1}{2}; 0\right], \qquad deg\, k_{\bar{1}2} = \left[\frac{1}{2}, \frac{1}{2}, -\frac{1}{2}; \frac{1}{2}, \frac{1}{2}, \frac{1}{2}; 0\right]. \tag{5.31}$$

In conclusion, we have now replaced the two tensor structures K_{12} and H_{12} of the previous subsection by the two tensor structures $k_{1\bar{2}}$ and $k_{\bar{1}2}$. Furthermore, one can show that the objects U_{ij3} can be decomposed into

$$U_{123} = \mho\, k_{1\bar{2}}\,, \qquad U_{213} = \mho\, k_{\bar{1}2}\,, \tag{5.32}$$

with a new tensor structure $\mho$ defined as

$$\mho = \sqrt{X_3^A\,(X_1 \wedge Z_1 \wedge W_1)_{ABC}\,(X_2 \wedge Z_2 \wedge W_2)^{BCD}\,X_{3\,D}}\,. \tag{5.33}$$

[1] More specifically the double cover of the Lorentz subgroup $\mathrm{SO}(1,3) \subset \mathrm{SO}(2,4)$.

	$-\Delta_1$	$-\Delta_2$	$-\Delta_3$	l_1	l_2	ℓ_1	ℓ_2
$k_{1\bar{2}}$	1/2	1/2	0	1/2	1/2	1/2	−1/2
$k_{\bar{1}2}$	1/2	1/2	0	1/2	1/2	−1/2	1/2
$\mho$	1/2	1/2	1	1/2	1/2	1/2	1/2
$\bar{\mho}$	1/2	1/2	1	1/2	1/2	−1/2	−1/2

Table 5.2: Degrees of additional tensor structures of the MST_2-MST_2-scalar 3-point function in $d = 4$.

The degree of $\mho$ is given by

$$deg\,\mho = \left[\frac{1}{2},\frac{1}{2},\frac{1}{2};\frac{1}{2},\frac{1}{2},\frac{1}{2};1\right] , \tag{5.34}$$

The tensor structure $\mho$ uses only W_i. Of course, it is also possible to construct a similar tensor structure $\overline{\mho}$ in terms of $\overline{W}_i$ as

$$\overline{\mho} = \sqrt{X_3^A \left(X_1 \wedge Z_1 \wedge \overline{W}_1\right)_{ABC} \left(X_2 \wedge Z_2 \wedge \overline{W}_2\right)^{BCD} X_{3\,D}} , \tag{5.35}$$

with

$$deg\,\overline{\mho} = \left[\frac{1}{2},\frac{1}{2},-\frac{1}{2};\frac{1}{2},\frac{1}{2},-\frac{1}{2};1\right] . \tag{5.36}$$

In direct analogy with eq. (5.32) we also find that

$$U_{\bar{1}23} = \overline{\mho}\, k_{\bar{1}2} , \qquad U_{\bar{2}13} = \overline{\mho}\, k_{1\bar{2}} . \tag{5.37}$$

At this point we have nine basic tensor structures at our disposal, namely $k_{\bar{1}2}, k_{1\bar{2}}, \mho$ and $\overline{\mho}$ in addition to $X_{12}, X_{23}, X_{13}, V_1$ and V_2. Their degrees certainly span the 7-dimensional space and in addition, we can construct the unique cross ratio $\mathcal{X}$ as

$$\mathcal{X} = 2\frac{k_{\bar{1}2}k_{1\bar{2}}}{V_1 V_2} . \tag{5.38}$$

Finally, the nine fundamental tensor structures that we introduced satisfy one relation,

$$(X_{23}V_1)(X_{13}V_2) = X_{12}\mho\,\overline{\mho} + 2k_{1\bar{2}}k_{\bar{1}2}X_{13}X_{23} . \tag{5.39}$$

For the reader's convenience we listed these additional tensor structures and their degrees in Tab. 5.2. Having introduced this new set of tensor structures for vertices of type III, we immediately see that the two solutions to the vanishing of the Gram determinant (5.23) in $d = 4$ arise very naturally when trying to construct a second $\mathcal{Y}$-like cross ratio. First, note that the cross ratio $\mathcal{Y}$ introduced in eq. (5.18) vanishes when ℓ_1 and ℓ_2 have the same sign,

$$\mathcal{Y}_{++} = \frac{X_{13}X_{23}V_1V_2K_{12}}{X_{12}U_{123}U_{213}} = 0 = \frac{X_{13}X_{23}V_1V_2K_{\bar{1}\bar{2}}}{X_{12}U_{\bar{1}23}U_{\bar{2}13}} = \mathcal{Y}_{--} , \tag{5.40}$$

because of the property (5.28). On the other hand, when the fields have opposite duality, one can only construct a cross ratio with the help of the non-vanishing tensor structures $k_{\bar{1}2}$ or $k_{1\bar{2}}$,

$$\mathcal{Y}_{-+} = \frac{X_{13}X_{23}V_1V_2k_{\bar{1}2}^2}{X_{12}U_{\bar{1}23}U_{213}} = \frac{1}{1-\mathcal{X}} = \frac{X_{13}X_{23}V_1V_2k_{1\bar{2}}^2}{X_{12}U_{123}U_{\bar{2}13}} = \mathcal{Y}_{+-} . \tag{5.41}$$

To compare with eq. (5.40), note that $K_{12} = k_{12}^2$. In evaluating the expressions for $\mathcal{Y}_{-+}$ and $\mathcal{Y}_{+-}$, we have used the relation (5.39) before inserting the definition (5.38) of the cross ratio $\mathcal{X}$. In this sense, the second zero of the Gram determinant can be associated with 3-point functions in which the spins ℓ_i of the MSTs have opposite sign.

Keeping in mind that we are also allowed to have negative values of the spin ℓ_i in $d = 4$, we can now write a generic 3-point function as in equation (5.20), but with the prefactor Ω given by

$$\Omega^{\Delta_1,\Delta_2,\Delta_3}_{l_1,l_2;\ell_1,\ell_2} = \frac{V_1^{l_1-|\ell_1|-|\ell_2|}V_2^{l_2-|\ell_1|-|\ell_2|}U_{s_1 23}^{|\ell_1|}U_{s_2 13}^{|\ell_2|}}{X_{12}^{\frac{\Delta_1+\Delta_2-\Delta_3+l_1+l_2-|\ell_1|-|\ell_2|}{2}}X_{23}^{\frac{\Delta_2+\Delta_3-\Delta_1-l_1+l_2+|\ell_1|+|\ell_2|}{2}}X_{31}^{\frac{\Delta_3+\Delta_1-\Delta_2+l_1-l_2+|\ell_1|+|\ell_2|}{2}}} \tag{5.42}$$

instead of (5.19). In spelling out the new prefactor that is defined for arbitrary integer values of ℓ_i, we have introduced the notation

$$s_i = \begin{cases} i & \ell_i \geq 0 \\ \bar{\imath} & \ell_i < 0 \end{cases} . \tag{5.43}$$

Note that, despite the presence of absolute values in (5.42), representations with any sign of ℓ_i are allowed, as the possible presence of $\overline{W}_i$ takes full care of negative homogeneity degrees. Formula (5.42) is the main result of this subsection.

As in the previous subsection, we can use our expression for the 3-point function to count the number of tensor structures when we impose spins to acquire integer values. In order to do so, we need to expand (5.42) in terms of the tensor structures specific to $d = 4$, in a form that depends specifically on the duality of the two MST_2 involved. To distinguish between those cases, we introduce the notation $\Omega_{\sigma_1\sigma_2}$, where $\sigma_i = +, -$ depending whether the field i is in a self-dual or anti-self-dual representation respectively. Those prefactors satisfy the relations $\Omega_{++} = \overline{\Omega}_{--}$ and $\Omega_{+-} = \overline{\Omega}_{-+}$, where the bar operation exchanges $W_i \leftrightarrow \overline{W}_i$ for both $i = 1, 2$; we can therefore focus on only the Ω_{++} and Ω_{+-} cases, as the results in these cases can easily be translated to the other two cases.

In analyzing the first case, involving Ω_{++}, we can express the prefactor in terms of $\mathcal{V}$, $k_{1\bar{2}}$ and $k_{\bar{1}2}$, leading to the 3-point function

$$\Omega_{++} t(\mathcal{X}) = \frac{V_1^{l_1-|\ell_1|-|\ell_2|} V_2^{l_2-|\ell_1|-|\ell_2|} \mathcal{V}^{|\ell_1|+|\ell_2|} k_{1\bar{2}}^{|\ell_1|} k_{\bar{1}2}^{|\ell_2|}}{X_{12}^{\frac{\Delta_1+\Delta_2-\Delta_3+l_1+l_2-|\ell_1|-|\ell_2|}{2}} X_{23}^{\frac{\Delta_2+\Delta_3-\Delta_1-l_1+l_2+|\ell_1|+|\ell_2|}{2}} X_{31}^{\frac{\Delta_3+\Delta_1-\Delta_2+l_1-l_2+|\ell_1|+|\ell_2|}{2}}} t(\mathcal{X}) . \tag{5.44}$$

By requiring polynomial dependence on the variables Z_i, W_i, $\overline{W}_i$ in this expression, it is easy to see that $t(\mathcal{X})$ must contain integer powers of the cross ratio (5.38), with exponents that are bounded from above by the minimum exponent of the V_i in the prefactor, and bounded from below by the minimum exponent of the k_{ij}. As a result, the function $t(\mathcal{X})$ must take the form

$$t(\mathcal{X}) = \sum_n c_n \mathcal{X}^n , \tag{5.45}$$

with the sum over exponents restricted by the inequalities

$$-\min(|\ell_1|, |\ell_2|) \leq n \leq \min(l_1, l_2) - |\ell_1| - |\ell_2| . \tag{5.46}$$

In cases where ℓ_1 and ℓ_2 have opposite sign, e.g. $\ell_1 > 0$, $\ell_2 < 0$ and the prefactor Ω_{+-} is used, the discussion is a bit different. Here we can use the relation (5.39) to eliminate one of the tensor structures $\mathcal{V}$ or $\overline{\mathcal{V}}$ from the prefactor and write the 3-point function as

$$\frac{V_1^{l_1-|\ell_1|-|\ell_2|} V_2^{l_2-|\ell_1|-|\ell_2|} \mathcal{V}^{|\ell_1|-\min(|\ell_1|,|\ell_2|)} \overline{\mathcal{V}}^{|\ell_2|-\min(|\ell_1|,|\ell_2|)} k_{1\bar{2}}^{|\ell_1|+|\ell_2|} (V_1 V_2 - 2k_{1\bar{2}}k_{\bar{1}2})^{\min(|\ell_1|,|\ell_2|)}}{X_{12}^{\frac{\Delta_1+\Delta_2-\Delta_3+l_1+l_2-|\ell_1|-|\ell_2|}{2}} X_{23}^{\frac{\Delta_2+\Delta_3-\Delta_1-l_1+l_2+|\ell_1|+|\ell_2|}{2}} X_{31}^{\frac{\Delta_3+\Delta_1-\Delta_2+l_1-l_2+|\ell_1|+|\ell_2|}{2}} \left(\frac{X_{12}}{X_{13}X_{23}}\right)^{\min(|\ell_1|,|\ell_2|)}} t(\mathcal{X}) .$$

In order to analyze the resulting constraints on the function $t(\mathcal{X})$, we shall think of t as a function of

$$1 - \mathcal{X} = \frac{V_1 V_2 - 2k_{1\bar{2}}k_{\bar{1}2}}{V_1 V_2} . \tag{5.47}$$

Requiring polynomial dependence on the polarization vectors, t is constrained to contain integer powers of $(1 - \mathcal{X})$ that are bounded from above by the minimum power of the V_i as in the previous case, and are bounded from below by the power of the factor $(V_1 V_2 - 2k_{1\bar{2}}k_{\bar{1}2})$. This can be written concretely as

$$t(\mathcal{X}) = \sum_n c'_n (1 - \mathcal{X})^n , \tag{5.48}$$

with the same constraint on the sum over exponents n that was spelled out in eq. (5.46). Thus, in both cases, we have determined that the space of tensor structures $t(\mathcal{X})$ has dimension

$$\min(l_1, l_2) - \max(|\ell_1|, |\ell_2|) + 1 , \tag{5.49}$$

which matches exactly the expected number from the representation theory of the conformal group.
For the computation of the vertex operator in section 5.3, it will prove useful to spell out an explicit relation between the prefactors Ω_{++} and Ω_{+-},

$$\Omega_{+-}\Big|_{|\ell_2|\to-|\ell_2|} = \left(\frac{\mathcal{X}(1-\mathcal{X})}{2}\right)^{-|\ell_2|}\Omega_{++}\,. \tag{5.50}$$

In other words, the prefactor for one self-dual and one anti-self-dual field is related to the one for two self-dual MSTs through a simple function of the cross ratio $\mathcal{X}$, plus a change of sign for the homogeneity of the field for which we are changing duality. This equation will allow us to relate the vertex operator computed in one case to the other one, see eq. (5.60).
We now address the tensor structures that can be constructed with the use of a six-dimensional Levi-Civita symbol for vertices of type II and III. Using only one W_i or $\overline{W}_i$ vector, it is possible to construct the structures

$$O^{(4)}_{ijk} = \epsilon_{ABCDEF}X_i^A X_j^B X_k^C Z_i^D Z_j^E W_i^F\,, \qquad O^{(4)}_{\bar{i}jk} = \epsilon_{ABCDEF}X_i^A X_j^B X_k^C Z_i^D Z_j^E \overline{W}_i^F\,. \tag{5.51}$$

These are however easily seen to be proportional to the U_{ijk} tensor structure

$$\left(O^{(4)}_{s_ijk}\right)^2 \propto (U_{s_ijk})^2\,, \tag{5.52}$$

so that the vertex function $t(\mathcal{X})$ is unaffected by the introduction of parity-odd tensor structures for vertices of type II in $d=4$. For vertices of type III we can also construct parity odd tensors of the form

$$\widetilde{O}^{(4)}_{12} = \epsilon_{ABCDEF}X_1^A X_2^B Z_1^C Z_2^D W_1^E W_2^F\,, \qquad \widetilde{O}^{(4)}_{\bar{1}2} = \epsilon_{ABCDEF}X_1^A X_2^B Z_1^C Z_2^D \overline{W}_1^E W_2^F\,, \tag{5.53}$$

as well as their images under $1\leftrightarrow\bar{1}$ and $2\leftrightarrow\bar{2}$. However, these structures are once again proportional to tensors that we have already introduced:

$$\left(\widetilde{O}^{(4)}_{12}\right)^2 \propto (K_{12})^2 \overset{d=4}{=} 0\,, \qquad \left(\widetilde{O}^{(4)}_{\bar{1}2}\right)^2 \propto (K_{\bar{1}2})^2\,. \tag{5.54}$$

We can therefore conclude that structures of the type (5.51) or (5.53) do not extend the space of $t(\mathcal{X})$ for vertices of type II and III.
Before ending this section, we would like to point out that the construction of $d=4$ 3-point tensor structures in this section is the embedding space version of the twistor based construction of tensor structures in [21, 89]. We describe in more detail in Appendix C.1 the dictionary from embedding space variables to twistor variables and vice versa.

5.3 The Single Variable Vertex Operator

Having assembled all of the required background, including in particular a detailed discussion of single variable 3-point functions of the form (5.20), we now move on to our central goal. In this section, we work out the explicit expression for the action of our vertex differential operators on the function $t(\mathcal{X})$ that multiplies the prefactors (5.19) or (5.42). Our strategy is to obtain the results for all three sub-cases listed in eq. (5.3) by studying the MST_2-MST_2-scalar vertex in $d\geq 4$. Note that passing through this 2-variable vertex is just a trick that allows us to shorten the discussion and avoid displaying multiple long expressions for all different cases; using the same procedure described in this section, one can compute the vertex operator in each individual case and easily verify that the answer is the same as what is obtained by reduction of the more general vertex. The results of this section should be seen as providing raw data that we will process in the subsequent sections. We will also comment on the relation between our formulas and the vertex differential operator of a 5-point function in $d\geq 3$, see [42]. To this end, we shall look at both shadow integrals and OPE limits in the second subsection.

5.3.1 Construction of the reduced vertex operator

As we had argued in chapter 3, there is a distinguished basis for the vertex functions t that is selected by solving the eigenvalue equations of some commuting set of vertex differential operators. For the MST_2-MST_2-scalar vertex there are two such operators, one of order four and the other of order six. When we descend from there to the single variable vertices in the list (5.3) via the constraint $\mathcal{Y}=0$, the sixth order operator becomes dependent. Hence to achieve our goals it is sufficient to work out the fourth order operator. The operator starts its existence as a differential operator on the space of coordinates and polarizations of three fields. We use the embedding space constructions that were reviewed in the previous section to write the operator

$$\mathcal{D}_{\mathfrak{v}} \equiv \mathcal{D}^{4,3}_{\mathfrak{v},13} = \mathrm{str}\left(\mathcal{T}^{(1)}\mathcal{T}^{(1)}\mathcal{T}^{(1)}\mathcal{T}^{(3)}\right) \tag{5.55}$$

in terms of the simple first order differential operators (2.58) encoding the action of the conformal generators on the variables (X_i, Z_i, W_i). Let us also recall that str stands for symmetrized trace. The action of the differential operator (5.55) can be reduced to the cross-ratio space of $t(\mathcal{X})$ by conjugation with the prefactor $\Omega^{\Delta_1,\Delta_2,\Delta_3}_{l_1,l_2;\ell_1,\ell_2}$, as in the case for Casimir differential operators,

$$H^{(d,\Delta_i,l_i,\ell_i)}t(\mathcal{X}) = \frac{1}{\Omega^{\Delta_1,\Delta_2,\Delta_3}_{l_1,l_2;\ell_1,\ell_2}}\mathcal{D}_{\mathfrak{v}}\left(\Omega^{\Delta_1,\Delta_2,\Delta_3}_{l_1,l_2;\ell_1,\ell_2}t(\mathcal{X})\right). \tag{5.56}$$

By plugging eqs. (2.58) and (5.55) in eq. (5.56), it is then possible to compute the action of $\mathcal{D}^{\mathcal{X}}_{\mathfrak{v}}$ in cross ratio space. To do this, we implemented the action of generators (2.58) in `Mathematica` and first obtained the conjugation with the prefactor expressed in terms of scalar products of X_i, Z_i, W_i. We then solved the expressions of the cross ratios (5.18) for two scalar products, set $\mathcal{Y}=0$, and plugged these expressions in the conjugated differential operator; due to conformal invariance all of the remaining scalar products drop out, and one is left with a differential operator in one cross ratio of the form

$$H^{(d,\Delta_i,l_i,\ell_i)} = h_0(\mathcal{X}) + \sum_{q=1}^{4} h_q(\mathcal{X})\mathcal{X}^{q-1}(1-\mathcal{X})^{q-1}\partial^q_{\mathcal{X}}\,. \tag{5.57}$$

Apart from a constant piece in $h_0(\mathcal{X})$, all of the coefficients $h_q(\mathcal{X})$ are symmetric under exchange of fields $1\leftrightarrow 2$, and we can therefore represent them as

$$h_q^{(d,\Delta_i,l_i,\ell_i)}(\mathcal{X}) = \chi_q^{(d,\Delta_i,l_i,\ell_i)}(\mathcal{X}) + (1\leftrightarrow 2)\,. \tag{5.58}$$

Finally, we write h_0 as

$$h_0^{(d,\Delta_i,l_i,\ell_i)}(\mathcal{X}) = \left[\chi_0^{(d,\Delta_i,l_i,\ell_i)}(\mathcal{X}) + (1\leftrightarrow 2)\right] + \tilde{\chi}_0^{(d,\Delta_i,l_i,\ell_i)}\,. \tag{5.59}$$

These coefficients take the following form:

$$\begin{aligned}
\tilde{\chi}_0 \;=\;& \frac{1}{6}(\Delta_1-\Delta_2)(d-\Delta_1-\Delta_2)\left(d^2-3d(\Delta_1+\Delta_2+\Delta_3+1)+3\left(\Delta_1^2+\Delta_2^2+\Delta_3^2\right)\right)\\
&-\frac{1}{6}(l_1-l_2)(d+l_1+l_2-2)\left(d^2+3d(-\Delta_3+l_1+l_2-3)+3\left(\Delta_3^2+l_1^2-2l_1+l_2^2-2l_2+2\right)\right)\\
&-\frac{1}{6}(\ell_1-\ell_2)(d+\ell_1+\ell_2-4)\left(d^2+3d(-\Delta_3+\ell_1+\ell_2-5)+3\left(\Delta_3^2+\ell_1^2-4\ell_1+\ell_2^2-4\ell_2+8\right)\right),
\end{aligned}$$

$$
\begin{aligned}
\chi_0(\mathcal{X}) \;=\;& 2\mathcal{X}^2\big[l_1\left(-4l_2^2\ell_1+l_2\left(8\ell_1\left(\ell_1+\ell_2+1\right)+1\right)-2\ell_1\left(\ell_1+1\right)\left(2\ell_1+6\ell_2+1\right)\right)\\
&+2\ell_1\left(\ell_2\left(2\ell_1\left(-3l_2+2\ell_1+3\right)+1\right)+\left(\ell_1+1\right)\left(\ell_1-l_2\right)\left(-l_2+\ell_1+1\right)+3\ell_1\ell_2^2\right)\\
&+l_1^2\left(-2l_2\left(2\ell_1+1\right)+l_2^2+2\ell_1\left(\ell_1+2\ell_2+1\right)\right)\big]\\
&+\mathcal{X}\big[2\ell_1l_2\left(d^2-d\left(\Delta_1+\Delta_3+1\right)+2\left(\Delta_1\Delta_2+\Delta_3+1\right)+\ell_1\left(d-2\Delta_3+14\ell_2+6\right)+4\ell_1^2\right)\\
&-d\Delta_1l_2\ell_2+2\ell_1^2\left(-d^2+\Delta_1\left(d-2\Delta_2\right)+\left(d-2\right)\Delta_3-3\ell_2\left(d-2\Delta_3+4\right)+d-8\ell_2^2-2\right)\\
&+2\ell_1\ell_2\left(-d^2+2\Delta_1\left(d-\Delta_2\right)+\left(d-2\right)\Delta_3+d-2\right)-2\ell_1^3\left(d-2\Delta_3+10\ell_2+4\right)\\
&+l_1\big(-l_2\left(2\Delta_1\left(\Delta_2-d\right)+2\ell_1\left(d+9\ell_2+8\right)+\left(d-1\right)d+16\ell_1^2+2\right)\\
&+2\ell_1\left(-\Delta_1\left(d-2\Delta_2\right)-\left(d-2\right)\Delta_3+2\ell_2\left(d-2\Delta_3+6\right)+\left(d-1\right)d+2\right)\\
&-2d\Delta_1\ell_2+8\ell_1^3+2\ell_1^2\left(d-2\Delta_3+14\ell_2+6\right)+\Delta_3l_2\left(d+4\ell_1-2\right)+8l_2^2\ell_1\big)\\
&+2d\Delta_1\ell_2^2-4l_2^2\left(\ell_1+1\right)\ell_1-4\ell_1^4-2l_1^2\left(-2l_2\left(2\ell_1+1\right)+l_2^2+2\ell_1\left(\ell_1+2\ell_2+1\right)\right)\big]\\
&-\frac{\ell_1\ell_2}{2\mathcal{X}}\left(\Delta_3^2+4\Delta_3\left(l_1-\ell_1\right)+2\left(\Delta_1\left(\Delta_2-\Delta_1\right)+l_1\left(l_2-2\ell_1\right)+\ell_1\left(-2l_2+\ell_1+\ell_2\right)+l_1^2\right)\right)\\
&+\frac{1}{12}\big[6l_1\big(l_2\left(d^2+2\Delta_1\left(\Delta_2-d\right)-\left(d-2\right)\Delta_3+2\ell_1\left(d-2\Delta_3+7\ell_2+2\right)+8\ell_1^2-2\right)-(d-2)\Delta_3^2\\
&-2\left(\ell_1\left(d\left(d-\Delta_1-1\right)+(d+6)\ell_2+2\Delta_1\Delta_2\right)-d\Delta_1\ell_2+\ell_1^2\left(d+12\ell_2+2\right)+2\ell_1^3\right)\\
&+\Delta_3\left(2\ell_1\left(d+2\ell_1+6\ell_2-2\right)+(d-2)d\right)+2(d-2)(d-1)-4l_2^2\ell_1\big)\\
&-\Delta_3^2\left(6\Delta_1\left(\Delta_1-d\right)+(d-3)d\right)+d\Delta_3\left(6\Delta_1\left(\Delta_1-d\right)+(d-3)d\right)\\
&-6l_1^2\left(-d\Delta_3+(d-6)d+\Delta_3^2+4l_2\ell_1-l_2^2-2\ell_1\left(\ell_1+4\ell_2+1\right)+6\right)\\
&-6\Delta_1\big(\left(\Delta_1-\Delta_2\right)\left(\left(d-\Delta_1\right)^2+\Delta_1\Delta_2\right)+2l_2^2\left(d-\Delta_1\right)+2l_2\left(\left(d-2\right)\left(d-\Delta_1\right)-d\ell_2\right)\\
&+2\ell_2\left(\Delta_1-d\right)+2d\ell_2^2\big)\\
&+6\ell_1^2\big(\Delta_3\left(-3d+\Delta_3+4\right)+2\ell_2\left(3d-10\Delta_3+5\right)+(d-2)(d+8)-2\Delta_1\left(\Delta_1-2\Delta_2\right)\\
&+4l_2\left(\Delta_3-6\ell_2-2\right)+4l_2^2+15\ell_2^2\big)\\
&+6\ell_1\big(2l_2\left(\Delta_1\left(d-2\Delta_2\right)+\left(d-2\right)\Delta_3-5d+8\right)+(d-2)\Delta_3^2+2(d-3)\Delta_1\left(d-\Delta_1\right)\\
&+\ell_2\left(-2\Delta_1\left(d-3\Delta_2\right)+\Delta_3\left(-5d+2\Delta_3+10\right)+3(d-2)d-4\Delta_1^2\right)\\
&-(d-2)d\Delta_3+2(d-3)l_2^2-4d+8\big)\\
&-12(d-2)l_1^3+12\ell_1^3\left(-2\Delta_3-2l_2+8\ell_2+5\right)-6l_1^4+6\ell_1^4\big],\\
\chi_1(\mathcal{X}) \;=\;& 8\mathcal{X}^3\big[-3l_1\ell_1^2-3l_2\ell_1^2+l_1^2\ell_1+l_2^2\ell_1-6l_1\ell_1+4l_1l_2\ell_1-6l_2\ell_1-6l_1\ell_2\ell_1+l_1^2-3l_1-l_1^2l_2+2l_1l_2\\
&+2\ell_1^3+6\ell_2\ell_1^2+6\ell_1^2+6\ell_2\ell_1+6\ell_1+1\big]\\
&+\mathcal{X}^2\big[l_1\left(2d(d-\Delta_3-\Delta_1)+4\Delta_1\Delta_2-l_2\left(d-2\Delta_3+24\right)+4\ell_1\left(d-2\Delta_3+19\ell_2+18\right)+36\right)\\
&-2\ell_1\big(2d^2-2l_2\left(d+9\ell_1+18\right)+(3d+37)\ell_2+\ell_1(3d+40\ell_2+36)+d+6l_2^2+12\ell_1^2+36\big)\\
&-d^2+2d\Delta_1\left(-l_2+2\ell_1+2\ell_2+1\right)+\Delta_3\left(4\ell_1\left(d-2l_2+3\ell_1+3\ell_2+1\right)+d\right)-48l_1l_2\ell_1\\
&+36l_1\ell_1^2+12l_1^2\left(l_2-\ell_1-1\right)-2\Delta_1\Delta_2\left(4\ell_1+1\right)-12\big]\\
&+\frac{1}{2}\mathcal{X}\big[-2l_1\big(-2\Delta_1(d-2\Delta_2)-2l_2(d+10\ell_1+3)+4\ell_1(d+10\ell_2+7)+d(d+6)+16\ell_1^2+4\big)\\
&+2\ell_1\left(-2\Delta_1\left(d+\Delta_1-4\Delta_2\right)-4(d+7)l_2+(5d+34)\ell_2+d(3d+4)+6l_2^2+24\right)\\
&+4\Delta_3l_1\left(d-l_2+4\ell_1\right)+2\Delta_1\left(-(d-2)\Delta_1+2dl_2-2\ell_2\left(d+\Delta_1\right)+(d-4)d+2\Delta_2\right)\\
&+2\ell_1^2\left(5(d+6)-16l_2+42\ell_2\right)+8d+20\ell_1^3+2l_1^2\left(d-4l_2+6\ell_1+2\right)+\Delta_3^2\left(d+4\ell_1-2\right)\\
&-\Delta_3\left(d^2+4\ell_1\left(3d-4l_2+6\ell_1+7\ell_2+2\right)\right)\big]\\
&\frac{1}{4}\big[4\Delta_3\left(-l_1\left(d+2\ell_1-2\right)+\ell_1\left(d-2l_2+2\ell_1+4\ell_2+2\right)+d-2\right)-2\ell_1^2\left(d-4l_1-4l_2+6\right)\\
&+4\left(l_1+l_2-2\right)\ell_1\left(d-l_1-l_2\right)-2\ell_2\ell_1\left(d-16l_1+14\ell_1+10\right)-2(d-2)\left(l_1\left(l_1+l_2-4\right)+2\right)\\
&+2\Delta_1^2\left(d+2\ell_1+2\ell_2-2\right)-\Delta_3^2\left(d+4\ell_1-2\right)-2\Delta_1\Delta_2\left(d+4\ell_1-2\right)-4\ell_1^3\big],
\end{aligned}
$$

$$
\begin{aligned}
\chi_2(\mathcal{X}) &= -4\mathcal{X}^2\left(l_1\left(2l_2-6\ell_1-9\right)+6\ell_1\left(-l_2+\ell_1+\ell_2+3\right)+l_1^2+7\right)\\
&\quad +\mathcal{X}\big[-2l_1\left(d-2\Delta_3-2l_1-4l_2+12\ell_1+18\right)+2\ell_1\left(3d-6\Delta_3-12l_2+12\ell_1+13\ell_2+36\right)\\
&\qquad d^2-2d(\Delta_1-1)-\Delta_3(d+4)+2\Delta_1\Delta_2+28\big]\\
&\quad +l_1\left(-2\Delta_3-l_1-l_2+6\ell_1+2d+4\right)+\ell_1\left(-2d+6\Delta_3+6l_2-5\ell_1-7\ell_2-16\right)-3d+\Delta_1^2\\
&\quad -\Delta_1\Delta_2+\frac{\Delta_3}{2}(-\Delta_3+2d+4)-2\,,\\
\chi_3(\mathcal{X}) &= -8\mathcal{X}\left(l_1-2\left(\ell_1+1\right)\right)+2\Delta_3+4l_1-8\ell_1-d-8\,,\\
\chi_4(\mathcal{X}) &= -2\,.
\end{aligned}
$$

From the operator above, it is easy to reduce to the vertex operators of type I and II: one has to simply impose the corresponding $\ell_i = 0$. For vertices of type III, where representations labeled by Young diagrams are reducible, the reduction requires some further comments. Let us note that the prefactor (5.42) for two self-dual fields (respectively two anti-self-dual fields) acquires precisely the same form as the $d > 4$ one, modulo the replacement of both second polarizations with their $d = 4$ counterparts W_i (respectively $\overline{W}_i$), and the replacement of the ℓ_i with their absolute values $|\ell_i|$. This means that the computation of the vertex operator for these cases will proceed in exactly the same way as in $d > 4$ up to the replacements described above. Furthermore, we observed with equation (5.40) that the cross ratio $\mathcal{Y}$ vanishes in $d = 4$ when expressed only in terms of (anti-)self-dual variables. We can therefore conclude that the vertex operator for two (anti-)self-dual fields corresponds to (5.55) with $\ell_i \to |\ell_i|$, as we have already imposed $\mathcal{Y} = 0$ in the computation of the $d > 4$ vertex operator. If instead we wish to describe the type III vertex operator with one self-dual and one anti-self-dual field, we can use our observation (5.50) relating prefactors in the $\ell_1\ell_2 > 0$ case to the $\ell_1\ell_2 < 0$ case. In particular, labeling the operator with $\ell_1, \ell_2 > 0$ as $H = H_{++}$ and the operator for $\ell_1 > 0$, $\ell_2 < 0$ as H_{+-}, we find that

$$
H_{+-}^{(d=4;\Delta_i;l_i;|\ell_1|,-|\ell_2|)} = \left(\frac{\mathcal{X}(1-\mathcal{X})}{2}\right)^{|\ell_2|} H_{++}^{(d=4;\Delta_i;l_i;|\ell_1|,|\ell_2|)} \left(\frac{\mathcal{X}(1-\mathcal{X})}{2}\right)^{-|\ell_2|}\,. \tag{5.60}
$$

and analogously for H_{-+} with $\ell_1 \leftrightarrow \ell_2$. This concludes our construction of the vertex differential operators for all three single variable cases listed in eq. (5.3)

Having written out the results of our computations, let us add a few quick remarks and observations. First of all, it is important to note that almost all terms have a polynomial dependence on the cross ratio $\mathcal{X}$. The only exception appears in our expression for $\chi_0(\mathcal{X})$, which contains one term proportional to $\ell_1\ell_2\mathcal{X}^{-1}$. For vertices of type I and II, where $\ell_2 = 0$, this non-polynomial term is absent, while it remains present for vertices of type III. Let us stress again that our derivation is valid for $\ell_2 \neq 0$ and for arbitrary dimension $d \geq 4$. As we shall show in section 5.5, the mapping of our operator (5.57) to the elliptic CMS model of [75] also works for all cases, including MST_2-MST_2-scalar vertices $d > 4$ with kinematics reduced to $\mathcal{Y} = 0$. Nevertheless, it turns out that the map has significantly different features when it is applied beyond the list (5.3) of single variable vertex systems, c.f. section 5.5 and Appendix C.2 for a discussion. Our analysis of the results in the next section will be restricted to the cases with $\ell_2 = 0$ which possess polynomial coefficients.

5.3.2 Relation with vertex operator for 5-point functions

It is worth to pause our analysis of the single variable vertex operators for a moment and to explain how this differential operator is related to the vertex operator for a 5-point function in $d \geq 3$ that can be worked out with the procedure of section 3.4. As usual, we split the scalar 5-point function

$$
\langle\phi_1(X_1)\phi_2(X_2)\phi_3(X_3)\phi_4(X_4)\phi_5(X_5)\rangle = \Omega_5^{\Delta_i}(X_i)\,F(u_i) \tag{5.61}
$$

into a function F of cross ratios and a prefactor Ω that accounts for the nontrivial covariance law of the scalar fields under conformal transformations. The former can be further decomposed into conformal

blocks,

$$F(u_i) = \sum_{\Delta_a, l_a, \Delta_b, l_b, \mathfrak{t}} \lambda_{12a}\lambda_{a3b;\mathfrak{t}}\lambda_{b45}\, g^{(\Delta_{12},\Delta_3,\Delta_{45})}_{\Delta_r,l_r,\mathfrak{t}}(u_i)\,, \tag{5.62}$$

while the latter is given by

$$\Omega_5^{(\Delta_i)}(X_i) = \frac{\left(\frac{X_2\cdot X_3}{X_1\cdot X_3}\right)^{\frac{\Delta_1-\Delta_2}{2}}\left(\frac{X_2\cdot X_4}{X_2\cdot X_3}\right)^{\frac{\Delta_3}{2}}\left(\frac{X_3\cdot X_5}{X_3\cdot X_4}\right)^{\frac{\Delta_4-\Delta_5}{2}}}{(X_1\cdot X_2)^{\frac{\Delta_1+\Delta_2}{2}}(X_3\cdot X_4)^{\frac{\Delta_3}{2}}(X_4\cdot X_5)^{\frac{\Delta_4+\Delta_5}{2}}}\,. \tag{3.80}$$

Once more, we rewrite the five cross ratios that can be constructed for $N = 5$ as

$$\begin{aligned}
u_1 &= \frac{(X_1\cdot X_2)\,(X_3\cdot X_4)}{(X_1\cdot X_3)\,(X_2\cdot X_4)} = z_1\bar{z}_1\,, \qquad v_1 = \frac{(X_1\cdot X_4)\,(X_2\cdot X_3)}{(X_1\cdot X_3)\,(X_2\cdot X_4)} = (1-z_1)(1-\bar{z}_1)\,,\\
u_2 &= \frac{(X_2\cdot X_3)\,(X_4\cdot X_5)}{(X_2\cdot X_4)\,(X_3\cdot X_5)} = z_2\bar{z}_2\,, \qquad v_2 = \frac{(X_2\cdot X_5)\,(X_3\cdot X_4)}{(X_2\cdot X_4)\,(X_3\cdot X_5)} = (1-z_2)(1-\bar{z}_2)\,,\\
U_1^{(5)} &= \frac{(X_1\cdot X_5)\,(X_2\cdot X_3)\,(X_3\cdot X_4)}{(X_2\cdot X_4)\,(X_1\cdot X_3)\,(X_3\cdot X_5)} = w(z_1-\bar{z}_1)(z_2-\bar{z}_2)+(1-z_1-z_2)(1-\bar{z}_1-\bar{z}_2)\,.
\end{aligned} \tag{5.63}$$

Since the OPE diagram for a 5-point function contains two internal fields of depth $L = 1$, i.e. two STTs, its blocks are characterized by four Casimir and one vertex operator.

One way to express the relation between this full vertex operator and the reduced 3-point vertex operator of the previous subsection makes use of the shadow formalism [90]. Shadow integrals turn the graphical representation of a conformal block, such as that of Fig. 2.8, into an integral formula. Just as in the case of Feynman integrals, the 'shadow integrand' is built from relatively simple building blocks that are assigned to the links and 3-point vertices of the associated OPE diagram. For a scalar 5-point function, the only non-trivial vertex is of type I. Within this subsection we resume the convention of chapter 4 to label the two internal STT lines by a and b rather than 1 and 2, to distinguish them from the external lines. The basic building block for the integrand of the shadow integral is the 3-point function Φ that was introduced in eq. (5.17). In the context of the 5-point function, only two special cases of this formula appear. On the one hand, there are two 1-STT-2 scalar vertices Φ_{1a2} and Φ_{b54} that are completely fixed by conformal symmetry, i.e. where t is trivial. On the other hand, there is the central vertex Φ_{ab3} of type I. With these notations, the shadow integral for scalar 5-point blocks of weight $\Delta_i, i = 1,\dots,5$ reads

$$\begin{aligned}
&\Psi^{(\Delta_1,\dots,\Delta_5)}_{(\Delta_a,\Delta_b;l_a,l_b;\mathfrak{t})}(X_1,\dots,X_5) \quad = \\
&\qquad = \prod_{s=a,b}\int \mathrm{d}\mu(X_a,X_b,Z_a,Z_b)\Phi_{1\tilde{a}2}(X_1,X_a,X_2;\bar{Z}_a)\,\Phi^t_{ab3}(X_a,X_b,X_3;Z_a,Z_b)\,\Phi_{\tilde{b}54}(X_b,X_5,X_4;\bar{Z}_b).
\end{aligned} \tag{5.64}$$

Here the tilde on the indices of the first and third vertex means that we use eq. (5.17) for two scalar legs but with Δ_a and Δ_b replaced by $d-\Delta_a$ and $d-\Delta_b$, respectively. We have placed a superscript t on the vertex function of the central vertex to remind the reader that this depends on a function t of the 3-point cross ratio. Integration is performed with the conformal invariant measure $\mathrm{d}\mu$ of the embedding space variables. After splitting off the prefactor (3.80),

$$\Psi^{(\Delta_i)}_{(\Delta_a,\Delta_b;l_a,l_b;t)}(X_i) = \Omega^{(\Delta_i)}(X_i)g^{(\Delta_{12},\Delta_3,\Delta_{45})}_{(\Delta_a,\Delta_b;l_a,l_b;t)}(u_i) \tag{5.65}$$

the shadow integral (5.64) gives rise to a finite conformal integral that defines the conformal block g as a function of the five conformal invariant cross ratios u_i. These integrals depend on the choice of (Δ_a, l_a), (Δ_b, l_b) and the function $t(\mathcal{X})$.

In chapter 3 we constructed five differential equations for these blocks. Four of these are given by the

eigenvalue equations for the second and fourth order Casimir operators for the intermediate channels,

$$\mathcal{D}^2_{(12)} = (\mathcal{T}_1+\mathcal{T}_2)_{[AB]}\,(\mathcal{T}_1+\mathcal{T}_2)^{[BA]}\,, \tag{3.75}$$
$$\mathcal{D}^2_{(45)} = (\mathcal{T}_4+\mathcal{T}_5)_{[AB]}\,(\mathcal{T}_4+\mathcal{T}_5)^{[BA]}\,, \tag{3.76}$$
$$\mathcal{D}^4_{(12)} = (\mathcal{T}_1+\mathcal{T}_2)_{[AB]}\,(\mathcal{T}_1+\mathcal{T}_2)^{[BC]}\,(\mathcal{T}_1+\mathcal{T}_2)_{[CD]}\,(\mathcal{T}_1+\mathcal{T}_2)^{[DA]}\,, \tag{3.77}$$
$$\mathcal{D}^4_{(45)} = (\mathcal{T}_4+\mathcal{T}_5)_{[AB]}\,(\mathcal{T}_4+\mathcal{T}_5)^{[BC]}\,(\mathcal{T}_4+\mathcal{T}_5)_{[CD]}\,(\mathcal{T}_4+\mathcal{T}_5)^{[DA]}\,. \tag{3.78}$$

5-point conformal blocks are eigenfunctions of these four differential operators with eigenvalues determined by the conformal weights Δ_a, Δ_b and the spins l_a, l_b of the two internal fields $a = (12)$ and $b = (45)$ that appear in the operator products $\phi_1\phi_2$ and $\phi_4\phi_5$, respectively. The shadow integrals Ψ for conformal 5-point blocks turn out to be eigenfunctions of the following fifth differential operator

$$\mathcal{D}^{4,3}_{\mathfrak{v},(12)3} = (\mathcal{T}_1+\mathcal{T}_2)_{[AB]}\,(\mathcal{T}_1+\mathcal{T}_2)^{[BC]}\,(\mathcal{T}_1+\mathcal{T}_2)_{[CD]}\,(\mathcal{T}_3)^{[DA]} \tag{3.79}$$

if and only if the vertex functions $t(\mathcal{X})$ we use in the integrand to represent the central vertex of the OPE diagram is an eigenfunction of the reduced vertex operator of the previous subsection, specialized to vertices of type I. In this sense, the shadow integral intertwines the full 5-point vertex operator of section 3.4 with the reduced vertex operator above.

There is another way to relate the full 5-point operator with the reduced one for type I vertices that employs the OPE limits of chapter 4. In order to work out the reduction, we make use of the OPE in the limit where fields (ϕ_1, ϕ_2) and (ϕ_4, ϕ_5) are taken to be colliding, and are replaced with fields ϕ_a and ϕ_b whose conformal dimension and spin belongs to the tensor product of their representations. The first step is to reduce the operators to act on a spinning 4-point function, as in Figure 5.2.

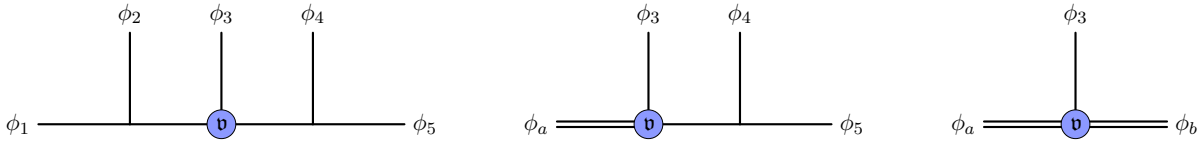

Figure 5.2: Scalar five point function (left), which in the OPE limit of fields ϕ_1 and ϕ_2 gets reduced to the 4-point function with a spinning leg ϕ_a (center), and after a second OPE limit for fields ϕ_4 and ϕ_5 gets fully reduced to a type I vertex (right).

Following the procedure of section 4.3.3 adapted to the five-points case, we start the reduction by taking the leading behavior in $\bar{z}_1$ as

$$g(z_1,\bar{z}_1,z_2,\bar{z}_2,w) \overset{\bar{z}_1\to 0}{\sim} \bar{z}_1^{\frac{\Delta_a-l_a}{2}}\, g(z_1,z_2,\bar{z}_2,w)\,. \tag{5.66}$$

Imposing this leading behavior in the eigenvalue equations for the differential operators (3.75)–(3.79) allows to reduce the action of the differential operators to a 4-dimensional subspace of cross ratios in the following way:

$$\lim_{\bar{z}_1\to 0}\left[\bar{z}_1^{-\frac{\Delta_a-l_a}{2}}\,\mathcal{D}\left(\bar{z}_1^{\frac{\Delta_a-l_a}{2}}\,g(z_1,z_2,\bar{z}_2,w)\right)\right] = \mathcal{E}\,g(z_1,z_2,\bar{z}_2,w). \tag{5.67}$$

To complete the OPE limit, one then considers the leading behavior in z_1 of the form

$$g(z_1,z_2,\bar{z}_2,w) \overset{z_1\to 0}{\sim} z_1^{\frac{\Delta_a+l_a}{2}}\, g(z_2,\bar{z}_2,w) \tag{5.68}$$

and takes a similar limit as in (5.67). After these conjugations and limits, both the quadratic and quartic Casimirs associated to the internal leg $a = (12)$ are reduced to constants, and the remaining three operators

$$\mathcal{D}^2_{(45)}\,, \qquad \mathcal{D}^4_{(45)}\,, \qquad \mathcal{D}^{4,3}_{\mathfrak{v},a3} \tag{5.69}$$

characterize the spinning 4-point function that is shown in Figure 5.2 (center). The latter depends only on three cross ratios $z_2, \bar{z}_2, w$, the spacetime dimension d, and the external data

$$\frac{\Delta_a - \Delta_3}{2}\,, \qquad \frac{\Delta_5 - \Delta_4}{2}\,, \qquad l_a\,. \tag{5.70}$$

It is straightforward to repeat the same procedure we just outlined for the leg $b = (45)$ in the remaining correlator, i.e. one can impose leading behaviors of the type

$$g(z_2, \bar{z}_2, w) \overset{\bar{z}_2 \to 0}{\sim} \bar{z}_2^{\frac{\Delta_b - l_b}{2}} g(z_2, w) \overset{z_2 \to 0}{\sim} z_2^{\frac{\Delta_b + l_b}{2}} \bar{z}_2^{\frac{\Delta_b - l_b}{2}} g(w) \tag{5.71}$$

to ensure that the quadratic and quartic Casimir of the internal leg $b = (45)$ assume constant values that are determined by the weight and spin of the intermediate field.
At the end of this procedure, one is left with a 3-point block of two STT's and one scalar, that is to say a vertex of type I, which is characterized by the sole vertex operator $\mathcal{D}^{4,3}_{\mathfrak{v},a3}$ acting on the remaining cross ratio w. By considering the OPE limit in embedding space as in section 4.3.2, and therefore writing

$$X_1 = X_a + \epsilon Z_a\,, \qquad X_2 = X_a - \epsilon Z_a\,, \qquad X_5 = X_b - \epsilon' Z_b\,, \qquad X_4 = X_b + \epsilon' Z_b\,, \tag{5.72}$$

and taking $\epsilon, \epsilon' \to 0$, we find the following expression for w in terms of the external 3-point data:

$$w = 1 - \frac{(X_3 \cdot X_a)(X_3 \cdot X_b)\left[(X_a \cdot Z_b)(X_b \cdot Z_a) - (X_a \cdot X_b)(Z_a \cdot Z_b)\right]}{\left[(X_3 \cdot Z_b)(X_a \cdot X_b) - (X_3 \cdot X_b)(X_a \cdot Z_b)\right]\left[(X_3 \cdot Z_a)(X_a \cdot X_b) - (X_3 \cdot X_a)(X_b \cdot Z_a)\right]}\,. \tag{5.73}$$

After further inspection, this expression can be identified with

$$w = 1 - \frac{H_{ab}}{V_{a,3b} V_{b,a3}} = 1 - \mathcal{X}'\,, \tag{5.74}$$

where the cross ratio $\mathcal{X}'$ is equal to $\mathcal{X}$ with the replacement $(1,2,3) \to (a,b,3)$. The resulting operator can be easily identified with the $\ell_1 = \ell_2 = 0$ case of the general expression (5.57).

5.4 Vertex Operator and Generalized Weyl algebras

The Hamiltonians we discussed in the previous section have nice properties, even though they may look a bit uninviting at first. In this section we exhibit some of their underlying algebraic structure. This allows us to recast the vertex operator into a one-line expression, somewhat analogous to the harmonic oscillator that possesses a particularly simple representation in terms of creation and annihilation operators. Here we define a generalized Weyl algebra with relatively simple commutation relations and then build our vertex operators directly in terms of its generators. An important role in our discussion is played by the scalar product of the vertex system.

5.4.1 Single variable vertices and the Gegenbauer scalar product

Functions on the configuration space $\mathcal{M}$ inherit a scalar product from the Haar measure on the conformal group. This is the case in general, but in particular for the 1-dimensional spaces we are dealing with in this chapter. Working out this scalar product is straightforward in principle, but a bit cumbersome in practice; the full derivation can be found in [43, Appendix B]. The result is surprisingly simple: it turns out that, when written in the variable $s = 1 - 2\mathcal{X}$, the group theoretic scalar product on the configuration space $\mathcal{M}$ coincides with the Gegenbauer scalar product,

$$\langle f, g \rangle_{\alpha(d;\ell_i)} := \int_{-1}^{+1} \mathrm{d}s\, (1 - s^2)^{\alpha(d;\ell_i) - \frac{1}{2}}\, \overline{f(s)}\, g(s)\,, \tag{5.75}$$

with the parameter α given by

$$\alpha(d;\ell_i) := \ell_1 + \ell_2 + \frac{d-3}{2}\,. \tag{5.76}$$

In the following we shall implicitly assume that the parameters assume only those values that appear in the context of our three single parameter vertices, i.e. for $d = 3$ we have $\ell_1 = 0 = \ell_2$ while for $d > 3$ only $\ell_2 = 0$. The only case for which ℓ_2 can also be non-zero is in $d = 4$. Gegenbauer polynomials $C_n^{(\alpha)}(s)$ provide an orthogonal basis for $\langle -, - \rangle_\alpha$:

$$\langle C_m^{(\alpha)}, C_n^{(\alpha)} \rangle_\alpha = \frac{\pi\, 2^{1-2\alpha}}{\Gamma(\alpha)^2} \frac{\Gamma(n+2\alpha)\Gamma(n+\alpha)}{\Gamma(n+\alpha+1)\Gamma(n+1)}\, \delta_{mn}\,. \tag{5.77}$$

As one may check by explicit computation, the vertex differential operators $H^{(d;\Delta_i;l_i)}(\mathcal{X}, \partial_\mathcal{X})$ are hermitian with respect to a Gegenbauer scalar product whenever the conformal weights Δ_i and the STT spins l_i are analytically continued to satisfy,

$$\bar{\Delta}_i = d - \Delta_i\,, \qquad \bar{l}_i = 2 - d - l_i\,, \tag{5.78}$$

i.e. $(\Delta_i; l_i) \in \left(\frac{d}{2} + \mathrm{i}\mathbb{R}\right) \times \left(\frac{2-d}{2} + \mathrm{i}\mathbb{R}\right)$, while $(d; \ell_i)$ are kept as real parameters. Our goal now is to compute the Hamiltonian in the basis of Gegenbauer polynomials. In doing so we shall restrict to the case with $d > 3$ and $\ell_2 = 0$, i.e. we exclude the somewhat special case of $d = 4$ with $\ell_1 \neq 0 \neq \ell_2$ for which our Hamiltonian contains a non-polynomial term, see comments at the end of the previous section. The computation of the Hamiltonian in the Gegenbauer basis relies on its expression as

$$H^{(d,\Delta_i,l_i,\ell_i)} = h_0^{(s)}(s) + \sum_{q=1}^{4} h_q^{(s)}(s)(1-s^2)^{q-1}\partial_s^q\,, \tag{5.79}$$

where all $h_q^{(s)}(s)$ are polynomials of order at most 3 in s whenever $\ell_2 = 0$. It proceeds with the help of three well-known identities:

(S) the recursion relation of Gegenbauer polynomials

$$s \cdot C_n^{(\alpha)} = \frac{(n+1)C_{n+1}^{(\alpha)} + (n+2\alpha-1)C_{n-1}^{(\alpha)}}{2(n+\alpha)}\,, \tag{5.80}$$

(D) the Gegenbauer differential equation in self-adjoint form,

$$\mathcal{D}_\alpha \cdot C_n^{(\alpha)} = (1-s^2)^{\frac{1}{2}-\alpha}\partial_s\,(1-s^2)^{\frac{1}{2}+\alpha}\partial_s \cdot C_n^{(\alpha)} = -n(n+2\alpha)C_n^{(\alpha)}\,, \tag{5.81}$$

(Θ) and the first order differentiation operator

$$\partial_\Theta \cdot C_n^{(\alpha)} = (1-s^2)\partial_s \cdot C_n^{(\alpha)} = \frac{(n+2\alpha-1)(n+2\alpha)C_{n-1}^{(\alpha)} - n(n+1)C_{n+1}^{(\alpha)}}{2(n+\alpha)}\,. \tag{5.82}$$

Using these building blocks (S),(D),(Θ), our Hamiltonians can be recast into the form

$$\begin{aligned} H^{(d,\Delta_i,l_i,\ell_i)} =& \mathcal{D}_\alpha\partial_\Theta^2 + (k_{3,1}s + k_{3,0})\,\mathcal{D}_\alpha\partial_\Theta + \left(k_{2,2}s^2 + k_{2,1}s + k_{2,0}\right)\mathcal{D}_\alpha \\ &+ (k_{1,1}s + k_{1,0})\,\partial_\Theta + k_{0,2}s^2 + k_{0,1}s + k_{0,0}\,, \end{aligned} \tag{5.83}$$

where the coefficients $k_{i,j} = k_{i,j}(d, \Delta_i, l_i, \ell_i)$ are given by

$$\begin{aligned} k_{3,0} &= 2\mathrm{i}\gamma_3\,, \qquad k_{3,1} = 2(\nu_1+\nu_2+\alpha)+3\,, \\ k_{2,0} &= \gamma_1^2+\gamma_2^2-\gamma_3^2-2\nu_1\nu_2-2(\alpha-1)(\nu_1+\nu_2)-\alpha(1+3\alpha)+\frac{13}{4}\,, \\ k_{2,1} &= -2\gamma_1\gamma_2+\mathrm{i}\gamma_3\,(2(\nu_1+\nu_2+\alpha)+3)\,, \qquad k_{2,2} = \nu_1^2+\nu_2^2+4l\nu_1\nu_2+(4\alpha+1)(\nu_1+\nu_2)+4\alpha^2+3\,, \\ k_{1,0} &= 2(\nu_1+\nu_2+\alpha)\gamma_1\gamma_2+\mathrm{i}\gamma_3\left(-2\nu_1\nu_2+(2\alpha+1)(\nu_1+\nu_2)-4\alpha^2+2\alpha+2\right), \\ k_{1,1} &= -2(\nu_1^2\nu_2+\nu_2^2\nu_1)+(1-2\alpha)\left(\nu_1^2+\nu_2^2+4\nu_1\nu_2+(1+4\alpha)(\nu_1+\nu_2+\alpha+1)-\alpha-2\right), \\ k_{0,1} &= 2\nu_1\nu_2\left(\gamma_1\gamma_2+\mathrm{i}\gamma_3(\alpha+\frac{1}{2})\right), \qquad k_{0,2} = -\nu_1\nu_2(\nu_1-1)(\nu_2-1)\,. \end{aligned} \tag{5.84}$$

The parameters γ_k, ν_k are defined through

$$\Delta_k := \frac{d}{2} + \mathrm{i}\gamma_k\,, \qquad k = 1,2,3\,, \qquad\qquad \nu_k := l_k - \ell_1\,, \qquad k = 1,2\,, \tag{5.85}$$

and α was introduced in eq. (5.76). Let us stress once again that the solution we have displayed here applies to $\ell_2 = 0$ and $d \geq 3$. When $\ell_2 \neq 0$, the Hamiltonian contains a non-polynomial term in $h_0^{(s)}(s)$ which is proportional to $(1-s)^{-1}$. So, while it is in principle possible to compute the action of the MST_2-MST_2-scalar Hamiltonian in $d = 4$ on Gegenbauer polynomials with $\alpha = (d-3)/2 + \ell_1 + \ell_2$, it does not directly fit our ansatz (5.83).

Plugging the identities (5.80), (5.81), (5.82) back into (5.83) one can obtain simple explicit formulas for the matrix elements

$$H_{mn}^{(d;\Delta_i;l_i;\ell_i)} = \frac{\langle C_m^{(\alpha)}, H^{(d;\Delta_i;l_i;\ell_i)} \cdot C_n^{(\alpha)} \rangle_\alpha}{\langle C_m^{(\alpha)}, C_m^{(\alpha)} \rangle_\alpha}\,. \tag{5.86}$$

One observes that these vanish whenever $|n-m| > 2$, so our Hamiltonian in the Gegenbauer basis has non-vanishing matrix elements only close to the diagonal. In terms of the matrix elements, the hermiticity property of the vertex differential operators reads

$$H_{mn}^{(d;\Delta_i;l_i;\ell_i)} = \frac{\langle C_n^{(\alpha)}, C_n^{(\alpha)} \rangle_\alpha}{\langle C_m^{(\alpha)}, C_m^{(\alpha)} \rangle_\alpha} H_{nm}^{(d;d-\Delta_i;2-d-l_i;\ell_i)}\,. \tag{5.87}$$

With our formulas (5.83) and (5.84) we have fulfilled our first promise, namely to write the Hamiltonian in a much more compact form that fully replaces the two pages of formulas we spelled out in the previous section.

5.4.2 A generalized Weyl algebra acting on tensor structures

We want to go one step further and write the vertex Hamiltonians in terms of the generators of some Weyl-like algebraic structure that acts on Gegenbauer polynomials and hence on 3-point tensor structures. Our algebra contains three generators $A, A^\dagger$ and N and it depends on the parameters α, ν_1 and ν_2 which we introduced in eqs. (5.76) and (5.85). When acting on Gegenbauer polynomials, these three operators are given by

$$N C_n^{(\alpha)} := n C_n^{(\alpha)}, \tag{5.88}$$

$$A C_n^{(\alpha)} := (n + \nu_1 + 2\alpha)(n + \nu_2 + 2\alpha)\frac{n + 2\alpha - 1}{n + \alpha} C_{n-1}^{(\alpha)}\,, \tag{5.89}$$

$$A^\dagger C_n^{(\alpha)} := (n - \nu_1)(n - \nu_2)\frac{n+1}{n+\alpha} C_{n+1}^{(\alpha)}, \tag{5.90}$$

where eq. (5.89) applies to all $n > 0$, and $A C_0^{(\alpha)} = 0$ when $n = 0$, i.e. the state $C_0^{(\alpha)}$ is annihilated by the lowering operator A. Similarly, the action of the raising operator $A^\dagger$ vanishes if $n = \nu_1$ or $n = \nu_2$. Consequently, one can restrict the action of $A, A^\dagger$ and N to the finite dimensional subspace that is spanned by $C_n^{(\alpha)}$ for $n = 0, \ldots, \min(\nu_1, \nu_2)$. This should remind us of the space of 3-point tensor structures we discussed at the very end of section 5.2. There we argued that the space of 3-point tensor structures has dimension $n_t + 1$ with $n_t = \min(l_1 - \ell_1, l_2 - \ell_1) = \min(\nu_1, \nu_2)$ in the case of $\ell_2 = 0$, using the definition (5.85) of ν_k. Therefore, the truncation of the action of $A, A^\dagger$ and N to a finite dimensional subspace of Gegenbauer polynomials we observe here is fully consistent with the finiteness of the space of 3-point tensor structures, at least for $d > 3$. We will discuss the special case of $d = 3$ below.

From the action on Gegenbauer polynomials it is possible to check that the operators $A, A^\dagger$ and N obey

the following relations

$$[N, A^\dagger] = A^\dagger, \tag{5.91}$$
$$[N, A] = -A\,, \tag{5.92}$$
$$AA^\dagger = \frac{(N+1)(N+2\alpha)}{(N+\alpha)(N+\alpha+1)}(N-\nu_1)(N+2\alpha+\nu_1+1)(N-\nu_2)(N+2\alpha+\nu_2+1)\,, \tag{5.93}$$
$$A^\dagger A = \frac{N(N+2\alpha-1)}{(N+\alpha-1)(N+\alpha)}(N+\nu_1+2\alpha)(N-\nu_1-1)(N+\nu_2+2\alpha)(N-\nu_2-1)\,. \tag{5.94}$$

We can use these to define a family of abstract algebras that depends parametrically on $\alpha = \ell_1 + (d-3)/2$ and $\nu_k = l_k - \ell_1$. This family comes equipped with an involutive antiautomorphism $(-)^*$ defined by $N^* = N$ and $A^* = A^\dagger$. It coincides with the adjoint whenever d is real and the spins l_i satisfy the relation (5.78) that is needed in order for our vertex operators to be hermitian or, equivalently,

$$\bar\alpha = \alpha\,, \qquad \bar\nu_1 = -(2\alpha+1+\nu_1)\,, \qquad \bar\nu_2 = -(2\alpha+1+\nu_2)\,. \tag{5.95}$$

Having introduced the algebra generated by $A, A^\dagger$ and N, the vertex operator H can now be written as a rational combination of the generators of this algebra:

$$H^{(d;\Delta_i;l_i;\ell_i)} = B^\dagger B - \Gamma(N+\alpha)^2 + \frac{\alpha(\alpha-1)\,K}{(N+\alpha)^2-1} + E^{(d;\Delta_i;l_i;\ell_i)}. \tag{5.96}$$

Here, we defined the operators

$$B^\dagger := \frac{A-A^\dagger}{2\mathrm{i}} - \mathrm{i}(2\gamma_1\gamma_2 + \mathrm{i}\gamma_3)(N+\alpha)\,, \tag{5.97}$$
$$B := \frac{A-A^\dagger}{2\mathrm{i}} + \mathrm{i}(2\gamma_1\gamma_2 - \mathrm{i}\gamma_3)(N+\alpha)\,, \tag{5.98}$$

and the two parameters

$$\Gamma := \frac{1}{4}(1+4\gamma_1^2)(1+4\gamma_2^2)\,, \tag{5.99}$$
$$K := (\nu_1+\alpha)(\nu_2+\alpha)(\nu_1+\alpha+1)(\nu_2+\alpha+1)\,. \tag{5.100}$$

The constant term $E^{(d;\Delta_i;l_i;\ell_i)}$ is obtained by relating $H^{(d;\Delta_i;l_i;\ell_i)} \cdot 1 = h_0^{(d;\Delta_i;l_i;\ell_i)}(0)$ to the action of $A, A^\dagger, N$ on $C_0^{(\alpha)}$. In this way we find

$$\begin{aligned} E^{(d;\Delta_i;l_i;\ell_i)} =& h_0^{(d;\Delta_i;l_i;\ell_i)}(0) - \alpha^4 - (1+2\nu_1+2\nu_2)\alpha^3 \\ &+ \alpha^2\left(\frac{1}{4} + \gamma_1^2 + \gamma_2^2 - \gamma_3^2 + \nu_1(\nu_1+1) + \nu_2(\nu_2+1) + 4\nu_1\nu_2\right) \\ &- 2\nu_1\nu_2\alpha - \nu_1\nu_2(1+\nu_1\nu_2). \end{aligned}$$

This concludes the algebraic reformulation of our vertex Hamiltonians. It is remarkable that the algebra only depends on the spins and dimension d, i.e. that all the dependence on the conformal weights of the three fields resides in the Hamiltonian.

The case of $d = 3$, which implies $\ell_1 = 0$, requires additional consideration since in this case one can also have odd-parity tensor structures, see our discussion at the end of subsection 5.2.1. As we saw there, the STT-STT-scalar vertex in $d = 3$ is unique in that it admits a total number

$$(\min(\nu_1,\nu_2)+1) + \min(\nu_1,\nu_2) = \min(2l_1+1, 2l_2+1) \tag{5.101}$$

of 3-point tensor structures. A complete and orthogonal basis can be obtained from the union of Chebyshev polynomials of the first and second kind,

$$\{C_n^{(0)}(s)\}_{n=0,\ldots,\min(l_1,l_2)} \quad , \quad \{\sqrt{1-s^2}C_n^{(1)}(s)\}_{n=1,\ldots,\min(l_1,l_2)}\,.$$

The action of $A, A^\dagger, N$ in $d = 3$, however, is more conveniently written in the Fourier basis $e^{in\theta}$, where $n = -\min(l_1, l_2), \ldots, +\min(l_1, l_2)$ and the new variable θ is related to our cross ratio $\mathcal{X}$ by $\mathcal{X} = \sin^2 \frac{\theta}{2}$. In this case, the action of $A, A^\dagger$ and N on the Fourier basis is

$$N\, e^{in\theta} := n e^{in\theta}, \qquad A^\dagger e^{in\theta} := (n - l_1)(n - l_2) e^{i(n+1)\theta}, \qquad A\, e^{in\theta} := (n + l_1)(n + l_2) e^{i(n-1)\theta}.$$

It is easy to see that these operators satisfy the following polynomial relations

$$[N, A^\dagger] = A^\dagger, \tag{5.102}$$
$$[N, A] = -A\,, \tag{5.103}$$
$$AA^\dagger = (N - l_1)(N - l_2)(N + l_1 + 1)(N + l_2 + 1)\,, \tag{5.104}$$
$$A^\dagger A = (N - l_1 - 1)(N - l_2 - 1)(N + l_1)(N + l_2)\,. \tag{5.105}$$

These relations agree with those we found in eqs. (5.91)-(5.93) above for the special choice $\alpha = \ell_1 + (d-3)/2 = 0$ relevant for vertices in $d = 3$, where $\ell_1 = 0$. In other words, we have now shown that for $d = 3$, the algebra we have introduced above possesses a finite dimensional representation on the space of Chebyshev polynomials of first and second kind.

For $\alpha = 0$ and $\alpha = 1$, the algebra of $A, A^\dagger$ and N is one special example of a larger family of algebras of the form $A^\dagger A = f(N)$, $AA^\dagger = f(N + 1)$ that can be associated with a polynomial $f(N)$. Such families of algebras have been studied for a long time in the mathematics literature, going back at least as early as [91, §3]. The representation theory of these algebras was studied in [92] and in [93], where the latter author first used the term "generalized Weyl algebra". It was then in [94] that these algebras were first reformulated as non-commutative deformations of the Kleinian singularity of type $\tilde{A}_{n-1}$ when f is a polynomial of degree n. Finally, using quiver theory, the authors of [95] generalized this analysis to non-commutative deformations of the Kleinian singularities associated to any finite subgroup of $\mathrm{SL}_{\mathbb{C}}(2)$. In this context, the algebra with relations (5.102) — (5.105) is thus called a generalized Weyl algebra or deformed Kleinian singularity of type $\tilde{A}_3$.

For $\alpha \neq 0, 1$, the relations (5.93) and (5.94) are no longer polynomial, at least not in the way we wrote them. Nevertheless, they can be recast as an α-dependent family of generalized Weyl algebras if we are willing to sacrifice the property $A^* = A^\dagger$. Indeed, any rescaling of the operators A and $A^\dagger$ by a rational function of N defines a homomorphism of algebras[2]. In the case of eqs. (5.93) and (5.94), it is natural to take

$$U := \frac{(N + \alpha)(N + \alpha + 1)}{(N + 1)(N + 2\alpha)} A\,, \qquad V := A^\dagger\,, \tag{5.106}$$

in which case the modified relations read

$$[N, V] = V\,, \tag{5.107}$$
$$[N, U] = -U\,, \tag{5.108}$$
$$UV = (N - \nu_1)(N + \nu_1 + 2\alpha + 1)(N - \nu_2)(N + \nu_2 + 2\alpha + 1)\,, \tag{5.109}$$
$$VU = (N - \nu_1 - 1)(N + \nu_1 + 2\alpha)(N - \nu_2 - 1)(N + \nu_2 + 2\alpha)\,, \tag{5.110}$$

and also define a generalized Weyl algebra of type $\tilde{A}_3$, but now with an extra deformation parameter α. In any given representation, the homomorphism $A \longleftrightarrow U$ in (5.106) is bijective if and only if $-1, -\alpha, -(\alpha + 1), -2\alpha \notin \mathrm{Spec}(N)$. This condition is indeed satisfied in the Gegenbauer polynomial representations, where U is explicitly represented as

$$U \cdot C_n^{(\alpha)} = (n + \nu_1 + 2\alpha)(n + \nu_2 + 2\alpha) \frac{n + \alpha - 1}{n} C_{n-1}, \quad \forall n > 0, \qquad U \cdot C_0^{(\alpha)} = 0. \tag{5.111}$$

As a result, $(A, A^\dagger, N) \mapsto (U, V, N)$ defines an isomorphism, and all vertex systems of type I and II are representations of the generalized $\tilde{A}_3$ Weyl algebra with relations (5.107) — (5.110).

[2] We thank Pavel Etingof for pointing this out to us.

Our final comment in this subsection concerns the fact that our expression (5.96) for the Hamiltonian depends on parameters only through the combinations α, ν_i, γ_i, at least up to the constant term. It follows that (see Appendix C.2 for a further generalization)

$$H^{(d;\Delta_i;l_i;\ell_1,0)} = H^{(d+2\ell_1;\Delta_i+\ell_1;l_i-\ell_1;0,0)} + \Delta E^{(d;\Delta_i;l_i;\ell_1)}, \tag{5.112}$$

where

$$\begin{aligned}\ell_1^{-1}\Delta E^{(d;\Delta_i;l_i;\ell_1)} = &-\frac{2}{3}\ell_1^3 + \frac{8\alpha+26}{3}\ell_1^2 \\ &+ \frac{4}{3}\left(-2\alpha^2 + 2(\nu_1-\nu_2-41/2)\alpha - \gamma_1^2+\gamma_2^2-\gamma_3^2+\nu_1(\nu_1+1)-\nu_2(\nu_2+1)-33\right)\ell_1 \\ &+ \frac{16}{3}\alpha^2(\nu_2-\nu_1+17/4) + \frac{8}{3}\alpha\left(\gamma_1^2-\gamma_2^2+\gamma_3^2-\nu_1(\nu_1+4)+\nu_2(\nu_2+5/2)+9\right) \\ &+ 2\left(2\gamma_1^2-\gamma_2^2+\gamma_3^2-2\nu_1(\nu_1+1)+\nu_2(\nu_2+1)+\frac{9}{2}\right).\end{aligned}$$

Now, the α-deformed relations (5.93) and (5.94) of the generalized Weyl algebra coincide with the $d=3$ relations (5.104), (5.105) whenever $\alpha=0$ or $\alpha=1$. In the former case, $\alpha=0 \iff (d,\ell_1)=(3,0)$. On the other hand, the latter case $\alpha=1$ can occur in two situations,

$$(d,\ell_1)=(5,0)\,, \qquad \text{or} \qquad (d,\ell_1)=(4,\frac{1}{2})\,, \tag{5.113}$$

in which case

$$\nu_i = l_i\,, \qquad \text{or} \qquad \nu_i = l_i - \frac{1}{2}\,, \tag{5.114}$$

and the two operators are the same up to a constant shift,

$$H^{(d=5;\Delta_i;l_i;0,0)}(\mathcal{X},\partial_{\mathcal{X}}) = H^{(d=4;\Delta_i-\frac{1}{2};l_i+\frac{1}{2};\frac{1}{2},0)}(\mathcal{X},\partial_{\mathcal{X}}) + \Delta E\,. \tag{5.115}$$

In both of these cases, the Gegenbauer polynomials become Chebyshev polynomials of the second kind $\{C_n^{(1)}(s)\}_{n=0,\ldots,\min(l_1,l_2)}$, and the two vertex operators are related to the $d=3$ operator by a similarity transformation,

$$H^{(d=5;\Delta_i;l_i;0,0)}(\mathcal{X},\partial_{\mathcal{X}}) = \frac{1}{\sqrt{\mathcal{X}(1-\mathcal{X})}} H^{(d=3;\Delta_i-1;l_i+1)}(\mathcal{X},\partial_{\mathcal{X}})\sqrt{\mathcal{X}(1-\mathcal{X})} + \Delta E\,. \tag{5.116}$$

In particular, the parity-even 3-point tensor structures of two STTs in $d=5$, are equivalent to the parity-odd 3-point tensor structures of two STTs in $d=3$.

5.5 Map to the Lemniscatic CMS model

In the previous section we have found quite an elegant reformulation of our vertex operators that makes it seem a bit more tractable than the original formulas we displayed in section 5.3. All this is somewhat similar to the Casimir operators of Dolan and Osborn, which may appear a bit uninviting at first, but were found to possess interesting algebraic structure that led to explicit solutions, in particular in even dimensions. In [76], it was discovered that the usual Casimir operator can be mapped to another well studied operator, namely the Hamiltonian of an integrable 2-particle CMS model. Here we state a very similar result for the vertex operators. By explicit computations, these operators can be mapped to the lemniscatic CMS model, a special case of the crystallographic elliptic CMS models found by Etingof, Felder, Ma and Veselov [75]. We review this model in the first subsection before constructing the map from our vertex differential operator. The third subsection contains a complete identification of parameters.

5.5.1 The elliptic $\mathbb{Z}/4\mathbb{Z}$ CMS model

While our vertex system examples have received little attention, there has been much discussion in similar cases of the relation between deformations of Kleinian singularities on the one hand, and CMS models for the corresponding complex reflection group on the other hand — see e.g. [96] for $\tilde{A}_{n-1}$, and [97] for the general case, both of which are based on [98]. Thus, the identification of our operator with a lemniscatic CMS model is less surprising in light of the $\tilde{A}_3$ singularity of §5.4.2. That said, apart from $\tilde{A}_1$, the only integrable models explicitly studied in this particular context have so far always been rational. And while the integrable systems in [99] include, amongst others, the compact $\mathfrak{so}_{\mathbb{R}}(6)$ analogue of our MST_2-MST_2-scalar vertex in $d = 4$, the authors do not make the connection with the elliptic integrable models of [75].

The elliptic CMS models associated with the complex reflection groups $\mathbb{Z}_m$ form a family of quantum mechanical integrable systems with (complexified) coordinate on an orbifold curve of the form

$$\mathcal{M} = \mathbb{C}/\left(\mathbb{Z}_m \ltimes (\mathbb{Z} \oplus \tau\mathbb{Z})\right), \tag{5.117}$$

where $\mathbb{Z} \oplus \tau\mathbb{Z} \subset \mathbb{C}$ is a 2-dimensional lattice with elliptic modulus τ in the upper half of the complex plane, and elements of the group $\mathbb{Z}_m \subset \mathrm{SO}(2)$ act on the lattice as a point group, i.e. through rotations by angles $\varphi_n = n/2m\pi$ where $n = 1, \dots, m$. It is well known that the only 2-dimensional lattices with a non-trivial point group $\mathbb{Z}_m$ appear for $m = 2, 3, 4, 6$. Apart from $m = 2$, the elliptic modulus τ is also fixed so that spaces $\mathcal{M}$ of the form (5.117) only appear for

$$(m, \tau) \in \{2\} \times \mathbb{C}_+\,, \qquad \text{or} \qquad (m, \tau) \in \{3, e^{2\pi\mathrm{i}/3}\} \cup \{4, \mathrm{i}\} \cup \{6, e^{\pi\mathrm{i}/3}\}\,. \tag{5.118}$$

In [75], the authors construct new integrable models on each of these curves, but only the case $\tau = \mathrm{i}$ with group action of $\mathbb{Z}_4$ turns out to be relevant for us. In order to proceed, let us write the associated curve (5.117) as the quotient of the so-called lemniscatic elliptic curve E_{i} by a $\mathbb{Z}_4$ action,

$$\mathcal{M} = E_{\mathrm{i}}/\mathbb{Z}_4\,, \quad \textit{where} \quad E_{\mathrm{i}} = \mathbb{C}/(\mathbb{Z} \oplus \mathrm{i}\mathbb{Z}) = \{z \in \mathbb{C} \,|\, z \sim z + 1 \sim z + \mathrm{i}\}\,. \tag{5.119}$$

Here, the $\mathbb{Z}_4$ action is the obvious one that is given by multiplication of $z \in E_{\mathrm{i}}$ with any fourth root of unity $\zeta^4 = 1$, i.e. $z \mapsto \zeta \cdot z$. Under this action, the lemniscatic curve E_{i} has four fixed points:

$$\omega_0 := 0\,, \qquad \zeta \cdot 0 = 0\,, \tag{5.120}$$

$$\omega_1 := \frac{1+\mathrm{i}}{2}\,, \qquad \zeta \cdot \frac{1+\mathrm{i}}{2} = \frac{-1+\mathrm{i}}{2} \sim \frac{1+\mathrm{i}}{2}\,, \tag{5.121}$$

$$\omega_2 := \frac{\mathrm{i}}{2}\,, \qquad \zeta^2 \cdot \frac{\mathrm{i}}{2} = -\frac{\mathrm{i}}{2} \sim \frac{\mathrm{i}}{2}\,, \tag{5.122}$$

$$\zeta^3 \cdot \omega_2 = \omega_3 := \frac{1}{2}\,, \qquad \zeta^2 \cdot \frac{1}{2} = -\frac{1}{2} \sim \frac{1}{2}\,, \tag{5.123}$$

where $\zeta \in \mathbb{Z}_4$ denotes the generating element $\zeta = \mathrm{i}$, and the equivalence relation $\sim$ identifies points that are obtained from one another by lattice shifts. From the short computation in the second column we conclude that ω_0, ω_1 are fixed points stabilized by the entire $\mathbb{Z}_4$, i.e. they are fixed points of order 4, while ω_2, ω_3 are fixed points of order 2 with a stabilizer subgroup $\mathbb{Z}_2 \subset \mathbb{Z}_4$. These last two fixed points are mapped to each other by the nontrivial $\mathbb{Z}_4$ transformation on E_{i}. They thus give rise to the same point in the quotient $\mathcal{M} = E_{\mathrm{i}}/\mathbb{Z}_4$. We conclude that $\mathcal{M}$ has three (singular) orbifold points which we denote as

$$z_0 := \omega_0\,, \quad z_1 := \omega_1\,, \quad z_2 := \omega_2 \sim \omega_3\,. \tag{5.124}$$

At these points, the orbifold singularities are of orders $4, 4, 2$, respectively. The elliptic CMS model associates to each of these singular points z_ν, $\nu = 0, 1, 2$, a family of multiplicities $m_{i,\nu}$, $i = 1, \dots, 4$ such that

$$\sum_{i=1}^{4} m_{i,\nu} := 6\,, \quad \nu = 0, 1, 2\,, \qquad m_{1,2} + m_{2,2} = 1\,, \qquad m_{3,2} + m_{4,2} = 5\,. \tag{5.125}$$

Note that there is one relation among the four multiplicities we associate with the fixed points of order four, while there are three relations among the four multiplicities that are associated with the fixed point of order two. Given that there are three relations that constrain the four multiplicities $m_{i,2}$, it is often convenient to parametrize the solutions in terms of a single parameter k which we define as

$$m_{1,2} := k + 1\,. \tag{5.126}$$

The Hamiltonian L_{EFMV} of the lemniscatic CMS model has a relatively complicated dependence on the multiplicities. On the other hand, it may be uniquely characterized by a rather simple set of conditions: if we require that that the $\mathbb{Z}_4$-invariant operator $L_{\text{EFMV}}(z,\partial_z)$ takes the normalized form

$$L_{\text{EFMV}} = \partial_z^4 + \mathcal{O}(\partial_z^2)\,, \tag{5.127}$$

then its dependence on the multiplicities is uniquely determined by the following set of conditions

$$L_{\text{EFMV}}(z,\partial_z)\cdot(z-z_0)^r = \prod_{i=1}^{4}(r-m_{i,0})\,(z-z_0)^{r-4} + \mathcal{O}((z-z_0)^r)\,, \tag{5.128}$$

$$L_{\text{EFMV}}(z,\partial_z)\cdot(z-z_1)^r = \prod_{i=1}^{4}(r-m_{i,1})\,(z-z_1)^{r-4} + \mathcal{O}((z-z_1)^r)\,, \tag{5.129}$$

$$\begin{aligned} L_{\text{EFMV}}(z,\partial_z)\cdot(z-z_2)^r = &\prod_{i=1}^{4}(r-m_{i,2})\,(z-z_2)^{r-4} \\ &+ \lambda(r-m_{1,2})(r-m_{2,2})(z-z_2)^{r-2} + \mathcal{O}((z-z_2)^r)\,, \end{aligned} \tag{5.130}$$

which we assume to hold for some constant $\lambda \in \mathbb{C}$, in the neighborhood of the singular points $z = z_\nu$. In order to write the Hamiltonian explicitly over the full orbifold $\mathcal{M}$, we first introduce the Weierstrass elliptic function

$$\wp(z) := \frac{1}{z^2} + \sum_{w\in(\mathbb{Z}\oplus i\mathbb{Z})\setminus\{0\}}\left(\frac{1}{(z-w)^2} - \frac{1}{w^2}\right), \tag{5.131}$$

which is double-periodic by construction, $\wp(z) = \wp(z+1) = \wp(z+\mathrm{i})$. Then the Hamiltonian of the lemniscatic $\mathbb{Z}/4\mathbb{Z}$ CMS model is given by [75, Eq. 4.3]

$$L_{\text{EFMV}}(z,\partial_z) = \partial_z^4 + \sum_{p=0}^{2} g_p^{(z)}(z)\partial_z^p\,, \tag{5.132}$$

where

$$c_2^{(z)}(z) = \sum_{\nu=0}^{3} a_\nu\,\wp(z-\omega_\nu)\,, \tag{5.133}$$

$$c_1^{(z)}(z) = \sum_{\nu=0}^{3} b_\nu\,\wp'(z-\omega_\nu)\,, \tag{5.134}$$

$$c_0^{(z)}(z) = \sum_{\nu=0}^{3} c_\nu\,\wp^2(z-\omega_\nu) + \wp(\omega_3)(a_0-a_1)k(k+1)\,(\wp(z-\omega_2)-\wp(z-\omega_3))\,. \tag{5.135}$$

The various coefficients (a_ν, b_ν, c_ν) for $\nu = 0,1,2$ are related to the multiplicities as [75, Example 7.7]

$$a_\nu := -11 + \sum_{1\le i<j\le 4} m_{i,\nu}m_{j,\nu}\,, \tag{5.136}$$

$$b_\nu := \frac{1}{2}\left(-a_\nu - 6 + \sum_{1\le i<j<k\le 4} m_{i,\nu}m_{j,\nu}m_{k,\nu}\right), \tag{5.137}$$

$$c_\nu := \prod_{i=1}^{4} m_{i,\nu}\,, \tag{5.138}$$

$(a_3, b_3, c_3) = (a_2, b_2, c_2)$ and the parameter k is $k = m_{1,2} - 1$. Note that in eq. (5.133)-(5.135) we are summing over the four fixed points $(\omega_0, \omega_1, \omega_2, \omega_3)$ of the elliptic curve E_{i}, and that we need $(a_3, b_3, c_3) \equiv (a_2, b_2, c_2)$ to ensure the $\mathbb{Z}_4$-symmetry of the Hamiltonian.

5.5.2 Construction of the map

In order to recast our vertex operator H in the form (5.127) of the lemniscatic CMS Hamiltonian, we need to find a change of variables from our cross-ratio $\mathcal{X}$ to a new variable ϕ and a 'gauge transformation' $\Theta(\mathcal{X}(\phi))$ such that

$$\Theta^{-1} H \Theta = (\text{const}) \partial_\phi^4 + \mathcal{O}(\partial_\phi^2)\,. \tag{5.139}$$

Looking at the terms of order $\partial_{\mathcal{X}}^4$ and $\partial_{\mathcal{X}}^3$, we see that ϕ can be taken to solve the differential equation

$$\frac{\mathrm{d}\phi}{\mathrm{d}\mathcal{X}} = \frac{(-)^{\frac{1}{4}}}{4} \mathcal{X}^{-\frac{3}{4}} (1-\mathcal{X})^{-\frac{3}{4}}, \qquad \phi(\mathcal{X}=0) = 0\,, \tag{5.140}$$

and Θ must be of the form

$$\Theta = \Theta_0\, \mathcal{X}^{\frac{l_1+l_2-2(\ell_1+\ell_2)+\Delta_3+(1-d)/2}{4}} (1-\mathcal{X})^{\frac{l_1+l_2-2(\ell_1+\ell_2)-\Delta_3+(1+d)/2}{4}}\,, \tag{5.141}$$

where $\Theta_0 \in \mathbb{C}\backslash\{0\}$ is an arbitrary multiplicative constant. The solution to eq. (5.140) is proportional to the incomplete Beta function, which has the known analytic expression (see [100, Eq. 8.17.7])

$$\phi(\mathcal{X}) = \frac{(-)^{\frac{1}{4}}}{4} \int_0^{\mathcal{X}} \mathrm{d}\mathcal{X}'\, \mathcal{X}'^{-\frac{3}{4}} (1-\mathcal{X}')^{-\frac{3}{4}} = (-\mathcal{X})^{\frac{1}{4}}\, {}_2F_1\left(\frac{1}{4}, \frac{3}{4}; \frac{5}{4}; \mathcal{X}\right). \tag{5.142}$$

If we now apply the Pfaff transformation of the Gauss hypergeometric function,

$${}_2F_1\left(a, b; c; \mathcal{X}\right) = (1-\mathcal{X})^{-a}\, {}_2F_1\left(a, c-b; c; \frac{\mathcal{X}}{\mathcal{X}-1}\right), \tag{5.143}$$

the above function can be expressed in terms of the inverse arc length function for the lemniscate curve (see [101, Eq. 5]),

$$\phi(\mathcal{X}) = \left(\frac{\mathcal{X}}{\mathcal{X}-1}\right)^{\frac{1}{4}} {}_2F_1\left(\frac{1}{4}, \frac{1}{2}; \frac{5}{4}; \frac{\mathcal{X}}{\mathcal{X}-1}\right) \equiv \text{arcsinlemn}\left(\frac{\mathcal{X}}{\mathcal{X}-1}\right)^{\frac{1}{4}}. \tag{5.144}$$

Using [101, Eq. 21], the change of variables can be inverted to

$$\sqrt{\frac{\mathcal{X}}{\mathcal{X}-1}} = \frac{\mathrm{sd}^2\left(\phi\sqrt{2}, \frac{1}{\sqrt{2}}\right)}{2}\,, \tag{5.145}$$

where $\mathrm{sd}(u,k)$ is one of the Jacobi elliptic functions. This can be equivalently expressed in terms of the Weierstrass function $\wp(z)$ defined in eq. (5.131),

$$\mathcal{X} = \frac{\wp(\omega_3)^2}{\wp(\omega_3)^2 - \wp(z)^2}\,, \qquad \phi = \wp(\omega_3)\, z\,, \tag{5.146}$$

To re-express the corresponding operator in the form (5.132) and solve the parameters k, a_ν, b_ν, c_ν in eqs. (5.133), (5.134), (5.135) for Δ_i, l_i, ℓ_i, d, we made a symbolic computation in `Mathematica`. This symbolic computation specifically avoids the use of the special functions `JacobiSD` and `WeierstrassP` that appear in eqs. (5.145) and (5.146), because the version of `Mathematica` we used does not efficiently make use of the derivative and addition formulas of these special functions. Instead, we only use the `Hypergeometric2F1` in eq. (5.144) to compute the coefficients $c_0^{(z)}, c_1^{(z)}, c_2^{(z)}$ as functions of $\mathcal{X}$. More specifically, we start by determining the three functions

$$\begin{aligned}
h_0^{(\phi)}(\phi(\mathcal{X})) &= H(\mathcal{X}, \partial_{\mathcal{X}}) \cdot 1\,, \\
h_1^{(\phi)}(\phi(\mathcal{X})) &= H(\mathcal{X}, \partial_{\mathcal{X}}) \cdot \phi(\mathcal{X}) - \phi(\mathcal{X}) h_0^{(\phi)}(\phi(\mathcal{X}))\,, \\
h_2^{(\phi)}(\phi(\mathcal{X})) &= H(\mathcal{X}, \partial_{\mathcal{X}}) \cdot \frac{\phi(\mathcal{X})^2}{2} - \phi(\mathcal{X}) h_1^{(\phi)}(\mathcal{X}) - \frac{\phi(\mathcal{X})^2}{2} h_0^{(\phi)}(\mathcal{X})\,,
\end{aligned}$$

that are related to the c-coefficients by

$$c_p^{(z)}(z(\mathcal{X})) = 4^3 \wp(\omega_3)^{2-\frac{p}{2}} \left(h_p^{(\phi)}(\phi(\mathcal{X})) - \delta_{p,0} E_{\text{EFMV}} \right), \qquad p = 0, 1, 2, \tag{5.147}$$

where $E_{\text{EFMV}}^{(d;\Delta_i;l_i;\ell_i)}$ is the constant shift of the Hamiltonian given in Appendix C.2.2. Following eq. (5.146), it is easy to show that the $c_p^{(z)}$ computed from $H(\mathcal{X}, \partial_{\mathcal{X}})$ are algebraic functions of $\wp(z)$. Similarly, we can express each term in eqs. (5.133), (5.134), (5.135) as a rational function of $\wp(z)$ using the addition formulas

$$\wp(z - \omega_1) = -\frac{\wp(\omega_3)^2}{\wp(z)}, \tag{5.148}$$

$$\wp(z - \omega_2) = -\wp(\omega_3) \frac{\wp(z) - \wp(\omega_3)}{\wp(z) + \wp(\omega_3)}, \tag{5.149}$$

$$\wp(z - \omega_3) = \wp(\omega_3) \frac{\wp(z) + \wp(\omega_3)}{\wp(z) - \wp(\omega_3)}, \tag{5.150}$$

and the derivative formula

$$\wp'(z)^2 = 4\wp(z) \left(\wp(z)^2 - \wp(\omega_3)^2 \right), \tag{5.151}$$

for the lemniscatic Weierstrass elliptic function. Following these identities, each of the coefficient functions $c_p^{(z)}$ in the Hamiltonian is the product of $\wp^{\frac{p}{2}-2} \left(\wp(\omega_3)^2 - \wp^2 \right)^{\frac{p}{2}-2}$ with a polynomial function in $\wp$. We can then identify each polynomial coefficient expressed as a function of k, a_ν, b_ν, c_ν with its expression in terms of Δ_i, l_i, ℓ_i, d to obtain the map from spins and conformal dimensions to multiplicities.

5.5.3 CMS multiplicities from weights and spins

In all cases, the multiplicity associated to z_2 (see eq. (5.126)) can be computed from the spin quantum numbers l_1, l_2 as

$$k = l_1 - l_2 - \frac{1}{2} \qquad \text{or} \qquad k = l_2 - l_1 - \frac{1}{2}. \tag{5.152}$$

Going from one choice to the other in eq. (5.152) is equivalent to the change of parameters $k \to -(k+1)$, which leaves the CMS Hamiltonian invariant. For the MST_2-STT-scalar (type II) vertex in all $d \geq 3$ we have

$$m_{1,0} = 3\frac{5-d}{2} - (l_1 + l_2) - \Delta_3 - 2\ell_1, \tag{5.153}$$

$$m_{2,0} = \frac{d-1}{2} - (l_1 + l_2) - \Delta_3 + 2\ell_1, \tag{5.154}$$

$$m_{3,0} = \frac{d-1}{2} + (l_1 + l_2) + \Delta_3 + 2(\Delta_1 - \Delta_2), \tag{5.155}$$

$$m_{4,0} = \frac{d-1}{2} + (l_1 + l_2) + \Delta_3 - 2(\Delta_1 - \Delta_2), \tag{5.156}$$

and

$$m_{1,1} = -5\frac{d-3}{2} - (l_1 + l_2) + \Delta_3 - 2\ell_1, \tag{5.157}$$

$$m_{2,1} = -\frac{d+1}{2} - (l_1 + l_2) + \Delta_3 + 2\ell_1, \tag{5.158}$$

$$m_{3,1} = -\frac{d+1}{2} + (l_1 + l_2) - \Delta_3 + 2(\Delta_1 + \Delta_2), \tag{5.159}$$

$$m_{4,1} = \frac{7d-1}{2} + (l_1 + l_2) - \Delta_3 - 2(\Delta_1 + \Delta_2), \tag{5.160}$$

which also contains the particular case of type I with two spinning fields in $d \geq 3$ simply by setting $\ell_1 = 0$. It is easy to observe from eqs. (5.153)—(5.160) that

$$m_{i,\nu}(d; \Delta_i, l_i; \ell_1) = m_{i,\nu}\left(d + \delta d; \Delta_i + \frac{\delta d}{2}; l_i - \frac{\delta d}{2}; \ell_1 - \frac{\delta d}{2} \right), \tag{5.161}$$

or equivalently

$$m_{i,\nu}(2\alpha+3-2\ell_1;\alpha-\ell_1+\frac{3}{2}+\mathrm{i}\gamma_i,l_i;\nu_i+\ell_1;\ell_1)=\text{function}\,(\alpha;\gamma_i;\nu_i)\,. \tag{5.162}$$

This is a direct consequence of the observation made in eq. (5.112). We conclude that the three weight and three spin labels along with the dimension d of the MST_2-STT-scalar vertices do not exhaust the full 7-dimensional parameter space of the elliptic $\mathbb{Z}_4$ CMS model. In fact, it is easy to see that the parameters are constrained by

$$m_{1,0}-m_{2,0}=m_{1,1}-m_{2,1}\,. \tag{5.163}$$

When specializing to $d=4$, this last constraint defines the restriction of the generic MST_2-MST_2-scalar (type III) vertex to the MST_2-STT-scalar case. We have determined that the full MST_2-MST_2-scalar vertex in $d=4$ yields the CMS multiplicities

$$m_{1,0}=\frac{3}{2}-(l_1+l_2)-\Delta_3-2(\ell_1-\ell_2)\,, \tag{5.164}$$
$$m_{2,0}=\frac{3}{2}-(l_1+l_2)-\Delta_3+2(\ell_1-\ell_2)\,, \tag{5.165}$$
$$m_{3,0}=\frac{3}{2}+(l_1+l_2)+\Delta_3+2(\Delta_1-\Delta_2)\,, \tag{5.166}$$
$$m_{4,0}=\frac{3}{2}+(l_1+l_2)+\Delta_3-2(\Delta_1-\Delta_2)\,, \tag{5.167}$$
$$m_{1,1}=-\frac{5}{2}-(l_1+l_2)+\Delta_3-2(\ell_1+\ell_2)\,, \tag{5.168}$$
$$m_{2,1}=-\frac{5}{2}-(l_1+l_2)+\Delta_3+2(\ell_1+\ell_2)\,, \tag{5.169}$$
$$m_{3,1}=-\frac{5}{2}+(l_1+l_2)-\Delta_3+2(\Delta_1+\Delta_2)\,, \tag{5.170}$$
$$m_{4,1}=\frac{27}{2}+(l_1+l_2)-\Delta_3-2(\Delta_1+\Delta_2)\,. \tag{5.171}$$

Let us note that this set of multiplicities does not satisfy any additional constraints. This concludes our description of the precise relation between the vertex differential operators for single variable vertices and the lemniscatic CMS model of [75]. We would like to finish this section off with two additional comments.

Comments on algebraic integrability: The CMS operator is said to be algebraically integrable if the multiplicities $m_{i,\nu}$ defined by eqs. (5.128), (5.129), (5.130) are integers (see [102, Corollary 2.4]). In this case, according to [102, Theorem 2.5], a generic eigenfunction of L_{EFMV} will take the form

$$\psi_\lambda(z)=e^{\beta z}\prod_{i=1}^{4}\frac{\theta(z-\alpha_i)}{\theta(z-\beta_i)}, \tag{5.172}$$

where $\theta(z)$ is the first Jacobi theta-function of the lemniscatic elliptic curve, and $\beta,\beta_1,\alpha_1,\ldots,\beta_4,\ \alpha_4$ are certain parameters that can be solved in terms for the multiplicities and eigenvalue λ by writing the eigenvalue equation $L_{\mathrm{EFMV}}\psi_\lambda=\lambda\psi_\lambda$ for (5.172) near the singular points $z=z_0,z_1,z_2$. We have determined above that all multiplicities are linear combinations of the quantum numbers $(\Delta_i;l_i;\ell_i)$ and the dimension d, with coefficients in $\frac{1}{2}\mathbb{Z}$. Therefore, depending on whether d is odd or even, the vertex operator is algebraically integrable when the quantum numbers $[-\Delta_i;l_i;\ell_i]$ that define the representation at each point are either integers or half-integers. This setup is equivalent to placing unitary irreducible representations of the compact real form $\mathrm{SO}_{\mathbb{R}}(d+2)$ at each point (or the double cover thereof). It would be interesting to explore the generalization of this result to non-integer conformal weights.

CMS multiplicities for all vertex systems: As a final comment we want to rewrite the relations between the CMS multiplicities and the weight and spin quantum numbers in terms of the parameters that appeared

in our discussion of the generalized Weyl algebra, see previous section. Recall the parameters of the generalized Weyl algebra,

$$\alpha := \frac{d-3}{2} + \ell_1 + \ell_2\,, \qquad \nu_1 = l_1 - \ell_1 - \ell_2\,, \qquad \nu_2 = l_2 - \ell_1 - \ell_2\,. \tag{5.173}$$

To determine a universal formula for the CMS multiplicities of all 1-dimensional vertex systems, we use the four extra parameters

$$\beta := \ell_1 - \ell_2 + \frac{d-5}{2}\,, \qquad \gamma_i := -\mathrm{i}\left(\Delta_i - \frac{d}{2}\right)\,. \tag{5.174}$$

The parameters γ_i had appeared in our construction of the Hamiltonian already, see eq. (5.85). Only the parameter β is new. Of course, the map from spin quantum numbers $(l_i;\ell_i)$ to α,β,ν_1,ν_2 can be inverted as

$$l_1 = \nu_1 + \alpha + \frac{3-d}{2}\,, \qquad l_2 = \nu_2 + \alpha + \frac{3-d}{2}\,, \tag{5.175}$$

$$\ell_1 = \frac{\alpha+\beta+4-d}{2}\,, \qquad \ell_2 = \frac{\alpha-\beta-1}{2}\,. \tag{5.176}$$

If we insert these formulas into the expressions for multiplicities we listed above, these become completely universal to all 1-dimensional vertex systems, i.e. they no longer depend on type of the vertex (I, II, or III). Explicitly one finds

$$k = \nu_1 - \nu_2 - \frac{1}{2}\,, \qquad \text{or} \qquad k = \nu_2 - \nu_1 - \frac{1}{2}\,, \tag{5.177}$$

and

$$m_{1,0} = -\frac{1}{2} - (\nu_1+\nu_2) - \mathrm{i}\gamma_3 - 2\alpha - 2\beta\,, \tag{5.178}$$

$$m_{2,0} = \frac{3}{2} + (\nu_1+\nu_2) - \mathrm{i}\gamma_3 - 2\alpha + 2\beta\,, \tag{5.179}$$

$$m_{3,0} = \frac{5}{2} + (\nu_1+\nu_2) + \mathrm{i}\gamma_3 + 2\alpha + 2\mathrm{i}(\gamma_1-\gamma_2)\,, \tag{5.180}$$

$$m_{4,0} = \frac{5}{2} + (\nu_1+\nu_2) + \mathrm{i}\gamma_3 + 2\alpha - 2\mathrm{i}(\gamma_1-\gamma_2)\,, \tag{5.181}$$

$$m_{1,1} = \frac{3}{2} - (\nu_1+\nu_2) + \mathrm{i}\gamma_3 - 4\alpha\,, \tag{5.182}$$

$$m_{2,1} = -\frac{1}{2} - (\nu_1+\nu_2) + \mathrm{i}\gamma_3\,, \tag{5.183}$$

$$m_{3,1} = \frac{5}{2} + (\nu_1+\nu_2) - \mathrm{i}\gamma_3 + 2\alpha + 2\mathrm{i}(\gamma_1+\gamma_2)\,, \tag{5.184}$$

$$m_{4,1} = \frac{5}{2} + (\nu_1+\nu_2) - \mathrm{i}\gamma_3 + 2\alpha - 2\mathrm{i}(\gamma_1+\gamma_2)\,. \tag{5.185}$$

In particular, the MST_2-STT-scalar (type II) case in all $d \geq 3$ is obtained by imposing the additional relation $\beta = \alpha - 1$, equivalent to $\ell_2 = 0$.

Chapter 6

Conclusions

In this thesis we addressed the problem of the computation of multipoint conformal blocks in Conformal Field Theories, introducing techniques and obtaining results that have improved the general understanding of this complicated subject.

After an introduction to basic concepts in CFT, we immediately delved into the characterization of multipoint conformal blocks from the perspective of differential equations. This brought to the statement, in chapter 3, of the first main result of this thesis: the construction of a full set of relevant differential equations for any conformal block with any number of external legs, in any channel, and any dimension. More concretely, we managed to construct a number of independent commuting differential operators for N-point functions which matches in all cases the number of conformally invariant cross ratios. This result has been achieved by making use of the integrability properties of the $\mathfrak{so}(d+1,1)$ Gaudin models, which could then be passed down to the computation of conformal blocks, allowing us to characterize also this one as an integrable problem. In fact, the possibility in Gaudin models to construct infinite families of commuting operators that are automatically invariant under diagonal conformal symmetry, made it such that the commuting operators that characterize conformal blocks could be simply recovered from limits of these families, with a procedure tailored to the OPE channel in consideration. The outcome of these limits is thus a set of operators which depends on the choice of an OPE channel, but which is in all cases made by only two distinct types of operators: Casimir differential operators, associated with internal legs of OPE diagrams and whose relevance is naturally expected in an extension of the work of Dolan and Osborn [51], and vertex differential operators, constructed around every non-trivial vertex of the OPE diagram and which constitute a novel type of operator that was never considered before in the context of CFT.

All of these new vertex operators produce differential equations of order higher than two, which makes them rather difficult to handle, especially when coupled with other differential equations. To have a good starting point to tackle their solution theory, we sought out limits in which the system simplifies and can be connected with known solutions. We discussed and analyzed one such type of limit, the OPE limits, in chapter 4. The central result there is the introduction of a set of conformal cross ratios in which each coordinate is naturally associated with just one of the basic elements of a comb-channel OPE diagram. This allows simple analysis of the leading contributions associated with any OPE of a comb-channel diagram, which can be used to project on certain exchanges of operators in the internal legs, or specific three-point tensor structures at the vertices. We claim that after extraction of the leading behavior on the three variables associated with an internal leg r, the $d \leq 4$ differential equations associated with the two branches connected to said leg decouple, and the conformal blocks thus factorize in a product of lower-point conformal blocks. The same claim also applies to N-point functions with $N \leq 6$ in any dimension. We verified this claim explicitly for $N \leq 6$, producing the remarkable OPE-factorization formulas in section 4.3 and matching the reduced quadratic Casimir equations with those of spinning four-point functions, obtained with Harish-Chandra's radial component map.

Being in possession of this knowledge on how multipoint conformal blocks can be explicitly reduced to lower-point ones, one can now formulate a plan on how explicit and complete solution could be computed for the general multipoint case. Ideally, one should first be able to solve all the fundamental subsystems that appear in the OPE diagram, i.e. the differential equations associated with internal legs and those for internal vertices. Once that is well under control, more general solutions could then be approached by turning on interactions between those subsystems, "gluing together" the elementary building blocks to form bigger OPE diagrams. The first main constituent, the Casimir equations associated with internal legs of OPE diagrams, is already under relatively good control. Many explicit solutions have been built in the literature for the simplest scalar and low-spin cases, and the general system is known to be in general equivalent to spinning generalizations of the hyperbolic BC_2 Calogero-Moser-Sutherland model [79, 80]. The understanding of the vertex systems, on the other hand, is not as advanced. For this reason, in chapter 5 we analyzed the simplest of these systems, namely those vertices that possess only one conformally invariant degree of freedom. These correspond precisely to all the possible vertices that can appear in a comb-channel diagram in $d \leq 4$, and can thus be obtained from the reduction of multipoint conformal blocks using our OPE factorization results. Despite the rather cumbersome form in which the explicit operators are initially computed, see section 5.3, we find after some manipulation that these objects can be recast in expressions that only span a few lines. The first simplification has been achieved by re-expressing the vertex differential operator in terms of generators of a generalized Weyl algebra that acts on Gegenbauer polynomials. We then constructed explicitly a map from the daunting two-page formula of section 5.3 to the Hamiltonian of a crystallographic elliptic Calogero-Moser-Sutherland model introduced in [75], showing yet another time how the realm of conformal blocks and that of integrable systems are strongly interconnected. We believe that these connections can lead to future insight on the solution theory for these vertex systems, which would then represent a solid base for the construction of general expressions for multipoint blocks.

There are many directions that are still left to explore from the work we just outlined, ranging from the understanding of more abstract mathematical properties to more concrete applications. For instance, it would be very intriguing to check whether the integrable nature of the multipoint block equations can lead to the construction and usage of powerful tools of integrability such as the Dunkl operators [103] for the BC_2 Calogero-Moser-Sutherland models. Objects of this type could lead to the decomposition of the Casimir or vertex operators into combinations of simpler objects, which could then make the study of solutions far more manageable. Another promising direction is represented by the construction of weight-shifting operators [20, 28]. These are already used in the four-point context to allow for a recursive construction of conformal blocks with spinning internal/external legs in terms of blocks with only scalars. One expects similar type of operators to be constructible also in a multipoint context, which would then make the computation of low-spin multipoint blocks within reach.

Ultimately, the main ambition of our differential approach for multipoint conformal blocks is to gain strong control over these functions, allowing this way the application of the conformal bootstrap logic to correlators with more than four external legs. At the current stage, it seems still unclear how this can be done in a numerical approach, as current numerical bootstrap techniques seem to depend on aspects that are only specific to the four-point case. Nonetheless, some non-trivial ideas are currently being considered, and it is possible that with proper refinement these could flourish and lead to functioning techniques. On the other hand, analytical bootstrap techniques are more directly extended to a higher-point setting. This is an aspect which has already seen some success in recent works [32–34]. The main approach followed by these involves the use of an expression of the OPE of two fields in the limit in which these are light-like separated [104]. This allows the computation of conformal blocks directly in certain multiple light-cone limits, which is all one needs for a light-cone bootstrap analysis. The main limitation of this approach, however, is that the light-cone OPE between one internal and one external field is not yet under sufficient control to be used for explicit computations. This means that, at the current stage,

this approach cannot produce results beyond the snowflake channel for six-point correlators. According to some recent early results, however, our approach involving differential equations seems to have high chances of success in leading to concrete expressions for more complicated light-cone conformal blocks, such as the null-polygon limit for six-point correlators in the comb-channel. This is rather promising, as it could open up the doors for bootstrap of more general operators on which very little information is currently available, such as triple-twist operators or more general MSTs. We are planning to address this very concretely in future work, walking along the pathway opened by the results of this thesis.

Appendix A

Appendices to Chapter 3

A.1 Proof of the induction in the limits of Gaudin models

In this appendix, we detail the induction in the proof of the limit procedure of section 3.3. We thus refer to this section for notation and definitions. Our main goal is to show that for every vertex $\mathfrak{v} \in V$, the Lax matrix of the N-sites Gaudin model satisfies the limit (3.52). For the purposes of this appendix, it will be useful to rewrite this limit as

$$\varpi^{n_\mathfrak{v}} \mathcal{L}_\alpha\big(h_\mathfrak{v}(z,\varpi)\big) \xrightarrow{\varpi\to 0} \mathcal{L}^\mathfrak{v}_\alpha(z) = \frac{\mathcal{T}_\alpha^{(I_{\mathfrak{v},1})}}{z} + \frac{\mathcal{T}_\alpha^{(I_{\mathfrak{v},2})}}{z-1}, \tag{A.1}$$

where we introduced

$$h_\mathfrak{v}(z,\varpi) = \varpi^{n_\mathfrak{v}} z + g_\mathfrak{v}(\varpi). \tag{A.2}$$

In the left-hand side of (A.1), and in all this appendix, we fix the sites w_i of the Gaudin model to their value $w_i = f_i(\varpi)$ prescribed by the limit procedure of Subsection 3.3.1. Recall that $\mathfrak{v}$ is either the reference vertex $\mathfrak{v}_*$, in V' or in V''. We will treat these three cases separately.

A.1.1 Reference vertex

Let us first consider the reference vertex $\mathfrak{v}_*$. The definition of $n_{\mathfrak{v}_*}$ and $g_{\mathfrak{v}_*}$ made in Subsection 3.3.1 can be simply rewritten as

$$n_{\mathfrak{v}_*} = 0 \qquad \text{and} \qquad h_{\mathfrak{v}_*}(z,\varpi) = z. \tag{A.3}$$

We then have

$$\varpi^{n_{\mathfrak{v}_*}} \mathcal{L}_\alpha\big(h_{\mathfrak{v}_*}(z,\varpi)\big) = \mathcal{L}_\alpha(z) = \sum_{i=1}^{N} \frac{\mathcal{T}_\alpha^{(i)}}{z-w_i}. \tag{A.4}$$

To proceed further, we decompose this sum over external edges $i \in \{1,\cdots,N\}$ into three parts.

Contribution of the reference edge. The first part is the contribution from the reference edge N, with corresponding site $w_N = f_N(\varpi) = \varpi^{-1}$, according to eq. (3.51). It simply reads

$$\frac{\mathcal{T}_\alpha^{(N)}}{z-w_N} = \frac{\varpi\,\mathcal{T}_\alpha^{(N)}}{\varpi\, z - 1} \xrightarrow{\varpi\to 0} 0 \tag{A.5}$$

and thus does not contribute to the limit of (A.4) when $\varpi \to 0$.

Contribution of the subtree T'. The second part is the contribution from the subtree T' attached to e', for which we should distinguish the cases where e' is external or not. If e' is external (in which case T' is trivial and e' is the only contribution from this subtree), recall from the first case of eq. (3.67) that we then have $w_{e'} = f_{e'}(\varpi) = \varpi$, so that the contribution to (A.4) simply is

$$\frac{\mathcal{T}_\alpha^{(e')}}{z-\varpi} \xrightarrow{\varpi\to 0} \frac{\mathcal{T}_\alpha^{(e')}}{z}. \tag{A.6}$$

Note that as e' is external, we have $E' = \{e'\}$ so that the generators $\mathcal{T}_\alpha^{(e')}$ coincide with $\mathcal{T}_\alpha^{(E')}$.
If e' is intermediate in the initial diagram then the contribution from the subtree T' comes from the edges $i \in E' \subset \underline{N}$, with corresponding sites $w_i = f_i(\varpi) = \varpi\, f_i'(\varpi)$ as in the second line of eq. (3.67). By construction, the functions $f_i'(\varpi)$ associated with the external edges $i \in E'$ stay finite when $\varpi \to 0$: indeed, as we supposed T' non-trivial, the edges $i \in E'$ are not the reference edge e' of T' and are thus associated with polynomial functions $f_i'(\varpi)$. Thus, we get that the corresponding sites $w_i = \varpi\, f_i'(\varpi)$ in the initial tree tend to 0 when $\varpi \to 0$. In this limit, the contribution of this subtree T' to the sum (A.4) then simply becomes

$$\sum_{i\in E'} \frac{\mathcal{T}_\alpha^{(i)}}{z - w_i} \xrightarrow{\varpi\to 0} \frac{1}{z} \sum_{i\in E'} \mathcal{T}_\alpha^{(i)}. \tag{A.7}$$

To conclude, let us observe that the sum in the right-hand side of the above equation is by definition $\mathcal{T}_\alpha^{(E')}$. Combined with the eq. (A.6) and the discussion that followed it for the case where e' is external, we thus observe that in both cases e' external and internal, the contribution of the subtree T' in the limit $\varpi \to 0$ of eq. (A.4) is simply

$$\sum_{i\in E'} \frac{\mathcal{T}_\alpha^{(i)}}{z - w_i} \xrightarrow{\varpi\to 0} \frac{\mathcal{T}_\alpha^{(E')}}{z}. \tag{A.8}$$

Contribution of the subtree T''. A similar argument applies to the contribution of the right subtree T'', attached to e''. If the latter is external, this contribution is simply equal to

$$\frac{\mathcal{T}_\alpha^{(e'')}}{z-1}, \tag{A.9}$$

since we then have $w_{e''} = 1$ – see the first line of eq. (3.68). If e'' is intermediate, the corresponding sites w_i, $i \in E''$, are given by the second line of eq. (3.68) and read $w_i = f_i(\varpi) = 1 + \varpi\, f_i''(\varpi)$, which thus tend to 1 when $\varpi \to 0$. In both cases, we find that the contribution to (A.4) is given by

$$\sum_{i\in E''} \frac{\mathcal{T}_\alpha^{(i)}}{z - w_i} \xrightarrow{\varpi\to 0} \frac{\mathcal{T}_\alpha^{(E'')}}{z-1}, \tag{A.10}$$

where in the first case $\mathcal{T}_\alpha^{(E'')} = \mathcal{T}_\alpha^{(e'')}$ while in the second case $\mathcal{T}_\alpha^{(E'')}$ is a composite operator formed by the sum of $\mathcal{T}_\alpha^{(i)}$ for $i \in E''$.

Conclusion. Summing the contributions (A.5), (A.8) and (A.10) in the limit of eq. (A.4) when $\varpi \to 0$, we then find

$$\varpi^{n_{\mathfrak{v}_*}} \mathcal{L}_\alpha\big(h_{\mathfrak{v}_*}(z,\varpi)\big) \xrightarrow{\varpi\to 0} \frac{\mathcal{T}_\alpha^{(E')}}{z} + \frac{\mathcal{T}_\alpha^{(E'')}}{z-1}. \tag{A.11}$$

To conclude, we observe that the labeling of branches at vertices made in Subsection 3.3.1 using the plane rooted tree representation T of the diagram implies that $E' = I_{\mathfrak{v}_*,1}$ and $E'' = I_{\mathfrak{v}_*,2}$. This shows that the limit (A.1) is satisfied for the reference vertex $\mathfrak{v}_*$.

A.1.2 Vertices in V'.

Let us now consider the case of a vertex $\mathfrak{v} \in V'$ in the subtree attached to e'. Note that the existence of this vertex requires the subtree T' to be non-trivial and thus the edge e' to be intermediate in the initial diagram. The definition of $n_\mathfrak{v}$ and the recursion relation for $g_\mathfrak{v}(\varpi)$ in the first line of eq. (3.66) can be rewritten as

$$n_\mathfrak{v} = n'_\mathfrak{v} + 1 \qquad \text{and} \qquad h_\mathfrak{v}(z,\varpi) = \varpi\, h'_\mathfrak{v}(z,\varpi), \tag{A.12}$$

where we have defined $h'_\mathfrak{v}(z,\varpi) = \varpi^{n'_\mathfrak{v}} z + g'_\mathfrak{v}(\varpi)$ as the equivalent of $h_\mathfrak{v}(z,\varpi)$ for the subtree T'. We thus have

$$\varpi^{n_\mathfrak{v}} \mathcal{L}_\alpha\big(h_\mathfrak{v}(z,\varpi)\big) = \varpi^{n'_\mathfrak{v}+1} \mathcal{L}_\alpha\big(\varpi\, h'_\mathfrak{v}(z,\varpi)\big) = \sum_{i=1}^{N} \frac{\varpi^{n'_\mathfrak{v}+1} \mathcal{T}_\alpha^{(i)}}{\varpi\, h'_\mathfrak{v}(z,\varpi) - w_i}. \tag{A.13}$$

We will once again separate this expression in three parts, coming from the contributions of the reference edge N and the two subtrees.

Contribution of the reference edge. Let us start with the edge N, with associated site $w_N = f_N(\varpi) = \varpi^{-1}$. Its contribution to (A.13) in the limit $\varpi \to 0$ is then given by

$$\frac{\varpi^{n'_\mathfrak{v}+1}\mathcal{T}_\alpha^{(N)}}{\varpi\, h'_\mathfrak{v}(z,\varpi) - w_N} = \frac{\varpi^{n'_\mathfrak{v}+2}\mathcal{T}_\alpha^{(N)}}{\varpi^2\, h'_\mathfrak{v}(z,\varpi) - 1} \xrightarrow{\varpi\to 0} 0. \tag{A.14}$$

Contribution of the subtree T''. Let us now consider the contribution coming from the subtree T'' attached to e''. If e'' is external in the initial tree T, then we simply have $w_{e''} = 1$ according to the first line of eq. (3.68) and the contribution to (A.13) is

$$\frac{\varpi^{n'_\mathfrak{v}+1}T_\alpha^{(e'')}}{\varpi\, h'_\mathfrak{v}(z,\varpi) - 1} \xrightarrow{\varpi\to 0} 0. \tag{A.15}$$

If e'' is initially intermediate, then the contribution comes from the external edges $i \in E'' \subset \underline{N}$ whose corresponding sites are given by the second line of eq. (3.68) to be $w_i = f_i(\varpi) = 1 + \varpi\, f_i''(\varpi)$. In particular, these tend to 1 when $\varpi \to 0$. Thus, in this case, the contribution of the subtree T'' to (A.13) also vanishes:

$$\sum_{i\in E''} \frac{\varpi^{n'_\mathfrak{v}+1}\mathcal{T}_\alpha^{(i)}}{\varpi\, h'_\mathfrak{v}(z,\varpi) - w_i} \xrightarrow{\varpi\to 0} 0. \tag{A.16}$$

Contribution of the subtree T'. Thus, the only non-vanishing contribution to (A.13) in the limit $\varpi \to 0$ comes from the subtree T' attached to e'. Recall that T' is non-trivial since it possesses a vertex $\mathfrak{v}$: the external edges $i \in E' \subset \underline{N}$ are thus different from e' and are associated with the sites $w_i = f_i(\varpi) = \varpi f'_i(\varpi)$, according to the second line of eq. (3.67). The contribution of T' to (A.13) then reads

$$\sum_{i\in E'} \frac{\varpi^{n'_\mathfrak{v}+1}\mathcal{T}_\alpha^{(i)}}{\varpi\, h'_\mathfrak{v}(z,\varpi) - w_i} = \sum_{i\in E'} \frac{\varpi^{n'_\mathfrak{v}}\mathcal{T}_\alpha^{(i)}}{h'_\mathfrak{v}(z,\varpi) - f'_i(\varpi)}. \tag{A.17}$$

The Gaudin Lax matrix of the subtree T' (the one of the full tree, not the ones associated with vertices) is given by eq. (3.69) and thus can be rewritten as

$$\mathcal{L}'_\alpha(z) = \sum_{i\in E'} \frac{\mathcal{T}_\alpha^{(i)}}{z - f'_i(\varpi)} + \frac{\varpi\, \mathcal{T}_\alpha^{(e')}}{\varpi\, z - 1}, \tag{A.18}$$

where we used the fact that $f'_{e'}(\varpi) = \varpi^{-1}$ since e' is the reference edge of T'. Thus, we can rewrite the above contribution (A.17) as

$$\sum_{i\in E'} \frac{\varpi^{n'_\mathfrak{v}+1}\mathcal{T}_\alpha^{(i)}}{\varpi\, h'_\mathfrak{v}(z,\varpi) - w_i} = \varpi^{n'_\mathfrak{v}}\mathcal{L}'_\alpha\big(h'_\mathfrak{v}(z,\varpi)\big) - \frac{\varpi^{n'_\mathfrak{v}+1}\mathcal{T}_\alpha^{(e')}}{\varpi\, h'_\mathfrak{v}(z,\varpi) - 1}. \tag{A.19}$$

The second term vanishes in the limit $\varpi \to 0$. Moreover, by the induction hypothesis (3.70) for the subtree T', the first term tends to $\mathcal{L}^\mathfrak{v}_\alpha(z)$ in this limit. In conclusion, we thus get

$$\sum_{i\in E'} \frac{\varpi^{n'_\mathfrak{v}+1}\mathcal{T}_\alpha^{(i)}}{\varpi\, h'_\mathfrak{v}(z,\varpi) - w_i} \xrightarrow{\varpi\to 0} \mathcal{L}^\mathfrak{v}_\alpha(z). \tag{A.20}$$

Conclusion. Since the contribution (A.20) is the only non-vanishing term in the limit of eq. (A.13) when $\varpi \to 0$, we thus get in the end that

$$\varpi^{n_\mathfrak{v}}\mathcal{L}_\alpha\big(h_\mathfrak{v}(z,\varpi)\big) \xrightarrow{\varpi\to 0} \mathcal{L}^\mathfrak{v}_\alpha(z), \tag{A.21}$$

as required. This indeed shows that the limit (A.1) is satisfied for vertices $\mathfrak{v} \in V'$, using the induction hypothesis (3.70) that a similar property also holds in the subtree T'.

A.1.3 Vertices in V''

Let us finally consider a vertex $\mathfrak{v} \in V''$. The procedure here will resemble the one in the previous subsection so we will not describe it in detail. The definition of $n_{\mathfrak{v}}$ and the recursion relation for $g_{\mathfrak{v}}(\varpi)$ in the second line of eq. (3.66) can be rewritten as

$$n_{\mathfrak{v}} = n''_{\mathfrak{v}} + 1 \qquad \text{and} \qquad h_{\mathfrak{v}}(z,\varpi) = 1 + \varpi\, h''_{\mathfrak{v}}(z,\varpi). \tag{A.22}$$

The main difference with the case of a vertex in V' is that we introduced a shift by 1 in the expression of $h_{\mathfrak{v}}(z,\varpi)$. The effect of this shift is that in the computation of the limit of $\varpi^{n_{\mathfrak{v}}}\mathcal{L}_\alpha\big(h_{\mathfrak{v}}(z,\varpi)\big)$ when $\varpi \to 0$, the only non-vanishing contribution now comes from the subtree T'' and not from T'. More precisely, using the fact that the shift by 1 cancels with the 1 in the recursive expression (3.68) of the sites w_i, $i \in E''$, we find in the end that

$$\lim_{\varpi\to 0} \varpi^{n_{\mathfrak{v}}}\mathcal{L}_\alpha\big(h_{\mathfrak{v}}(z,\varpi)\big) = \lim_{\varpi\to 0} \varpi^{n''_{\mathfrak{v}}}\mathcal{L}''_\alpha\big(h''_{\mathfrak{v}}(z,\varpi)\big) = \mathcal{L}^{\mathfrak{v}}_\alpha(z), \tag{A.23}$$

with $\mathcal{L}''_\alpha$ the Lax matrix (3.71) associated with the subtree T'', and where the last equality follows from the induction hypothesis (3.72) for the subtree T''. This then completes the proof of the induction.

A.2 Classical Embedding space formalism

For the proof in Appendix A.3 we are going to need a classical version of the embedding space formalism for the spinning fields that we have just discussed. For this purpose, we introduce P_A as the conjugate momentum to X^A, and Q^p_A as conjugate momenta of the auxiliary variables Z^A_p.
To see which constraints are imposed on these classical variables, one can check the action of the operators

$$X \cdot \frac{\partial}{\partial X}\,, \qquad X \cdot \frac{\partial}{\partial Z_p}\,, \qquad Z_p \cdot \frac{\partial}{\partial X}\,, \qquad Z_p \cdot \frac{\partial}{\partial Z_q} \tag{A.24}$$

on fields or correlation functions to get conditions that need to be satisfied by scalar products of coordinates and momenta. Some of the operators in (A.24) are in fact evaluated to constants on correlation functions. By imposing the same behavior when replacing derivatives with momenta, one obtains the following relations for phase space variables:

$$\begin{aligned} X^2 = Z_p^2 = Z_p \cdot Z_q = 0\,,\\ X \cdot Z_p = X \cdot Q_p = 0\,,\\ Z_p \cdot Q_q = 0 \quad \forall\, p < q\,,\\ X \cdot P = -\Delta\,, \quad Z_p \cdot Q_p = j_p\,. \end{aligned} \tag{A.25}$$

One can directly verify that the conditions (A.25) combined with the classical version of the generators (2.58)

$$\bar{\mathcal{T}}_{[AB]} = X_A P_B + \sum_{p=1}^{L} Z_{p\,A} Q_{p\,B} - (A \leftrightarrow B) \tag{A.26}$$

lead to the correct classical Casimirs associated to mixed-symmetry tensors:

$$\mathcal{C}as^{\,2n} = 2\Delta^{2n} + 2\sum_{i=1}^{L} j_p^{2n}\,. \tag{A.27}$$

A.3 Relations among vertex differential operators

Our goal in this appendix is to justify the relations (3.36) and (3.37) for the total symbols of our vertex differential operators. There are many ways to derive these relations. Here we shall follow a more pedestrian approach that does not require much background from representation theory.

In order to derive the relations (3.36), (3.37) we first note that these were formulated in terms of the coordinates and momenta of the external scalar fields. The representation of the conformal algebra that is associated to the index set I decomposes into an infinite number of spinning representations. Each of the irreducible components can be prepared in embedding space formalism. Here we shall study the relations (3.36) for a given irreducible component so that the coefficients $\varrho_{f,s}$ are functions of the associated weight and spins rather than functions of symbols of the Casimir differential operators.

After these introductory comments let us approach relation (3.36) by considering the simplest example in which the intermediate irreducible representation is scalar. We can construct explicitly the first three matrices $(\bar{\mathcal{T}}^n)^A{}_B$[1] in the classical embedding space that we introduced in Appendix A.2:

$$\begin{aligned}\left(\bar{\mathcal{T}}^1\right)^A{}_B &= X^A P_B - X_B P^A \\ \left(\bar{\mathcal{T}}^2\right)^A{}_B &= \Delta\left(X^A P_B + X_B P^A\right) - P^2 X^A X_B \\ \left(\bar{\mathcal{T}}^3\right)^A{}_B &= \Delta^2\left(X^A P_B - X_B P^A\right) = \Delta^2\left(\bar{\mathcal{T}}^1\right)^A{}_B\,.\end{aligned} \tag{A.28}$$

It is then clear that, when considering scalar representations, the powers of generators $\bar{\mathcal{T}}^n$ with $n \geq 3$ will be dependent on lower powers of the generators. This directly implies that any vertex operator of the type (3.34) that contains a power of a scalar generator higher than two will become dependent on operators of lower order, e.g.

$$\bar{\mathcal{T}}^3 \cdot \mathcal{B} \propto \bar{\mathcal{T}} \cdot \mathcal{B}\,. \tag{A.29}$$

We would now like to prove that something analogous to (A.28) is valid for representations of higher depth $\mathfrak{d}$ and higher powers, respectively. Let us then consider the generators for a mixed symmetry tensor of depth $\mathfrak{d}$,

$$\bar{\mathcal{T}}_{[AB]} = X_A P_B + \sum_{p=1}^{\mathfrak{d}-1} Z_{p\,A} Q_{p\,B} - (A \leftrightarrow B); \tag{A.30}$$

we expect the n-fold contractions of generators $\bar{\mathcal{T}}^n$ to be independent up to power $n = 2\mathfrak{d}$, with the first dependent object produced at power $n = 2\mathfrak{d}+1$. To prove this, let us focus on a specific matrix entry $(\bar{\mathcal{T}}^n)^A{}_B$ of the powers $\bar{\mathcal{T}}^n$ and construct the following submatrix of the Jacobian for fixed indices A, B and C:

$$\begin{pmatrix} \frac{\partial(\bar{\mathcal{T}}^1)^A{}_B}{\partial X^C} & \frac{\partial(\bar{\mathcal{T}}^1)^A{}_B}{\partial P^C} & \frac{\partial(\bar{\mathcal{T}}^1)^A{}_B}{\partial Z_1^C} & \frac{\partial(\bar{\mathcal{T}}^1)^A{}_B}{\partial Q_1^C} & \cdots & \frac{\partial(\bar{\mathcal{T}}^1)^A{}_B}{\partial Q_{\mathfrak{d}-1}^C} \\ \vdots & \vdots & \vdots & \vdots & & \vdots \\ \frac{\partial(\bar{\mathcal{T}}^{2\mathfrak{d}+1})^A{}_B}{\partial X^C} & \frac{\partial(\bar{\mathcal{T}}^{2\mathfrak{d}+1})^A{}_B}{\partial P^C} & \frac{\partial(\bar{\mathcal{T}}^{2\mathfrak{d}+1})^A{}_B}{\partial Z_1^C} & \frac{\partial(\bar{\mathcal{T}}^{2\mathfrak{d}+1})^A{}_B}{\partial Q_1^C} & \cdots & \frac{\partial(\bar{\mathcal{T}}^{2\mathfrak{d}+1})^A{}_B}{\partial Q_{\mathfrak{d}-1}^C} \end{pmatrix}. \tag{A.31}$$

If what we argued above holds, we should be able to see that some $2\mathfrak{d}$-minors of (A.31) are equal to zero, while the same matrix with the last row dropped out has all nonzero $2\mathfrak{d}$-minors. We checked this with Mathematica symbolically for the case of symmetric traceless tensors, and numerically for mixed symmetry tensors of depth $\mathfrak{d} \leq 6$, exhausting all tensorial representations that are allowed in the range of dimensions of known CFTs. One can use a similar reasoning to show eq. (3.37).

Let us finally comment on a more conceptual interpretation of the results of this appendix. We consider first the case of a scalar representation, whose generators can be gathered in the matrix $(\bar{\mathcal{T}}_f)^A{}_B = X^A P_B - X_B P^A$ in the fundamental representation. Using the relations $X^A X_A = 0$ and $X^A P_A = -\Delta$, one can show that the matrix $\bar{\mathcal{T}}_f$ is diagonalizable, with eigenvalues Δ, $-\Delta$ and 0 (with multiplicity d). It is a standard result of linear algebra that $\bar{\mathcal{T}}_f$ is then annihilated by the polynomial with simple roots equal to these eigenvalues, namely $T(T-\Delta)(T+\Delta) = T^3 - \Delta^2 T$: we recover this way that $\bar{\mathcal{T}}_f^3 = \Delta^2 \bar{\mathcal{T}}_f$. A similar argument can be formulated for a representation with higher depth $\mathfrak{d} = L+1$, characterized by a weight Δ and L spins $j_1, \ldots, j_L$. The (symbols of the) generators of this representation are given by eq. (A.26) and can be gathered in a matrix $\bar{\mathcal{T}}_f$ valued in the fundamental representation. The traces of odd powers of $\bar{\mathcal{T}}_f$ vanish, while the traces of even powers are given by the classical Casimirs

[1] Here and in the discussion below we shall drop the subscript f.

(A.27). These traces are the Newton sums $\sum_{i=1}^{d+2} \lambda_i^p$ of the eigenvalues $\lambda_1, \cdots, \lambda_{d+2}$ of $\bar{\mathcal{T}}_f$ and thus determine these eigenvalues uniquely (up to permutation). More precisely, we find that $\bar{\mathcal{T}}_f$ has eigenvalues $\Delta, -\Delta, j_1, -j_1, \ldots, j_L, -j_L$ and 0 (with multiplicity $d-2L$). If we suppose that $\bar{\mathcal{T}}_f$ is diagonalizable, it is then annihilated by the polynomial with simple roots equal to these eigenvalues, hence

$$\bar{\mathcal{T}}_f\big(\bar{\mathcal{T}}_f^2 - \Delta^2\big)\big(\bar{\mathcal{T}}_f^2 - j_1^2\big)\cdots\big(\bar{\mathcal{T}}_f^2 - j_L^2\big) = 0. \tag{A.32}$$

This shows that the power $\bar{\mathcal{T}}_f^{2L+3} = \bar{\mathcal{T}}_f^{2\mathfrak{d}+1}$ is expressible in terms of lower power $\bar{\mathcal{T}}_f^n$, $n \leq 2\mathfrak{d}$, as expected. Let us finally note that the coefficients in the relation (A.32) are elementary symmetric polynomials in the variables $(\Delta^2, j_1^2, \ldots, j_L^2)$: by the Newton identities, these coefficients are then also polynomials in the Newton sums $\Delta^{2p} + \sum_{i=1}^{L} j_i^{2p}$ and thus in the values (A.27) of the classical Casimirs. This ensures that the coefficients $\varrho_{f;AB}^{(n,m)}$ in eq. (3.36) are polynomials in the total symbols of the Casimir operators.

Appendix B

Appendices to Chapter 4

B.1 Radial decomposition of the Casimir

The quadratic Casimir $\mathcal{C}as^2 = -\frac{1}{2}M^{AB}M_{AB}$ can be written as

$$M_{-1,0}^2+M_{-1,1}^2+M_{-1,2}^2-M_{01}^2-M_{02}^2-M_{12}^2-M^{-1,a}M_{-1,a}-M^{0a}M_{0a}-M^{1a}M_{1a}-M^{2a}M_{2a}-\frac{1}{2}M^{ab}M_{ab}\,. \tag{B.1}$$

Here, indices a, b take values $3, 4, ..., d$. Using relations

$$M_{-1,a} = \coth t_1 M_{1a} - \frac{1}{\sinh t_1}M'_{1a} \quad M_{0a} = i\left(\coth t_2 M_{2a} - \frac{1}{\sinh t_2}M'_{2a}\right), \tag{B.2}$$

$$M_{01} \mp iM_{-1,2} = -\coth(t_1 \pm t_2)D_\pm + \frac{D'_\pm}{\sinh(t_1 \pm t_2)}, \tag{B.3}$$

$$[M_{1a}, M'_{1a}] = -\sinh t_1 H_1, \quad [M_{2a}, M'_{2a}] = -\sinh t_2 H_2, \quad [D_\pm, D'_\pm] = 2\sinh(t_1 \pm t_2)(H_1 \pm H_2), \tag{B.4}$$

we obtain

$$-M^{-1,a}M_{-1,a} - M^{1a}M_{1a} = \frac{M'_{1a}M'_{1a} - 2\cosh t_1 M'_{1a}M_{1a} + M_{1a}M_{1a}}{\sinh^2 t_1} + (d-2)\coth t_1 H_1,$$

$$-M^{0a}M_{0a} - M^{2a}M_{2a} = \frac{M'_{2a}M'_{2a} - 2\cosh t_2 M'_{2a}M_{2a} + M_{2a}M_{2a}}{\sinh^2 t_2} + (d-2)\coth t_2 H_2,$$

and

$$M_{-1,0}^2 - M_{12}^2 + M_{-1,2}^2 - M_{01}^2 = -\frac{D'^2_+ - 2\cosh(t_1+t_2)D'_+D_+ + D^2_+}{2\sinh^2(t_1+t_2)} - \frac{D'^2_- - 2\cosh(t_1-t_2)D'_-D_- + D^2_-}{2\sinh^2(t_1-t_2)}$$
$$+\coth(t_1+t_2)(H_1+H_2) + \coth(t_1-t_2)(H_1-H_2)\,.$$

Adding these terms gives the radial decomposition used in the main text.

B.2 Construction of a six-point conformal frame

In this section, we construct a conformal frame for the six-point function by appending x_6 to the conformal frame of the (12345) five-point function, namely:

$$x_1 = \rho_1\vec{n}(\theta_1, 0, 0), \quad x_2 = 0, \quad x_3 = \infty, \quad x_4 = \vec{e}_1, \quad x_5 = \vec{e}_1 - \rho_2\vec{n}(\theta_2, \phi_1, 0), \tag{B.5}$$

where we parametrize unit vectors in S^4 as

$$\vec{n}(\theta,\phi,\varphi) := \cos\theta\,\vec{e}_1 + \sin\theta\big\{\cos\phi\,\vec{e}_2 + \sin\phi\,(\cos\varphi\,\vec{e}_3 + \sin\varphi\,\vec{e}_4)\big\} = e^{\varphi M_{34}}e^{\phi M_{23}}e^{\theta M_{12}}\vec{e}_1. \tag{B.6}$$

It will also be useful to define the rotation matrices

$$R(\theta,\phi,\varphi) := e^{-\theta M_{12}} e^{-\phi M_{23}} e^{-\varphi M_{31}} \Longrightarrow \vec{n}(\theta,\phi,\varphi) = R(\theta,\phi,\varphi)^{-1}\vec{e}_1. \tag{B.7}$$

Finally, we parametrize cross ratios as in (4.34),

$$z_r := \rho_r e^{\mathrm{i}\theta_r}, \quad \bar{z}_r := \rho_r e^{-\mathrm{i}\theta_r}, \quad w_s := \sin^2\frac{\phi_s}{2}, \quad \Upsilon := \pm\mathrm{i}\frac{\cos\varphi}{\sin\theta_2}. \tag{B.8}$$

To understand how x_6 depends on the cross ratios, we compute a distinguished vector in this frame:

$$\psi_{56} := (x_{45}^{-1} - x_{46}^{-1})^{-1} \in \mathbb{R}^4_{1234}, \tag{B.9}$$

where $x^{-1} := x/x^2$ denotes the image of the vector x under conformal inversion. Note that we implicitly used the residual $\mathrm{SO}(d-4)$ symmetry preserving (B.5) to fix a gauge where $x_6 \in \mathrm{Span}(\vec{e}_1,\vec{e}_2,\vec{e}_3,\vec{e}_4)$. In Euclidean signature, we can parametrize the latter by its norm and its unit vector on the S^4, which we write as

$$\psi_{56} = |\psi_{56}|\,\hat{\psi}_{56}, \quad |\psi_{56}| = \rho_2\rho_3^{-1}, \tag{B.10}$$

Then the unit vector $\hat{\psi}_{56}$ is determined by three equations:

$$\hat{\psi}_{56}\cdot\hat{x}_{45} = \frac{1+u_2-v_2}{2\rho_2}, \quad \hat{\psi}_{56}\cdot x_4 = \frac{\mathcal{U}_2^{(5)}}{2\rho_2\rho_3}, \quad \hat{\psi}_{56}\cdot\hat{x}_1 = \frac{\mathcal{U}_1^{(6)}}{2\rho_1\rho_2\rho_3}, \tag{B.11}$$

where the $\mathcal{U}_r^{(m)}$ are polynomials in the polynomial cross ratios:

$$\mathcal{U}_r^{(5)} := 1 - v_r - v_{r+1} + U_r^{(5)}, \quad \mathcal{U}_1^{(6)} := (1-v_1)(1-v_3) - v_2 + U_1^{(5)} + U_2^{(5)} - U_1^{(6)}. \tag{B.12}$$

Using the change of variables (4.30) and (4.31), we can express the scalar products of (B.11) in terms of the angle cross ratios $(\theta_s,\phi_r,\varphi)$:

$$\frac{\mathcal{U}_1^{(5)}}{2\rho_2\rho_3} = \cos\theta_2\cos\theta_3 + \sin\theta_2\sin\theta_3\cos\phi_2 \tag{B.13}$$

$$\begin{aligned}\frac{\mathcal{U}_1^{(6)}}{2\rho_1\rho_2\rho_3} &= \cos\theta_1\cos\theta_2\cos\theta_3 + \cos\theta_1\sin\theta_2\cos\phi_2\sin\theta_3 + \sin\theta_1\sin\theta_2\cos\phi_1\cos\theta_3 \\ &\quad - \sin\theta_1\left(\cos\theta_2\cos\phi_1\cos\phi_2 + \sin\phi_1\sin\phi_2\cos\varphi\right)\sin\theta_3.\end{aligned} \tag{B.14}$$

Given that $x_4 = \vec{e}_1$, $\hat{x}_1 \in \mathrm{Span}(\vec{e}_1,\vec{e}_2)$, $\hat{x}_{45} \in \mathrm{Span}(\vec{e}_1,\vec{e}_2,\vec{e}_3)$, we can recursively compute the components of $\hat{\psi}_{56}$ as

$$\begin{aligned}&\hat{\psi}_{56}\cdot x_4 = \hat{\psi}_{56}\cdot\vec{e}_1 \Longrightarrow \hat{\psi}^1_{56},\\ &\hat{\psi}_{56}\cdot\hat{x}_1 = \hat{\psi}_{56}\cdot\vec{n}(\theta_1,0,0) \Longrightarrow \hat{\psi}^2_{56},\\ &\hat{\psi}_{56}\cdot\hat{x}_{45} = \hat{\psi}_{56}\cdot\vec{n}(\theta_2,\phi_1,0) \Longrightarrow \pm\hat{\psi}^3_{56},\\ &(\hat{\psi}^1_{56})^2 + (\hat{\psi}^2_{56})^2 + (\hat{\psi}^3_{56})^2 + (\hat{\psi}^4_{56})^2 = 1 \Longrightarrow \pm\hat{\psi}^4_{56}.\end{aligned}$$

There is a sign indeterminacy in the third step coming from the convention for $\Upsilon \propto \pm\cos\varphi$, and there is also a sign indeterminacy in the last step coming from the two solutions to the quadratic equation. We compute the solution to each of these equations and find

$$\hat{\psi}_{56} = R(\theta_2,\phi_1,0)^{-1}\vec{n}(-\theta_3,\pm\phi_2,\pm\varphi) \overset{\text{choice}}{=} R(\theta_2,\phi_1,0)^{-1}\vec{n}(-\theta_3,\phi_2,\varphi). \tag{B.15}$$

Now, we can obtain x_6 in the conformal frame by a conformal transformation of ψ_{56},

$$\psi_{56} = (x_{64}^{-1} - x_{54}^{-1})^{-1} = e^{-x_{45}^{-1}\cdot K} e^{x_4\cdot P}\cdot x_6 = e^{-\rho_2^{-1}\vec{n}(\theta_2,\phi_1,0)\cdot K} e^{P_1} x_6. \tag{B.16}$$

After simplifying and inverting the conformal transformation in (B.16), we then obtain

$$x_6 = e^{-P_1}\rho_2^{-D}R(\theta_2,\phi_1,0)^{-1}\mathcal{I}\,e^{P_1}\cdot\rho_3 n(-\theta_3,\phi_2,\varphi), \tag{B.17}$$

where $\mathcal{I} : x \mapsto x^{-1}$ is conformal inversion. To better understand the meaning of these conformal transformations, let's take a closer look at the conformal group element

$$g \equiv g(\rho_2,\theta_2,\phi_1) = e^{-P_1}\rho_2^{-D}R(\theta_2,\phi_1,0)^{-1}\mathcal{I}\,e^{P_1}. \tag{B.18}$$

Its inverse acts as

$$g^{-1} : x \mapsto \rho_2^{-1}R(\theta_2,\phi_1)(x-\vec{e}_1)^{-1} + \vec{e}_1, \tag{B.19}$$

such that when g^{-1} acts on the points of the original conformal frame, the images are given by

$$g^{-1}(x_6) = \rho_3\vec{n}(-\theta_3,\phi_2,\varphi), \quad g^{-1}(x_5) = 0, \quad g^{-1}(x_4) = \infty, \quad g^{-1}(x_3) = \vec{e}_1. \tag{B.20}$$

This suggests a general method to characterize the comb-channel conformal frame of $N > 6$ points in $d = 4$, which depends on the cross ratios $(\rho_r,\theta_r)_{r=1}^{N-3}$, $(\phi_s)_{s=1}^{N-4}$ and $(\varphi_r)_{r=2}^{N-4}$ defined in (4.40). First, define the conformal transformation

$$h^{-1}(\rho_2,\theta_2,\phi_1,0,\varphi_2) := e^{-\varphi_2 M_{34}}\sigma_1\,e^{P_1}g^{-1}(\rho_2,\theta_2,\phi_1) = \rho_2^{-D}\mathcal{I}\sigma_1 e^{-\varphi_2 M_{zt}}R(\theta_2,\phi_1)e^{P_1}, \tag{B.21}$$

where $\sigma_1 : (x^1,x^2,x^3,x^4) \mapsto (-x^1,x^2,x^3,x^4)$ is a reflection along the hyperplane orthogonal to $\vec{e}_1$. Its action on a point is given by

$$h^{-1}(x) = \rho_2\sigma_1 e^{-\varphi_2 M_{34}}R(\theta_2,\phi_1)(x-\vec{e}_1)^{-1}. \tag{B.22}$$

From the previous discussion, we determined that this conformal transformation acts on the six-point conformal frame as follows:

$$h^{-1}(x_2) = \rho_2\vec{n}(\theta_2,0,0), \quad h^{-1}(x_3) = 0, \quad h^{-1}(x_4) = \infty, \quad h^{-1}(x_5) = \vec{e}_1, \quad h^{-1}(x_6) = \vec{e}_1 - \rho_3\vec{n}(\theta_3,\phi_2,0). \tag{B.23}$$

Thus, h^{-1} shifts the framing from the constraints (B.5) on x_i, to the same constraints on x_{i+1}, $i = 1,\dots,5$. We can similarly express the seventh point as

$$h^{-1}(x_7) = h'\left(\vec{e}_1 - \rho_4\vec{n}(\theta_4,\phi_3,0)\right), \tag{B.24}$$

where $h' \equiv h(\rho_3,\theta_3,\phi_2,\varphi_2,\varphi_3)$ is now uniquely defined by

$$h'^{-1}(0) = \rho_3\vec{n}(\theta_3,0,0), \quad h'^{-1}(\infty) = 0, \quad h'^{-1}(e_x) = \infty,$$
$$h'^{-1}(h^{-1}(x_6)) = \vec{e}_1, \quad h'^{-1}(h^{-1}(x_7)) = \vec{e}_1 - \rho_4\vec{n}(\theta_4,\phi_3,0).$$

A quick comparison with the action of h^{-1} on $x_2,\dots,x_6$ implies that

$$h'^{-1} := \rho_3^{-D}\mathcal{I}\sigma_1 e^{-\varphi_3 M_{34}}R(\theta_3,\phi_2,\varphi_2)^{-1}e^{P_1}. \tag{B.25}$$

We can then iterate this procedure until reaching x_N. More specifically, the frame will be given by

$$
\begin{aligned}
x_1 &= \rho_1 \vec{n}(\theta_1, 0, 0), \\
x_2 &= 0, \\
x_3 &= \infty, \\
x_4 &= \vec{e}_1, \\
x_5 &= \vec{e}_1 - \rho_2 \vec{n}(\theta_2, \phi_1, 0), \\
x_6 &= h(\rho_2, \theta_2, \phi_1, \varphi_1, 0)(\vec{e}_1 - \rho_3 \vec{n}(\theta_3, \phi_2, 0)) \\
x_7 &= h(\rho_2, \theta_2, \phi_1, \varphi_1, 0) \circ h(\rho_3, \theta_3, \phi_2, \varphi_1, \varphi_2)(\vec{e}_1 - \rho_4 \vec{n}(\theta_4, \phi_3, 0)), \\
&\cdots\cdots\cdots \\
x_N &= h(\rho_2, \theta_2, \phi_1, \varphi_1, 0) \circ \prod_{r=3}^{N-4} h(\rho_r, \theta_r, \phi_{r-1}, \varphi_{r-1}, \varphi_r)\left(\vec{e}_1 - \rho_N \vec{n}(\theta_N, \phi_{N-1}, \varphi_{N-2}, 0)\right),
\end{aligned}
$$

where

$$
h^{-1}(\rho_r, \theta_r, \phi_{r-1}, \varphi_{r-1}, \varphi_r) := \rho_r^{-D} \mathcal{I} \sigma_1 e^{-\varphi_r M_{34}} R(\theta_r, \phi_{r-1}, \varphi_{r-1})^{-1} e^{P_1}. \tag{B.26}
$$

The action of this conformal group element on points is then given by

$$
h^{-1}(\rho_r, \theta_r, \phi_{r-1}, \varphi_{r-1}, \varphi_r) : x \mapsto \rho_r \sigma_1 e^{-\varphi_r M_{34}} R(\theta_r, \phi_{r-1}, \varphi_{r-1})^{-1} (x - \vec{e}_1)^{-1}. \tag{B.27}
$$

B.3 Middle leg OPE limit in embedding space

In the six-point function, the limit $\bar{z}_2 \to 0$ at the middle leg b can be lifted to embedding space as

$$
X_{45}, X_{46}, X_{56} \to 0, \quad \frac{X_{45}}{X_{46}}, \frac{X_{56}}{X_{46}} = \text{finite}. \tag{B.28}
$$

In other words, all distances between the three points x_4, x_5 and x_6 vanish at the same rate in spacetime. By first quantising around x_6 and then mapping to the cylinder, a triplet satisfying (B.28) is mapped to past timelike infinity. The infinite distance between (x_4, x_5, x_6) and (x_1, x_2, x_3) in this limit factorizes the six-point function into a product of two four-point functions in a manner reminiscent of the cluster decomposition principle.

To compute this limit in embedding space, it will be useful to define the vector

$$
Y_5 := (X_4 - X_5) - \frac{X_{45}}{X_{46}}(X_4 - X_6). \tag{B.29}
$$

In particular, $X_4 \wedge Y_5$ is a homogeneous tensor in both X_4 and X_5. For a spacetime interpretation of these vectors, we can use the mapping $X, Z \mapsto x, z$ provided by the Poincaré patches (4.55) and (4.56), from which we obtain

$$
Y_5 = \frac{x_{56}^2}{x_{46}^2} Z_{x_4, \psi_{56}}, \quad \psi_{56} := (x_{45}^{-1} - x_{46}^{-1})^{-1}. \tag{B.30}
$$

Note also that $Y_5^2 = -2\frac{X_{45}X_{56}}{X_{46}} \to 0$ in the limit (B.28). We now define the full b OPE limit $z_2, \Upsilon \to 0$ in embedding space as

$$
X_5 = X_4 + \epsilon Z_4, \quad Y_5 = \epsilon\, \epsilon' W_4, \quad \epsilon, \epsilon' \to 0. \tag{B.31}
$$

where Z_4 and W_4 are MST_2 polarisation vectors for X_4. To make the connection with the prescription of section 4.3.2 more explicit, we can rewrite the second equation in (B.31) as

$$
\epsilon' W_4 = Z_4' - Z_4, \quad \epsilon Z_4' := \frac{X_{45}}{X_{46}}(X_6 - X_4). \tag{B.32}
$$

We thereby obtain the same prescription as eq. (4.61) up to projective equivalence, with a rescaling of Z_4' outside of the conventional Poincaré patch to simplify computations. Note that the permutation $(4,5,6) \leftrightarrow (3,2,1)$ leads to an identical parametrization of the b OPE limit. Thus, to make expressions more symmetric, we also define

$$Y_2 := Y_5|_{(4,5,6)\leftrightarrow(3,2,1)}. \tag{B.33}$$

Now, to understand how Υ encodes MST_2 transfer along the internal leg b, we would like to compute the b OPE limit of

$$\frac{X_{34}(X_3 \wedge X_2 \wedge Y_2)\cdot(X_4 \wedge X_5 \wedge Y_5)}{X_{24}^2 X_{35}^2} = \mathcal{U}_1^{(5)}\mathcal{U}_2^{(5)} - (1-v_2)\mathcal{U}_1^{(6)}, \tag{B.34}$$

where $\mathcal{U}_r^{(m)}$ are the same functions of the polynomial cross-ratios defined in (B.12). To relate them to the left hand side of (B.34), we expressed them in embedding space as follows:

$$\mathcal{U}_1^{(5)} = \frac{(X_3 \wedge Y_2)\cdot(X_4 \wedge X_5)}{X_{24}X_{35}}, \quad \mathcal{U}_2^{(5)} = \frac{(X_3 \wedge X_2)\cdot(X_4 \wedge Y_5)}{X_{24}X_{35}}, \quad \mathcal{U}_1^{(6)} = \frac{(X_3 \wedge Y_2)\cdot(X_4 \wedge Y_5)}{X_{24}X_{35}}. \tag{B.35}$$

On the left hand side of (B.34), the OPE limit (B.31) is simple to compute:

$$\mathrm{LHS} = \epsilon^2\epsilon' \frac{X_{23}U_{4,123}}{X_{13}X_{24}^2X_{34}} + \mathcal{O}(\epsilon^3\epsilon'), \quad U_{4,123} := (X_4 \wedge Z_4 \wedge W_4)_{ABC}X_1^A X_2^B X_3^C.$$

Note that $U_{4,123}$ is the unique independent MST_2 tensor structure of the four-point function of three scalars and one MST_2 field. On the other hand, the right hand side of (B.34) can be written in cross ratio space using

$$\mathcal{U}_1^{(5)} = z_1'z_2 + \bar{z}_1'\bar{z}_2, \tag{B.36}$$

$$\mathcal{U}_2^{(5)} = z_2z_3' + \bar{z}_2\bar{z}_3', \tag{B.37}$$

$$\mathcal{U}_1^{(6)} = z_1'z_2z_3' + \bar{z}_1'\bar{z}_2\bar{z}_3' - \left[(z_1-\bar{z}_1)\sqrt{w_1(1-w_1)}\right](z_2-\bar{z}_2)\Upsilon\left[(z_3-\bar{z}_3)\sqrt{w_2(1-w_2)}\right], \tag{B.38}$$

where we defined

$$z_1' := w_1z_1 + (1-w_1)\bar{z}_1, \quad \bar{z}_1' := w_1\bar{z}_1 + (1-w_1)z_1, \tag{B.39}$$

$$z_3' := w_2z_3 + (1-w_2)\bar{z}_3, \quad \bar{z}_3' := w_2\bar{z}_3 + (1-w_2)z_3. \tag{B.40}$$

Taking $\bar{z}_2 = 0$, we then find

$$\mathcal{U}_1^{(5)}\mathcal{U}_2^{(5)} - (1-v_2)\mathcal{U}_1^{(6)} = \frac{1}{4}\left[(z_1-\bar{z}_1)\sqrt{w_1(1-w_1)}\right]z_2^2\Upsilon\left[(z_3-\bar{z}_3)\sqrt{w_2(1-w_2)}\right]. \tag{B.41}$$

At the same time, using

$$1-v_2 = z_2 = \epsilon\frac{J_{4,23}}{X_{24}X_{34}} + \mathcal{O}(\epsilon^2), \quad J_{4,23} := (X_4 \wedge Z_4)_{BC}X_2^B X_3^C, \tag{B.42}$$

we find that $\Upsilon = \mathcal{O}(\epsilon')$ in the b OPE limit (B.31) with leading behaviour

$$\Upsilon = \epsilon' \frac{U_{4,123}X_{23}X_{34}}{X_{13}J_{4,23}^2}\left[\frac{z_1-\bar{z}_1}{2}\frac{z_3-\bar{z}_3}{2}\sqrt{w_1(1-w_1)}\sqrt{w_2(1-w_2)}\right]^{-1} + \mathcal{O}(\epsilon\epsilon'). \tag{B.43}$$

In particular, if we define

$$\deg X_4^{-\Delta}Z_4^l W_4^\ell := [\Delta, l, \ell] \Longrightarrow \deg J_{4,23} = [-1,1,0], \quad \deg U_{4,123} = [-1,1,1], \tag{B.44}$$

then we find from (B.42) and (B.43) that

$$\deg z_2 = [1,1,0], \quad \deg \bar{z}_2 = [1,-1,0],, \quad \deg \Upsilon = [0,-1,1]. \tag{B.45}$$

This fits directly with the asymptotic behaviour (4.70) of conformal blocks in the b OPE limit.

B.4 OPE limit factorization of six-point blocks in $d = 1$ CFT

Let us consider the case of six-point conformal blocks in the comb channel for the $d = 1$ case. The conformal blocks for this case have been computed in [36]. To match the convention of that paper, we will introduce the three cross ratios

$$\chi_1 = \frac{x_{12}x_{34}}{x_{13}x_{24}}\,, \qquad \chi_2 = \frac{x_{23}x_{45}}{x_{24}x_{35}}\,, \qquad \chi_3 = \frac{x_{34}x_{56}}{x_{35}x_{46}}\,, \tag{B.46}$$

which make a complete set of independent cross ratios in $d = 1$, and we rename conformal dimensions as

$$\Delta_i = h_i\,, \qquad \Delta_a = \mathbb{h}_1\,, \qquad \Delta_b = \mathbb{h}_2\,, \qquad \Delta_c = \mathbb{h}_3\,. \tag{B.47}$$

Note that when reducing to $d = 1$, the Gram determinant relations impose $z_i = \bar{z}_i$, and that

$$\chi_i = z_i = \bar{z}_i\,. \tag{B.48}$$

The one-dimensional six-point conformal blocks can then be written as in [36, equation 2.11]

$$g^{h_1,\ldots,h_6}_{\mathbb{h}_1,\mathbb{h}_2,\mathbb{h}_3} = \chi_1^{\mathbb{h}_1}\chi_2^{\mathbb{h}_2}\chi_3^{\mathbb{h}_3} F_K\left[\begin{matrix} h_{12}+\mathbb{h}_1,\ \mathbb{h}_1+\mathbb{h}_2-h_3,\ \mathbb{h}_2+\mathbb{h}_3-h_4,\ \mathbb{h}_3+h_{65} \\ 2\mathbb{h}_1,\ 2\mathbb{h}_2,\ 2\mathbb{h}_3 \end{matrix};\chi_1,\chi_2,\chi_3\right], \tag{B.49}$$

where the comb function F_K can be expressed as

$$F_K\left[\begin{matrix} a_1,\ b_1,\ b_2,\ a_2 \\ c_1,\ c_2,\ c_3 \end{matrix};\chi_1,\chi_2,\chi_3\right] = \sum_{n=0}^{\infty}\frac{(b_1)_n(b_2)_n}{(c_2)_n}\frac{\chi_2^n}{n!}\,{}_2F_1\left[\begin{matrix} b_1+n,\ a_1 \\ c_1 \end{matrix};\chi_1\right]{}_2F_1\left[\begin{matrix} b_2+n,\ a_2 \\ c_3 \end{matrix};\chi_3\right]. \tag{B.50}$$

It is immediate to see that taking the leading behaviour on the cross ratio χ_2, which is the one-dimensional analogue of $\bar{z}_2$, corresponds to simply setting $n = 0$ in eq. (B.50), leading to the factorized expression

$$g^{h_1,\ldots,h_6}_{\mathbb{h}_1,\mathbb{h}_2,\mathbb{h}_3} \overset{\chi_2\to 0}{\sim} \chi_2^{\mathbb{h}_2}\left(\chi_1^{\mathbb{h}_1}\,{}_2F_1\left[\begin{matrix} \mathbb{h}_1+\mathbb{h}_2-h_3,\ h_{12}+\mathbb{h}_1 \\ 2\mathbb{h}_1 \end{matrix};\chi_1\right]\right)\left(\chi_3^{\mathbb{h}_3}\,{}_2F_1\left[\begin{matrix} \mathbb{h}_2+\mathbb{h}_3-h_4,\ \mathbb{h}_3+h_{65} \\ 2\mathbb{h}_3 \end{matrix};\chi_3\right]\right). \tag{B.51}$$

Expression (B.51) is an explicit factorization of six-point conformal blocks into the product of two four-point blocks, providing an explicit example of equation (4.70) for the one-dimensional case.

Appendix C

Appendices to Chapter 5

C.1 Map from $\mathfrak{so}_{\mathbb{C}}(6)$ embedding space to $\mathfrak{sl}_{\mathbb{C}}(4)$ twistors

We use indices $A, B, C = 0, \ldots, 5$ to label an orthonormal basis in the fundamental representation of $\mathfrak{so}_{\mathbb{C}}(6)$, and $a, b, c = 1, 2, 3, 4$ to label a basis in the fundamental representation of $\mathfrak{sl}_{\mathbb{C}}(4)$. We saw that irreducible representations of $\mathfrak{so}_{\mathbb{C}}(6)$ are sections of a line bundle over the space of isotropic flags in $\mathbb{C}^6$

$$\mathrm{Span}(X) \subset \mathrm{Span}(X, Z) \subset \mathrm{Span}(X, Z, W) = \mathrm{Span}(X, Z, W)^{\perp} \subset \mathrm{Span}(X, Z)^{\perp} \subset \mathrm{Span}(X)^{\perp} \subset \mathbb{C}^6, \quad \text{(C.1)}$$

where $\mathbb{V}^{\perp}$ is the orthogonal complement of the vector subspace $\mathbb{V} \subset \mathbb{C}^6$ with respect to the 6-dimensional metric (η_{AB}). These sections are equivalent to certain functions $F(X, Z, W)$ of three vectors in $\mathbb{C}^6$ that are null and mutually orthogonal with respect to the Minkowski metric,

$$X^2 = Z^2 = W^2 = X \cdot Z = X \cdot W = Z \cdot W = 0\,. \quad \text{(C.2)}$$

Said functions must be homogeneous of fixed multi-degree, and invariant under the gauge transformations that preserve the isotropic flag,

$$F(X, Z + \beta_{10} X, W + \beta_{20} X + \beta_{21} Z) = F(X, Z, W)\,. \quad \text{(C.3)}$$

Depending on the choice of real form of $\mathfrak{so}_{\mathbb{C}}(6)$ (or equivalently the signature of (η_{AB})), as well as the choice of representation, one must either apply reality conditions on some of the X, Z, W or impose that F is holomorphic in some of the X, Z, W variables. For the reflection positive and integer spin representations of CFT_4, X is real and F is holomorphic in $Z, W \in \mathbb{C}^6$. In this case, the space of vectors $(X, Z, W) \in \mathbb{R}^6 \times (\mathbb{C}^6)^2$ satisfying (C.2) is informally known as embedding space. The gauge constraints can be explicitly solved by a change of variables

$$C^{(0)}_A := X_A, \qquad C^{(1)}_{AB} := (X \wedge Z)_{AB}, \qquad C^{(2)}_{ABC} := (X \wedge Z \wedge W)_{ABC}, \quad \text{(C.4)}$$

such that $F(X, Z, W) = F'(C^{(0)}, C^{(1)}, C^{(2)})$ for some function F'.
Similarly, irreducible representations of $\mathfrak{sl}_{\mathbb{C}}(4)$ are sections of a line bundle over the space of flags in $\mathbb{C}^4$,

$$\mathrm{Span}(Y_1) \subset \mathrm{Span}(Y_1, Y_2) \subset \mathrm{Span}(Y_1, Y_2, Y_3) \subset \mathbb{C}^4\,. \quad \text{(C.5)}$$

This is equivalent to functions $\Psi(Y_1, Y_2, Y_3)$ of three (arbitrary) vectors in $\mathbb{C}^4$. Said functions must also be homogeneous of fixed multi-degree, and invariant under the gauge transformations that preserve the flag,

$$\Psi(Y_1, Y_2 + c_{21} Y_1, W + c_{31} Y_1 + c_{32} Y_2) = \Psi(Y_1, Y_2, Y_3)\,. \quad \text{(C.6)}$$

Once again, the gauge constraints can be explicitly solved by the change of variables to gauge-invariant tensors

$$S_a := Y_{1a}, \qquad X_{ab} := (Y_1 \wedge Y_2)_{ab}, \qquad \bar{S}_{abc} := (Y_1 \wedge Y_2 \wedge Y_3)_{abc}\,, \quad \text{(C.7)}$$

such that $\Psi(Y_1, Y_2, Y_3) = \Psi'(S, X, \bar{S})$ for some function Ψ'. The gauge invariant, anti-symmetric, and $\mathfrak{su}(2,2)$-covariant tensors $(S, X, \bar{S})$ are known as *twistor* variables in the physics literature. Similarly to the previous case, reality conditions on Y_1, Y_2, Y_3 or holomorphicity conditions on Ψ are required to realize irreducible representations of real forms of $\mathfrak{sl}_{\mathbb{C}}(4)$. In particular, the reflection positive and half-integer spin representations of CFT_4 are realized by imposing that X_{ab} is real and Ψ' is a holomorphic function of S and $\bar{S}$. This follows from the fact that $\text{SU}(2,2)$ is the double cover of the Lorentzian conformal group $\text{SO}(2,4)$.

More generally, as $\mathfrak{so}_{\mathbb{C}}(6) \cong \mathfrak{sl}_{\mathbb{C}}(4)$, representations of the latter can be mapped to representations of the former. As a result, there exists a map from homogeneous, gauge-invariant functions on $\mathfrak{so}_{\mathbb{C}}(6)$ embedding space to homogeneous functions of the twistor variables (C.7). This translates into a map from the gauge-invariant tensors (C.4) in $\mathbb{C}^6$ to the gauge-invariant tensors (C.7) in $\mathbb{C}^4$. To determine explicit expressions, we make use of the chiral Γ-matrices Γ^A_{ab} defined for example in [21, Appendix B]. If $M^A{}_B \in \mathfrak{so}_{\mathbb{C}}(6)$, then there exists $L_a{}^b \in \mathfrak{sl}_{\mathbb{C}}(4)$ such that

$$M^A{}_B \Gamma^B_{ab} = L_a{}^c \Gamma^A_{cb} + L_b{}^d \Gamma^A_{ad} \,. \tag{C.8}$$

These Γ-matrices are anti-symmetric, such that we can define their duals with respect to the 4-dimensional ϵ-tensor,

$$\bar{\Gamma}^{Aab} := \frac{1}{2}\epsilon^{abcd}\Gamma^A_{ab} \,. \tag{C.9}$$

The fundamental identities of the Γ-matrices can also be found in [21, Appendix B]. The Clifford relations are

$$\bar{\Gamma}^{Aab}\Gamma^B_{bc} + \bar{\Gamma}^{Bab}\Gamma^A_{bc} = -2\eta^{AB}\delta^a_c \,, \tag{C.10}$$

while the contraction identity is

$$\eta_{AB}\Gamma^A_{ab}\Gamma^B_{cd} = 2\epsilon_{abcd} \,. \tag{C.11}$$

The map from gauge-invariant tensors in $\mathfrak{so}(1,5)$ embedding space to twistor variables is then given by

$$C^{(0)}_A = X_A = \frac{1}{4}X_{ab}\bar{\Gamma}^{ab}_A \,, \tag{C.12}$$

$$C^{(1)}_{AB} = (X \wedge Z)_{AB} = \frac{1}{\sqrt{2}}\bar{S}^a\Gamma_{Aab}\bar{\Gamma}^{bc}_B S_c \,, \tag{C.13}$$

$$C^{(2)}_{ABC} = (X \wedge Z \wedge W)_{ABC} = \frac{1}{2\sqrt{2}}S_a\bar{\Gamma}^{ab}_A\Gamma_{Bbc}\bar{\Gamma}^{cd}_B S_d \,, \tag{C.14}$$

$$\bar{C}^{(2)}_{ABC} = (X \wedge Z \wedge \bar{W})_{ABC} = \frac{1}{2\sqrt{2}}\bar{S}^a\Gamma_{Aab}\bar{\Gamma}^{bc}_B\Gamma_{Ccd}\bar{S}^d \,. \tag{C.15}$$

Here, we defined the dual tensors

$$\bar{S}^a := \frac{1}{3!}\epsilon^{abcd}\bar{S}_{bcd}, \qquad \bar{X}^{ab} := \frac{1}{2}\epsilon^{abcd}X_{cd}. \tag{C.16}$$

We can now summarize our nomenclature for various spinning representations of maximal spin depth in $d = 4$:

- we call a self-dual (respectively anti-self-dual) representation any function on embedding space that is a homogeneous polynomial of order $\ell \in \mathbb{Z}_+$ in W (respectively a polynomial of order $-\ell \in \mathbb{Z}_+$ in $\overline{W}$). In twistor space, we see that these representations correspond to homogeneous polynomials of order $J \in 2\mathbb{Z}_+$ in S and $\bar{J} \in 2\mathbb{Z}_+$ with $J > \bar{J}$ (respectively $J < \bar{J}$).

- We call a chiral (respectively anti-chiral) representation any function on twistor space that is a polynomial of order $J \in \mathbb{Z}_+$ in S (respectively $\bar{J} \in \mathbb{Z}_+$ in $\bar{S}$) with $\bar{J} = 0$ (respectively $J = 0$). In cases where J (respectively $\bar{J}$) is an even integer, these coincide with the self-dual (respectively anti-self-dual) parts of $\mathfrak{so}(4)$ representations with rectangular Young tableaux of height $h_1 = \cdots = h_l = 2$ and length $l = \ell = J/2$ (respectively $l = -\ell = \bar{J}/2$).

With this map, it is easy to directly relate the MST_2-MST_2-scalar tensor structures in $\mathfrak{so}(1,5)$ embedding space with those of twistor space:

$$X_i \cdot X_j = \frac{1}{4}\bar{X}_i^{ab} X_{jab} = -\frac{1}{4}\mathrm{tr}\,\bar{X}_i X_j, \tag{C.17}$$

$$X_{jk} V_{i,jk} = \bar{S}_i X_j \bar{X}_k S_i \tag{C.18}$$

$$(k_{\bar{i}j})^2 = (\bar{S}_i S_j)^2 \tag{C.19}$$

$$\mho^2_{ij,k} = (S_i \bar{X}_k S_j)^2 \tag{C.20}$$

$$\bar{\mho}^2_{ij,k} = (\bar{S}_i X_k \bar{S}_j)^2. \tag{C.21}$$

It is important to note that the squared tensor structures on the left hand side of (C.19), (C.20), (C.21) are also perfect squares of $\mathfrak{so}_{\mathbb{C}}(6)$ embedding space variables. This means that we can compute 3-point functions of any half-integer spin fields in our formalism.

C.2 The d-deformation of the MST_2-MST_2-scalar vertex operator

C.2.1 Comparison with one-dimensional vertex systems

For all combinations of $(d;\Delta_i;l_i;\ell_i)$ that yield one-dimensional vertex systems, the Hamiltonian can be written as

$$H^{(d;\Delta_i;l_i;\ell_i)} = \tilde{H}^{(\gamma_i;\nu_i;\alpha;\beta)} + \Delta\tilde{E}^{(\gamma_i;\nu_i;\alpha;\beta;d)}\,, \tag{C.22}$$

where $(\Delta_i;l_i;\ell_i) \leftrightarrow (\gamma_i;\nu_i;\alpha;\beta)$ is the d-dependent bijection of seven parameters defined in subsection 5.5.3, and $\Delta\tilde{E}^{(\gamma_i;\nu_i;\alpha;\beta;d)}$ is a constant energy shift determined by

$$\Delta\tilde{E} - E_{\mathrm{EFMV}} = L_{\mathrm{EFMV}} - \tilde{H}, \tag{C.23}$$

with $E^{(\Delta_i;l_i;\ell_i;d)}_{\mathrm{EFMV}}$ given in C.2.2. Even for the two-dimensional vertex systems $d > 4, \ell_1, \ell_2 \neq 0$, we can obtain a d-dependent, MST_2-MST_2-scalar Hamiltonian for a one-dimensional system by restricting to the $\mathcal{Y} = 0$ plane:

$$H^{(d>4;\Delta_i;l_i;\ell_1,\ell_2)}(\mathcal{X},\partial_{\mathcal{X}}) := H^{(d>4;\Delta_i;l_i;\ell_1,\ell_2)}(\mathcal{X},\mathcal{Y}=0,\partial_{\mathcal{X}},\partial_{\mathcal{Y}}=0)\,. \tag{C.24}$$

This d-deformation of the MST_2-MST_2-scalar operator is qualitatively different from the $d = 4$ or $\ell_2 = 0$ cases for several reasons:

1) First, while we can still write the whole operator $H^{(d>4;\Delta_i;l_i;\ell_1,\ell_2)}$ in (C.26) as an elliptic CMS Hamiltonian, two of its multiplicities will no longer be linear in the quantum numbers — instead

$$m_{1,0} = \frac{7-d}{2} - (l_1+l_2) - \Delta_3 - 2\sqrt{\left(\ell_1 + \frac{d-4}{2}\right)^2 + 2\ell_2\left(\frac{d-4}{2} - \ell_1\right) + \ell_2^2}\,,$$

$$m_{2,0} = \frac{7-d}{2} - (l_1+l_2) - \Delta_3 + 2\sqrt{\left(\ell_1 + \frac{d-4}{2}\right)^2 + 2\ell_2\left(\frac{d-4}{2} - \ell_1\right) + \ell_2^2}\,,$$

and the remaining multiplicities are

$$k(d;\Delta_i;l_i;\ell_1,\ell_2) = k(d;\Delta_i;l_i;\ell_1,0)\,,$$
$$m_{i,\nu}(d;\Delta_i;l_i;\ell_1,\ell_2) = m_{i,\nu}(d;\Delta_i;l_i;\ell_1+\ell_2,0)\,, \qquad (i,\nu) \in \{3,4\}\times\{0\} \cup \{1,2,3,4\}\times\{1\}\,.$$

2) Second, there is no choice of α such that $H^{(d>4;\Delta_i;l_i;\ell_1,\ell_2)}$ is hermitian with respect to the Gegenbauer scalar product $\langle -,-\rangle_\alpha$, nor any scalar product with a measure of the form $\mathcal{X}^a(1-\mathcal{X})^b$, $\mathcal{X} \in [0,1]$.

3) It goes hand in hand with reason (1) that $H^{(d>4;\Delta_i;l_i;\ell_1,\ell_2\neq 0)}$ will now exhibit an explicit dependence on dimension after the reparametrization $(\Delta_i;l_i;\ell_i)\leftrightarrow(\gamma_i;\nu_i;\alpha;\beta)$, i.e.

$$H^{(d>4;\Delta_i;l_i;\ell_1,\ell_2\neq 0)}=\tilde{H}^{(d>4;\gamma_i;\nu_i;\alpha;\beta)}. \tag{C.25}$$

In fact, the generalization of (C.22) to $H^{(d>4;\Delta_i;l_i;\ell_1,\ell_2\neq 0)}$ is given by

$$H^{(d;\Delta_i;l_i;\ell_i)}=\tilde{H}^{(\gamma_i;\nu_i;\alpha;\beta)}+(d-4)(\alpha-\beta-1)H_{\mathrm{def}}^{(\gamma_i;\nu_i;\alpha;\beta)}(\mathcal{X},\partial_{\mathcal{X}})+\Delta\tilde{E}^{(\gamma_i;\nu_i;\alpha;\beta;d)}\,, \tag{C.26}$$

where

$$\begin{aligned}H_{\mathrm{def}}^{(\gamma_i;\nu_i;\alpha;\beta)}(\mathcal{X},\partial_{\mathcal{X}})=&4\mathcal{X}(1-\mathcal{X})^2\partial_{\mathcal{X}}^2\\&+2(1-\mathcal{X})\left[(\nu_1+\nu_2-1)\mathcal{X}-(\nu_1+\nu_2+1)-2\alpha-2\mathrm{i}\gamma_3\right]\partial_{\mathcal{X}}+4\nu_1\nu_2\mathcal{X}\\&+\frac{1}{4\mathcal{X}}\left(4\left(\gamma_1-\gamma_2\right)^2+\left(2\alpha+2\mathrm{i}\gamma_3+2\nu_1+2\nu_2+3\right)^2\right),\end{aligned}$$

is the $d\neq 4$ deformation, and $\Delta\tilde{E}^{(\gamma_i;\nu_i;\alpha;\beta;d>4)}$ is also a constant obtained from

$$\Delta\tilde{E}-E_{\mathrm{EFMV}}=L_{\mathrm{EFMV}}-\tilde{H}-(d-4)(\alpha-\beta-1)H_{\mathrm{def}}. \tag{C.27}$$

C.2.2 The constant shift for the CMS Operator

In section 5.5 (more specifically Eq. (5.147)), we determined the Hamiltonian of all one-dimensional vertex systems in terms of the CMS operator L_{EFMV} up to a constant shift E_{EFMV}. This was generalized in the previous section to $H^{(d\neq 4;\Delta_i;l_i;\ell_i\neq 0)}(\mathcal{X},\mathcal{Y}=0,\partial_{\mathcal{X}},\partial_{\mathcal{Y}}=0)$ with generalized CMS multiplities that are no longer linear in the dimension and quantum numbers. In all of these cases, the constant shift in the Hamiltonian is given by

$$H^{(d;\Delta_i;l_i;\ell_i)}(\mathcal{X},\partial_{\mathcal{X}})=L_{\mathrm{EFMV}}(\mathcal{X},\partial_{\mathcal{X}})+E_{\mathrm{EFMV}}^{(d;\Delta_i;l_i;\ell_i)}. \tag{C.28}$$

To write out E_{EFMV} explicitly, we make use of the previous change of variables to $(\gamma_i;\nu_i;\alpha,\beta)$ and expand the dimension around $d=4$, $\beta=0$, and $\alpha=0$, i.e.

$$d:=4+2\varepsilon,\quad E_{\mathrm{EFMV}}:=\sum_{m=0}^{4}\varepsilon^m E_{\mathrm{EFMV}}^{(m)},\qquad E_{\mathrm{EFMV}}^{(m)}:=\sum_{n=0}^{3}\beta^n E_{\mathrm{EFMV}}^{(m,n)},\qquad E_{\mathrm{EFMV}}^{(m,n)}:=\sum_{p=0}^{4}\alpha^p E_{\mathrm{EFMV}}^{(m,n,p)}.$$

The simplest coefficients are at the highest order in each of the three expansion parameters,

$$\begin{aligned}&E_{\mathrm{EFMV}}^{(4)}=-128/3,\qquad E_{\mathrm{EFMV}}^{(3)}=\frac{64(\beta-\alpha)-1856}{3},\qquad E_{\mathrm{EFMV}}^{(2,2)}=32,\\&E_{\mathrm{EFMV}}^{(1,3)}=E_{\mathrm{EFMV}}^{(0,0,4)}=-16,\qquad E_{\mathrm{EFMV}}^{(0,3)}=8(1-2\alpha).\end{aligned}$$

The next highest order terms are also relatively simple,

$$\begin{aligned}&E_{\mathrm{EFMV}}^{(2,1)}=\frac{64(\alpha-3\mathrm{i}\gamma_3)+896}{3},\qquad E_{\mathrm{EFMV}}^{(1,2)}=16(2\mathrm{i}\gamma_3+\alpha-2),\qquad E_{\mathrm{EFMV}}^{(1,0,2)}=16(15+6\nu_1-2\nu_2),\\&E_{\mathrm{EFMV}}^{(0,1,2)}=8(1+8\nu_1-8\nu_2),\qquad E_{\mathrm{EFMV}}^{(0,0,3)}=80\nu_2-176\nu_1-16\mathrm{i}\gamma_3-64.\end{aligned}$$

We can then write all terms at $\mathcal{O}(\varepsilon,\beta)$ as

$$\begin{aligned}E_{\mathrm{EFMV}}^{(1,1)}=&56\nu_1(\nu_1-\frac{12}{7}\alpha-1)+8\nu_2(\nu_2+4\alpha+1)+16\nu_1\nu_2+8(4\gamma_1^2-4\gamma_2^2+\gamma_3^2)\\&-16\mathrm{i}\gamma_3(\nu_1+\nu_2-2\alpha)+\frac{688}{3}\alpha-16\alpha^2+\frac{230}{3}.\end{aligned}$$

The remaining terms that fit on one line are

$$\begin{aligned}&E_{\mathrm{EFMV}}^{(0,1,1)}=-16\nu_1(2\nu_1-1)+16\nu_2(2\nu_2+1)+16\mathrm{i}\gamma_3+32(\gamma_1^2-\gamma_2^2+\gamma_3^2)+\frac{1120}{3},\\&E_{\mathrm{EFMV}}^{(0,1,0)}=28\nu_1(\nu_1+1)-4\nu_2(\nu_2+1)-8\nu_1\nu_2+8\mathrm{i}\gamma_3(\nu_1+\nu_2+\frac{3}{2})-4\gamma_3^2+16(\gamma_2^2-\gamma_1^2)-\frac{347}{3}\\&E_{\mathrm{EFMV}}^{(0,0,2)}=60\nu_2(\nu_2+\frac{31}{15})-124\nu_1(\nu_1+1)+88\nu_1\nu_2+4\mathrm{i}\gamma_3(1-2\nu_1-2\nu_2)+60\gamma_3^2-32(\gamma_1^2+\gamma_2^2)+183.\end{aligned}$$

Finally, we have

$$\begin{aligned}
E^{(1,0,1)}_{\mathrm{EFMV}} =& 56\nu_1^2 - 8\nu_2^2 - 16\nu_1\nu_2 - \frac{1208}{3}\nu_2 - \frac{1928}{3}\nu_1 \\
&+ 16\mathrm{i}\gamma_3(\nu_1+\nu_2+\frac{3}{2}) - 8\gamma_3^2 + 32(\gamma_2^2-\gamma_1^2) - \frac{278}{3}, \\
E^{(1,0,0)}_{\mathrm{EFMV}} =& \frac{856}{3}\nu_1(\nu_1+1) - \frac{616}{3}\nu_2(\nu_2+1) + 16\nu_1\nu_2 \\
&+ 16\mathrm{i}\gamma_3(\nu_1+\nu_2-\frac{3}{2}) - \frac{616}{3}\gamma_3^2 + \frac{544}{3}\gamma_2^2 - \frac{928}{3}\gamma_1^2 - \frac{4874}{3}, \\
E^{(0,2)}_{\mathrm{EFMV}} =& 16\alpha\left(-\alpha+\nu_1+\nu_2+\mathrm{i}\gamma_3+2\right) + 12\nu_1(\nu_1+1) + 12\nu_2(\nu_2+1) + 8\nu_1\nu_2 \\
&+ 4\mathrm{i}\gamma_3(2\nu_1+2\nu_2+3) + 59,
\end{aligned}$$

along with

$$\begin{aligned}
E^{(0,0,1)}_{\mathrm{EFMV}} =& 16\nu_2^3 - 240\nu_1^3 + 52\nu_2^2 - 364\nu_1^2 \\
&+ 48\nu_1\nu_2(\nu_1+\nu_2+104) + \frac{2168}{3}\nu_1 - \frac{1352}{3}\nu_2 + 4\mathrm{i}\gamma_3(3+2\nu_1+2\nu_2) \\
&+ 4\gamma_3^2(13+28\nu_1-4\nu_2) + \gamma_1^2(32\nu_1-96\nu_2) - 32\gamma_2^2(1+3\nu_1-\nu_2) + 64\mathrm{i}\gamma_1\gamma_2\gamma_3 + \frac{899}{3},
\end{aligned}$$

and

$$\begin{aligned}
E^{(0,0,0)}_{\mathrm{EFMV}} =& 4\nu_2^4 - 60\nu_1^4 + 8\nu_2^3 - 120\nu_1^3 + 24\nu_1^2\nu_2^2 + \frac{1084}{3}\nu_1^2 - \frac{724}{3}\nu_2(\nu_2+1) + 28\nu_1\nu_2 + \frac{1276}{3}\nu_1 \\
&+ 16\mathrm{i}\gamma_1\gamma_2\gamma_3(1+2\nu_1+2\nu_2) - 2\gamma_3^4 - 64\gamma_1^2(\gamma_1^2-\gamma_2^2) \\
&- \gamma_3^2\left(\frac{751}{3} + 56\gamma_1^2 - 8\gamma_2^2 - 52\nu_1^2 - 56\nu_1 + 8\nu_1 - 8\nu_1\nu_2 + 12\nu_2^2\right) \\
&- \gamma_1^2\left(\frac{1330}{3} + 56\nu_2^2 - 8\nu_1^2 + 40\nu_2 - 24\nu_1 - 16\nu_1\nu_2\right) \\
&+ \gamma_2^2\left(\frac{766}{3} + 8\nu_2^2 - 56\nu_1^2 + 24\nu_2 - 40\nu_1 + 16\nu_1\nu_2\right).
\end{aligned}$$

Bibliography

[1] K. G. Wilson and J. B. Kogut, *"The Renormalization group and the epsilon expansion"*, Phys. Rept. 12, 75 (1974).

[2] P. A. M. Dirac, *"Wave equations in conformal space"*, Annals Math. 37, 429 (1936).

[3] A. Belavin, A. Polyakov and A. Zamolodchikov, *"Infinite conformal symmetry in two-dimensional quantum field theory"*, Nuclear Physics B 241, 333 (1984), https://www.sciencedirect.com/science/article/pii/055032138490052X.

[4] A. M. Polyakov, *"Nonhamiltonian approach to conformal quantum field theory"*, Zh. Eksp. Teor. Fiz. 66, 23 (1974).

[5] R. Rattazzi, V. S. Rychkov, E. Tonni and A. Vichi, *"Bounding scalar operator dimensions in 4D CFT"*, JHEP 0812, 031 (2008), arxiv:0807.0004.

[6] Z. Komargodski and A. Zhiboedov, *"Convexity and Liberation at Large Spin"*, JHEP 1311, 140 (2013), arxiv:1212.4103.

[7] S. El-Showk and M. F. Paulos, *"Bootstrapping Conformal Field Theories with the Extremal Functional Method"*, Phys. Rev. Lett. 111, 241601 (2013), arxiv:1211.2810.

[8] A. L. Fitzpatrick, J. Kaplan, D. Poland and D. Simmons-Duffin, *"The Analytic Bootstrap and AdS Superhorizon Locality"*, JHEP 1312, 004 (2013), arxiv:1212.3616.

[9] F. Kos, D. Poland and D. Simmons-Duffin, *"Bootstrapping Mixed Correlators in the 3D Ising Model"*, JHEP 1411, 109 (2014), arxiv:1406.4858.

[10] L. F. Alday, A. Bissi and T. Lukowski, *"Large spin systematics in CFT"*, JHEP 1511, 101 (2015), arxiv:1502.07707.

[11] D. Simmons-Duffin, *"A Semidefinite Program Solver for the Conformal Bootstrap"*, JHEP 1506, 174 (2015), arxiv:1502.02033.

[12] L. F. Alday, *"Large Spin Perturbation Theory for Conformal Field Theories"*, Phys. Rev. Lett. 119, 111601 (2017), arxiv:1611.01500.

[13] R. Gopakumar, A. Kaviraj, K. Sen and A. Sinha, *"Conformal Bootstrap in Mellin Space"*, Phys. Rev. Lett. 118, 081601 (2017), arxiv:1609.00572.

[14] S. Caron-Huot, *"Analyticity in Spin in Conformal Theories"*, JHEP 1709, 078 (2017), arxiv:1703.00278.

[15] D. Mazac and M. F. Paulos, *"The analytic functional bootstrap. Part I: 1D CFTs and 2D S-matrices"*, JHEP 1902, 162 (2019), arxiv:1803.10233.

[16] M. Reehorst, S. Rychkov, D. Simmons-Duffin, B. Sirois, N. Su and B. van Rees, *"Navigator Function for the Conformal Bootstrap"*, SciPost Phys. 11, 072 (2021), arxiv:2104.09518.

[17] F. Kos, D. Poland, D. Simmons-Duffin and A. Vichi, *"Precision Islands in the Ising and $O(N)$ Models"*, JHEP 1608, 036 (2016), arxiv:1603.04436.

[18] F. A. Dolan and H. Osborn, *"Conformal four point functions and the operator product expansion"*, Nucl. Phys. B 599, 459 (2001), hep-th/0011040.

[19] F. Dolan and H. Osborn, *"Conformal partial waves and the operator product expansion"*, Nucl. Phys. B 678, 491 (2004), hep-th/0309180.

[20] M. S. Costa, J. Penedones, D. Poland and S. Rychkov, *"Spinning Conformal Blocks"*, JHEP 1111, 154 (2011), arxiv:1109.6321.

[21] D. Simmons-Duffin, *"Projectors, Shadows, and Conformal Blocks"*, JHEP 1404, 146 (2014), arxiv:1204.3894.

[22] M. Hogervorst and S. Rychkov, *"Radial Coordinates for Conformal Blocks"*, Phys. Rev. D 87, 106004 (2013), arxiv:1303.1111.

[23] A. Castedo Echeverri, E. Elkhidir, D. Karateev and M. Serone, *"Deconstructing Conformal Blocks in 4D CFT"*, JHEP 1508, 101 (2015), arxiv:1505.03750.

[24] J. a. Penedones, E. Trevisani and M. Yamazaki, *"Recursion Relations for Conformal Blocks"*, JHEP 1609, 070 (2016), arxiv:1509.00428.

[25] L. Iliesiu, F. Kos, D. Poland, S. S. Pufu, D. Simmons-Duffin and R. Yacoby, *"Fermion-Scalar Conformal Blocks"*, JHEP 1604, 074 (2016), arxiv:1511.01497.

[26] A. Castedo Echeverri, E. Elkhidir, D. Karateev and M. Serone, *"Seed Conformal Blocks in 4D CFT"*, JHEP 1602, 183 (2016), arxiv:1601.05325.

[27] M. S. Costa, T. Hansen, J. a. Penedones and E. Trevisani, *"Projectors and seed conformal blocks for traceless mixed-symmetry tensors"*, JHEP 1607, 018 (2016), arxiv:1603.05551.

[28] D. Karateev, P. Kravchuk and D. Simmons-Duffin, *"Weight Shifting Operators and Conformal Blocks"*, JHEP 1802, 081 (2018), arxiv:1706.07813.

[29] M. Isachenkov and V. Schomerus, *"Integrability of conformal blocks. Part I. Calogero-Sutherland scattering theory"*, JHEP 1807, 180 (2018), arxiv:1711.06609.

[30] R. S. Erramilli, L. V. Iliesiu and P. Kravchuk, *"Recursion relation for general 3d blocks"*, JHEP 1912, 116 (2019), arxiv:1907.11247.

[31] J.-F. Fortin, W.-J. Ma, V. Prilepina and W. Skiba, *"Efficient Rules for All Conformal Blocks"*, arxiv:2002.09007.

[32] C. Bercini, V. Gonçalves and P. Vieira, *"Light-Cone Bootstrap of Higher Point Functions and Wilson Loop Duality"*, Phys. Rev. Lett. 126, 121603 (2021), arxiv:2008.10407.

[33] C. Bercini, V. Gonçalves, A. Homrich and P. Vieira, *"The Wilson Loop - Large Spin OPE Dictionary"*, arxiv:2110.04364.

[34] A. Antunes, M. S. Costa, V. Goncalves and J. V. Boas, *"Lightcone Bootstrap at higher points"*, arxiv:2111.05453.

[35] T. Anous, A. Belin, J. de Boer and D. Liska, *"OPE statistics from higher-point crossing"*, arxiv:2112.09143.

[36] V. Rosenhaus, *"Multipoint Conformal Blocks in the Comb Channel"*, JHEP 1902, 142 (2019), arxiv:1810.03244.

[37] V. Gonçalves, R. Pereira and X. Zhou, *"20′ Five-Point Function from $AdS_5 \times S^5$ Supergravity"*, JHEP 1910, 247 (2019), arxiv:1906.05305.

[38] S. Hoback and S. Parikh, *"Dimensional reduction of higher-point conformal blocks"*, JHEP 2103, 187 (2021), arxiv:2009.12904.

[39] J.-F. Fortin, W.-J. Ma and W. Skiba, *"Seven-point conformal blocks in the extended snowflake channel and beyond"*, Phys. Rev. D 102, 125007 (2020), arxiv:2006.13964.

[40] D. Poland and V. Prilepina, *"Recursion relations for 5-point conformal blocks"*, JHEP 2110, 160 (2021), arxiv:2103.12092.

[41] I. Buric, S. Lacroix, J. A. Mann, L. Quintavalle and V. Schomerus, *"From Gaudin Integrable Models to d-dimensional Multipoint Conformal Blocks"*, Phys. Rev. Lett. 126, 021602 (2021), arxiv:2009.11882.

[42] I. Buric, S. Lacroix, J. A. Mann, L. Quintavalle and V. Schomerus, *"Gaudin models and multipoint conformal blocks: general theory"*, JHEP 2110, 139 (2021), arxiv:2105.00021.

[43] I. Buric, S. Lacroix, J. A. Mann, L. Quintavalle and V. Schomerus, *"Gaudin Models and Multipoint Conformal Blocks II: Comb channel vertices in 3D and 4D"*, JHEP 2111, 182 (2021), arxiv:2108.00023.

[44] I. Buric, S. Lacroix, J. A. Mann, L. Quintavalle and V. Schomerus, *"Gaudin Models and Multipoint Conformal Blocks III: Comb channel coordinates and OPE factorisation"*, arxiv:2112.10827.

[45] D. Poland, S. Rychkov and A. Vichi, *"The Conformal Bootstrap: Theory, Numerical Techniques, and Applications"*, Rev. Mod. Phys. 91, 015002 (2019), arxiv:1805.04405.

[46] V. Bargmann and I. T. Todorov, *"Spaces of analytic functions on a complex cone as carriers for the symmetric tensor representations of SO(n)"*, Journal of Mathematical Physics 18, 1141 (1977).

[47] V. K. Dobrev, G. Mack, V. B. Petkova, S. G. Petrova and I. T. Todorov, *"Harmonic Analysis on the n-Dimensional Lorentz Group and Its Application to Conformal Quantum Field Theory"*, Lect. Notes Phys. 63, 1 (1977).

[48] M. S. Costa, J. Penedones, D. Poland and S. Rychkov, *"Spinning Conformal Correlators"*, JHEP 1111, 071 (2011), arxiv:1107.3554.

[49] M. S. Costa and T. Hansen, *"Conformal correlators of mixed-symmetry tensors"*, JHEP 1502, 151 (2015), arxiv:1411.7351.

[50] E. Lauria, M. Meineri and E. Trevisani, *"Spinning operators and defects in conformal field theory"*, JHEP 1908, 066 (2019), arxiv:1807.02522.

[51] F. A. Dolan and H. Osborn, *"Conformal Partial Waves: Further Mathematical Results"*, arxiv:1108.6194.

[52] S. Parikh, *"Holographic dual of the five-point conformal block"*, JHEP 1905, 051 (2019), arxiv:1901.01267.

[53] J.-F. Fortin and W. Skiba, *"New methods for conformal correlation functions"*, JHEP 2006, 028 (2020), arxiv:1905.00434.

[54] S. Parikh, *"A multipoint conformal block chain in d dimensions"*, JHEP 2005, 120 (2020), arxiv:1911.09190.

[55] J.-F. Fortin, W. Ma and W. Skiba, *"Higher-Point Conformal Blocks in the Comb Channel"*, JHEP 2007, 213 (2020), arxiv:1911.11046.

[56] N. Irges, F. Koutroulis and D. Theofilopoulos, *"The conformal N-point scalar correlator in coordinate space"*, arxiv:2001.07171.

[57] J.-F. Fortin, W.-J. Ma and W. Skiba, *"Six-point conformal blocks in the snowflake channel"*, JHEP 2011, 147 (2020), arxiv:2004.02824.

[58] A. Pal and K. Ray, *"Conformal Correlation functions in four dimensions from Quaternionic Lauricella system"*, Nucl. Phys. B 968, 115433 (2021), arxiv:2005.12523.

[59] S. Hoback and S. Parikh, *"Towards Feynman rules for conformal blocks"*, JHEP 2101, 005 (2021), arxiv:2006.14736.

[60] J.-F. Fortin, W.-J. Ma and W. Skiba, *"All Global One- and Two-Dimensional Higher-Point Conformal Blocks"*, arxiv:2009.07674.

[61] M. Gaudin, *"Diagonalisation d'une classe d'hamiltoniens de spin"*, Journal de Physique 37 (10), 1087 (1976).

[62] M. Gaudin, *"La fonction d'onde de Bethe"*, Masson (1983).

[63] B. Feigin, E. Frenkel and N. Reshetikhin, *"Gaudin model, Bethe ansatz and correlation functions at the critical level"*, Commun. Math. Phys. 166, 27 (1994), hep-th/9402022.

[64] B. Feigin and E. Frenkel, *"Affine Kac-Moody algebras at the critical level and Gelfand-Dikii algebras"*, Int. J. Mod. Phys. A7S1A, 197 (1992).

[65] D. Talalaev, *"Quantization of the Gaudin system"*, hep-th/0404153.

[66] A. Chervov and D. Talalaev, *"Quantum spectral curves, quantum integrable systems and the geometric Langlands correspondence"*, hep-th/0604128.

[67] A. I. Molev, *"Feigin-Frenkel center in types B, C and D"*, Inventiones Mathematicae 191, 1 (2013), arxiv:1105.2341.

[68] A. Molev, *"Sugawara Operators for Classical Lie Algebras"*, Mathematical surveys and monographs, American Mathematical Society (2018).

[69] O. Yakimova, *"Symmetrisation and the Feigin-Frenkel centre"*, arxiv:1910.10204.

[70] A. Chervov, G. Falqui and L. Rybnikov, *"Limits of Gaudin algebras, quantization of bending flows, Jucys-Murphy elements and Gelfand-Tsetlin bases"*, Lett. Math. Phys. 91, 129 (2010), arxiv:0710.4971.

[71] A. Chervov, G. Falqui and L. Rybnikov, *"Limits of Gaudin Systems: Classical and Quantum Cases"*, SIGMA 5, 029 (2009), arxiv:0903.1604.

[72] L. Rybnikov, *"Cactus group and monodromy of Bethe vectors"*, arxiv:1409.0131.

[73] P. Argyres, O. Chalykh and Y. Lü, *"Inozemtsev System as Seiberg-Witten Integrable system"*, arxiv:2101.04505.

[74] L. Eberhardt, S. Komatsu and S. Mizera, *"Scattering equations in AdS: scalar correlators in arbitrary dimensions"*, JHEP 2011, 158 (2020), arxiv:2007.06574.

[75] P. Etingof, G. Felder, X. Ma and A. Veselov, *"On elliptic Calogero-Moser systems for complex crystallographic reflection groups"*, Journal of Algebra 329, 107 (2011), arxiv:1003.4689, See also erratum 2.14 in http://www-math.mit.edu/~etingof/errorsinpapers.pdf.

[76] M. Isachenkov and V. Schomerus, *"Superintegrability of d-dimensional Conformal Blocks"*, Phys. Rev. Lett. 117, 071602 (2016), arxiv:1602.01858.

[77] G. J. Heckman and E. M. Opdam, *"Root systems and hypergeometric functions. I"*, Compositio Mathematica 64, 329 (1987).

[78] A. Castedo Echeverri, E. Elkhidir, D. Karateev and M. Serone, *"Seed Conformal Blocks in 4D CFT"*, JHEP 1602, 183 (2016), arxiv:1601.05325.

[79] V. Schomerus, E. Sobko and M. Isachenkov, *"Harmony of Spinning Conformal Blocks"*, JHEP 1703, 085 (2017), arxiv:1612.02479.

[80] V. Schomerus and E. Sobko, *"From Spinning Conformal Blocks to Matrix Calogero-Sutherland Models"*, JHEP 1804, 052 (2018), arxiv:1711.02022.

[81] I. Burić, V. Schomerus and M. Isachenkov, *"Conformal Group Theory of Tensor Structures"*, arxiv:1910.08099.

[82] Harish-Chandra, *"Spherical Functions on a Semisimple Lie Group, I"*, Amer. J. Math. 80, 241 (1958).

[83] I. Buric and V. Schomerus, *"Universal Spinning Casimir Equations. Applications to Defect CFTs - in preparation"*.

[84] T. G. Raben and C.-I. Tan, *"Minkowski conformal blocks and the Regge limit for Sachdev-Ye-Kitaev-like models"*, Phys. Rev. D 98, 086009 (2018), arxiv:1801.04208.

[85] I. Buric, V. Schomerus and E. Sobko, *"Superconformal Blocks: General Theory"*, arxiv:1904.04852.

[86] I. Burić, V. Schomerus and E. Sobko, *"The superconformal X-ing equation"*, JHEP 2010, 147 (2020), arxiv:2005.13547.

[87] J. Stokman and N. Reshetikhin, *"N-point spherical functions and asymptotic boundary KZB equations"*, arxiv:2002.02251.

[88] N. Reshetikhin and J. Stokman, *"Asymptotic boundary KZB operators and quantum Calogero-Moser spin chains"*, arxiv:2012.13497.

[89] E. Elkhidir, D. Karateev and M. Serone, *"General Three-Point Functions in 4D CFT"*, JHEP 1501, 133 (2015), arxiv:1412.1796.

[90] S. Ferrara, A. F. Grillo, G. Parisi and R. Gatto, *"The shadow operator formalism for conformal algebra. Vacuum expectation values and operator products"*, Lett. Nuovo Cim. 4S2, 115 (1972), [Lett. Nuovo Cim.4,115(1972)].

[91] A. Joseph, *"A generalization of Quillen's lemma and its application to the Weyl algebras"*, Israel Journal of Mathematics 28, 177 (1977).

[92] S. P. Smith, *"A Class of Algebras Similar to the Enveloping Algebra of* sl(2)*"*, Transactions of the American Mathematical Society 322, 285 (1990).

[93] V. V. Bavula, *"Generalized Weyl algebras and their representations"*, Algebra i Analiz 4, 75 (1992).

[94] T. J. Hodges, *"Noncommutative deformations of type-A Kleinian singularities"*, Journal of Algebra 161, 271 (1993).

[95] W. Crawley-Boevey and M. P. Holland, *"Noncommutative deformations of Kleinian singularities"*, Duke mathematical journal 92, 605 (1998).

[96] A. Oblomkov, *"Deformed Harish-Chandra homomorphism for the cyclic quiver"*, Math. Res. Lett 14, 359 (2007), math/0504395.

[97] P. Etingof, W. L. Gan, V. Ginzburg and A. Oblomkov, *"Harish–Chandra homomorphisms and symplectic reflection algebras for wreath-products"*, Publications mathémati 105, 91 (2007), math/0511489.

[98] M. P. Holland, *"Quantization of the Marsden-Weinstein reduction for extended Dynkin quivers"*, Annales Scientifiques de l'École Normale Supérieure 32, 813 (1999).

[99] P. Etingof, S. Loktev, A. Oblomkov and L. Rybnikov, *"A Lie-theoretic construction of spherical symplectic reflection algebras"*, Transformation Groups 13, 541 (2008), arxiv:0801.2339.

[100] *"NIST Digital Library of Mathematical Functions"*, F. W. J. Olver, A. B. Olde Daalhuis, D. W. Lozier, B. I. Schneider, R. F. Boisvert, C. W. Clark, B. R. Miller, B. V. Saunders, H. S. Cohl, and M. A. McClain, eds., http://dlmf.nist.gov/.

[101] E. W. Weisstein, *"'Lemniscate Function'. From MathWorld — a Wolfram Web Resource"*, https://mathworld.wolfram.com/LemniscateFunction.html.

[102] P. Etingof and E. Rains, *"On algebraically integrable differential operators on an elliptic curve"*, SIGMA 7, 062 (2011), arxiv:1011.6410.

[103] C. F. Dunkl, *"Reflection groups and orthogonal polynomials on the sphere"*, Mathematische Zeitschrift 197, 33 (1988).

[104] S. Ferrara, A. F. Grillo, R. Gatto and G. Parisi, *"Analyticity properties and asymptotic expansions of conformal covariant green's functions"*, Nuovo Cim. A 19, 667 (1974).